

PDF hosted at the Radboud Repository of the Radboud University Nijmegen

The following full text is a publisher's version.

For additional information about this publication click this link.

<http://hdl.handle.net/2066/19230>

Please be advised that this information was generated on 2017-12-05 and may be subject to change.

**ANTIFUNGAL SUSCEPTIBILITY TESTING
AND
DRUG INTERACTION MODELING IN MOULDS**

JOSEPH MELETIADIS

CIP data, Koninklijke Bibliotheek, Den Haag

ISBN: 90-9015970-3

Copyright © 2002 by J. Meletiadis

All papers were reprinted with permission and credit to their original source.

Printing: Drukkerij Benda, Nijmegen, The Netherlands

ANTIFUNGAL SUSCEPTIBILITY TESTING AND DRUG INTERACTION MODELING IN MOULDS

Een wetenschappelijke proeve op het gebied van de Medische Wetenschappen

PROEFSCHRIFT

ter verkrijging van de graad van doctor
aan de Katholieke Universiteit Nijmegen
op gezag van de Rector Magnificus Prof. dr. C. W. P. M. Blom
volgens besluit van het College van Decanen
in het openbaar te verdedigen op
woensdag 18 September 2002
des namiddags om 1:30 uur precies

door

JOSEPH MELETIADIS

Geboren op 13 juli 1975 te Hannover, Duitsland

Promotor: Prof. Dr. B. E. de Pauw

Co-promotores: Dr. P. E. Verweij
Dr. J. F. G. M. Meis, Canisius-Wilhelmina Ziekenhuis

Manuscriptcommissie: Prof. Dr. D. Ruiter
Dr. B-J. Kullberg
Prof. Dr. G. S. de Hoog, CBS Utrecht

Cover illustration:

Scanning electron micrograph of *Aspergillus fumigatus* conidiophores. The picture was kindly provided by Hein van der Lee. A background color of the MTT-formazan dye and the three-dimensional graph of response surface concentration effect approach for modeling interactions based on the fully parametric Greco model are shown.

The research described in this thesis was performed at the Department of Medical Microbiology, University Medical Center Nijmegen, in collaboration with the Department of Medical Microbiology and Infectious Diseases, Canisius-Wilhelmina Hospital Nijmegen, The Netherlands and was supported by the European Commission Training and Mobility of Researchers program (EC-TMR-EUROFUNG network ERBFMRXCT97-0145).

The publication of this thesis was supported by contributions of:

- Mycology Research Center Nijmegen
- Center for Pharmacodynamic Research Nijmegen
- Gilead
- ICN-Pharmaceuticals
- Merck
- Pfizer
- Janssen
- Wyeth Pharmaceuticals
- Bayer
- Pharmacia
- Novartis
- AB-Biodisk

**To my grandparents, Iosif and Sophia
and
to my parents, Despina and Emmanouil**

CONTENTS

CHAPTER 1: GENERAL INTRODUCTION

1.1 In vitro susceptibility testing of filamentous fungi	
Adapted from <i>Reviews in Medical Microbiology 2002; 13: (in press)</i>	12
1.2 Drug interaction modeling	
Adapted from <i>Reviews in Medical Microbiology 2002; 13: (in press)</i>	14
1.3 Outline of the thesis	19

CHAPTER 2: IN VITRO SUSCEPTIBILITY TESTING OF FILAMENTOUS FUNGI

2.1 Analysis of growth characteristics of filamentous fungi in different nutrient media	
<i>Journal of Clinical Microbiology 2001; 39: 478-484</i>	27
2.2 Comparison of NCCLS and 3-(4,5-dimethyl-2-thiazyl)-2,5-diphenyl-2H-tetrazolium bromide (MTT) methods of in vitro susceptibility testing of filamentous fungi and development of a new simplified method	
<i>Journal of Clinical Microbiology 2000; 38: 2949-2954</i>	39
2.3 Colorimetric assay for antifungal susceptibility testing of <i>Aspergillus</i> species	
<i>Journal of Clinical Microbiology 2001; 39: 3402-3408</i>	49
2.4 Comparison of spectrophotometric and visual readings of NCCLS method and evaluation of a colorimetric method based on reduction of a soluble tetrazolium salt 2,3-bis{2-methoxy-4-nitro-5-[(sulphenylamino)carbonyl]-2H-tetrazolium hydroxide} for antifungal susceptibility testing of <i>Aspergillus</i> species	
<i>Journal of Clinical Microbiology 2001; 39: 4256-4263</i>	59

CHAPTER 3: DRUG INTERACTION MODELING OF ANTIFUNGALS

3.1 In vitro interaction of terbinafine with itraconazole against clinical isolates of <i>Scedosporium prolificans</i> <i>Antimicrobial Agents and Chemotherapy 2000; 44: 470-472</i>	73
3.2 Drug interaction modeling of in vitro combination of azoles with terbinafine against clinical <i>Scedosporium prolificans</i> isolates <i>(submitted for publication)</i>	79
3.3 Assessing the in vitro interaction of antifungal drugs: Comparison of different drug interaction models <i>(submitted for publication)</i>	95

CHAPTER 4: GENERAL CONCLUSIONS

4.1 Summary	117
4.2 Samenvatting (summary in Dutch)	118
4.3 Περίληψη (summary in Greek)	120
4.4 Future perspectives Adapted from <i>Reviews in Medical Microbiology 2002; 13: (in press)</i>	122

ACKNOWLEDGMENTS	125
------------------------------	------------

CURRICULUM VITAE	127
-------------------------------	------------

LIST OF PUBLICATIONS	129
-----------------------------------	------------

CHAPTER

1

GENERAL INTRODUCTION

- In vitro susceptibility testing of filamentous fungi
- Drug interaction modeling
- Outline of the thesis

Adapted from *Reviews in Medical Microbiology* 2002; 13: (in press)

IN VITRO SUSCEPTIBILITY TESTING OF FILAMENTOUS FUNGI AND DRUG INTERACTION MODELING OF ANTIFUNGAL DRUGS

JOSEPH MELETIADIS¹, JOHAN W. MOUTON², JACQUES F. G. M. MEIS², AND PAUL E. VERWEIJ¹

Department of Medical Microbiology, University Medical Center Nijmegen¹, and Department of Medical Microbiology and Infectious Diseases, Canisius-Wilhelmina Hospital², The Netherlands

Given the high mortality of invasive infections caused by filamentous fungi and the limitations of current antifungal therapies, the interest in combination therapy is increasing. However, assessment of the nature and the intensity of antifungal interactions depend on the in vitro methodology used as well as on the approach chosen to analyze the data. Regarding the in vitro methodology many variables in antifungal susceptibility testing of filamentous fungi such as the inoculum, incubation conditions, medium, and minimal inhibitory concentration (MIC) endpoints remain unstandardized. The proposed standard medium RPMI 1640, although it provides reproducible results, inadequately supports the growth of many fungi and is considered less optimal for detection of amphotericin B resistance. Visual determination of the MICs is subjective and does not allow precise quantification of fungal growth. Determination of the MICs could be facilitated using colorimetric assays based on the conversion of tetrazolium salts. These salts are converted to colored formazan derivatives by enzymes with dehydrogenase activity and therefore can be used as indicators of reducing systems. Regarding the assessment of drug interactions, the standard approach in medical microbiology is the calculation of the fractional inhibitory concentration index despite its drawbacks. Alternative approaches of drug interaction modeling consist of response surface approaches and fully parametric models which incorporate modern concepts of statistical and regression analysis and provide an objective and quantitative tool for the study of drug interaction.

Systemic infections caused by filamentous fungi can be differentiated to two groups; endemic and opportunistic mycoses. True human pathogens (dimorphic fungi) are responsible for endemic mycoses, which are able to cause infections even in individuals with normal host defense and which have their habitat in specific geographical areas (71). Less virulent and less well-adapted organisms (opportunists) are responsible for opportunistic mycoses, which cause infections in debilitated and immunocompromised hosts and which are distributed worldwide. In the last two decades a dramatic increase in the latter infections has been observed and incidence rates up to 36% have been reported in particular patient populations such as bone marrow transplant recipients (16, 21). This increase was associated with an increasing number of immunocompromised individuals mainly due to organ transplantation, HIV infection and cancer where cytotoxic and immunosuppressive therapies are used (19, 57, 78). Corticosteroid therapy, diabetes and other underlying diseases were also recognized as predisposing factors (58). The most commonly identified pathogens were *Aspergillus* species, especially *Aspergillus fumigatus*. A growing number of uncommon organisms have been implicated in invasive human infections including members of the Zygomycota (*Rhizopus* spp., *Mucor* spp., and *Absidia* spp.), *Fusarium* spp. and *Scedosporium* spp. (28, 77).

Since the immune system of immunocompromised patients may be suppressed for long periods, antifungal therapy is employed to prevent and/or control invasive fungal infections (79). Amphotericin B and itraconazole are licensed drugs to treat invasive infections caused by filamentous fungi although new drugs are under investigation (34). However, the mortality rates of these infections remain as high as 95% despite the use of aggressive antifungal chemotherapy (78). Furthermore, there are several drawbacks to the currently available antifungal agents such as the high toxicity, the low level of penetration into some tissues, the irregular pharmacokinetic profile, the drug interactions, and the emergence of resistance (35). Given these limitations, new approaches for the management of invasive infections caused by filamentous fungi are warranted. Combination therapy might be an effective approach (49) since new azoles with better pharmacokinetic profiles (i.e. voriconazole and posaconazole) and drugs with novel antifungal actions (i.e. echinocandins, nikkomycin) are under investigation. The increased arsenal of antifungal agents facilitates the number of possible combinations and the probability of synergistic interactions (47).

Combination therapy has been shown to be beneficial for several difficult-to-treat infections such as HIV (<http://www.hivatis.org>) and mycobacterial infections (42) which do not respond well to single-

Table 1. NCCLS guidelines for antifungal susceptibility testing of conidium forming filamentous fungi

Parameter	NCCLS M-38P
Suitability	Conidium- and spore forming fungi
Format	Microdilution, two-fold dilution scheme
Inoculum	Conidial suspensions of $0.4 \times 10^4 - 5 \times 10^4$ CFU/ml
Inoculum standardization	Spectrophotometric adjustment at 530 nm 68-70% transmittance (T) for <i>Scedosporium</i> spp. and <i>Rhizopus</i> spp. 78-80% T for the remaining fungi incl. <i>Aspergillus</i> spp.
Incubation conditions	35°C in ambient conditions
Duration of incubation	24 h (<i>Rhizopus</i> spp.), 72 h (<i>Scedosporium</i> spp.) 48 h (most fungi including <i>Aspergillus</i> spp. and <i>Fusarium</i> spp.)
Solvent	Dimethylsulfoxid for amphotericin B and all azoles, 1% of final concentration
Test medium	RPMI 1640 buffered at pH 7.0 with 0.165 M 3-N-morpholinopropanesulfonic acid
Endpoint	Lowest drug concentration with absence of visible growth (for amphotericin B) or with prominent growth reduction (50%) from control (for azoles)

drug therapy either due to lack of efficacy or rapid emergence of resistance. Combination therapy has also been proven to be beneficial in clinical mycology such as the combination of amphotericin B and flucytosine for the treatment of cryptococcal meningitis (35, 62). However, adverse events can either eliminate or reverse the benefits of combination therapy by worsening the clinical outcome (43, 44). The problem with the testing of the toxicity and superior efficacy of a given combination compared to monotherapy in the clinical setting is that large, time-consuming and expensive clinical trials are required in order to have sufficient power to show significant differences. Although animal models might predict efficacy and toxicity in humans, current models are often inappropriate since antifungal drugs exhibit different pharmacokinetic characteristics compared with humans (61). However, recently models have been published that help to characterize the pharmacodynamic profile of antifungal agents (2). Nevertheless, in vitro systems are needed in order to help to predict drug interaction in clinical practice using the fungal strain that caused the infection. Furthermore, in vitro data, although they are obtained from simplified systems, could be combined with in vivo data in order to design proper, feasible, and less costly clinical trials by optimizing for instance the dosing of regimens in combination (18, 22).

However, assessing the nature and the intensity of drug interactions in vitro depends both on the methodology used (50) as well as on the approach used to analyze the results (6). Although different methodologies, such as agar dilution, disc diffusion, and Etest have been used for testing the in vitro

interaction of antifungal drugs (4, 13, 47, 48, 53, 56, 60, 72), the most common approach in antifungal susceptibility testing is the microdilution checkerboard technique. According to this technique a serial dilution of drug A is combined with a serial dilution of drug B (including zero concentrations of each drug) in small volumes of broth medium in microtiter plates in such a way to obtain a two-dimensional checkerboard (41). Conclusions are then inferred by comparing the growth in the wells containing single drugs with the growth in the wells where the drugs are combined.

1.1 IN VITRO SUSCEPTIBILITY TESTING OF FILAMENTOUS FUNGI

Despite the considerable progress in in vitro antifungal susceptibility testing (AST) of moulds leading to the publication of the M-38P standard proposed by the USA National Committee of Clinical Laboratory Standards for antifungal susceptibility testing of conidium forming fungi (55), several variables remain unstandardized. The M-38P method specifies the inoculum size and preparation, incubation time and temperature, the format of the methodology, test medium, and assessment of the minimal inhibitory concentration (MIC) endpoint for various drugs (Table 1). Although the large differences between the different methodologies used previously, are now eliminated and more reproducible results are obtained with this method (24, 25), the appropriateness of some parameters is questionable given the absence of clinical correlation of the results.

Although it is more convenient to use conidial suspensions as an inoculum for AST, the invasive forms of filamentous fungi are hyphae, which exhibit higher MICs compared to conidia (24, 38). An inoculum of 10^4 CFU/ml seems to be satisfactory although inoculum effects (increased MICs with higher inocula) suggest specific adjustments based on the organism tested and the drug. In addition higher inocula may facilitate the detection of resistant strains (20, 24, 30). According to the reference method, the incubation period required for obtaining the inoculum takes several days and the technique advocated to harvest the conidia or spores results in an inoculum that may contain also hyphal fragments which could give variable MIC results (15, 54). Spectrophotometric adjustment of the inocula provides a fast and reproducible way to obtain inocula within a range of $1 \log_{10}$ CFU/ml (27) but the transmittance measured might be affected by the proportion of hyphal fragments present in the inoculum (24, 54). Furthermore, differences in color and size (64) of conidia and fungal spores affect spectrophotometric reading resulting in a wider range of CFU/ml compared to counting with a hemacytometer (59).

Regarding the incubation conditions of AST, although temperatures of 35-37°C correspond to body temperatures and appear adequate for AST, filamentous fungi seem to grow better at lower temperatures i.e. 25-30°C (66, 67). Incubation periods were established arbitrary based on the presence of visual growth, which is different for various species, without considering the dynamic nature of fungal growth. Prolonged incubation results in higher MICs (3, 24, 30) and different levels of reproducibility may be achieved with different incubation periods (51). The degree of differentiation between resistant and susceptible strains is variable with different incubation periods (20).

Although the microdilution format is less troublesome and generates similar results compared to the well-evaluated macrodilution method (26, 65), it is more sensitive to evaporation and assessment of fungicidal activities is problematic (67). The synthetic and fully defined medium RPMI 1640 buffered at pH 7.0 is used for AST, supports the growth of different fungal species and generates reproducible results. However, the inability of this medium to distinguish amphotericin B-resistant *Aspergillus* and *Candida* strains from susceptible ones (46, 68) and the poor growth of dermatophytes and *Cryptococcus neoformans* (24, 32), raises questions concerning the appropriateness of this medium for susceptibility testing of filamentous fungi given that no extensive evaluation has been reported that addresses the suitability of this medium for these fungi. Better growth was achieved by supplementing RPMI 1640 with extra glucose for *Candida* strains or by using alternative nutrient media such as yeast nitrogen base medium for *C. neoformans*.

Other media used for fungi include Antibiotic Medium 3, Sabouraud's medium, and SAAM-F. Although the use of one standard medium for in vitro susceptibility testing of all fungi is desirable, the diversity in growth rate and nutrient requirements among members of the fungal kingdom and the differences in properties of various antifungal drugs suggest that the use of different media will be inevitable. The medium pH as well as the buffering capacity is also critical factors for AST since they may alter the action of some antifungal drugs (69).

The MIC determination based on visual observation simplifies the M-38P since special equipment is not required. However, this introduces subjectivity and variability in methodology and precludes the precise quantification of fungal growth. The latter is complicated by the non-homogenous growth of moulds in liquid media and the fungistatic activity of azoles, which inhibit the growth over a range of drug concentrations. Thus automation of AST for filamentous fungi is impossible and detailed information about the antifungal effect-drug concentration relationship is not obtained. In order to avoid these problems alternative methodologies have been proposed based on spectrophotometric, radiometric, direct microscopic, colorimetric, flow cytometric, and fluorescent assays (14, 69, 70). However, some of them are semi-quantitative (Alamar blue oxidation-reduction indicator dye), lack sensitivity (spectrophotometric), are time-consuming (measuring the rate of elongation of germ tubes), potentially hazardous (use of radioactive substances), or require expensive equipment (flow cytometer) thus limiting their use in routine clinical laboratories. Colorimetric assays based on the reduction of tetrazolium salts have many advantages and have found many applications in various fields including the susceptibility testing of cancer cells (73), viruses (45), parasites (17), bacteria (29) as well as yeasts (40).

Tetrazolium salts are heterocyclic organic compounds that got their name from the four nitrogens of the five-member unsaturated ring that contains a heteroatom. The most characteristic and important property of this class of dyes is that they are reduced into highly colored formazans with mild reduction giving rapid and strong reactions. Formazans are produced when the tetrazolium salts receive electrons from the hydrogen transport system, catalyzed by enzymes, substituting the natural final acceptor (oxygen) in the biological redox process or non-enzymatically from artificial electron transporters (phenazine methosulfate, menadione) (Fig. 1). This reaction takes place inside mitochondria or other intracellular sites with dehydrogenase activity of intact cells where tetrazolium salts can penetrate rapidly depending on the molecular size. Since the tetrazolium-

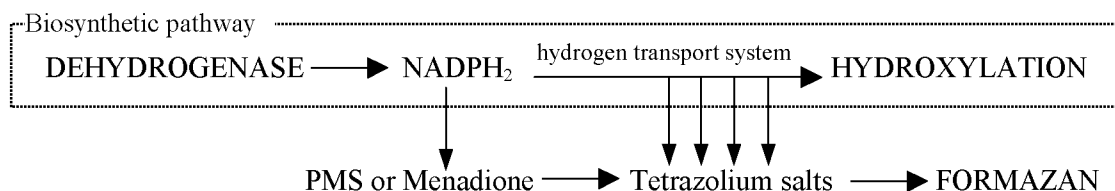


Figure 1. Generalized scheme showing the pathways leading to reduction of tetrazolium salts to their formazan derivatives. Dehydrogenases are cellular enzymes, which oxidize different biomolecules by reducing the cofactor NADP^+ to NADPH_2 . From NADPH_2 , e^- are transferred through the hydrogen transport system (cytochromes) to O_2 the oxidation of which causes the hydroxylation of other substrates. Tetrazolium salts can interact with components of hydrogen transport system and can be reduced to formazan derivatives by receiving e^- from carriers of this system (flavins) but not directly from NADPH unless an electron-coupling agent (PMS; phenazine methosulfate or Menadione) is added. NADPH_2 is oxidized back to NADP^+ by cellular enzymes called diaphorases.

formazan reaction assesses dehydrogenase activity, tetrazolium salts have been used as indicators of reducing systems with a number of applications in chemistry and biology including susceptibility testing (1).

Although some of the above mentioned factors of AST of filamentous fungi have little effect on the final results, their effect may increase when all these factors are combined simultaneously (67). This effect will be amplified when filamentous fungi are tested against combinations of antifungal drugs where the drug-fungus interaction becomes more complicated with the addition of one or more drugs. The analysis of such a system is difficult not only from a methodological point of view but also when the results are attempted to be evaluated in order to assess the nature and the degree of interaction taking place among the antifungal drugs against the fungus.

1.2 DRUG INTERACTION MODELING

Assessing the nature and the degree of drug interactions is a critical challenge and a debated area of chemotherapy. The importance of drug interactions in chemotherapy is related with the clinical outcome that can be improved or worsened when positive or negative drug interactions, respectively take place (44, 52). Drug interactions are of great interest particularly in antifungal chemotherapy given that treatment is initiated in patients who simultaneously receive a variety of anticancer, immune-suppressive, antiviral or antibacterial drugs, which increases the possibility for such interactions to take place. Drug interactions may occur at different levels i.e. absorption, metabolism, excretion of drugs altering their pharmacokinetic and finally their pharmacodynamic profiles (8, 39, 53) before the drugs reach the site of infection and exhibit their antifungal effects (Table 2). Even then drug interactions may occur at the cellular (fungus) (33, 81) and molecular (receptors) level (4) before an antifungal

effect occurs and at the population level before growth is arrested. In vitro susceptibility tests attempt to assess the drug interactions at this level.

Although different terms and classifications can be found in the literature in order to describe drug interactions, three classes can be recognized; 1. positive interaction or synergy which originates from the Greek words $\sigma\upsilon\nu$ (plus) and $\acute{\epsilon}\rho\gamma\omicron$ (work) and means working together (synonyms are potentiation, augmentation, sensitization, supraditiveness). 2. negative interaction or antagonism, which means working against each other (synonyms are depotentiation, desensitization, infraditiveness, negative synergy) and 3. zero-interaction, in which the drugs do neither of the above do not interact and therefore the effect of such a combination is precisely what is expected (synonyms are additivity, indifference, independence, autonomy). The definition of the latter has a central position in drug interaction theories since synergy or antagonism can be defined as departures of the zero interaction and thus a combination is deemed synergistic or antagonistic when its effect is greater or less, respectively than that expected from the zero interaction theory.

For the calculation of the expected effect of zero interaction various theories were developed based upon mechanistic and empirical models (7). The former models which are based on the mechanism of action of drugs for calculating the expected effects (11, 12) require a full understanding of the mode of actions of the drug, are dependent on the current state of knowledge and exclude analysis of the interaction of drugs which modes of action are not known. Even if the mechanisms were fully understood at the molecular level, the effect of a zero interactive combination might be different than expected based on these theories since the action of drugs might be different at the cellular level (7) and at the population level (5) as is the case for susceptibility tests. The empirical mechanism-free models rely on concentration-effect curves of individual drugs on which based the effect of zero interaction is calculated without making assumptions about the

Table 2. Classification of drug interactions

I.	Prior to administration
II.	Drug absorption
	Within the gut lumen
	By altering gut motility
	By altering gut flora
	Within the gut wall
III.	Protein-binding
IV.	Drug metabolism
	Stimulation
	Inhibition
V.	Drug excretion
	Changes in urine pH
	Competition for active renal tubular excretion
	Fluid and electrolyte changes
VI.	Interactions at the site of infection
	Physical conditions (pH, oxygen concentration)
	Population level (heteroresistant strains)
	Cellular level (influx pumps)
	Molecular level (receptor sites)

Adapted from Breckenridge (8).

mechanism of action. Among all theories described in the literature two are distinguished as reference models, the Bliss independence and the Loewe additivity theories.

Bliss independence implies that two drugs do not cooperate physically or chemically or biologically i.e. each drug acts independently from the other (36). In this case the effect (S_0) of a zero interactive combination would be equal with the product of the survival fractions S_A and S_B of its constituent doses of drug A and B when acting alone, respectively giving the equation:

$$S_0 = S_A \times S_B \quad [1].$$

If the combination of a dose of drug A and a dose of drug B results in a survival fraction of S_{A+B} greater than the S_0 antagonism is deemed while if it is smaller than S_0 synergy is claimed. The equation [1] can be derived from the probability theory. Given that the two drugs do not interact, their actions may be treated as statistically independent events (5). Thus, if $P(A)$ and $P(B)$ are the probabilities of independent event A and B, the probability of at least one of event A or B occurring $P(A \cup B)$ is

$$P(A \cup B) = P(A) + P(B) - P(A) \times P(B) \quad [2].$$

Now, let $P(A)$ and $P(B)$ be the action of two drugs A and B alone (which in case of susceptibility tests corresponds with growth inhibition I_A and I_B caused by each drug, respectively) and the $P(A \cup B)$ the

action of a zero interactive combination (I_0) the following equation is derived:

$$I_0 = I_A + I_B + I_A \times I_B \quad [3].$$

Since it holds that $S = 1 - I$ [4] where S is the percentage of growth and I the percentage of inhibition, the equation [3] is rewritten as

$$1 - S_0 = (1 - S_A) + (1 - S_B) + (1 - S_A) \times (1 - S_B)$$

which after resolution results in equation [1]. Equation [1] is also derived by the following paradigm. Let us consider a drug A that inhibits the growth of a fungal population for 30% ($= I_A$) and a drug B that inhibits the growth for 50% ($= I_B$). If the growth of the control is designated as 100%, the drug A alone would reduce the growth to 70% ($= S_A$). If the drug B now added the growth would be reduced further to 35% ($= S_0$ and based on equation [4] $I_0 = 65\%$) if the first drug did not affect the action of the second drug. Likewise if drug B is used alone, the growth would be reduced to 50% ($= S_B$) and the addition of drug A would reduce it to 35% again. Using the values in the brackets equation [1] and [3] come true (80).

The other candidate for the reference zero interaction theory is the Loewe additivity, which is based on the concept that a drug cannot interact with itself by definition. Therefore, the effect of a sham combination of one drug with itself in any arrangement of concentrations is what would be expected from the concentration effect curve of the drug selected, so such a combination is zero-interactive by construction. This must hold irrespective the shape of the concentration-effect curve of the drug and the type of the effect measured. Loewe additivity is described by the following equation:

$$1 = d_A/D_A + d_B/D_B \quad [5]$$

where d_A and d_B are the concentrations of the drugs A and B in a combination which elicits a certain effect and D_A and D_B the iso-effective concentrations of the drugs A and B when acting alone. When the right part of the equation [5] is less than 1, synergy is claimed while when it is greater than 1, antagonism is concluded. The power of equation [5] is supported by the following paradigm. Lets consider a drug A, 1 mg of which inhibits the growth by 30% and 2 mg by 50%. If the 2 mg powder is split into two portions of 1 mg and labeled as drug A_1 and drug A_2 , the combination of 1 mg of drug A_1 plus 1 mg of drug A_2 would have the same effect as 2 mg of drug A_1 or drug A_2 alone which actually is the effect of drug A i.e. 50% of inhibition based on the concentration-effect curve of drug A. Such a combination can only be zero interactive. Thus, for

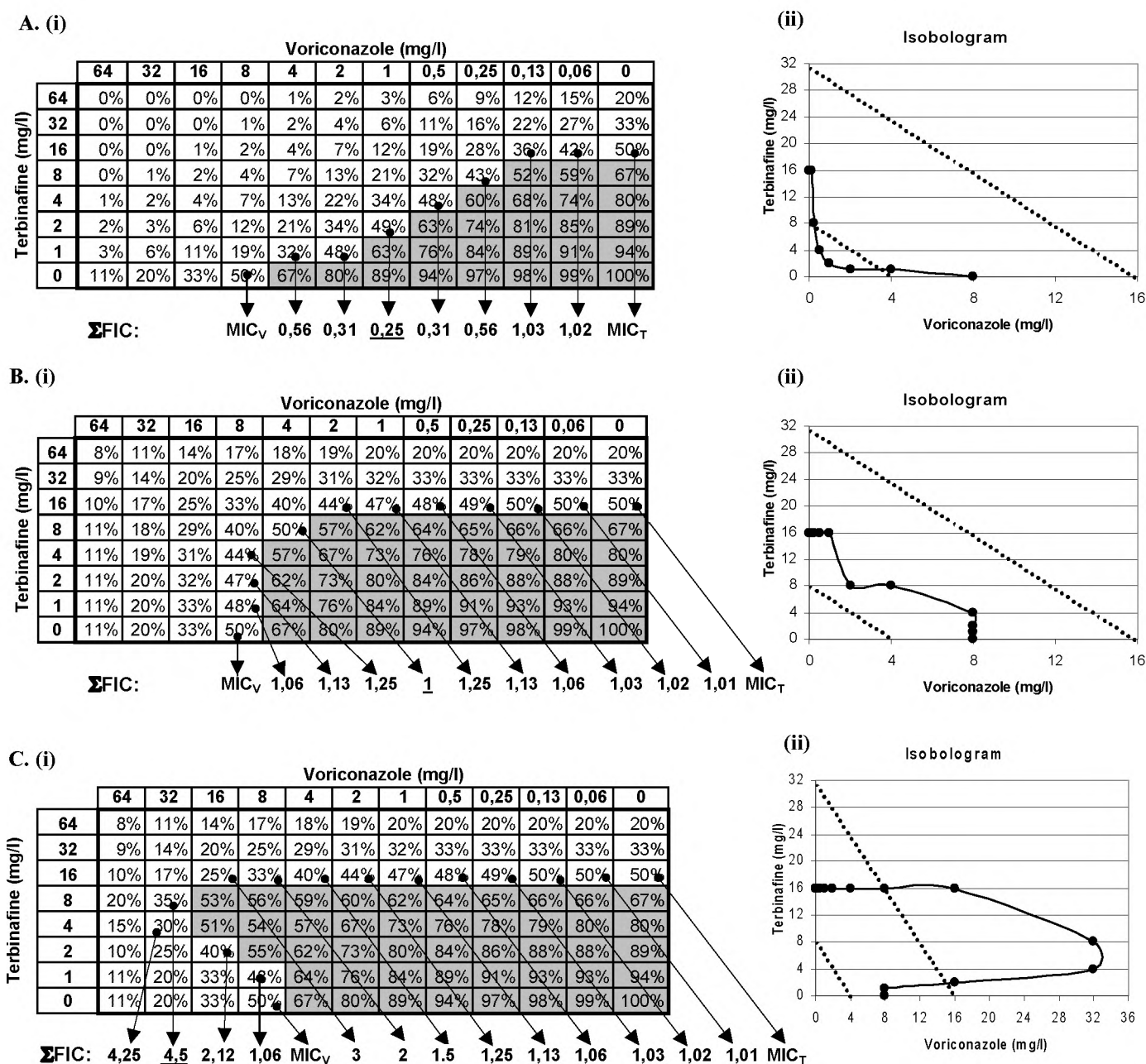


Figure 2. Layouts of the microdilution checkerboards (i) and isobolograms (ii) for a synergistic (A), additive/indifferent (B) and antagonistic (C) interaction between voriconazole and terbinafine. The percentages of growth at each combination of the two drugs are presented (shadow area indicates combination with higher than 50% of growth) together with the Σ FICs calculated for the iso-effective combinations (arrows). The underlined Σ FICs represent the minimum (for A and B) and maximum (for C) Σ FIC and correspond to the FIC indices. Isobolograms were also constructed (graphs on the right hand) by plotting the concentrations of the two drugs showing the same effects as the effect at the MICs. Dashed lines represent the cutoffs of 0.5 and 4 for synergy and antagonism respectively.

the zero-interactive combination of 1 mg of drug A_1 ($= d_A$) and 1 mg of drug A_2 ($= d_B$) iso-effective with 2 mg of drug A_1 (D_A) or drug A_2 (D_B), the equation [5] is true.

The graphical representation of equation [5] is a straight line (additivity line) which in case of susceptibility tests connects the individual MIC of drug A with the individual MIC of drug B as well as all iso-effective combinations of the two drugs in a graph (isobologram) where the two axes are the concen-

trations of the two drugs arithmetically scaled. Synergy is indicated when the line which connects iso-effective concentrations (isobols) concave up (Fig. 2Aii) above the additivity line (Fig. 2Bii) and antagonism when the isobols concave down (Fig. 2Cii).

However, the validity of both theories is not undisputed. The equation of the drug actions with statistically defined events and their probabilities in Bliss independence theory is questioned particularly for complex systems like cells or populations of cells given

the high degree of integration and interaction. Therefore, it was suggested that Bliss independence should be applied only in simple systems like single enzymes and simple biochemical pathways. Furthermore, using the paradigm of the sham combination of two doses of the same drug, equation [1] holds only when the concentration-effect curves of the individual drugs follow log-linear pattern, otherwise paradoxical results are obtained (5, 7). On the other side, Loewe additivity implies that drugs act similarly at the same biochemical site, which is a rare phenomenon, or that the concentration-effect curves of the drugs are the same and therefore it should not be applied when two drugs have different concentration-effect curves. Since neither model can be invalidated based on mechanistic explanations in complex systems such as cells or populations of cells, both models are used to assess drug interactions (36).

Although various approaches have been used for assessing the in vitro interaction of antimicrobials, the most common approach in medical microbiology and particularly for antifungal drug interaction studies is the calculation of the fractional inhibitory concentration index (FIC_i). The FIC_i model is a Loewe additivity based model, which is described by the following equation:

$$\Sigma FIC = FIC_A + FIC_B = \frac{C_A^{comb}}{MIC_A^{alone}} + \frac{C_B^{comb}}{MIC_B^{alone}}$$

where C_A^{comb} and C_B^{comb} are the concentrations of the drugs A and B at the iso-effective combinations and MIC_A^{alone} and MIC_B^{alone} represent the concentrations of the drugs A and B when acting alone (41). Given that in antimicrobial susceptibility testing a two-fold dilution scheme is followed, combinations are assessed as synergistic when the $\Sigma FIC \leq 0.5$, additive when $\Sigma FIC > 0.5$ and ≤ 1 , indifferent when $\Sigma FIC > 1$ and ≤ 4 and antagonistic when $\Sigma FIC > 4$ (23) (Fig. 2). Among all ΣFIC s calculated for a data set, the FIC_i corresponds to the lowest ΣFIC when synergy is present or to the highest ΣFIC when antagonism is pre-sent and expresses the degree of bowing of the isobols.

The majority of in vitro antifungal combinations published in the literature were analyzed with this model. However, controversial results can be obtained depending on the parameters used to assess the antifungal interaction, even when the same methodology was employed. Factors such as the level of antifungal effect (MIC endpoint), the way of reading the MICs, the analysis of the results of individual data sets or replicates, experimental errors, and interpretation of FIC indices (FIC endpoints) can influence the final conclusions (62).

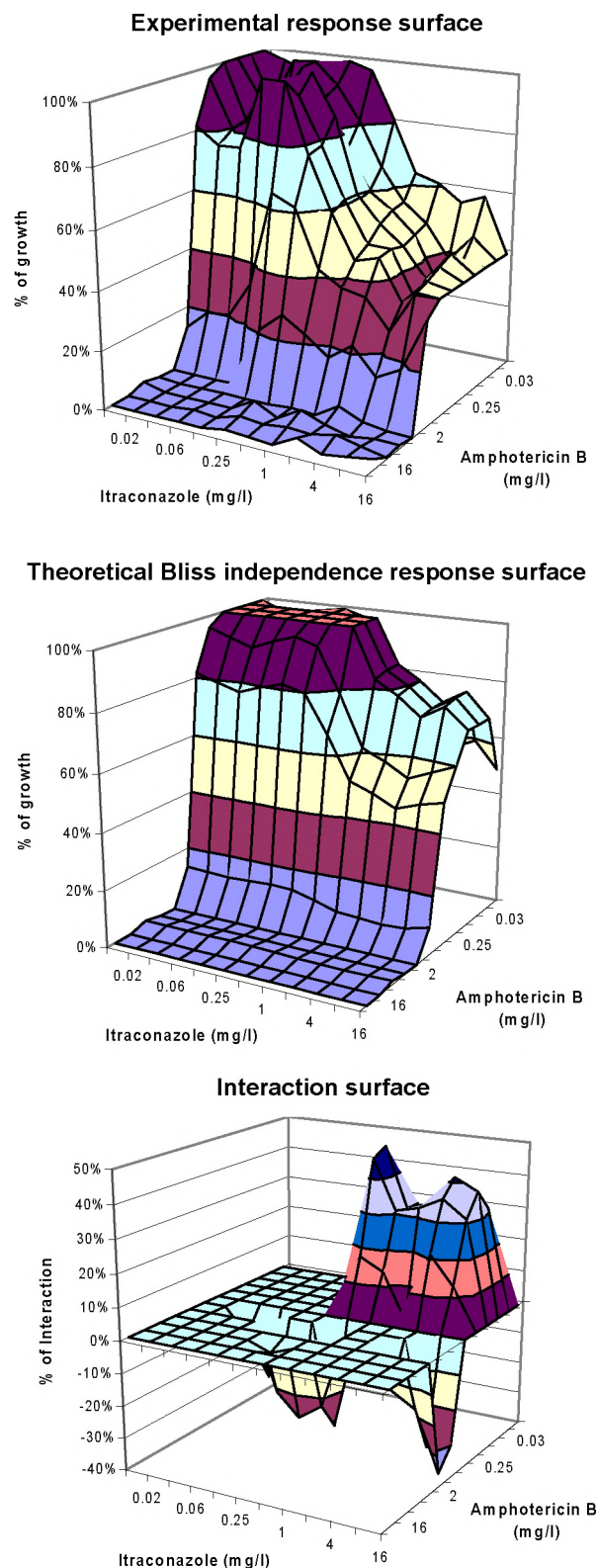


Figure 3. Three-dimensional analysis of interaction between amphotericin B and itraconazole based on the model of Prichard et al. (63). The subtraction of the experimental response surface from the theoretical Bliss independence response surface (the latter was calculated based on the concentration-effect relationships of the single drugs and the equation [1]) yields an interaction surface with a mosaic of statistically significant (as evaluated using replicates) synergistic and antagonistic combinations above and below the 0 plane (independent combinations), respectively.

Alternative models for assessing drug interactions have been developed based on response surface approaches that emphasize the three dimensional nature of drug interactions in contrast with the mono-dimensional FIC_i (9, 10, 31, 64, 74-76). With these approaches, the dependent variable such as the drug effect (i.e. measured % of growth) is related to any drug combination, thus generating a surface when this relationship is plotted three dimensionally (Fig. 3). This so called response surface is then compared with the zero interaction surface obtained based on the concentration-effect curves of the single drugs. Synergy is recognized when the experimental response surface is below the zero interaction surface and antagonism is recognized when the response surface is above the zero interaction surface. These approaches were further developed incorporating regression analysis for modeling the concentration-effect relationships and statistical analysis for the estimation of the significance of the departure from the zero interaction. Such a model is developed by Prichard et al. (62) based on the Bliss independence zero interaction theory. The observed effect (% of growth) of a particular combination of the two drugs is subtracted from the effect of the zero interaction, estimated for this combination, using equation [1] where E_A and E_B are the observed effects (or fitted effects, if regression analysis is used for modeling the concentration-effect curves) of the two drugs alone. This difference is calculated for all combinations of the two drugs and plotted three dimensionally where the volumes above and below the 0 plane (zero interaction) indicate the synergistic or antagonistic combinations, respectively. When replicates are performed the results can be evaluated statistically (64) (Fig. 3).

Modern approaches of drug interaction modeling relying on fully parametric response surface models that are fitted to the entire experimental response surface (Fig. 4). These models incorporate interaction parameters, which indicate both the nature and the intensity of the interaction for all combinations of two drugs over the concentration range of both drugs and importantly include the uncertainty of the estimates taking into account the variation of the data. Such a model is developed by Greco et al. (37) based on the Loewe additivity zero interaction theory and is described by the following equation:

$$1 = \frac{d_A}{IC_{50,A} \left(\frac{E}{E_{con}} - E \right)^{1/m_A}} + \frac{d_B}{IC_{50,B} \left(\frac{E}{E_{con}} - E \right)^{1/m_B}} + \alpha \frac{d_A d_B}{IC_{50,A} IC_{50,B} \left(\frac{E}{E_{con}} - E \right)^{0.5(1/m_A + 1/m_B)}} \quad [6]$$

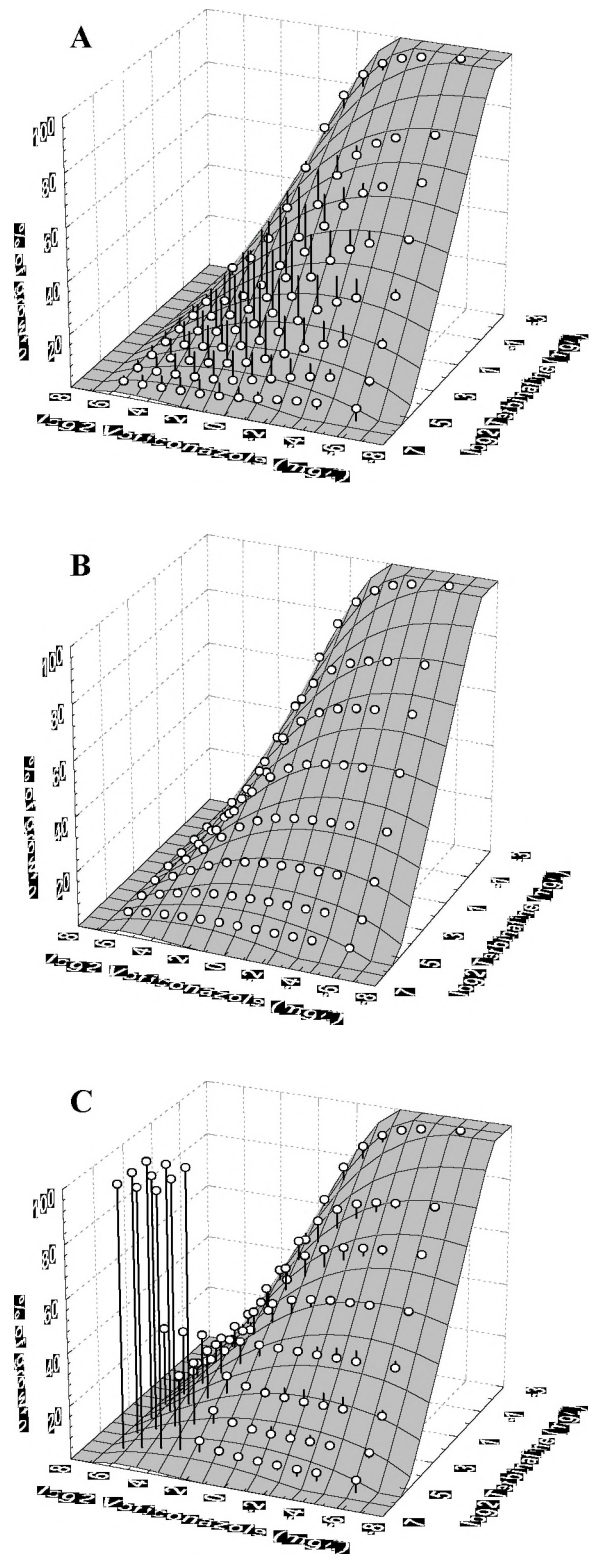


Figure 4. Modeling the interaction between voriconazole and terbinafine based on the fully parametric response surface model described by Greco et al. (37). The panels A, B, and C show the effect of the interaction parameter α relative to zero interaction response surface. In each of the three panels the gray surfaces represent the zero interaction response surfaces as obtained with the equation [6] using values for $E_{con}=100$, $IC_{50,A}=4$, $IC_{50,B}=4$, $m_A=-1$, $m_B=-1$. The white balls indicate the data obtained with $\alpha=50$ (synergy, panel A), $\alpha=0$ (no interaction, panel B) and $\alpha=-0.2$ (antagonism, panel C).

where d_A and d_B are the concentrations of drug A and drug B, respectively in a combination (independent variables), E is the percentage growth at this combination (dependent variable), $IC_{50,A}$ and $IC_{50,B}$ are the concentrations of the drug A and drug B result in 50% of the growth control E_{con} when acting alone and m_A and m_B are the slopes (Hill coefficients) of the E_{max} model [sigmoid curve that is described by the equation $E = E_{max} \times (D/IC_{50})^m / (1 + D/IC_{50})^m$]. The equation [6] is derived from equation [5] where D_A and D_B are obtained from the E_{max} model assuming that this model is an appropriate model of the concentration-effect curves of each drug alone. The third term in the right part of the equation [6] includes the interaction parameter α . In contrast with equation [5], which describes only additive interactions, equation [6] describes all types of interactions. The drug interaction is synergistic when α is positive, antagonistic when α is negative, and additive when α is 0. Equation [6] is not derived from a biological theory but is rather an empirical equation that often matches the shape of the response surface of experimental data. All estimates of the parameters of equation [6] are obtained with a measure of uncertainty, usually the 95% confidence interval deriving from the results of regression analysis. Moreover, by using the variation in measurement as input in the fitting procedure, the errors of the estimates are taken into account as well.

Fig. 5 represents a schematic diagram proposed as the general approach to assess the nature and the intensity of drug interactions (36). After choosing the most appropriate model (sigmoid, exponential, exponential with shoulder curve) to describe the concentration-effect curves of each drug alone (Step 1), and a data variation model (i.e. normal or poisson distribution) in order to take into account random variation caused for instance by biological variability or experimental errors (Step 2), the experimental data are compared with the predicted data of joint action from the zero interaction theory (left side of Fig. 5) or a full combined action model is fitted to all experimental data at once and interaction parameters are estimated (right side of Fig. 5). The FIC_i model and the responses surface approach developed by Prichard et al. (62) follows strategy on the strategy on left-hand side while the fully parametric model developed by Greco et al. (37) follows the strategy on the right-hand side.

1.3 OUTLINE OF THE THESIS

Given the great interest of combination therapy for treating invasive infections caused by filamentous fungi, objective and reliable analysis tools are required for assessing the in vitro interaction of antifungal drugs. However, before sophisticated and modern approaches

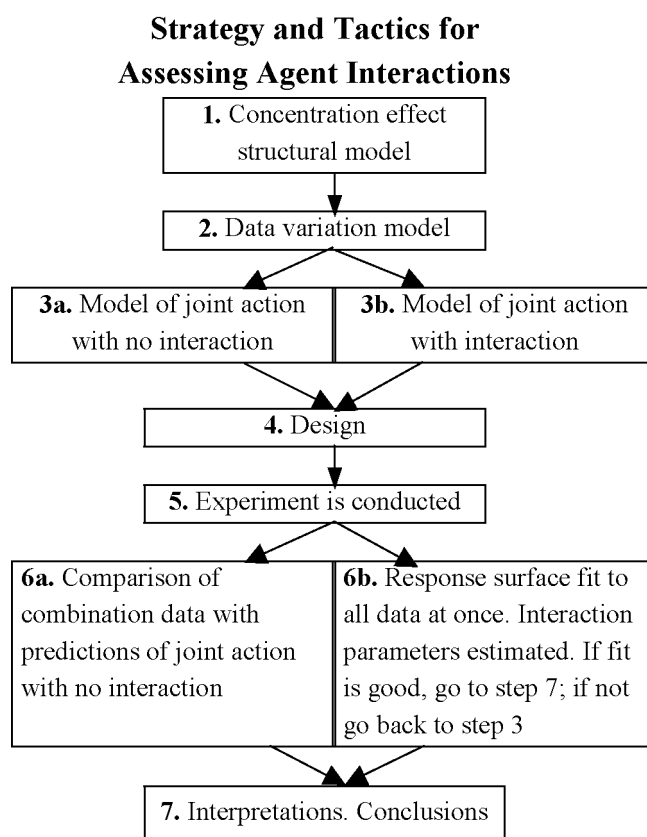


Figure 5. Schematic diagram of general approach to assessment of the nature and intensity of agent interactions, which include all specific approaches [adapted from Greco et al. (36)].

of drug interaction modeling can be applied to anti-fungal susceptibility testing of filamentous fungi, precise quantification of fungal growth and accurate estimation of antifungal effects are required. Due to the inability of the current proposed standard to determine these variables, further optimization is required.

Therefore, Chapter 2 is focused on different variables of AST of filamentous fungi. Since the nutrient medium is an important factor of susceptibility tests in this chapter different media were evaluated for the growth of various filamentous fungi. For this purpose a kinetic in vitro system was developed to monitor the growth of fungi and to describe the characteristics of their growth curves. In the remaining three studies, a spectrophotometric methodology and colorimetric assays based on tetrazolium salts are developed and optimized in order to overcome the limitations arising from the visual determination of the MICs and to provide detailed information of the concentration-effect relationships of antifungal drugs for filamentous fungi.

These methods were then used in Chapter 3 for the assessment of in vitro interaction of antifungal drugs for various fungi. Data were analyzed based on

conventional and modern approaches of drug interaction modeling using two different zero interaction theories. Thus, in vitro combinations were assessed with the standard approach of the FIC index model. Response surface modeling was applied and interactions were evaluated with fully parametric models incorporating modern concepts of statistical and non-linear regression analysis.

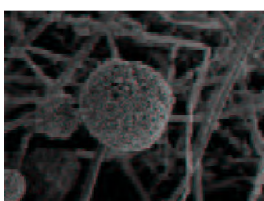
Finally, in Chapter 4, after summarizing the highlights of this thesis as described in the previous chapters, the future perspectives of antifungal susceptibility testing and drug interaction modeling together with their applications are explored and new directions in these fields are addressed.

REFERENCES

1. **Altman, F. P.** 1976. Tetrazolium salts and formazans. Progress in histochemistry and cytochemistry **9**:1-56.
2. **Andes, D., T. Stamsted, and R. Conklin.** 2001. Pharmacodynamics of amphotericin B in a neutropenic-mouse disseminated-candidiasis model. Antimicrob. Agents Chemother. **45**:922-926.
3. **Arikan, S., M. Lozano-Chiu, V. Paetznick, S. Nangia, and J. H. Rex.** 1999. Microdilution susceptibility testing of amphotericin B, itraconazole, and voriconazole against clinical isolates of *Aspergillus* and *Fusarium* species. J. Clin. Microbiol. **37**:3946-3951.
4. **Bartizal, K., T. Scott, G. K. Abruzzo, C. J. Gill, C. Pacholok, L. Lynch, and H. Kropp.** 1995. In vitro evaluation of the pneumocandin antifungal agent L-733560, a new water-soluble hybrid of L-705589 and L-731373. Antimicrob. Agents Chemother. **39**:1070-1076.
5. **Berenbaum, M. C.** 1981. Criteria for analyzing interactions between biologically active agents. Adv. Cancer Res. **35**:269-335.
6. **Berenbaum, M. C.** 1977. Synergy, additivism and antagonism in immunosuppression. A critical review. Clin. Exp. Immunol. **28**:1-18.
7. **Berenbaum, M. C.** 1989. What is synergy? Pharmacol. Rev. **41**:93-141.
8. **Breckenridge, A.** 1992. Clinical significance of interactions with antifungal agents. Br. J. Dermatol. **126**(Suppl. 39):19-22.
9. **Carter, W. H., Jr.** 1995. Relating isobolograms to response surfaces. Toxicology **105**:181-188.
10. **Carter, W. H., Jr., and G. L. Wampler.** 1986. Review of the application of response surface methodology in the combination therapy of cancer. Cancer Treat. Rep. **70**:133-140.
11. **Chou, T. C., and P. Talalay.** 1981. Generalized equations for the analysis of inhibitions of Michaelis-Menten and higher-order kinetic systems with two or more mutually exclusive and nonexclusive inhibitors. Eur. J. Biochem. **115**:207-216.
12. **Chou, T. C., and P. Talalay.** 1984. Quantitative analysis of dose-effect relationships: the combined effects of multiple drugs or enzyme inhibitors. Adv. Enzyme Regul. **22**:27-55.
13. **Clancy, C. J., Y. C. Yu, A. Lewin, and M. H. Nguyen.** 1998. Inhibition of RNA synthesis as a therapeutic strategy against *Aspergillus* and *Fusarium*: demonstration of in vitro synergy between rifabutin and amphotericin B. Antimicrob. Agents Chemother. **42**:509-513.
14. **Cormican, M. G., and M. A. Pfaller.** 1996. Standardization of antifungal susceptibility testing. J. Antimicrob. Chemother. **38**:561-578.
15. **Cuenca-Estrella, M., and J. L. Rodriguez-Tudela.** 2001. Present status of the detection of antifungal resistance: the perspective from both sides of the ocean. Clin. Microbiol. Infect. **7**:46-53.
16. **de Bock, R.** 1994. Epidemiology of invasive fungal infections in bone marrow transplantation. EORTC Invasive Fungal Infections Cooperative Group. Bone Marrow Transplant. **14**(Suppl 5):1-2.
17. **Delhaes, L., J. E. Lazaro, F. Gay, M. Thellier, and M. Danis.** 1999. The microculture tetrazolium assay (MTA): another colorimetric method of testing *Plasmodium falciparum* chemosensitivity. Ann. Trop. Med. Parasitol. **93**:31-40.
18. **den Hollander, J. G., J. W. Mouton, and H. A. Verbrugh.** 1998. Use of pharmacodynamic parameters to predict efficacy of combination therapy by using fractional inhibitory concentration kinetics. Antimicrob. Agents Chemother. **42**:744-748.
19. **Denning, D. W., A. Marinus, J. Cohen, D. Spence, R. Herbrecht, L. Pagano, C. Kibbler, V. Kermery, F. Offner, C. Cordonnier, U. Jehn, M. Ellis, L. Collette, and R. Sylvester.** 1998. An EORTC multicentre prospective survey of invasive aspergillosis in hematological patients: diagnosis and therapeutic outcome. EORTC Invasive Fungal Infections Cooperative Group. J. Infect. **37**:173-180.
20. **Denning, D. W., S. A. Radford, K. L. Oakley, L. Hall, E. M. Johnson, and D. W. Warnock.** 1997. Correlation between in-vitro susceptibility testing to itraconazole and in-vivo outcome of *Aspergillus fumigatus* infection. J. Antimicrob. Chemother. **40**:401-414.
21. **Denning, D. W., and D. A. Stevens.** 1990. Antifungal and surgical treatment of invasive aspergillosis: review of 2,121 published cases. Rev. Infect. Dis. **12**:1147-1201.
22. **Drusano, G. L., S. L. Preston, C. Hardalo, R. Hare, C. Banfield, D. Andes, O. Vesga, and W. A. Craig.** 2001. Use of preclinical data for selection of a phase II/III dose for evernimicin and identification of a preclinical MIC breakpoint. Antimicrob. Agents Chemother. **45**:13-22.
23. **Elliopoulou** 1993. Antimicrobial combinations, p. 432-492. In V. Lorian (ed.), Antibiotics in Laboratory Medicine, 3rd ed., The Williams and Wilkins Co., Baltimore.
24. **Espinel-Ingroff, A., F. Barchiesi, K. C. Hazen, J. V. Martinez-Suarez, and G. Scalise.** 1998. Standardization of antifungal susceptibility testing and clinical relevance. Med. Mycol. **36**:68-78.
25. **Espinel-Ingroff, A., M. Bartlett, R. Bowden, N. X. Chin, C. Cooper Jr, A. Fothergill, M. R. McGinnis, P. Menezes, S. A. Messer, P. W. Nelson, F. C. Odds, L. Pasarell, J. Peter, M. A. Pfaller, J. H. Rex, M. G. Rinaldi, G. S. Shankland, T. J. Walsh, and I. Weitzman.** 1997. Multicenter evaluation of proposed standar-

- dized procedure for antifungal susceptibility testing of filamentous fungi. *J. Clin. Microbiol.* **35**:139-143.
26. **Espinel-Ingroff, A., K. Dawson, M. Pfaller, E. Anaissie, B. Breslin, D. Dixon, A. Fothergill, V. Paetznick, J. Peter, M. Rinaldi, and T. Walsh.** 1995. Comparative and collaborative evaluation of standardization of antifungal susceptibility testing for filamentous fungi. *Antimicrob. Agents Chemother.* **39**:314-319.
 27. **Espinel-Ingroff, A., and T. M. Kerkering.** 1991. Spectrophotometric method of inoculum preparation for the in vitro susceptibility testing of filamentous fungi. *J. Clin. Microbiol.* **29**:393-394.
 28. **Fridkin, S. K., and W. R. Jarvis.** 1996. Epidemiology of nosocomial fungal infections. *Clin. Microbiol. Rev.* **9**:499-511.
 29. **Gattringer, R., M. Niks, R. Ostertag, K. Schwarz, H. Medvedovic, W. Graninger, and A. Georgopoulos.** 2002. Evaluation of MIDITECH automated colorimetric MIC reading for antimicrobial susceptibility testing. *J. Antimicrob. Chemother.* **49**:651-659.
 30. **Gehrt, A., J. Peter, P. A. Pizzo, and T. J. Walsh.** 1995. Effect of increasing inoculum sizes of pathogenic filamentous fungi on MICs of antifungal agents by broth microdilution method. *J. Clin. Microbiol.* **33**:1302-1307.
 31. **Gennings, C., W. H. Carter, Jr., E. D. Campbell, J. G. Staniswalis, T. J. Martin, B. R. Martin, and K. L. White, Jr.** 1990. Isobolographic characterization of drug interactions incorporating biological variability. *J. Pharmacol. Exp. Ther.* **252**:208-217.
 32. **Ghannoum, M. A., A. S. Ibrahim, Y. Fu, M. C. Shafiq, J. E. Edwards, Jr., and R. S. Criddle.** 1992. Susceptibility testing of *Cryptococcus neoformans*: a microdilution technique. *J. Clin. Microbiol.* **30**:2881-2886.
 33. **Ghannoum, M. A., and L. B. Rice.** 1999. Antifungal agents: mode of action, mechanisms of resistance, and correlation of these mechanisms with bacterial resistance. *Clin. Microbiol. Rev.* **12**:501-517.
 34. **Graybill, J. R.** 1992. Future directions of antifungal chemotherapy. *Clin. Infect. Dis.* **14**(Suppl. 1):170-181.
 35. **Graybill, J. R.** 1996. The future of antifungal therapy. *Clin. Infect. Dis.* **22**(Suppl 2):166-178.
 36. **Greco, W. R., G. Bravo, and J. C. Parsons.** 1995. The search for synergy: a critical review from a response surface perspective. *Pharmacol. Rev.* **47**:331-385.
 37. **Greco, W. R., H. S. Park, and Y. M. Rustum.** 1990. Application of a new approach for the quantitation of drug synergism to the combination of cis-diamminedichloroplatinum and 1-beta-D-arabinofuranosylcytosine. *Cancer Res.* **50**:5318-5327.
 38. **Guarro, J., C. Llop, C. Aguilar, and I. Pujol.** 1997. Comparison of in vitro antifungal susceptibilities of conidia and hyphae of filamentous fungi. *Antimicrob. Agents Chemother.* **41**:2760-2762.
 39. **Gupta, A. K., H. I. Katz, and N. H. Shear.** 1999. Drug interactions with itraconazole, fluconazole, and terbinafine and their management. *J. Am. Acad. Dermatol.* **41**:237-249.
 40. **Hawser SP, H. Norris, C. J. Jessup, and M. A. Ghannoum.** 1998. Comparison of a 2,3-bis(2-methoxy-4-nitro-5-sulfophenyl)-5-(phenylamino) carbonyl]-2H-tetrazolium hydroxide (XTT) colorimetric method with the standardized National Committee for Clinical Laboratory Standards method of testing clinical yeast isolates for susceptibility to antifungal agents. *J. Clin. Microbiol.* **36**:1450-1452.
 41. **Hindler, J.** 1995. Antimicrobial susceptibility testing, p. 5.18.11-15.18.20. In H. D. Isenberg (ed.), *Clinical Microbiology Procedures Handbook*, Washington, D. C.
 42. **Horsburgh, C. R., Jr., S. Feldman, and R. Ridzon.** 2000. Practice guidelines for the treatment of tuberculosis. *Clin. Infect. Dis.* **31**:633-639.
 43. **Jankel, C. A., and L. K. Fitterman.** 1993. Epidemiology of drug-drug interactions as a cause of hospital admissions. *Drug Saf.* **9**:51-59.
 44. **Jankel, C. A., and S. M. Speedie.** 1990. Detecting drug interactions: a review of the literature. *DICP.* **24**:982-989.
 45. **Jellinger, R. M., R. W. Shafer, and T. C. Merigan.** 1997. A novel approach to assessing the drug susceptibility and replication of human immunodeficiency virus type 1 isolates. *J. Infect. Dis.* **175**:561-566.
 46. **Johnson, E. M., K. L. Oakley, S. A. Radford, C. B. Moore, P. Warn, D. W. Warnock, and D. W. Denning.** 2000. Lack of correlation of in vitro amphotericin B susceptibility testing with outcome in a murine model of *Aspergillus* infection. *J. Antimicrob. Chemother.* **45**:85-93.
 47. **Kauffman, C. A., and P. L. Carver.** 1997. Antifungal agents in the 1990s. Current status and future developments. *Drugs* **53**:539-549.
 48. **Kontoyiannis, D. P., R. E. Lewis, N. Sagar, G. May, R. A. Prince, and K. V. Rolston.** 2000. Itra-conazole-amphotericin B antagonism in *Aspergillus fumigatus*: an Etest-based strategy. *Antimicrob. Agents Chemother.* **44**:2915-2918.
 49. **Kontoyiannis, D. P., and R. E. Lewis.** 2002. Antifungal drug resistance of pathogenic fungi. *Lancet* **359**:1135-1144.
 50. **Lewis, R. E., D. J. Diekema, S. A. Messer, M. A. Pfaller, and M. E. Klepser.** 2002. Comparison of Etest, checkerboard dilution and time-kill studies for the detection of synergy or antagonism between antifungal agents tested against *Candida* species. *J. Antimicrob. Chemother.* **49**:345-351.
 51. **Llop, C., I. Pujol, C. Aguilar, J. Sala, D. Riba, and J. Guarro.** 2000. Comparison of three methods of determining MICs for filamentous fungi using different end point criteria and incubation periods. *Antimicrob. Agents Chemother.* **44**:239-242.
 52. **Macgregor, A. G.** 1965. Clinical effects of interaction between drugs. Review of points at which drugs can interact. *Proc. R. Soc. Med.* **58**:943-946.
 53. **Maesaki, S., S. Kohno, M. Kaku, H. Koga, and K. Hara.** 1994. Effects of antifungal agent combinations administered simultaneously and sequentially against *Aspergillus fumigatus*. *Antimicrob. Agents Chemother.* **38**:2843-2845.
 54. **Moore, C. B., N. Sayers, J. Mosquera, J. Slaven, and D. W. Denning.** 2000. Antifungal drug resistance in *Aspergillus*. *J. Infect.* **41**:203-220.
 55. **NCCLS** 1998. Reference method for broth dilution antifungal susceptibility testing of conidium-forming

- filamentous fungi; proposed standard. Document M-38P. National Committee for Clinical Laboratory Standards, Wayne, Pa.
56. **Odds, F. C.** 1982. Interactions among amphotericin B, 5-fluorocytosine, ketoconazole, and miconazole against pathogenic fungi in vitro. *Antimicrob. Agents Chemother.* **22**:763-770.
 57. **Paterson, D. L., and N. Singh.** 1999. Invasive aspergillosis in transplant recipients. *Medicine (Baltimore)* **78**:123-138.
 58. **Perfect, J. R., and W. A. Schell.** 1996. The new fungal opportunists are coming. *Clin. Infect. Dis.* **22**(Suppl. 2):112-118.
 59. **Petrikkou, E., J. L. Rodriguez-Tudela, M. Cuenca-Estrella, A. Gomez, A. Molleja, and E. Mellado.** 2001. Inoculum standardization for antifungal susceptibility testing of filamentous fungi pathogenic for humans. *J. Clin. Microbiol.* **39**:1345-1347.
 60. **Polak, A.** 1993. Combination of amorolfine with various antifungal drugs in dermatophytosis. *Mycoses* **36**:43-49.
 61. **Polak, A.** 1998. Experimental models in antifungal chemotherapy. *Mycoses* **41**:1-30.
 62. **Polak, A.** 1999. The past, present and future of antimycotic combination therapy. *Mycoses* **42**:355-370.
 63. **Prichard, M. N., L. E. Prichard, W. A. Baguley, M. R. Nassiri, and C. Shipman, Jr.** 1991. Three-dimensional analysis of the synergistic cytotoxicity of ganciclovir and zidovudine. *Antimicrob. Agents Chemother.* **35**:1060-1065.
 64. **Prichard, M. N., and C. Shipman, Jr.** 1990. A three-dimensional model to analyze drug-drug interactions. *Antiviral Res.* **14**:181-205.
 65. **Pujol, I., J. Guarro, C. Llop, L. Soler, and J. Fernandez-Ballart.** 1996. Comparison study of broth macrodilution and microdilution antifungal susceptibility tests for the filamentous fungi. *Antimicrob. Agents Chemother.* **40**:2106-2110.
 66. **Pujol, I., J. Guarro, J. Sala, and M. D. Riba.** 1997. Effects of incubation temperature, inoculum size, and time of reading on broth microdilution susceptibility test results for amphotericin B against *Fusarium*. *Antimicrob. Agents Chemother.* **41**:808-811.
 67. **Rambali, B., J. A. Fernandez, L. Van Nuffel, F. Woestenborghs, L. Baert, D. L. Massart, and F. C. Odds.** 2001. Susceptibility testing of pathogenic fungi with itraconazole: a process analysis of test variables. *J. Antimicrob. Chemother.* **48**:163-177.
 68. **Rex, J. H., C. R. Cooper, Jr., W. G. Merz, J. N. Galgiani, and E. J. Anaissie.** 1995. Detection of amphotericin B-resistant *Candida* isolates in a broth-based system. *Antimicrob. Agents Chemother.* **39**:906-909.
 69. **Rex, J. H., M. A. Pfaller, M. G. Rinaldi, A. Polak, and J. N. Galgiani.** 1993. Antifungal susceptibility testing. *Clin. Microbiol. Rev.* **6**:367-381.
 70. **Rex, J. H., M. A. Pfaller, T. J. Walsh, V. Chaturvedi, A. Espinel-Ingroff, M. A. Ghan-noum, L. L. Gosey, F. C. Odds, M. G. Rinaldi, D. J. Sheehan, and D. W. Warnock.** 2001. Antifungal susceptibility testing: practical aspects and current challenges. *Clin. Microbiol. Rev.* **14**:643-658.
 71. **Richardson, M. D., and D. W. Warnock** 1997. Fungi as human pathogens, p. 2-8, *Fungal infection. Diagnosis and management*. 2nd ed., Blackwell Science Ltd.
 72. **Ryder, N. S., and I. Leitner.** 2001. Synergistic interaction of terbinafine with triazoles or amphotericin B against *Aspergillus* species. *Med. Mycol.* **39**:91-95.
 73. **Scudiero, D. A., R. H. Shoemaker, K. D. Paull, A. Monks, S. Tierney, T. H. Nofziger, M. J. Currens, D. Seniff, and M. R. Boyd.** 1988. Evaluation of a soluble tetrazolium/formazan assay for cell growth and drug sensitivity in culture using human and other tumor cell lines. *Cancer Res.* **48**:4827-33.
 74. **Suhnel, J.** 1992. Re: W. R. Greco et al., Application of a new approach for the quantitation of drug synergism to the combination of cis-diammine-dichloroplatinum and 1-beta-D-arabinofuranosyl-cytosine. *Cancer Res.*, **50**:5318-5327, 1990. *Cancer Res.* **52**:4560-4561.
 75. **Suhnel, J.** 1992. Zero interaction response surfaces, interaction functions and difference response surfaces for combinations of biologically active agents. *Arzneimittelforschung* **42**:1251-1258.
 76. **Unkelbach, H. D., and T. Wolf.** 1984. Drug combinations-concepts and terminology. *Arzneimittelforschung* **34**:935-938.
 77. **Vartivarian, S. E., E. J. Anaissie, and G. P. Bodey.** 1993. Emerging fungal pathogens in immunocompromised patients: classification, diagnosis, and management. *Clin. Infect. Dis.* **17**(Suppl. 2):487-491.
 78. **Viscoli, C., and E. Castagnola.** 1998. Emerging fungal pathogens, drug resistance and the role of lipid formulations of amphotericin B in the treatment of fungal infections in cancer patients: a review. *Int. J. Infect. Dis.* **3**:109-118.
 79. **Warnock, D. W.** 1998. Fungal infections in neutropenia: current problems and chemotherapeutic control. *J. Antimicrob. Chemother.* **41**(Suppl. D):95-105.
 80. **Webb, J. L.** 1963. Effect of more than one inhibitor, p. 66-79 & 487-512, *Enzymes and metabolic inhibitors*, vol. 1. Academic Press, New York.
 81. **White, T. C., K. A. Marr, and R. A. Bowden.** 1998. Clinical, cellular, and molecular factors that contribute to antifungal drug resistance. *Clin. Microbiol. Rev.* **11**:382-402.



CHAPTER

2

IN VITRO SUSCEPTIBILITY TESTING OF FILAMENTOUS FUNGI

- Analysis of growth characteristics of filamentous fungi in different nutrient media
- Comparison of NCCLS and 3-(4,5-dimethyl-2-thiazyl)-2,5-diphenyl-2H-tetrazolium bromide (MTT) methods of in vitro susceptibility testing of filamentous fungi and development of a new simplified method
- Colorimetric assay for antifungal susceptibility testing of *Aspergillus* species
- Comparison of spectrophotometric and visual readings of NCCLS method and evaluation of a colorimetric method based on reduction of a soluble tetrazolium salt 2,3-bis{2-methoxy-4-nitro-5-[(sulphenylamino) carbonyl]-2H-tetrazolium hydroxide} for antifungal susceptibility testing of *Aspergillus* species

Chapter 2.1

Analysis of Growth Characteristics of Filamentous Fungi in Different Nutrient Media

Journal of Clinical Microbiology 2001; 39: 478-484

ANALYSIS OF GROWTH CHARACTERISTICS OF FILAMENTOUS FUNGI IN DIFFERENT NUTRIENT MEDIA

JOSEPH MELETIADIS¹, JACQUES F. G. M. MEIS^{1,2}, JOHAN W. MOUTON², AND PAUL E. VERWEIJ¹

Department of Medical Microbiology, University Medical Center Nijmegen¹, and Department of Medical Microbiology and Infectious Diseases, Canisius-Wilhelmina Hospital², Nijmegen, The Netherlands

A microbroth kinetic model based on turbidity measurements was developed in order to analyze the growth characteristics of three species of filamentous fungi (*Rhizopus microsporus*, *Aspergillus fumigatus*, and *Scedosporium prolificans*) characterized by different growth rates in five nutrient media (antibiotic medium 3, yeast nitrogen base medium, Sabouraud broth, RPMI 1640 alone, and RPMI 1640 with 2% glucose). In general, five distinct phases in the growth of filamentous fungi could be distinguished, namely, the lag phase, the first transition period, the log phase, the second transition period, and the stationary phase. The growth curves were smooth and were characterized by the presence of long transition periods. Among the different growth phases distinguished, the smallest variability in growth rates among the strains of each species was found during the log phase in all nutrient media. The different growth phases of filamentous fungi were barely distinguishable in RPMI 1640, in which the poorest growth was observed for all fungi even when the medium was supplemented with 2% glucose. *R. microsporus* and *A. fumigatus* grew better in Sabouraud and yeast nitrogen base medium than in RPMI 1640, with growth rates three to four times higher. None of the media provided optimal growth of *S. prolificans*. The germination of *Rhizopus* spores and *Aspergillus* and *Scedosporium* conidia commenced after 2 and 5 h of incubation, respectively. The elongation rates ranged from 39.6 to 26.7, 25.4 to 20.2, and 16.9 to 9.9 $\mu\text{m/h}$ for *Rhizopus*, *Aspergillus*, and *Scedosporium* hyphae, respectively. The germination of conidia and spores and the elongation rates of hyphae were enhanced in antibiotic medium 3 and delayed in yeast nitrogen base medium. In conclusion, the growth curves provide a useful tool to gain insight into the growth characteristics of filamentous fungi in different nutrient media and may help to optimize the methodology for antifungal susceptibility testing.

In vitro susceptibility testing of filamentous fungi is becoming increasingly important because of the frequency and diversity of infections caused by them (24, 31, 37). In addition, more antifungal agents have been introduced for clinical use and other new drugs are undergoing clinical evaluation (34). Hence, standardized in vitro susceptibility tests that give reproducible results, predict the resistance of moulds, and correlate with clinical outcome are required (2, 3, 9). Better inter- and intralaboratory agreement has been achieved by standardizing various factors involved in testing filamentous fungi for their susceptibilities such as the inoculum preparation, the incubation conditions (time and temperature), the MIC determination (reading time and end points), and the nutrient medium (4, 5, 18, 27).

The influence of medium on antifungal susceptibility tests of yeasts is well established (3, 11, 15, 25, 28). Although there is no consensus as to the optimal nutrient medium, by definition the nutrient medium must be able to support adequate growth of the fungus without interfering with the action of the antifungal agents and must result in reproducible results that have clinical value (19). Many studies have shown

that synthetic medium RPMI 1640 gives reproducible results for the in vitro testing of the susceptibility of yeasts to various antifungal drugs (25, 28). This medium was also selected by the Subcommittee for Antifungal Susceptibility Testing of the National Committee for Clinical Laboratory Standards (NCCLS) for the in vitro susceptibility testing of conidium-forming filamentous fungi (23) although there was no evidence that this medium was suitable for filamentous fungi (3). RPMI 1640 has a number of advantages (28), but its suitability for the susceptibility testing of nonfermentative yeasts such as *Cryptococcus neoformans* has been questioned (10, 15, 33, 35). Therefore, the appropriateness of this medium for filamentous fungi should not be implicitly postulated.

Given the greater variability in the growth rate, mechanisms of sporulation, and nutrient requirements among the filamentous fungi than among yeasts, growth characteristics of moulds in relation to the medium should be studied in detail. Due to the filamentous and non-homogenous growth of moulds, the analysis of growth characteristics by growth curves is difficult. In the present study we developed a microbroth kinetic system in order to investigate the growth characteristics

of filamentous fungi in different nutrient media. Such a system would help to select the medium that optimally supports the growth of these fungi and to establish the optimal reading time of susceptibility testing of filamentous fungi.

MATERIALS AND METHODS

Isolates. Fifteen clinical isolates of filamentous fungi belonging to three species were selected based on their growth rates. *Rhizopus microsporus* var. *rhizopodiformis* was chosen as representative of fast-growing moulds, *Aspergillus fumigatus* was chosen as intermediate in growth rate, and *Scedosporium prolificans* was chosen as representative of slow-growing fungi. For each species five strains from our private collection were tested: *R. microsporus* var. *rhizopodiformis*, AZN190, AZN410, AZN5816, AZN5805, and AZN1185; *A. fumigatus*, AZN9618, AZN9619, AZN9620, AZN9621, and AZN9625; *S. prolificans*, AZN7898, AZN7901, AZN7902, AZN7906, and AZN7918.

Isolates had been frozen in 50% glycerol at -70°C and were revived by subculturing onto Sabouraud glucose agar (SGA) tubes supplemented with 0.5% chloramphenicol and incubated at 29°C for 7 days. The isolates were subcultured again on SGA tubes and incubated for another 5 to 7 days at 37°C .

Nutrient media. The following five nutrient media were used: RPMI 1640 medium with L-glutamine but without bicarbonate (GIBCO BRL, Life Technologies, Woerden, The Netherlands) prepared alone (RPMI) or supplemented with 2% glucose (RPMI+); yeast nitrogen base (YNB; Difco Laboratories, Amsterdam, The Netherlands); antibiotic medium 3 (AM3; Oxoid, Hampshire, United Kingdom), and Sabouraud broth (SAB; Oxoid).

All media were prepared according to the manufacturer's instructions and buffered to pH 7.0 with 0.165 M 3-N-morpholinopropanesulfonic acid (MOPS) (Sigma-Aldrich Chemie GmbH, Steinheim, Germany). Double-strength media were prepared and sterilized by filtration (RPMI, RPMI+, and YNB) or by autoclavation (SAB and AM3).

Growth curves. Conidia and spores were collected using a cotton swab from 7- to 10-day-old cultures and suspended in 0.1% Tween 80. The suspensions were adjusted to 2×10^4 spores/ml by counting the cells in a hemacytometer cell counting chamber. Viability was confirmed by plating serial dilutions on SGA plates. One hundred microliters of each suspension containing 0.1% Tween 80 was inoculated into 100 μl of double-strength medium in 96-well flat-bottom microtitration plates. Tween 80 was used in order to prevent the growth of fungi on the surfaces of the media inside the wells. The plates were sealed and incubated at 37°C for 100 h inside a plate reader (Rosys Anthos ht3; Anthos Labtec Instruments GmbH, Salzburg, Austria). The optical density (OD) at 405 nm was recorded for each well automatically every 15 min without shaking. The reader can detect changes of 0.001 in OD. Sequential OD measurements were used to generate growth curves for each fungus and medium in triplicate. All studies were conducted two times.

Microscopic examination. In order to correlate OD changes with the morphology of the fungi, conidia and spores were observed microscopically in microtitration plates by a reverse microscope at hourly intervals. At each time point, 100 conidia and spores were counted and the percentage of germination in each medium was estimated in triplicate. The lengths of hyphae formed by 15 germinated conidia or spores were measured, and the average length was calculated in triplicate. Furthermore, the change in hyphal length over time was computed as $(\text{average length at } t_2 - \text{average length at } t_1) / (t_2 - t_1)$, where t_1 and t_2 are the times at the beginning and end of the measurement period, respectively. The mean elongation rate was calculated by averaging the changes during sequential time periods of the growth.

Kinetic parameters. In order to compare the growth curves for each species in the five different nutrient media, various parameters were calculated based on the changes of the OD over time using the MicroWin, version 3, software (Mikrotek Laborsysteme GmbH, Overath, Germany). From the growth curve of each strain in each of the media the following parameters were calculated: the highest OD (OD_{max}), the average of all changes in OD (ΔOD) per minute, where $\Delta\text{OD} = \text{OD}_{\text{final}} - \text{OD}_{\text{initial}}$ in an interval of 15 min, the overall slope S obtained by linear regression analysis, and the maximal slope (S_{max}), which was the largest increase rate in OD repeated for 25 consecutive time points. Furthermore the following time-related parameters were recorded: the time of first detectable OD change, the time when 90% of the OD_{max} was reached (OD_{90}), and the time at which S_{max} of the growth curve was reached.

In addition, the S values for the growth curves were calculated and were used as estimates of the growth rates of the species in each nutrient medium. To visualize small changes in the growth rates during the growth curve and to determine the time point after which the growth rate changed significantly, a calculation model based on the area under the kinetic curve (AUKC) was developed. With this model the relative AUKC (rAUKC) was estimated by dividing each AUKC for each time point every 3 h by the corresponding time period. The changes in rAUKC, ΔrAUKC , were calculated for each time point by subtracting the rAUKC for each time point from the corresponding rAUKC of the previous time point. The ΔrAUKC is an estimate of changes in the slope of the growth curve and thus an estimate of the growth rate of fungus. When the ΔrAUKC value increases linearly over time, the OD increases with a constant rate, and when the ΔrAUKC value decreases or goes to zero over time, the growth rate decreases or goes to zero, respectively. Thus, increasing ΔrAUKC values corresponded to high growth rates. The ΔrAUKC values were used in order to distinguish different phases in the growth of filamentous fungi and the time employed for each phase.

RESULTS

A total of 225 growth curves based on 90,000 time points were obtained. The shapes of the growth curves were different depending on the nutrient medium used and the species tested (Fig. 1A, 2A, and

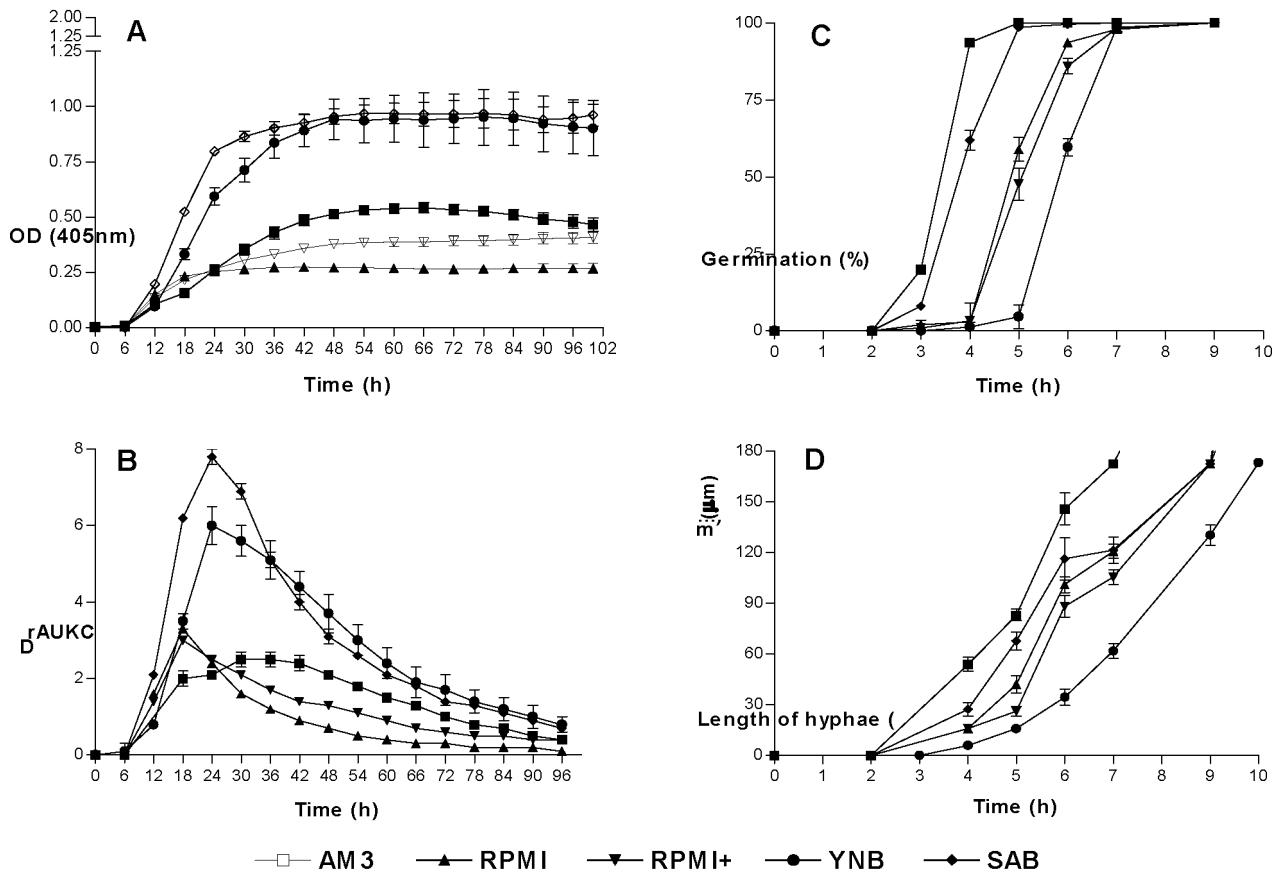


Figure 1. Graphical representation of the growth of *R. microsporus* var. *rhizopodiformis* in five nutrient media. (A) Changes in OD over time. (B) Changes in Δ AUKC over time. (C) Percentages of germination of conidia over time. (D) Extension of hyphae over time. Bars, SE.

3A). However they were very reproducible among the replicates and the strains tested. Since the results of the two experiments were similar, the data of the first experiment were used for analysis.

The growth curves were fragmented and were analyzed. In general the following phases in the growth of each of the tested genera could be distinguished based on OD changes and Δ AUKC values (Table 1). The first phase was the lag phase in which no changes in OD were measured and the Δ AUKC values were lower than 5% of the maximal Δ AUKC. Microscopic examination revealed that during this phase germination of spores and conidia took place followed by elongation of hyphae to a maximal length of 60 μ m (Fig. 1D, 2D, and 3D).

Further elongation of hyphae was detected spectrophotometrically and resulted in a rapid increase in OD (first transition period) until 30% of the maximal Δ AUKC was reached. After this phase, the Δ AUKC increased and the growth curve reached the maximal slope, the maximal Δ AUKC (log phase). Afterwards a second transition period, in which the slope of the growth curve decreased continuously until the Δ AUKC reached 70% of its maximum and the OD tended to reach a plateau, was apparent (second transition period).

The last phase was the stationary phase, where no changes in OD or negative slopes of the growth curve were observed and where values for Δ AUKC were lower than 70% of the maximum Δ AUKC (Fig. 1A and B, 2A and B, and 3A and B).

R. microsporus. The strains of *R. microsporus* var. *rhizopodiformis* showed the shortest lag phase, with the first significant change in OD after 4.8 to 6.5 h of incubation at 37°C, and the OD₉₀ for the five strains ranged between 20 and 40 h (Table 2). The OD₉₀ was reached earlier (after 20 h) when RPMI was used as the nutrient medium; however in this medium the growth rate was very low, with an OD_{max} of 0.29 and a slope of 0.61×10^{-4} (Table 2). Supplementation of RPMI with 2% glucose resulted in a slight increase of the growth rate of the fungus. By contrast the growth rates in SAB and YNB media were the highest, with OD_{max}s of 1.01 and 1.02 and slopes of 2.28×10^{-4} and 2.17×10^{-4} , respectively. The S_{max}s in these media were observed after 15.75 and 18.60 h, respectively. After 66 h of incubation a decrease in the OD was observed in AM3 but not in the other media (Fig. 1A). The microscopical observations showed that the germination of spores started after 2 h in AM3 and SAB, after 4 h in RPMI and RPMI+, and after 5 h in YNB (Fig. 1C). The highest

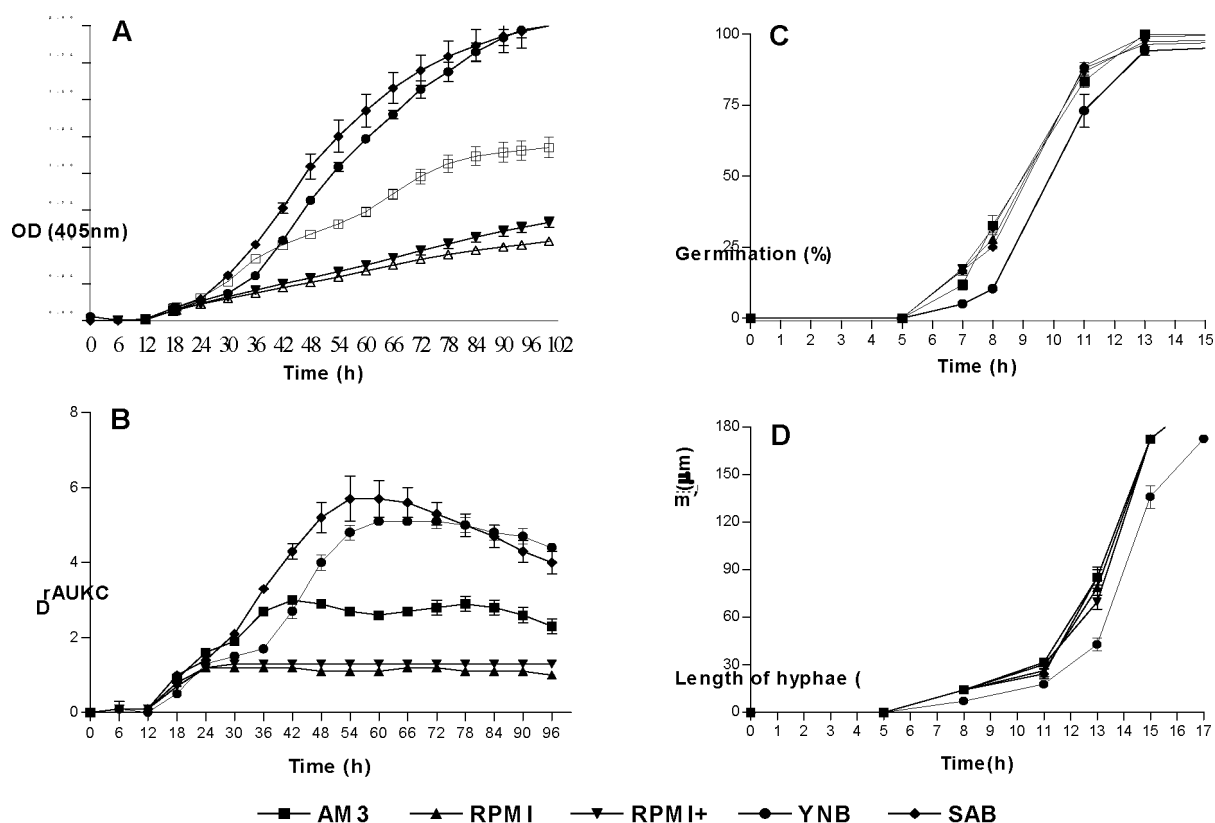


Figure 2. Graphical representation of the growth of *A. fumigatus* in five nutrient media. (A) Changes in OD over time. (B) Changes in Δ AUKC over time. (C) Percentages of germination of conidia over time. (D) Extension of hyphae over time. Bars, SE.

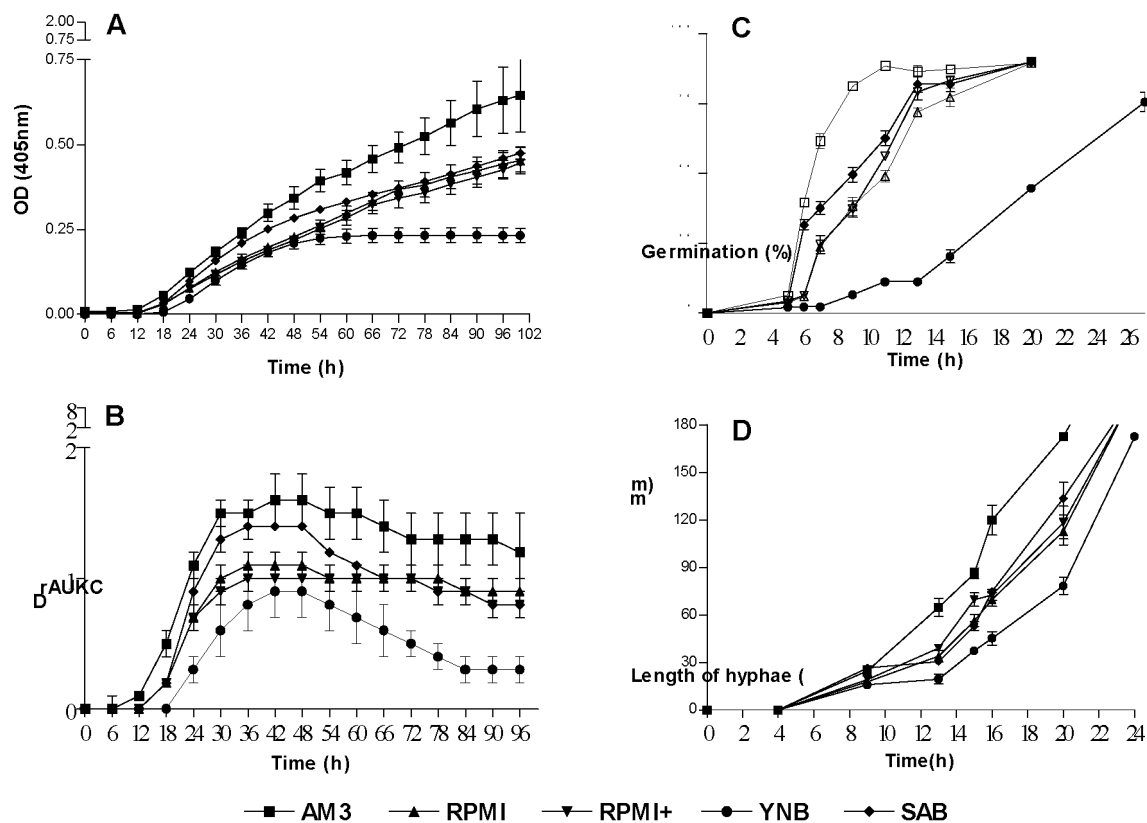


Figure 3. Graphical representation of the growth of *S. prolificans* in five nutrient media. (A) Changes in OD over time. (B) Changes in Δ AUKC over time. (C) Percentages of germination of conidia over time. (D) Extension of hyphae over time. Bars, SE.

Table 1. Time intervals at which different growth phases of *R. microsporus* var. *rhizopodiformis*, *A. fumigatus*, and *S. prolificans* were apparent in different media

Species	Medium	Time (h) of phase end \pm SD (Δ OD/min [10^{-5}] [CV ^a])				
		Lag ^b	1 st transition	Log	2 nd transition	Stationary
<i>R. microsporus</i>	AM3	5.40 \pm 1.12 (1.02 [68%])	6.60 \pm 1.12 (14.34 [13%])	27.60 \pm 4.18 (24.20 [14%])	54.00 \pm 2.51 (13.14 [20%])	>54 (-2.52 [71%])
	RPMI	6.00 \pm 0.95 (2.06 [23%])	7.80 \pm 1.20 (15.70 [14%])	15.60 \pm 0.60 (39.72 [9%])	24.00 \pm 0.95 (8.94 [37%])	>24 (4.36 [27%])
	RPMI+	6.60 \pm 0.60 (2.05 [23%])	9.00 \pm 0.00 (23.60 [10%])	15.60 \pm 0.60 (37.44 [10%])	27.60 \pm 1.75 (14.80 [19%])	>27.60 (2.52 [61%])
	SAB	9.00 \pm 0.00 (12.41 [18%])	9.00 \pm 0.00 (0 [0])	23.25 \pm 0.67 (84.48 [6%])	34.50 \pm 0.77 (25.20 [66%])	>34.50 (8.78 [175%])
<i>A. fumigatus</i>	YNB	8.40 \pm 0.60 (2.26 [33%])	12.00 \pm 0.00 (36.00 [17%])	25.20 \pm 0.73 (65.76 [14%])	43.80 \pm 4.31 (26.98 [49%])	>43.80 (0.03 [126%])
	AM3	13.20 \pm 1.53 (2.90 [45%])	16.20 \pm 1.53 (21.36 [24%])	54.60 \pm 8.35 (25.98 [11%])	97.80 \pm 2.24 (19.30 [21%])	>97.80 (5.83 [177%])
	RPMI	12.60 \pm 1.12 (2.48 [20%])	14.40 \pm 0.60 (17.36 [22%])	46.80 \pm 12.24 (11.50 [5%])	94.80 \pm 4.51 (9.16 [17%])	>94.80 (6.60 [127%])
	RPMI+	10.80 \pm 1.20 (1.12 [29%])	13.80 \pm 0.73 (13.92 [12%])	57.60 \pm 12.78 (12.38 [12%])	>99 (11.98 [11%])	>99 (NC ^c)
<i>S. prolificans</i>	SAB	13.80 \pm 1.20 (4.41 [8%])	24.60 \pm 1.12 (19.02 [9%])	56.40 \pm 4.18 (55.93 [12%])	92.40 \pm 3.47 (29.22 [28%])	>92.40 (14.24 [122%])
	YNB	13.80 \pm 0.73 (1.70 [14%])	30.00 \pm 1.64 (17.16 [9%])	65.40 \pm 2.58 (56.34 [5%])	>99 (31.46 [14%])	>99 (NC)
	AM3	13.50 \pm 3.19 (1.53 [40%])	17.40 \pm 1.47 (14.58 [28%])	55.80 \pm 9.23 (15.08 [26%])	87.60 \pm 9.60 (9.75 [64%])	>87.6 (7.49 [145%])
	RPMI	13.20 \pm 0.73 (0.59 [65%])	17.40 \pm 0.60 (7.61 [22%])	49.80 \pm 8.62 (11.04 [11%])	84.00 \pm 9.90 (8.15 [42%])	>84.00 (4.85 [124%])
<i>S. prolificans</i>	RPMI+	15.60 \pm 1.12 (1.76 [28%])	18.00 \pm 0.95 (10.93 [12%])	52.20 \pm 7.86 (10.06 [14%])	87.60 \pm 10.50 (7.20 [29%])	>87.60 (6.77 [34%])
	SAB	15.60 \pm 1.12 (1.70 [29%])	18.60 \pm 0.60 (15.44 [19%])	37.20 \pm 1.53 (16.30 [6%])	75.00 \pm 7.35 (7.22 [15%])	>75.00 (6.20 [38%])
	YNB	18.75 \pm 0.67 (0.91 [61%])	21.00 \pm 1.10 (9.07 [47%])	41.25 \pm 2.77 (13.05 [13%])	61.50 \pm 2.32 (4.34 [47%])	>61.50 (12.58 [171%])

^a CV, coefficient of variation. ^b The beginning of the lag phase is at time zero in each case. ^c NC, not calculated.

^a CV, coefficient of variation.^b The beginning of the lag phase is at time zero in each case. ^c NC, not calculated.

elongation rates of hyphae were observed in AM3 (39.6 μ m/h), and the lowest were observed in YNB (26.7 μ m/h) (Fig. 1D). The highest rate of increase in OD (Δ OD per minute) was observed during the log phase (0.5 to 3 times higher than those in the other growth phases (Table 1). Based on the Δ rAUKC model the log phase was from 9 to 15.6 h in RPMI and RPMI+, from 12 to 25.2 h in YNB, from 9 to 23.3 h in SAB, and from 6.6 to 27 h in AM3 (Fig. 1B and Table 1). Based on Δ OD-per-minute values the lowest interstrain variation for all media was found during the log phase. The mean variations \pm standard errors (SE) of Δ OD-per-minute values in the five media were 11% \pm 2% for the log phase, 14% \pm 1% for the first transition period, 33% \pm 9% for the lag phase, 38% \pm 9% for the second transition period, and 92% \pm 26% for the stationary phase (Table 1).

***A. fumigatus*.** The first detectable growth for the strains of *A. fumigatus* was after 9.65 h (Table 2) although the germination of conidia was completed after 13 h (Fig. 2C). In Fig. 2A the differences in the shapes of the growth curves for each nutrient medium are shown. The slopes of the growth curves in RPMI medium, even when supplemented with 2% glucose, were fourfold lower than those in SAB and YNB (Table 2). By contrast to that of *Rhizopus* strains, the growth of the *Aspergillus* strains failed to reach the stationary phase within 100 h. S_{\max} was reached after 30 h for all media except RPMI, in which S_{\max} occurred after 17 h (Table 2). The germination of conidia started after 5 h of incubation in all media although it was delayed for 1.5 h in YNB (Fig. 2C). Similar rates of elongation of *Aspergillus* hyphae occurred in all media (\approx 25 μ m/h) except in YNB, in which a lower elongation rate (20.2 μ m/h) was observed (Fig. 2D). The Δ OD-per-minute values in the log phase were higher than those in the other growth phases except in RPMI, where the Δ OD per minute was comparable to that in the first transition period. The log phase based on Δ rAUKC values was between 14.4 and 46.8 h in RPMI and RPMI+, between 24.6 and 56.4 h in SAB, between 30 and 65.4 h in YNB, and between 16.2 and 54.6 h in AM3 (Fig. 2B and Table 1). The lowest variation in Δ OD per minute among the five strains and among the growth phases was found during the log phase. The mean variations \pm SE of Δ OD per minute in the five media were 9% \pm 2% for the log phase, 15% \pm 3% for the first transition period, 18% \pm 3% for the second transition period, 22% \pm 2% for the stationary phase, and 23% \pm 6% for the lag phase (Table 1).

***S. prolificans*.** The growth of this fungus was the slowest among the species tested since after 100 h of incubation the OD_{\max} ranged from 0.27 in YNB to 0.64 in AM3 (Table 2). The highest growth rate occurred in AM3, and the lowest occurred in YNB, with

Table 2. Parameters calculated from the growth curves of the five strains from each fungal species in five nutrient media based on changes of OD^a

Species	Medium	OD _{max}	S (10 ⁻⁴)	S _{max} (10 ⁻⁴)	OD ₀ ^b (h)	OD ₉₀ (h)	Time of S _{max} (h)
<i>R. microsporus</i>	AM3	0.55 ± 0.05	1.17 ± 0.11	3.33 ± 0.74	4.80 ± 0.21	39.35 ± 5.10	12.06 ± 6.57
	RPMI	0.29 ± 0.03	0.61 ± 0.08	4.44 ± 0.50	4.95 ± 0.33	20.30 ± 6.10	11.15 ± 0.93
	RPMI+	0.41 ± 0.06	0.84 ± 0.06	3.96 ± 0.38	5.15 ± 0.29	37.15 ± 8.86	10.65 ± 1.04
	SAB	1.01 ± 0.10	2.28 ± 0.24	11.52 ± 4.76	5.38 ± 0.14	29.24 ± 6.04	15.75 ± 2.19
	YNB	1.02 ± 0.24	2.17 ± 0.60	8.52 ± 2.04	6.50 ± 0.35	40.18 ± 9.47	18.60 ± 1.15
<i>A. fumigatus</i>	AM3	1.17 ± 0.15	2.49 ± 0.32	4.68 ± 0.59	10.02 ± 0.78	73.33 ± 3.78	31.17 ± 0.76
	RPMI	0.53 ± 0.06	1.08 ± 0.11	1.69 ± 0.37	9.65 ± 0.38	76.05 ± 2.33	17.30 ± 5.04
	RPMI+	0.65 ± 0.08	1.27 ± 0.15	1.64 ± 0.22	9.70 ± 0.27	81.21 ± 0.53	17.13 ± 4.61
	SAB	2.00 ± 0.26	4.23 ± 0.53	6.69 ± 0.45	9.65 ± 0.76	72.80 ± 3.56	42.44 ± 4.79
	YNB	2.01 ± 0.12	4.28 ± 0.31	7.66 ± 0.67	11.35 ± 0.34	80.90 ± 4.03	43.63 ± 0.48
<i>S. prolificans</i>	AM3	0.64 ± 0.23	1.31 ± 0.45	2.63 ± 0.75	11.35 ± 0.89	71.49 ± 13.46	40.25 ± 14.15
	RPMI	0.45 ± 0.08	0.97 ± 0.14	1.92 ± 0.80	13.30 ± 1.01	74.05 ± 3.45	43.69 ± 19.90
	RPMI+	0.44 ± 0.06	0.87 ± 0.14	1.64 ± 0.35	12.95 ± 0.93	75.44 ± 7.36	39.63 ± 23.43
	SAB	0.47 ± 0.04	0.97 ± 0.06	1.82 ± 0.18	12.95 ± 0.72	69.10 ± 8.62	22.50 ± 1.62
	YNB	0.24 ± 0.04	0.53 ± 0.10	1.59 ± 0.16	17.75 ± 2.28	45.21 ± 5.41	26.31 ± 3.37

^a Values are means ± standard deviations.^b OD₀, Time of the first significant change in OD.

slopes of the growth curves of 1.31×10^{-4} and 0.53×10^{-4} , respectively. The S_{max} in these media occurred after 40 and 26 h, respectively (Table 2). In all the nutrient media the fungus continued to grow until 100 h, except for YNB, in which the plateau was reached within 50 h (Fig. 3A). The germination of *Scedosporium* conidia started after 4 h of incubation in AM3 and SAB, after 5 h of incubation in RPMI and RPMI+, and after 7 h of incubation in YNB, in which the delay in germination increased during the incubation. Complete germination was not achieved in any of the media after 20 h of incubation (Fig. 3C). The elongation rates ranged from 16.9 to 9.9 $\mu\text{m}/\text{h}$, with the highest in AM3 and the lowest in YNB (Fig. 3D). The ΔOD -per-minute values were higher during the log phase but were comparable to those of the first transition period (Fig. 3B and Table 1). The log phase based on the ΔrAUKC model was between 17.4 and 49.8 h in RPMI and RPMI+, between 18 and 55.8 h in AM3, between 18.6 and 37.2 h in SAB, and between 21 and 41.3 h in YNB. The lowest interstrain variation was found during the log phase, with a mean ± SE of $14\% \pm 3\%$ compared with those during the first transition period ($28\% \pm 5\%$), the second transition period ($39\% \pm 8\%$), the lag phase ($44\% \pm 8\%$), and the stationary phase ($82\% \pm 31\%$) (Table 1).

DISCUSSION

The nutrient medium is a major factor that influences the results of susceptibility tests (3, 30).

According to clinical laboratory standards an optimal nutrient medium should provide good or adequate growth of the microorganisms (19). The relativity of this definition is clear since all the media tested here supported the growth of filamentous fungi to various degrees. Moreover the definition of an adequate medium is really a minimal requirement that has to be fulfilled in order for a medium to be considered as a candidate for the susceptibility tests. An optimal nutrient medium should provide not simply adequate growth but the best possible growth in order to allow moulds to grow without restriction and express all phenotypes. Under these growth conditions, any failure of the fungus to grow in the presence of antifungal drugs should be considered as a true inability, i.e., lack of proper genetic predisposition to resist the antifungal drugs or interaction of the drug with the target.

The importance of the nutrient medium and the growth rate of the fungus in relation to in vitro susceptibility testing has been shown previously. The in vitro susceptibility of *Candida albicans* to fluconazole and miconazole depends on the stage of the growth of the fungus and the nutrient medium used (6, 17, 36). Yeasts in the exponential growth phase were more susceptible to fluconazole than those in the lag phase when they were cultivated in YNB-2% glucose medium (6, 17), and the in vitro activity of miconazole in CYG (0.5% casein gydrolase, 0.5% yeast extract, 0.5% glucose), NG (1% neopeptone, 0.5% glucose), and YNB-4% glucose media was greater when richer media were used (36). Differences in MICs for filamentous fungi were also observed when conidia (fungus in the

lag phase) and hyphae (fungus in the log or stationary phase) were cultivated in RPMI 1640 (12). In another study where RPMI and YNB were employed the interaction between antimicrobial agents and fungi depended on the type of medium used (22).

The previous findings can be correlated with the results of this study. Figures 1A, 2A, and 3A show that RPMI poorly supports the growth of the three species of filamentous fungi tested. Supplementation with glucose essentially had little effect, despite being proposed as a means of improving the characteristics of this medium (32), and resulted only in a slight increase in the fungal growth even after incubation for 100 h. SAB and YNB were the more nutritious media and provided the highest growth for *R. microsporus* and *A. fumigatus*, with growth rates three to four times higher than those achieved in RPMI. None of the media supported the growth of *S. prolificans* sufficiently. Apparent were other effects of the media, such as the delay of germination of spores and conidia as well as the lower elongation rates of hyphae of all species in YNB medium, processes which were enhanced in AM3. By contrast with the growth of yeasts, where the stationary phase is reached within 30 h (15, 36), the growth of filamentous fungi is characterized by smoother curves and long transition periods although it depended on the medium and species. Interestingly, during the growth of *R. microsporus* in AM3, an OD decrease after 66 h of incubation, which could be correlated with the death phase of bacterial growth, occurred (20).

The use of a poor medium such as RPMI, in which fungi grow slowly, might result in erroneous MICs. In an extreme situation a fungus unable to grow in a certain medium would seem to be susceptible despite the fact that the inhibition of growth is not due to the action of the antifungal agent but due to the medium. There might be other situations, which are difficult to prove experimentally, in which a poor medium, although it supports fungal growth, acts synergistically with the drug in inhibiting growth, resulting in an appearance of better activity. The discrepancy in the interaction of a fluoroquinolone with amphotericin B against *A. fumigatus* in YNB (synergistic) and in RPMI (antagonistic) (22), as well as the higher activity of miconazole in richer media (36), could be explained by the growth curves. The high growth in YNB and the poor growth in RPMI correlate with different levels of metabolic activity. Thus, in YNB the drugs might penetrate better into the intracellular site of action in sufficient concentrations to exhibit an effect.

RPMI has been evaluated extensively for in vitro susceptibility testing of yeasts and has been shown to provide reproducible results (2, 25, 28, 30). Therefore, the NCCLS has proposed to use this medium as the standard medium for antifungal susceptibility testing of

filamentous fungi (23). Like YNB, RPMI is a synthetic and completely defined medium and is characterized by small lot-to-lot variation, resulting in high reproducibility of susceptibility tests, unlike AM3, which has considerable variation from lot to lot and source to source. By contrast the use of chemically complex undefined media such as SAB medium is not recommended (19, 28) since undefined components that they may contain might interact with antifungal drugs (13, 14, 19, 26). Furthermore, acidic media such as YNB and SAB, if they were used unbuffered, may inactivate amphotericin B, which is not stable at low pH (16, 21).

Another important variable in susceptibility testing of filamentous fungi is the reading time. It is well known that prolonged incubation elevates the MICs of antifungal drugs (8, 29). The NCCLS addressed this by recommending different incubation periods for each species based on visual growth. Although the growth curves of filamentous fungi have not been previously studied in order to characterize the growth over time, the NCCLS recommended incubation periods of 24 h for the fast-growing species, usually belonging to the Zygomycetes, 72 h for the slow-growing species such as the black fungi, and 48 h for the other species (23).

In the field of antibacterial susceptibility testing, the MICs should be read when the growth control is in the log phase and not in the transition periods, i.e., between lag phase and log phase or between log phase and stationary phase, where unbalanced growth exists (20). Since the growth curves of filamentous fungi are characterized by long transition periods, the precise determination of these periods is a crucial parameter in order to obtain balanced growth. The same conclusion was made by Galgiani and Stevens (7) in terms of variability of MICs, when they observed that yeasts showed increased variation in the concentration of a drug producing 50% of the growth seen in a drug-free well when the MIC determination was made beyond 48 h of incubation. Beyond this incubation period, the drug-free culture reached the stationary phase and stopped growing resulting in higher variation in MICs (7). This effect is more obvious for fungistatic drugs since in the stationary phase the fungi in the drug-free control stop growing but those in drug-containing wells do not, which increases the difference in optical density between these two wells (unpublished observations). These findings could be correlated with our finding of high variation in the stationary phase compared with that in the other growth phases. That the growth phase is an important variable is supported by the findings that the inhibitory effects of ketoconazole and miconazole against *C. albicans* were indistinguishable when the yeasts were tested in the stationary phase (1).

Based on the results of this study (Table 1), the growth curves for filamentous fungi during the transition periods were characterized by rapid changes in slope and high variation compared with other parts of the growth curve. The slopes in the transition periods were either continuously decreasing until a plateau was reached (second transition period) or increasing until the log phase was reached (first transition period). Since the log phase is located between these two transition periods, precise determination of these periods is required in order to determine the boundaries of this growth phase. Due to long and smooth transition periods of the growth curves of filamentous fungi, the visualization of the start and end points of these periods by using the OD changes is difficult. Therefore, a calculation model based on Δ rAUKC was developed. With the Δ rAUKC model even small changes of the slopes, which might be an indication of transition between phases, can be observed. The log phase of the growth curve is that part of the curve where Δ rAUKC values increase linearly over time and the growth rate is constant at its highest value. This model can be used to describe the different growth phases of filamentous fungi and to determine the boundaries of each phase. The level of 30% (increase until 30% and decrease until 70%) of the maximal Δ rAUKC seems to be the crucial breakpoint of the growth curves of filamentous fungi indicating the presence of symmetry.

In summary, the above-mentioned studies indicate that during the log phase balanced growth takes place (20) and a greater distribution of MICs is obtained (1) and the reproducibility of MICs is higher (7) than in the other growth phases. In addition, this study shows that the lowest interstrain variation was observed during the log phase of the growth curve. Thus, the optimal reading time of antifungal susceptibility testing of filamentous fungi could be during the log phase. Therefore the precise knowledge of the growth phases during the growth of filamentous fungi would help to find the optimal reading time of the MICs.

Nevertheless, many factors are involved in the standardization of antifungal susceptibility testing. Unequivocally intercenter and intracenter reproducibility, as underlined by NCCLS, is a major issue for antifungal susceptibility testing of filamentous fungi. However another primary goal of susceptibility tests is the correlation of in vitro results with clinical response, and this does not favor necessarily and absolutely simplified methodologies.

Although an ultimate challenge would be to find a common medium that would be suitable for as many fungi as possible, this study indicates that the standardization of susceptibility testing of filamentous fungi may require different nutrient media for each species and consequently different reading times of the

MICs of antifungal drugs. Furthermore, findings for one species are not readily extrapolated to others, particularly for filamentous fungi, where significant morphological and physiological variations exist. Therefore, based on the results obtained from the growth curves further studies are required to investigate the effect of nutrient media and growth phases on MICs and ultimately to determine which approach correlates best with the clinical outcome.

ACKNOWLEDGMENTS

This study was supported by the European Commission Training and Mobility of Researchers grant ERBFMRXCT97-0145 to Joseph Meletiadis and by the Mycology Research Center of Nijmegen.

REFERENCES

1. **Beggs, W.** 1984. Growth phase in relation to ketoconazole and miconazole susceptibilities of *Candida albicans*. *Antimicrob. Agents Chemother.* **25**:316-318.
2. **Cormican, M. G., and M. A. Pfaller.** 1996. Standardization of antifungal susceptibility testing. *J. Antimicrob. Chemother.* **38**:561-578.
3. **Espinel-Ingroff, A., F. Barchiesi, K. C. Hazen, J. V. Martinez-Suarez, and G. Scalise.** 1998. Standardization of antifungal susceptibility testing and clinical relevance. *Med. Mycol.* **36**(Suppl. 1):68-78.
4. **Espinel-Ingroff, A., M. Bartlett, R. Bowden, N. X. Chin, C. Cooper, Jr., A. Fothergill, M. R. McGinnis, P. Menezes, S. A. Messer, P. W. Nelson, F. C. Odds, L. Pasarell, J. Peter, M. A. Pfaller, J. H. Rex, M. G. Rinaldi, G. S. Shankland, T. J. Walsh, and I. Weitzman.** 1997. Multicenter evaluation of proposed standardized procedure for antifungal susceptibility testing of filamentous fungi. *J. Clin. Microbiol.* **35**:139-143.
5. **Espinel-Ingroff, A., K. Dawson, M. Pfaller, E. Anaissie, B. Breslin, D. Dixon, A. Fothergill, V. Paetznick, J. Peter, M. G. Rinaldi, and T. Walsh.** 1995. Comparative and collaborative evaluation of standardization of antifungal susceptibility testing for filamentous fungi. *Antimicrob. Agents Chemother.* **39**:314-319.
6. **Gale, E. F., A. M. Johnson, D. Kerridge, and T. Y. Koh.** 1975. Factors affecting the changes in amphotericin B sensitivity of *Candida albicans* during growth. *J. Gen. Microbiol.* **87**:20-36.
7. **Galgiani, J. N., and D. A. Stevens.** 1976. Antimicrobial susceptibility testing of yeasts: a turbidimetric technique independent of inoculum size. *Antimicrob. Agents Chemother.* **10**:721-728.
8. **Gehrt, A., J. Peter, P. A. Pizzo, and T. J. Walsh.** 1995. Effect of increasing inoculum sizes of pathogenic

- filamentous fungi on MICs of antifungal agents by broth microdilution method. *J. Clin. Microbiol.* **33**:1302-1307.
9. **Ghannoum, M. A.** 1997. Susceptibility testing of fungi and correlation with clinical outcome. *J. Chemother.* **9**(Suppl. 1):19-24.
 10. **Ghannoum, M. A., A. S. Ibrahim, Y. Fu, M. C. Shafiq, J. E. Edwards, Jr., and R. S. Criddle.** 1992. Susceptibility testing of *Cryptococcus neoformans*: a microdilution technique. *J. Clin. Microbiol.* **30**:2881-2886.
 11. **Ghannoum, M. A., and L. B. Rice.** 1999. Antifungal agents: mode of action, mechanisms of resistance, and correlation of these mechanisms with bacterial resistance. *Clin. Microbiol. Rev.* **12**:501-517.
 12. **Guarro, J., C. Llop, C. Agular, and I. Pujol.** 1997. Comparison of in vitro antifungal susceptibilities of conidia and hyphae of filamentous fungi. *Antimicrob. Agents Chemother.* **41**:2760-2762.
 13. **Hoeprich, P. D., and P. D. Finn.** 1972. Obfuscation of the activity of antifungal antimicrobics by culture media. *J. Infect. Dis.* **126**:353-361.
 14. **Hoeprich, P. D., and A. C. Huston.** 1976. Effect of culture media on the antifungal activity of miconazole and amphotericin B methyl ester. *J. Infect. Dis.* **134**:336-341.
 15. **Hoeprich, P. D., and J. M. Merry.** 1986. Influence of culture medium on susceptibility testing with BAY n 7133 and ketoconazole. *J. Clin. Microbiol.* **24**:269-271.
 16. **Johnson, B., R. J. White, and G. M. Williamson.** 1978. Factors influencing the susceptibility of *Candida albicans* to the polyenic antibiotics nystatin and amphotericin B. *J. Gen. Microbiol.* **104**:325-333.
 17. **Kerridge, D., T. Y. Koh, M. S. Marriott, and E. F. Gale.** 1976. Microbiology and plant protoplasts, p. 23-28. In J. F. Peberdy, A. H. Rose, H. J. Rodger, and E. C. Cocking (ed.), *Microbiology and plant protoplasts*. Churchill Livingstone, London, England.
 18. **Llop, C., I. Pujol, C. Aguilar, J. Sala, D. Riba, and J. Guarro.** 2000. Comparison of three methods of determining MICs for filamentous fungi using different end point criteria and incubation periods. *Antimicrob. Agents Chemother.* **44**:239-242.
 19. **McGinnis, M. R., and M. G. Rinaldi.** 1991. Antifungal drugs: mechanisms of action, drug resistance, susceptibility testing, and assays of activity in biological fluids, p. 198-251. In V. Lorian (ed.), *Antibiotics in laboratory medicine*, 3rd ed. Williams & Wilkins, Baltimore, Md.
 20. **McGinnis, M. R., and M. G. Rinaldi.** 1991. Determining the effects of antibiotics on bacterial growth by optical and electrical methods, p.64-75. In V. Lorian (ed.), *Antibiotics in laboratory medicine*, 3rd ed. Williams & Wilkins, Baltimore, Md.
 21. **Minagawa, H., K. Kitaura, and N. Nakamizo.** 1983. Effects of pH on the activity of ketoconazole against *Candida albicans*. *Antimicrob. Agents Chemother.* **23**:105-107.
 22. **Nakajima, R., A. Kitamura, K. Someya, M. Tanaka, and K. Sato.** 1995. In vitro and in vivo antifungal activities of DU-6859a, a fluoroquinolone, in combination with amphotericin B and fluconazole against pathogenic fungi. *Antimicrob. Agents Chemother.* **39**:1517-1521.
 23. **National Committee for Clinical Laboratory Standards.** 1998. Reference method for broth dilution antifungal susceptibility testing of conidium forming filamentous fungi. Proposed standard M38-P. National Committee for Clinical Laboratory Standards, Wayne, Pa.
 24. **Perfect, J. R., and W. A. Schell.** 1996. The new fungal opportunists are coming. *Clin. Infect. Dis.* **22**(Suppl. 2):112-118.
 25. **Pfaller, M. A., M. G. Rinaldi, J. N. Galgiani, M. S. Bartlett, B. A. Body, A. Espinel-Ingroff, R. A. Fromtling, G. S. Hall, C. E. Hughes, and F. C. Odds.** 1990. Collaborative investigation of variables in susceptibility testing of yeasts. *Antimicrob. Agents Chemother.* **34**:1648-1654.
 26. **Polak, A., and H. J. Scholer.** 1973. Fungistatic activity, uptake and incorporation of 5-fluorocytosine in *Candida albicans*, as influenced by pyrimidines and purines. I. Reversal experiments. *Pathol. Microbiol.* **39**:148-159.
 27. **Pujol, I., J. Guarro, J. Sala, and M. D. Riba.** 1997. Effects of incubation temperature, inoculum size, and time of reading on broth microdilution susceptibility test results for amphotericin B against *Fusarium*. *Antimicrob. Agents Chemother.* **41**:808-811.
 28. **Radetsky, M., R. C. Wheeler, M. H. Roe, and J. K. Todd.** 1986. Microtiter broth dilution method for yeast susceptibility testing with validation by clinical outcome. *J. Clin. Microbiol.* **24**:600-606.
 29. **Reuben, A., E. Anaissie, P. E. Nelson, R. Hashem, C. Legrand, D. H. Ho, and G. P. Bodey.** 1989. Antifungal susceptibility of 44 clinical isolates of *Fusarium* species determined by using a broth microdilution method. *Antimicrob. Agents Chemother.* **33**:3290-3295.
 30. **Rex, J. H., M. A. Pfaller, M. G. Rinaldi, A. Polak, and J. N. Galgiani.** 1993. Antifungal susceptibility testing. *Clin. Microbiol. Rev.* **6**:367-381.
 31. **Richardson, M. D.** 1991. Opportunistic and patho-genic fungi. *J. Antimicrob. Chemother.* **28**(Suppl. A):1-11.
 32. **Rodriguez-Tudela, J. L., and J. V. Martinez-Suarez.** 1995. Defining conditions for microbroth antifungal susceptibility tests: influence of RPMI and RPMI-2% glucose on the selection of endpoint criteria. *J. Antimicrob. Chemother.* **35**:739-749.
 33. **Rodriguez-Tudela, J. L., F. Martin-Diez, M. Cuenca-Estrella, L. Rodero, Y. Carpintero, and B. Gorgojo.** 2000. Influence of shaking on antifungal susceptibility testing of *Cryptococcus neoformans*: a comparison of the NCCLS standard M27A medium, buffered yeast nitrogen base, and RPMI-2% glucose. *Antimicrob. Agents Chemother.* **44**:400-404.
 34. **Sheehan, D. J., C. A. Hitchcock, and C. M. Sibley.** 1999. Current and emerging azole antifungal agents. *Clin. Microbiol. Rev.* **12**:40-79.
 35. **St-Germain, G., and C. Dion.** 1996. Effect of media on growth rate and susceptibility testing of *Cryptococcus neoformans*. *Mycoses* **39**:201-206.
 36. **van den Bossche, H., G. Willemsens, and J. M. van Cutsem.** 1975. The action of miconazole on the growth of *Candida albicans*. *Sabouraudia* **13**:63-73.

37. **Vartivarian, S. E., E. J. Anaissie, and G. P. Bodey.** 1993. Emerging fungal pathogens in immuno-compromised patients: classification, diagnosis, and management. *Clin. Infect. Dis.* **17**(Suppl. 2):487-491.



Chapter 2.2

Comparison of NCCLS and 3-(4,5-Dimethyl-2-Thiazyl)-2,5-Diphenyl-2H-Tetrazolium Bromide (MTT) Methods of In Vitro Susceptibility Testing of Filamentous Fungi and Development of a New Simplified Method

Journal of Clinical Microbiology 2000; 38: 2949-2954

COMPARISON OF NCCLS AND 3-(4,5-DIMETHYL-2-THIAZYL)-2,5-DIPHENYL-2H-TETRAZOLIUM BROMIDE (MTT) METHODS OF IN VITRO SUSCEPTIBILITY TESTING OF FILAMENTOUS FUNGI AND DEVELOPMENT OF A NEW SIMPLIFIED METHOD

JOSEPH MELETIADIS¹, JACQUES F. G. M. MEIS^{1,2}, JOHAN W. MOUTON², J. PETER DONNELLY³,
AND PAUL E. VERWEIJ¹

Departments of Medical Microbiology¹ and Hematology³, University Medical Center Nijmegen, and Department of Medical Microbiology and Infectious Diseases, Canisius-Wilhelmina Hospital², Nijmegen, The Netherlands

The susceptibility of 30 clinical isolates belonging to six different species of filamentous fungi (*Aspergillus fumigatus*, *Aspergillus flavus*, *Scedosporium prolificans*, *Scedosporium apiospermum*, *Fusarium solani*, and *Fusarium oxysporum*) was tested against six antifungal drugs (miconazole, voriconazole, itraconazole, UR9825, terbinafine, and amphotericin B) with the microdilution method recommended by the National Committee for Clinical Laboratory Standards (NCCLS) (M38-P). The MICs were compared with the MICs obtained by a colorimetric method measuring the reduction of the dye 3-(4,5-dimethyl-2-thiazyl)-2,5-diphenyl-2H-tetrazolium bromide (MTT) to formazan by viable fungi. The levels of agreement between the two methods were 96 and 92% for MIC-0 (clear wells) and MIC-1 (75% growth reduction), respectively. The levels of agreement were always higher for *Aspergillus* spp. (97% \pm 2.5%), followed by *Scedosporium* spp. (87% \pm 10.3%) and *Fusarium* spp. (78% \pm 7.8%). The NCCLS method was more reproducible than the MTT method: 98 versus 95% for MIC-0 and 97 versus 90% for MIC-1. However, the percentage of hyphal growth as determined visually by the NCCLS method showed several discrepancies when they were compared with the percentages of MTT reduction. A new simplified assay that incorporates the dye MTT with the initial inoculum and in which the fungi are incubated with the dye for 48 h or more was developed, showing comparable levels of agreement and reproducibility with the other two methods. Furthermore, the new assay was easier to perform and more sensitive than the MTT method.

Filamentous fungi may cause invasive mycoses in both immunocompromised and non-immunocompromised individuals. These infections require prompt systemic antifungal therapy, the effectiveness of which depends, among other things, on the in vitro susceptibility of the fungus to antifungal drugs. Therefore, there is a demand for reproducible and reliable methods of antifungal susceptibility testing of filamentous fungi. Many variables that decrease the inter- and intralaboratory agreement are now defined (2, 4, 5, 16, 19). Broth macrodilution methods are time-consuming and labor-intensive (1), and therefore, efforts have focused on microdilution methods that are more practical and more user-friendly in the clinical laboratory (18). Based on these principles, the Subcommittee on Antifungal Susceptibility Testing of the National Committee for Clinical Laboratory Standards (NCCLS) has proposed the M38-P standard for the antifungal susceptibility testing of conidium-forming fungi (14).

The determination of MICs for filamentous fungi can be facilitated with a method which overcomes observer bias and quantifies the hyphal growth of moulds. Because turbidity measurements and colony counts (9) are not useful in the case of filamentous

fungi, colorimetric methods based on the measurement of metabolic activity may facilitate determination of the MIC (17). One of these is an assay using the dye 3-(4,5-dimethyl-2-thiazyl)-2,5-diphenyl-2H-tetrazolium bromide (MTT). This yellow tetrazolium salt is cleaved by dehydrogenases inside mitochondria or in other cellular locations possessing dehydrogenase activity (7) to form its purple formazan derivative (11), which can be measured spectrophotometrically at 550 nm. MTT is cleaved by all living, metabolically active fungi independent of proliferation and irrespective of unicellular or multicellular growth and thus is a measure of metabolic activity.

A method based on MTT has been used for susceptibility testing of fungi. The MTT method demonstrated excellent agreement with the standard macrodilution method for the antifungal susceptibility testing of yeasts (1, 9). For filamentous fungi, the MTT method has been used for *Aspergillus fumigatus*, resulting in interpretable data (10). In order to overcome the shortcomings of visual MIC determination for filamentous fungi and to develop a reliable, subjective, and less variable method for the antifungal susceptibility testing of filamentous fungi, we evaluated the performance of a method using MTT and compared

the results with those obtained with the proposed standard of the NCCLS. The correlation between the metabolic activity and the growth of fungi was examined. Furthermore, a simplified method using MTT was developed and compared with the previous methods.

MATERIALS AND METHODS

Test isolates. Thirty clinical isolates of filamentous fungi (part of our private collection) were tested. These included five isolates of each of the following species: *A. fumigatus* (AZN7151, AZN7275, AZN8249, AZN8248, and AZN7272), *Aspergillus flavus* (AZN501, AZN6837, AZN6803, AZN6686, and AZN6578), *Scedosporium prolificans* (AZN7886, AZN7903, AZN7946, AZN7921, and AZN7895), *Scedosporium apiospermum* (AZN1252, AZN7309, AZN7110, AZN7111, and AZN6474), *Fusarium solani* (AZN729, AZN646, AZN2106, AZN7844, and AZN2784), and *Fusarium oxysporum* (AZN685, AZN441, AZN1859, AZN8263, and AZN1188). *Candida parapsilosis* (ATCC 22019) and *Candida krusei* (ATCC 6258) were used for quality controls.

Isolates were passaged twice at an interval of 5 to 7 days at 30 to 37°C. All isolates were tested three times on three different days. All the solutions were prepared ex novo with powders from the same lot. Conidia of the isolates were obtained from fresh cultures each time.

NCCLS method. A broth microdilution method was performed according to NCCLS guidelines (M38-P) (14). The drugs that were used included miconazole (Janssen Research Foundation, Beerse, Belgium), terbinafine (Novartis, Basel, Switzerland), itraconazole (Janssen Research Foundation), UR9825 (Ureach, Madrid, Spain), voriconazole (Pfizer Central Research, Sandwich, United Kingdom), and amphotericin B (Bristol-Myers Squibb, Woerden, The Netherlands). The drug dilutions were made in RPMI 1640 medium (with L-glutamine, without bicarbonate) (GIBCO BRL, Life Technologies, Woerden, The Netherlands) buffered to pH 7.0 with 0.165 M 3-N-morpholinopropanesulfonic acid (MOPS) (Sigma-Aldrich Chemie GmbH, Steinheim, Germany). The final concentrations of the antifungal agents ranged from 0.015 to 16 mg of amphotericin B/liter, 0.06 to 64 mg of miconazole/liter, and 0.03 to 32 mg of itraconazole, terbinafine, UR9825, and voriconazole per liter.

The tests were performed in 96-well flat-bottom microtitration plates, which were kept at -70°C until the day of testing. Spores were collected with a cotton stick and suspended in sterile water. After the heavy particles were allowed to settle, the turbidity of the supernatants were measured spectrophotometrically (Spectronic 20D; Milton Roy, Rochester, N.Y.) at 530 nm and transmission was adjusted to 68 to 70% (*Scedosporium* spp. and *Fusarium* spp.) or to 80 to 82% (*Aspergillus* spp.). Each suspension was diluted 1:50 in RPMI 1640 to obtain two times the desired inoculum. The inoculum size was confirmed by plating serial dilutions on Sabouraud dextrose agar (SDA) plates, with final inocula ranging from 1×10^4 to 5×10^4 CFU/ml. After agitation, the plates were incubated at 37°C for 48 h

(*Aspergillus* spp. and *Fusarium* spp.) and 72 h (*Scedosporium* spp.). The growth was assessed by visual observation with the aid of a concave mirror. Growth was scaled according to the NCCLS guidelines as follows: 4, no reduction in growth; 3, slight reduction in growth, or approximately 75% of the growth control; 2, prominent reduction in growth, or approximately 50% of the growth control; 1, slight growth, or approximately 25% of growth control; and 0, optically clear, or the absence of growth. MIC-1 and MIC-0 were determined to be the lowest concentrations of drug showing slight growth (25%) and absence of growth (100% visible-growth inhibition) compared with that of the drug-free control, respectively. For amphotericin B, only the MIC-0 was determined.

MTT method (MTT-3h). The MICs were also determined by a colorimetric method using the dye MTT (Sigma Chemical, St. Louis, Mo.). After the MICs were visually determined on each of the microtitration plates, 25 μ l of RPMI 1640 containing 5 mg of MTT/ml was added to each well. Incubation was continued at 37°C for 3 h. The content of each well was removed (centrifugation is not required for filamentous fungi due their adherence to the wells), and 200 μ l of isopropanol containing 5% 1 M HCl was added to extract the dye. After 30 min of incubation at room temperature and gentle agitation, the optical density (OD) was measured with a microtitration plate spectrophotometer (MS2 reader, Titertekplus; ICN Biomedical Ltd., B.V., Zoetermeer, The Netherlands) at 550 nm. The OD of the blank, which consisted of an uninoculated plate incubated together with the inoculated plates, was subtracted from the ODs of the inoculated plates. The percentage of MTT conversion to its formazan derivative for each well was calculated by comparing the OD at 550 nm (OD₅₅₀) of the wells with that of the drug-free control based on the following equation: (OD₅₅₀ of wells that contained the drug/OD₅₅₀ of the drug-free well) \times 100%. MIC-0 and MIC-1 were considered to be the lowest concentrations of drug showing at least 95 and 75% reductions in the OD compared with that of the drug-free well, respectively.

Toxicity test. The dye MTT was tested for possible inhibitory effects on the growth of filamentous fungi. The isolates were incubated in RPMI 1640 with different concentrations of MTT ranging from 4 to 0.06 mg/ml, for 72 h at 37°C. A final inoculum of 10^4 CFU/ml was used. Growth inhibition was assessed by visual observation of the wells containing MTT and compared with the MTT-free wells. The level of inhibition of the fungal growth was assessed and scored as described above.

Modified MTT method. The MICs for each of the isolates were also determined by a modification of the MTT method previously described. For this method, conidia suspensions were prepared as described above. Each suspension was diluted 1:50 in RPMI 1640 containing 0.2 mg of MTT/ml to obtain two times the desired inoculum. Then, the inoculum that contained MTT was added to microtitration plates, which resulted in a final concentration of MTT of 0.1 mg/ml, and the microtitration plates were incubated for 72 h (*Scedosporium* spp.) and 48 h (other species). After incubation, the formed formazan was extracted and the MICs were determined as described above.

Analysis of results. Each of the 30 isolates was tested

Table 1. The MICs of six antifungal drugs against 30 clinical isolates of filamentous fungi obtained by NCCLS method for the two endpoints

Species ^a	MIC Endpoint ^b	MIC (mg/liter) range (median) of the following drugs:					
		Miconazole	Terbinafine	Itraconazole	UR9825	Voriconazole	Amphotericin B
<i>A. fumigatus</i>	MIC-0	4-16 (4)	2-4 (4)	0.5-2 (1)	0.25-1 (0.5)	0.25-1 (0.5)	0.5-1 (0.5)
	MIC-1	4-16 (4)	0.5-4 (1)	0.5-1 (0.5)	0.13-0.25 (0.25)	0.13-0.5 (0.25)	ND ^c
<i>A. flavus</i>	MIC-0	1-16 (4)	0.03-0.5 (0.06)	0.13-1 (1)	0.13-0.25 (0.25)	0.25-1 (0.5)	0.5-1 (1)
	MIC-1	0.13-8 (2)	0.03-0.13 (0.03)	0.06-1 (0.5)	0.06-0.13 (0.13)	0.06-0.5 (0.25)	ND
<i>S. apiospermum</i>	MIC-0	1-8 (2)	>32	2->32 (32)	1-8 (2)	0.5-2 (0.5)	2-4 (2)
	MIC-1	0.5-2 (1)	>32	0.5-4 (1)	0.25-2 (1)	0.13-1 (0.25)	ND
<i>S. prolificans</i>	MIC-0	16->64 (>64)	>32	>32	8-32 (16)	16->32 (32)	0.5->16 (16)
	MIC-1	4->64 (64)	>32	>32	1-8 (2)	1-8 (4)	ND
<i>F. oxysporum</i>	MIC-0	1->64 (16)	0.13->32 (8)	0.5->32 (32)	0.5->32 (8)	0.5-16 (4)	0.25-2 (1)
	MIC-1	0.25->64 (8)	0.03-8 (2)	0.13->32 (32)	0.13-16 (4)	0.13-8 (2)	ND
<i>F. solani</i>	MIC-0	4->64 (16)	1->32 (4)	4->32 (32)	4->32 (8)	2-32 (4)	0.5-2 (1)
	MIC-1	2->64 (8)	0.5-8 (2)	2->32 (16)	2->32 (4)	1-16 (2)	ND

^a There were five isolates per species.

^b MIC-0, the lowest concentration of drug showing completely inhibition of growth (NCCLS method); MIC-1, the lowest concentration of drug showing slight growth (25%) (NCCLS method).

^c ND, not determined.

three times by the three methods against the six drugs. For each isolate, there was one reading per test. The MICs derived from the three readings by the NCCLS method and the two MTT methods were compared for each drug-isolate combination.

(i) Agreement between NCCLS and MTT methods.

The percentage of agreement between the NCCLS method and the MTT methods was defined as the proportion of MIC-0 and MIC-1 determined by MTT methods which fell within 1 dilution of the MIC-0 and MIC-1 determined by the NCCLS method, respectively, for each reading. The high and low off-scale MICs were included in the analysis by converting to the next higher or lower drug concentration, respectively. The differences were analyzed by two-way analysis of variance and were considered not statistically significant when the probability (*P*) exceeded 0.05.

(ii) Correlation of visual reading of growth with OD reduction. The correlation of the visual reading of growth with the OD reduction was estimated for each MIC endpoint by comparing the MIC-0 and MIC-1, as these were determined visually by the NCCLS method and spectrophotometrically by the MTT method (MTT-3h). The frequency of visual MICs, which fulfilled the criteria defined above for the MIC endpoints of the MTT method (at least 95 and 75% reductions of the OD for MIC-0 and MIC-1, respectively) as well as the average of percentage of OD reduction compared with the visual MIC endpoints were calculated.

(iii) Reproducibility of methods. For each method, the median of the three MICs measured was calculated and the proportion of the MICs that fell within 1 dilution of the

median was estimated. Based on these calculations, the reproducibility of each method for determining the drug-MIC endpoint was determined.

RESULTS

A total of 1,620 MICs obtained by the three methods were evaluated in this study. All the isolates produced detectable growth at 48 and 72 h. The MICs of quality control strains were within the reference ranges for the three replicates.

MIC data. The MIC ranges for both MIC endpoints obtained by the NCCLS method for six antifungal drugs against the six fungal species are summarized in Table 1. Table 1 also provides the median MIC of the three readings. In most of the endpoint-drug-species combinations, the MIC range and the median MIC were the same for the two methods, with very few exceptions with the *Fusarium* spp. The MICs were distributed over all the drug concentrations used.

Toxicity of MTT. MTT did not have any effect on the growth of the fungi at concentrations of 0.125 mg/ml and lower (Fig. 1). At the higher concentrations, MTT was toxic for *Scedosporium* spp. and *Fusarium* spp. since the growth was completely inhibited. By contrast, *Aspergillus* spp. appeared resistant to MTT even at higher concentrations.

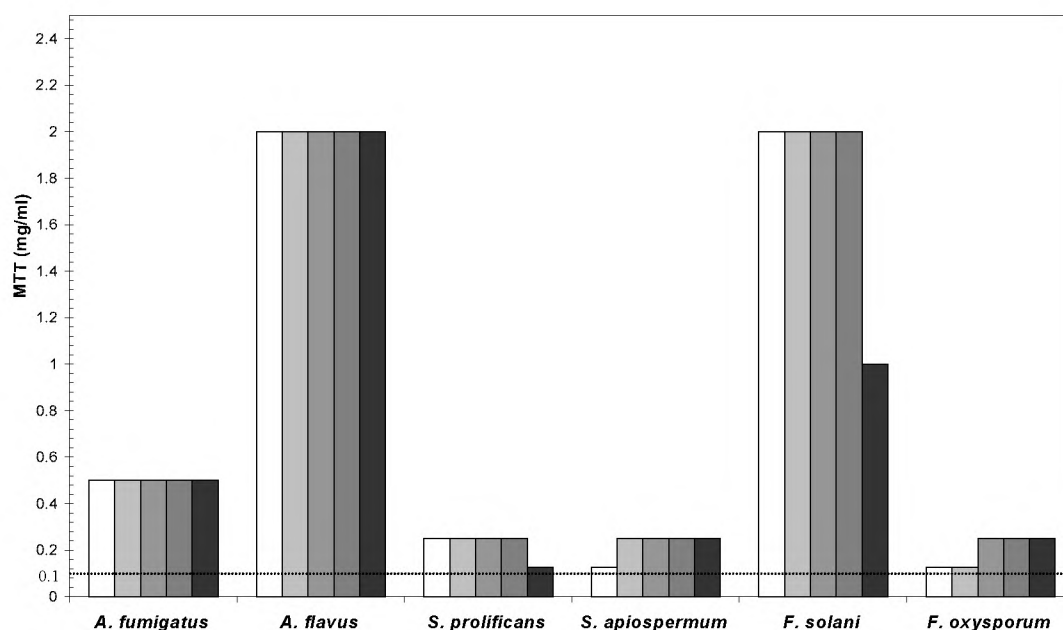


Figure 1. Toxicity of MTT for six species of filamentous fungi. The bars for each species represent each of five individual strains tested and indicate the lowest concentration of MTT at which no inhibition of growth was observed. The dotted line shows the concentration of MTT used for MIC determination (0.1 mg/ml) by the modified MTT method.

Agreement between methods. The percentages of agreement within 1 dilution between MICs obtained by the NCCLS and MTT methods for each species-drug-MIC endpoint combination are presented in Table 2. The results were stratified by antifungal agents and MIC endpoint. High levels of agreement (96% for MIC-0 and 92% for MIC-1) were found for the comparison of the NCCLS method with the MTT method. Lower levels of agreement were found when results of the modified MTT method were compared with those of the NCCLS method and the MTT method (MTT-3h). The agreement for MIC-0 was always higher than that for MIC-1. The observed differences among the methods were not statistically significant except for those derived from the comparison of the modified MTT method with the other two methods for both MIC endpoints of voriconazole and for MIC-1 of UR9825.

The levels of agreement for each drug-MIC endpoint combination between the methods were

always the highest for the *Aspergillus* spp. ($97\% \pm 2.5\%$), followed by *Scedosporium* spp. ($87\% \pm 10.3\%$). For *Fusarium* spp., the levels of agreement were relatively low ($78\% \pm 7.8\%$) (data not shown).

Representative curves of the OD and percentage of MTT conversion of miconazole against *S. apiospermum* are presented in Fig. 2. MIC-0 and MIC-1 determined visually by the NCCLS method were 1 and 0.5 mg/liter, respectively.

Correlation between visual reading of growth and OD reduction. Visual reading of growth was correlated with the colorimetric assessment of metabolic activity of fungi by comparing the results of the NCCLS method with the results of the MTT method (MTT-3h) (Table 3). The off-scale MICs were excluded from the analysis. For the MIC-0 endpoint, 84.7% of the MIC-0s of all drugs determined by the NCCLS method corresponded to a 95% or greater reduction of the OD.

Table 2. Agreement between NCCLS- and MTT- derived MICs

Drug	% Agreement within ± 1 dilution (P-value)					
	NCCLS-MTT		NCCLS-modified MTT		MTT-modified MTT	
	MIC-0	MIC-1	MIC-0	MIC-1	MIC-0	MIC-1
Miconazole	99 (0.94)	93 (0.79)	89 (0.36)	88 (0.66)	86 (0.36)	83 (0.48)
Terbinafine	92 (0.82)	84 (0.45)	93 (0.85)	78 (0.36)	94 (0.96)	75 (0.89)
Itraconazole	97 (1)	95 (0.43)	90 (0.66)	81 (0.18)	91 (0.66)	82 (0.46)
UR9825	99 (0.98)	96 (0.53)	76 (0.04)	77 (0.09)	86 (0.03)	76 (0.25)
Voriconazole	94 (0.91)	94 (0.21)	83 (0.006)	69 (0.003)	86 (0.01)	81 (0.05)
Amphotericin B	94 (0.60)		88 (0.16)		87 (0.35)	
Overall agreement	95.8	92.3	86.6	78.5	88.4	79.4

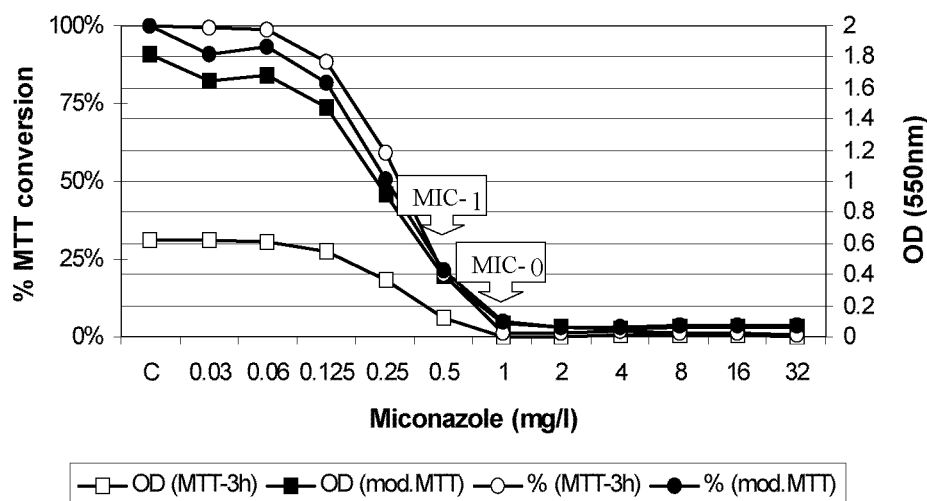


Figure 2. Testing of susceptibility of a *S. apiospermum* strain to miconazole. Representative curves generated by the MTT method (MTT-3h) and its modification (mod. MTT). The curves with the circles represent the percentage of OD reduction compared with the OD of drug-free well, and the curves with the squares represent the absorption of formed formazan at 550 nm. The MIC-0 and MIC-1 determined by the NCCLS method were 1 and 0.5 mg/l, respectively.

For the MIC-1 endpoint, 63.9% of the MIC-1s obtained by the NCCLS method corresponded to a 75% or greater reduction of the OD.

Reproducibility of methods. Overall, the three methods were very reproducible, since the levels of the reproducibility were higher than 89% for both MIC endpoints. The NCCLS method was more reproducible than the MTT methods, since the reproducibility for MIC-0 and MIC-1 were 94.8 and 93.4% for the NCCLS method compared with 94.8 and 89.5% for the MTT method and 92.8 and 89.6% for the modified MTT method, respectively. Between the two MIC endpoints, MIC-0 was more reproducible than MIC-1. For all drugs tested, the reproducibility of MIC-0 ranged from 90 to 100% and that of MIC-1 ranged from 82 to 99%. The lowest reproducibility among the drug-MIC

endpoint-method combinations was exhibited by MIC-1 of terbinafine determined by the MTT method and the modified MTT method (82 and 84%, respectively).

DISCUSSION

There are several problems in the determination of the MICs of antifungal agents, such as trailing effect caused by partial inhibition of fungal growth (8) and the subjectivity of visual reading with the aid of a magnifying mirror (16). These shortcomings are increased for filamentous fungi, which produce hyphae, making quantification of growth difficult. Moreover, the unequal growth, clumping, and adherence (13) of moulds in assay tubes makes establishing a clear

Table 3. Correlation of visually determined MICs (NCCLS MICs) with the percentages of MTT conversion, as calculated by MTT method^a

Drug	MTT conversion of isolates with NCCLS MIC-0		MTT conversion of isolates with NCCLS MIC-1			
	% of isolates with <5 % conversion	% Conversion [median (range)] ^b	% of isolates with:			% Conversion [median (range)]
			<25 %	26-50 %	51-75 %	
Miconazole	89.5	0 (0-36)	74.7	21.5	3.8	13 (0-75)
Terbinafine	76.9	2 (0-24)	53.6	31.9	14.5	24 (0-75)
Itraconazole	84.9	1 (0-30)	68.8	25.0	6.2	15.5 (0-75)
UR9825	83.3	1 (0-36)	61.3	31.2	7.5	21 (0-75)
Voriconazole	87.8	1 (0-35)	61.7	27.7	10.6	21 (0-71)
Amphotericin B	84.3	0 (0-28)				
Overall	84.7	1 (0-36)	63.9	27.6	8.5	20 (0-75)

^a Percentage of MTT conversion was calculated by comparing the OD of the drug containing well with that of the drug-free well.

^b The median and range of percentage of MTT conversion calculated by the MTT method were corresponded to MIC endpoints determined by the NCCLS method.

endpoint impossible both by visual reading as well as by spectrophotometer.

The colorimetric method using the dye MTT has been investigated as an alternative method for the NCCLS method for in vitro susceptibility testing of fungi. Its applicability was investigated for the MIC of fluconazole against 101 yeast isolates, and high levels of agreement with the NCCLS method were reported (1). In the same study, the authors found that the MICs could be determined 24 h earlier with the MTT method. Although previous studies have shown that the MTT method resulted in interpretable dose-response curves with both amphotericin B and itraconazole against *A. fumigatus* (9, 10), the applicability of the MTT method for the antifungal susceptibility testing of various filamentous fungi against different antifungal drugs and the comparison of this method with the NCCLS method (M-38P) had not been studied.

Overall, the levels of agreement between the MTT and NCCLS methods within 1 dilution were 95.8% based on MIC-0 and 92.3% based on MIC-1 (Table 2). The MTT method relies on metabolic activity of mycelia (6, 11) and, thus, not directly on growth. Any factor which influences the metabolic rate might have an effect on reduction of MTT even if the biomass remains the same. The high levels of agreement with the NCCLS method might indicate that growth corresponds directly with the metabolic status of fungi. However, different levels of agreement were found between the genera, with *Aspergillus* spp. showing higher levels of agreement ($97\% \pm 2.5\%$) than *Scedosporium* spp. ($87\% \pm 10.3\%$) and *Fusarium* spp. ($78\% \pm 7.8\%$). This could be explained by the different rates and manner of sporulation and, if true, indicates potential difficulties in developing a general, accurate, comprehensive assay for testing the susceptibility of conidium-forming filamentous fungi in vitro.

Although the microtitration plates were prepared ex novo, the two methods showed high reproducibility since the levels of agreement among the replicates were 97.6 and 96.7% (NCCLS) and 94.8 and 89.5% (MTT) based on MIC-0 and MIC-1, respectively. The lower reproducibility of MIC-1 compared with that of MIC-0 in the MTT method could be explained by the high sensitivity of the assay. Different variables in the conditions of incubation, such as batch of medium, temperature, and evaporation, might have an effect in the reduction of MTT influencing the less-stable MIC-1 endpoint to a higher degree.

The correlation of the MIC endpoints in two methods showed some discrepancies since only 84.7% of the MIC-0s determined by the NCCLS method corresponded with metabolic activity lower than 5%, as assessed by MTT conversion, and 63.9% of visually determined MIC-1s by the NCCLS method corresponded to MTT conversion lower than 25% (Table 3).

The discrepancies that occurred from the comparison of MIC endpoints were expected since the accurate method of MTT precisely quantifies the growth in each well, which is very difficult to achieve by visual reading.

In order to increase the reduction of MTT and diminish the incubation period required for the MIC determination, it has been suggested to use menadione, an electron-coupling agent that increases the reduction of MTT (3, 6, 9, 10). However, we were able to increase the reduction of MTT just by adding the dye to the inoculum and by incubating the fungi with the dye for 48 and 72 h. This resulted in a 1.5- to 5-fold increase of absorption due to the higher production of formazan (Fig. 2). To ensure that MTT does not inhibit the growth of fungi, we incubated the fungi with different concentrations of MTT. All fungi were inhibited by a high concentration of MTT, although the susceptibility varied among the species. No inhibition was observed at a concentration of 0.125 mg/ml or lower when all the isolates were incubated for 72 h with the dye (Fig. 1). Therefore, a final concentration of 0.1 mg of MTT/ml was used in the modified MTT assay.

The agreement of this new assay with the NCCLS method was lower than that of the MTT method (86.6% for MIC-0 and 78.5% for MIC-1), probably due to interexperimental variability (different plates) and its higher sensitivity, since small differences in the growth rate can result in large differences in the amount of formazan that is produced. The discrepancies for UR9825 and voriconazole were statistically significant. This could be related to the trailing effect, which might influence the results obtained by the modified MTT method more than those derived by the MTT assay. However, the modified assay was very reproducible (92.8% for MIC-0 and 89.6% for MIC-1), compared to the MTT method.

The MTT method incorporates several advantages. It is easy to perform and objective (1). The MICs of antifungal drugs can be determined rapidly since it can produce results after 24 h for *Aspergillus* spp. and 48 h for *Scedosporium* spp., although the reduction of MTT increased during prolonged incubation (unpublished observations). The MTT method is reproducible and reliable. It provides good agreement with the NCCLS method while overcoming some of its drawbacks. The main advantage of the MTT method is that it enables precise quantification of hyphal proliferation of moulds and can assess even very small differences. This property is very important in cases that interactions between combinations of antifungal agents are studied (12).

A drawback of the MTT method is the requirement of high numbers of cells, especially if they have low metabolic activity (6), in order to achieve measurable MTT reduction. Furthermore, the high

sensitivity can decrease the reproducibility in some experimental designs. The extraction of formazan crystals is performed by dissolution in organic solvents (15), which precludes direct spectrophotometric measurement of absorption (20) and prevents the assessment of fungicidal concentration of the drugs. Furthermore, an additional extraction step is required to visualize the reduction of MTT (20). Alternatively, 2,3-bis(2-methoxy-4-nitro-5-[(sulfophenylamino)carbonyl]-2H-tetrazolium-hydroxide) (XTT) could be considered an alternative since it is reduced to a water-soluble formazan product (8, 20; J. Meletiadis, unpublished observations).

In conclusion, the MTT method can be used as an alternative method to the NCCLS method since it shows high levels of agreement with the NCCLS method. The spectrophotometric reading provides more detailed information on the antifungal activity in each well. Furthermore, optimization of the MTT method may overcome the above-mentioned drawbacks. The modified assay we described in this study could be the starting point for further optimization of the MTT method.

ACKNOWLEDGMENTS

This study was supported by the European Commission Training and Mobility of Researchers grant ERBFMRXCT97-0145 to Joseph Meletiadis and by the Mycology Research Center of Nijmegen.

REFERENCES

1. Clancy, C. J., and M. H. Nguyen. 1997. Comparison of a photometric method with standardized methods of antifungal susceptibility testing of yeasts. *J. Clin. Microbiol.* **35**:2878-2882.
2. Cormican, M. G., and M. A. Pfaller. 1996. Standardization of antifungal susceptibility testing. *J. Antimicrob. Chemother.* **38**:561-578.
3. Denizot, F., and R. Lang. 1986. Rapid colorimetric assay for cell growth and survival. Modifications to the tetrazolium dye procedure giving improved sensitivity and reliability. *J. Immunol. Methods* **89**:271-277.
4. Espinel-Ingroff, A., K. Dawson, M. Pfaller, E. Anaissie, B. Breslin, D. Dixon, A. Fothergill, V. Paetznick, J. Peter, M. G. Rinaldi, and T. Walsh. 1995. Comparative and collaborative evaluation of standardization of antifungal susceptibility testing for filamentous fungi. *Antimicrob. Agents Chemother.* **39**:314-319.
5. Espinel-Ingroff, A., M. Bartlett, R. Bowden, N. X. Chin, C. Cooper, Jr., A. Fothergill, M. R. McGinnis, P. Menezes, S. A. Messer, P. W. Nelson, F. C. Odds, L. Pasarell, J. Peter, M. A. Pfaller, J. H. Rex, M. G. Rinaldi, G. S. Shankland, T. J. Walsh, and I. Weitzman. 1997. Multicenter evaluation of proposed standardized procedure for antifungal susceptibility testing of filamentous fungi. *J. Clin. Microbiol.* **35**:139-143.
6. Garn, H., H. Krause, V. Enzmann, and K. Drossler. 1990. An improved MTT assay using the electron-coupling agent menadione. *J. Immunol. Methods* **168**:253-256.
7. Hansen, M. B., S. E. Nielsen, and K. Berg. 1989. Re-examination and further development of a precise and rapid dye method for measuring cell growth/cell kill. *J. Immunol. Methods* **119**:203-210.
8. Hawser, S. P., H. Norris, C. J. Jessup, and M. A. Ghannoum. 1998. Comparison of a 2,3-bis(2-methoxy-4-nitro-5-sulfophenyl)-5-(phenylamino) carbonyl-2H-tetrazolium hydroxide (XTT) colorimetric method with the standardized National Committee for Clinical Laboratory Standards method of testing clinical yeast isolates for susceptibility to antifungal agents. *J. Clin. Microbiol.* **36**:1450-1452.
9. Jahn, B., E. Martin, A. Stueben, and S. Bhakdi. 1995. Susceptibility testing of *Candida albicans* and *Aspergillus* species by a simple microtiter menadione-augmented 3-(4,5-dimethyl-2-thiazolyl)-2,5-diphenyl-2H-tetrazolium bromide assay. *J. Clin. Microbiol.* **33**:661-667.
10. Jahn, B., A. Stueben, and S. Bhakdi. 1996. Colorimetric susceptibility testing for *Aspergillus fumigatus*: comparison of menadione-augmented 3-(4,5-dimethyl-2-thiazolyl)-2,5-diphenyl-2H-tetrazolium bromide and Alamar blue tests. *J. Clin. Microbiol.* **34**:2039-2041.
11. Levitz, S. M., and R. D. Diamond. 1985. A rapid colorimetric assay of fungal viability with the tetrazolium salt MTT. *J. Infect. Dis.* **152**:938-945.
12. Meletiadis, J., J. W. Mouton, J. L. Rodriguez-Tudela, J. F. G. M. Meis, and P. E. Verweij. 2000. In vitro interaction of terbinafine with itraconazole against clinical isolates of *Scedosporium prolificans*. *Antimicrob. Agents Chemother.* **44**:470-472.
13. Meshulam, T., S. M. Levitz, L. Christin, and R. D. Diamond. 1995. A simplified new assay for assessment of fungal cell damage with the tetrazolium dye, (2,3)-bis-(2-methoxy-4-nitro-5-sulphenyl)-(2H)-tetrazolium-5-carboxanilide (XTT). *J. Infect. Dis.* **172**:1153-1156.
14. National Committee for Clinical Laboratory Standards. 1998. Reference method for broth dilution antifungal susceptibility testing of conidium forming filamentous fungi. Proposed standard M38-P. National Committee for Clinical Laboratory Standards, Wayne, Pa.
15. Niks, M., and M. Otto. 1990. Towards an optimized MTT assay. *J. Immunol. Methods* **130**:149-151.
16. Pfaller, M. A., and M. G. Rinaldi. 1993. Antifungal susceptibility testing. Current state of technology, limitations, and standardization. *Infect. Dis. Clin. N. Am.* **7**:435-444.
17. Pfaller, M. A., Q. Vu, M. Lancaster, A. Espinel-Ingroff, A. Fothergill, C. Grant, M. R. McGinnis, L. Pasarell, M. G. Rinaldi, and L. Steele-Moore. 1994. Multisite reproducibility of colorimetric broth microdilution method for antifungal susceptibility testing of yeast isolates. *J. Clin. Microbiol.* **32**:1625-1628.

18. **Pujol, I., J. Guarro, C. Llop, L. Soler, and J. Fernandez-Ballart.** 1996. Comparison study of broth macrodilution and microdilution antifungal susceptibility tests for the filamentous fungi. *Antimicrob. Agents Chemother.* **40**:2106-2110.
19. **Rex, J. H., M. A. Pfaller, M. G. Rinaldi, A. Polak, and J. N. Galgiani.** 1993. Antifungal susceptibility testing. *Clin. Microbiol. Rev.* **6**:367-381.
20. **Roehm, N. W., G. H. Rodgers, S. M. Hatfield, and A. L. Glasebrook.** 1991. An improved colorimetric assay for cell proliferation and viability utilizing the tetrazolium salt XTT. *J. Immunol. Methods* **142**:257-265.



Chapter 2.3

Colorimetric Assay for Antifungal Susceptibility Testing of *Aspergillus* Species

Journal of Clinical Microbiology 2001; 39: 3402-3408

COLORIMETRIC ASSAY FOR ANTIFUNGAL SUSCEPTIBILITY TESTING OF *ASPERGILLUS* SPECIES

JOSEPH MELETIADIS¹, JOHAN W. MOUTON², JACQUES F. G. M. MEIS², BIANCA A. BOUMAN¹, J. PETER DONNELLY³, PAUL E. VERWEIJ¹, AND EUROFUNG NETWORK*

Departments of Medical Microbiology¹ and Hematology³, University Medical Center Nijmegen, and Department of Medical Microbiology and Infectious Diseases, Canisius-Wilhelmina Hospital², Nijmegen, The Netherlands

A colorimetric assay for antifungal susceptibility testing of *Aspergillus* species (*Aspergillus fumigatus*, *Aspergillus flavus*, *Aspergillus terreus*, *Aspergillus nidulans*, and *Aspergillus ustus*) is described based on the reduction of the tetrazolium salt 2,3-bis{2-methoxy-4-nitro-5-[(sulphenylamino) carbonyl]-2H-tetrazolium-hydroxide} (XTT) in the presence of menadione as an electron-coupling agent. The combination of 200 µg of XTT/ml with 25 µM menadione resulted in a high production of formazan within 2 h of exposure, allowing the detection of hyphae formed by low inocula of 10² CFU/ml after 24 h of incubation. Under these settings, the formazan production correlated linearly with the fungal biomass and less-variable concentration effect curves for amphotericin B and itraconazole were obtained.

Tetrazolium salts are heterocyclic organic compounds that substitute the natural final acceptor (oxygen) in the biological redox process and are reduced to formazan derivatives by receiving electrons enzymically from substances of the hydrogen transport system or nonenzymically from artificial electron transporters (phenazine methosulfate and menadione), which enhance the reaction. Tetrazolium salts can penetrate rapidly into intact cells and directly into subcellular membranes with dehydrogenase activity, where they are converted to colored formazan derivatives (1, 14). Therefore, they were used as indicators of reducing systems. The tetrazolium salt MTT has been used for antifungal susceptibility testing of various yeasts and filamentous fungi, and testing was in agreement with the corresponding standard methods recommended by the National Committee for Clinical Laboratory Standards (NCCLS) (2, 7, 11). The disadvantage of MTT, however, is that the process includes the solubilization of formazan derivatives. As an alternative, a new tetrazolium salt, 2,3-bis{2-methoxy-4-nitro-5-[(sulphenylamino) carbonyl]-2H-tetrazolium-hydroxide} (XTT) (10), has been employed for antifungal susceptibility testing of yeasts and resulted in

clear-cut endpoints for various antifungal agents (4, 15). XTT is converted into a water-soluble formazan, thereby avoiding the additional steps for the solubilization of formazan derivatives (8, 12), but needs the presence of an electron-coupling agent. The nature and the concentration of this agent are critical in order to obtain a good correlation between the formazan production and the number of viable fungi and less-variable concentration effect curves (1, 15).

We developed a colorimetric assay for the quantification of fungal growth of five different *Aspergillus* species based on the tetrazolium salt XTT by standardizing various factors that influence XTT conversion. This assay was also tested in the presence of antifungal drugs in order to ascertain its potential for antifungal susceptibility testing of filamentous fungi.

MATERIALS AND METHODS

Isolates. Two clinical isolates of *Aspergillus fumigatus* [AZN5161 (S) and AZN 5241 (R)] and one each of *Aspergillus flavus* (AZN 510), *Aspergillus terreus* (AZN 7320), *Aspergillus nidulans* (AZN 8933), and *Aspergillus ustus* (AZN 9420) from our private collection was selected, and *Candida parapsilosis* (ATCC 22019) and *Candida krusei* (ATCC 6258) were used for quality control. Isolates were revived by subculturing them twice onto Sabouraud glucose agar (SAB) plates with chloramphenicol first at 30°C and then at 37°C for 5 to 7 days. Conidia were collected with a swab and suspended in sterile saline containing 0.05% Tween 20. After the heavy particles were allowed to settle for 5 to 10 min, the turbidity of the supernatants were measured spectrophotometrically (Spectronic 20D; Milton Roy, Rochester, N.Y.) at 530 nm and transmission was adjusted to 80 to 82%, corresponding to an inoculum size of 1 × 10⁶ to 5 × 10⁶ CFU/ml. The inoculum size was confirmed by plating serial dilutions of conidia suspensions on SAB plates.

*EC-TMR-EUROFUNG network (ERBFMRXCT97-0145). The Eurofung Network consists of the following participants: Emmanuel Roilides and Nicos Maglaveras, Aristotle University, Thessaloniki, Greece; Tore Abrahamsen and Peter Gaustad, Rikshospitalet National Hospital, Oslo, Norway; David W. Denning, University of Manchester, Manchester, United Kingdom; Paul E. Verweij and Jacques F. G. M. Meis, University of Nijmegen, Nijmegen, The Netherlands; Juan L. Rodriguez-Tudela, Instituto de Salud Carlos III, Madrid, Spain; and George Petrikos, Athens University, Athens, Greece.

Medium. RPMI 1640 medium (with L-glutamine; without bicarbonate) (GIBCO BRL, Life Technologies, Woerden, The Netherlands) buffered to pH 7.0 with 0.165 M 3-*N*-morpholinopropanesulfonic acid (MOPS) (Sigma-Aldrich Chemie GmbH, Steinheim, Germany) was used throughout.

XTT. XTT (Sigma Chemical, St. Louis, Mo.) was dissolved in saline at a final concentration of 1 mg/ml. The solution was filtered through a 0.22 μ m-pore-size filter.

Electron-coupling agents. Two electron acceptors were evaluated, menadione (Sigma-Aldrich Chemie GmbH) and phenazine methosulfate (PMS) (Sigma-Aldrich Chemie GmbH). Menadione was first dissolved in acetone at a concentration of 10 mM and was then diluted 1:10 in saline. PMS was directly dissolved in saline at a final concentration of 1 mM. Further dilutions of both agents were made in saline.

Antifungal drugs. Itraconazole (Janssen-Cilag, Beerse, Belgium) and amphotericin B (Bristol-Myers Squibb, Woerden, The Netherlands) were dissolved in dimethyl sulfoxide (DMSO) at final concentrations of 3,200 and 1,600 mg/liter, respectively.

XTT assay. Conidia suspensions of each species were diluted 1:100 in the medium, and 200 μ l was inoculated in 96-well flat-bottom microtitration plates (Costar, Corning, N.Y.). After 24 or 48 h of incubation at 37°C, 50- μ l aliquots of various concentrations of XTT with either menadione or PMS were added to the wells in order to obtain final concentrations of 200, 100, and 50 μ g of XTT/ml and 100, 25, 6.25, 1.56, and 0.39 μ M menadione or PMS. The microtitration plates were incubated further for 6 h at 37°C and the optical density at 450 nm (OD_{450}) was measured at hourly intervals by spectrophotometer (Rosys Anthos ht3; Anthos Labtec Instruments GmbH, Salzburg, Austria). The XTT assay was performed for each species in triplicate and the ODs after 1, 2, and 4 h of exposure to various concentrations of XTT and the two electron coupling agents of fungi incubated for 24 and 48 h were plotted.

Quantitative assay of fungal viability. The relationship between the number of viable fungi and the amount of XTT reduction was tested by incubating various inocula of *Aspergillus* conidia (10^2 to 10^6 CFU/ml) with XTT and various concentrations of menadione. Conidia suspensions were diluted 1:10 serially in the medium to up to 10^2 CFU/ml. Then, 96-well flat-bottom microtitration plates were inoculated with 200 μ l of each conidia dilution. After 24 h of incubation at 37°C, 50- μ l aliquots of XTT and various concentrations of menadione were added to each well in order to obtain final concentrations of 200 μ g/ml for XTT and 100, 25, 6.25, 1.56, and 0.39 μ M for menadione. The microtitration plates were then incubated for another 2 h, after which 100 μ l of the supernatant of each well was transferred in clean wells. The OD_{450} was measured spectrophotometrically. This experiment was performed in triplicate for each species, and the data were analyzed by linear regression analysis. Regression lines were plotted for each concentration of menadione and for each species, together with the 95% confidence intervals. The slopes and the r^2 of each regression line were reported as an estimation of steepness of the line and the goodness of fit, respectively. An r^2 value of

1 indicates perfect correlation. The nonlinearity of the curves was checked by a runs test following the linear regression.

Antifungal susceptibility assay. Stock solutions of antifungal drugs were serially diluted twofold in DMSO, and then each drug concentration was diluted 1:50 in the medium in order to obtain twofold final concentrations which ranged from 0.015 to 16 mg of amphotericin B/liter and 0.03 to 32 mg of itraconazole/liter. Wells of 96-well flat-bottom microtitration plates were filled with 100 μ l of each drug concentration. A drug-free well containing 2% DMSO in the medium served as the growth control. Each well was inoculated with 100 μ l of conidia suspensions diluted 1:50 in medium in order to obtain a final inoculum of 1×10^4 to 5×10^4 CFU/ml. The plates were incubated for 24 or 48 h at 37°C, and the MIC-0 was determined visually by four different observers to be the lowest drug concentration showing no visible growth (NCCLS) (9). Afterwards, the OD of each well at 405 nm was measured in order to quantify the biomass of fungal growth (spectrophotometric method). Then, 50 μ l of XTT-menadione was added to each well in order to obtain final concentrations of 200 μ g/ml and 25 μ M, respectively. After 2 h of further incubation, the OD of each well at 450 nm was measured in order to quantify the formazan production (colorimetric method). Background OD was obtained by spectrophotometric measurements of noninoculated wells processed in the same way as the inoculated wells. The relative ODs for each well based on both measurements at 405 and 450 nm were calculated (in percent) based on the following equation: [(OD of drug containing well – background OD)/(OD of drug-free well – background OD of drug-free well)] \times 100%. The tests were carried out in triplicate in three independent experiments for each strain. Results from each experiment were analyzed by nonlinear regression analysis by using a four parameter logistic model (sigmoid curve with variable slope) known as the E_{\max} model, which is described by the following equation: $E = E_{\max} \times (D/EC_{50})^m / [1 + (D/EC_{50})^m]$, where E is the relative OD (dependent variable), E_{\max} is the maximum relative OD, D is the drug concentration (independent variable), EC_{50} is the drug concentration producing 50% of the E_{\max} , and m is the slope that describes the steepness of the curve (3). Since data were normalized by using the relative ODs, the top and the bottom of the E_{\max} model corresponded to 100 and 0%, respectively. Analysis was carried out using the GraphPad Prism Software (San Diego, Calif.). Deviation from the model was tested by the runs test, and goodness of fit was checked by the r^2 values. In order to compare the concentration effect curves generated by the spectrophotometric and colorimetric methods, the best-fit values of EC_{50} and slope (m) obtained by the regression analysis were used. The differences between the best-fit values of the concentration effect curves for all species were analyzed by analysis of variance followed by a Bonferroni post test. The significance level of 0.05 was chosen.

RESULTS

XTT assay. The tetrazolium salt XTT was not metabolized by any of the *Aspergillus* species until an

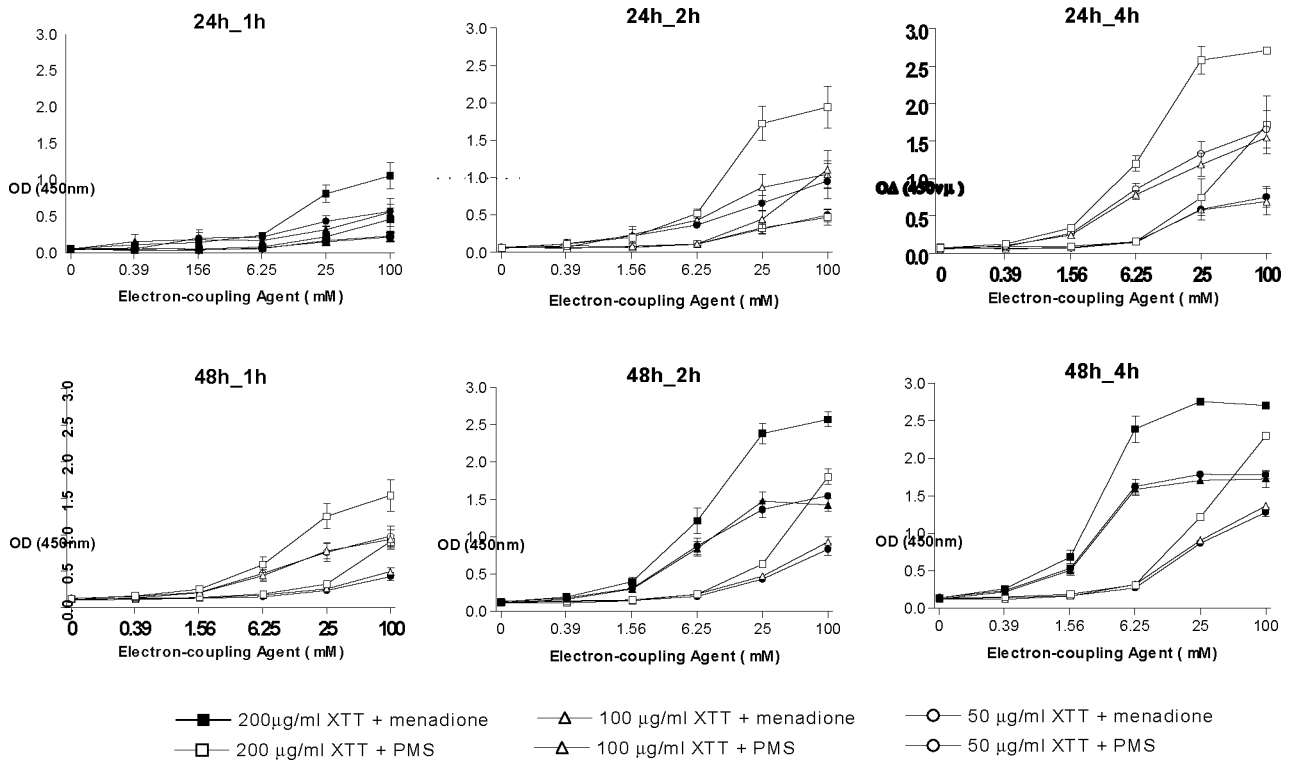


Figure 1. XTT reduction by *Aspergillus* species. The *Aspergillus* strains were incubated for 24 or 48 h and were then exposed for 1, 2, and 4 h to various concentrations of XTT, 200 (squares), 100 (triangles) and 50 (circles) µg/ml, combined with menadione (close symbols) or PMS (open symbols) at various concentrations (0.39, 1.56, 6.25, 25, and 100 µM). Each data point represents the average of all strains tested in triplicate.

electron-coupling agent was added. Conversion of XTT by a certain amount of hyphae depended on the concentration of XTT and the exposure time as well as the electron-coupling agent and its concentration (Fig. 1). Between the three concentrations of XTT used, 200 µg/ml resulted in two-times-higher formazan production than 100 and 50 µg/ml, for which the formazan production was similar. Among the two electron-coupling agents, menadione was eight times more potent than PMS for all *Aspergillus* species. The use of PMS resulted in a background absorbance higher than that of menadione, especially at the concentration of 100 µM, where the OD of the blank after 6 h of exposure was 0.805 for PMS and 0.347 for menadione. Relatively lower background absorbances (≈ 0.2) were observed at maximal concentrations of 25 µM menadione and 1.56 µM PMS (data not shown). Any increase of menadione concentration beyond 25 µM did not have any effect in formazan production when XTT was exposed for longer than 2 h to fungi which were incubated for 48 h.

Quantitative assay of fungal viability. The relationship between the XTT conversion and increasing inocula of *Aspergillus* species was tested using 200 µg of XTT/ml with 25 µM menadione after 2 h of exposure. The analysis of results showed a linear relationship between the OD and log CFU (Fig. 2). The

slopes and the coefficients obtained by the regression analysis depended on the concentration of menadione used for each species.

A general pattern of concentration dependence was observed for all five species. At menadione concentrations lower than 1.56 µM, low XTT conversion rates were apparent (slopes ranged between 0.01 and 0.13) for all species. For *A. nidulans* and *A. flavus*, low conversion rates were also observed at a menadione concentration of 6.25 µM (Table 1). The conversion rates increased at higher concentrations of menadione, generating higher slopes, up to 0.65, as in the case of *A. terreus* with 100 µM menadione. However, at this concentration of menadione, larger deviations from linearity were observed for all species (except *A. ustus*) and very low slopes were obtained for *A. fumigatus* (R) and *A. flavus* (0.05 and 0.22, respectively). In addition, at the concentration of 100 µM menadione, formazan production exceeded an OD of 3 after 4 h of exposure of XTT, which was the detection limit of the spectrophotometer, especially when hyphae were exposed to XTT after 48 h of incubation.

Among the different concentrations of menadione that were evaluated, relatively higher conversion rates and more linear relationships between formazan production and viable fungi were generated with the concentration of 25 µM for all species (Table 1). In ad-

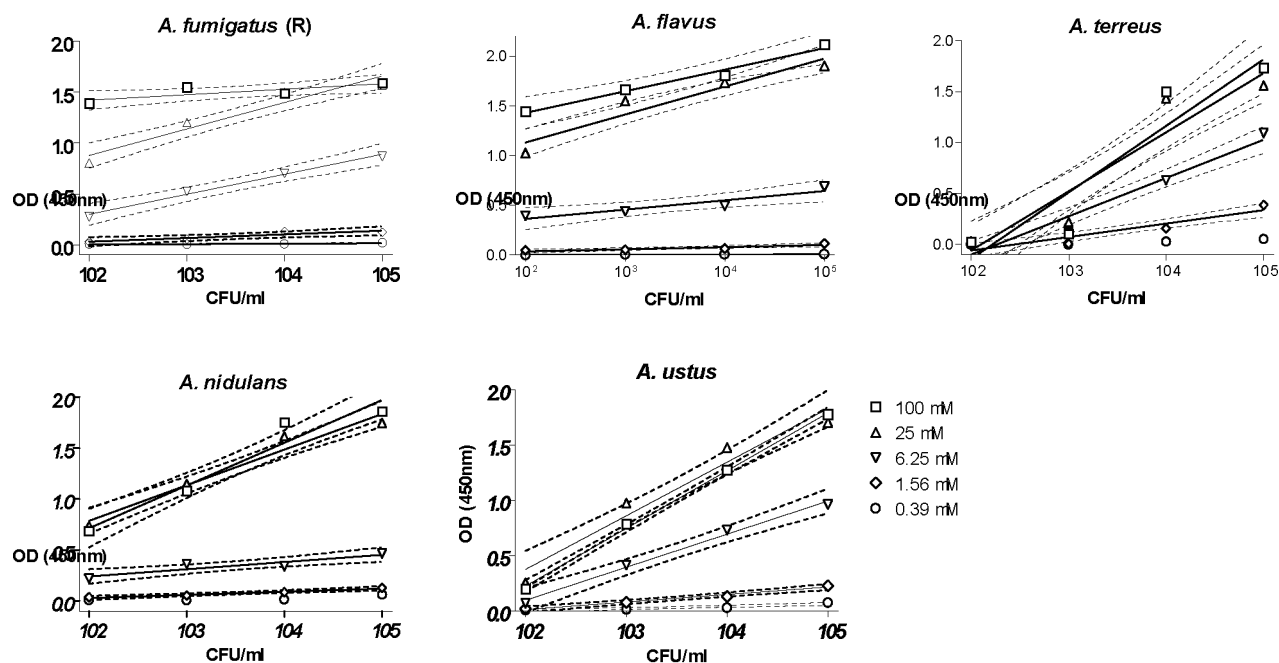


Figure 2. Relationship between the amount of XTT and increasing inocula of each *Aspergillus* species. The reduction of 200 μ g of XTT/ml in the presence of various concentrations of menadione (0.39, 1.56, 6.25, 25, and 100 μ M) was tested in triplicate for each strain. The symbols are the means of the triplicates, and the lines were generated by linear regression analysis. Dotted lines represent the 95% confidence intervals of the regression lines.

dition, the formazan production at this concentration was high within 2 h of exposure without exceeding the detection limit of the spectrophotometer (OD of 3) and low background absorbance was obtained.

Antifungal susceptibility assay. For all *Aspergillus* species, the NCCLS MICs of amphotericin B ranged from 0.5 to 4 mg/liter and those of itraconazole ranged from 0.25 to 0.5 mg/liter except for *A. fumigatus* (R) and for *A. ustus*, for which the MICs were higher than 2 mg/liter (Table 2). Concentration effect curves based on the conversion of XTT by hyphae are shown in Fig. 3 (right-hand). All curves show similar patterns and are characterized by two plateaus connected by a drop in relative OD. In the case of a resistant strain, significant XTT conversion was observed in higher concentrations [*A. ustus* and

A. fumigatus (R) against itraconazole; Fig. 3]. The three phases of XTT conversion were clearly distinguishable for amphotericin B, for which steep concentration effect curves were obtained. In contrast, for itraconazole, more shallow curves were generated.

The concentration effect curves obtained by the colorimetric and the spectrophotometric assessments of fungal growth (Fig. 3) were analyzed by the E_{\max} model with variable slope, and the best-fit values of the two variables EC_{50} and slope (m) were compared for each species, drug, and incubation period. The model fitted the data very well since the r^2 ranged between 0.85 and 0.99 (median, 0.95) and no statistically significant deviations from the model were found ($P > 0.1$). No statistically significant differences were found by analysis of variance between the best-fit values of the

Table 1. Results of linear regression analysis of the relationship between the amount of XTT reduction in the presence of different concentrations of menadione and increasing inocula of each *Aspergillus* species after 24 h of incubation^a

Species	Relationship between menadione concentration and <i>Aspergillus</i> inoculum (log CFU/ml)									
	100 μ M		25 μ M		6.25 μ M		1.563 μ M		0.39 μ M	
	Slope	r^2	Slope	r^2	Slope	r^2	Slope	r^2	Slope	r^2
<i>A. fumigatus</i> (R)	0.05	0.368	0.26	0.884	0.20	0.853	0.04	0.524	0.01	0.359
<i>A. flavus</i>	0.22	0.756	0.28	0.873	0.09	0.549	0.02	0.671	0.01	0.529
<i>A. terreus</i>	0.65	0.869	0.57	0.878	0.38	0.934	0.13	0.862	0.02	0.745
<i>A. nidulans</i>	0.42	0.894	0.35	0.929	0.07	0.635	0.03	0.787	0.02	0.462
<i>A. ustus</i>	0.52	0.994	0.49	0.936	0.30	0.926	0.08	0.908	0.02	0.802

^a Each replicate was analyzed as a separate point. Data used for calculations were OD and log CFU.

Table 2. Best-fit values and the 95% CIs obtained by non-linear regression analysis^a

Drug and incubation period	Species	Results of antifungal susceptibility assay				
		MICs-0 (NCCLS) ^b	EC ₅₀ ± 95% CI (mg/l)		Slope <i>m</i> ± 95% CI	
			SP	XTT	SP	XTT
AB, 24 h	<i>A. fumigatus</i> (S)	0.5 (0.125-0.5)	0.20 ± 0.05	0.22 ± 0.04	-1.65 ± 0.63	-2.18 ± 0.78
	<i>A. fumigatus</i> (R)	2 (1-4)	0.51 ± 0.06	0.38 ± 0.11	-7.04 ± 7.04	-1.33 ± 0.44
	<i>A. flavus</i>	1 (0.5-1)	0.42 ± 0.19	0.65 ± 0.08	-1.27 ± 0.61	-7.33 ± 3.18
	<i>A. nidulans</i>	1 (1-4)	0.21 ± 0.09	0.33 ± 0.03	-1.47 ± 0.72	-4.11 ± 1.09
	<i>A. terreus</i>	1 (1-2)	0.27 ± 0.12	0.66 ± 0.10	-1.00 ± 0.41	-8.69 ± 4.71
	<i>A. ustus</i>	2 (1-2)	0.47 ± 0.09	0.35 ± 0.12	-3.58 ± 2.56	-1.11 ± 0.34
AB, 48 h	<i>A. fumigatus</i> (S)	1	0.41 ± 0.07	0.37 ± 0.05	-2.88 ± 1.25	-5.09 ± 2.14
	<i>A. fumigatus</i> (R)	4 (2-4)	1.13 ± 0.93	1.00 ± 0.68	-6.42 ± 6.42	-1.22 ± 0.51
	<i>A. flavus</i>	1 (1-2)	0.73 ± 0.18	1.23 ± 0.14	-2.94 ± 1.79	-8.41 ± 4.29
	<i>A. nidulans</i>	2 (2-4)	0.25 ± 0.10	1.09 ± 0.12	-1.24 ± 0.51	-5.10 ± 3.98
	<i>A. terreus</i>	4 (2-4)	0.63 ± 0.16	0.96 ± 0.09	-2.67 ± 1.54	-7.00 ± 7.00
	<i>A. ustus</i>	2 (1-2)	0.27 ± 0.09	0.45 ± 0.13	-1.08 ± 0.37	-1.14 ± 0.31
ICZ, 24 h	<i>A. fumigatus</i> (S)	0.5 (0.5-1)	0.15 ± 0.02	0.16 ± 0.04	-1.26 ± 0.23	-1.39 ± 0.42
	<i>A. fumigatus</i> (R)	>32	6.27 ± 5.80	> 32	-0.42 ± 0.17	-0.24 ± 0.12
	<i>A. flavus</i>	0.25 (0.25-0.5)	0.07 ± 0.01	0.09 ± 0.02	-1.42 ± 0.25	-1.64 ± 0.54
	<i>A. nidulans</i>	0.5 (0.25-0.5)	0.07 ± 0.01	0.10 ± 0.01	-2.54 ± 0.86	-1.86 ± 0.41
	<i>A. terreus</i>	0.5 (0.25-0.5)	0.07 ± 0.02	0.05 ± 0.01	-1.46 ± 0.44	-1.32 ± 0.21
	<i>A. ustus</i>	2 (0.5->32)	0.20 ± 0.08	0.37 ± 0.08	-0.89 ± 0.26	-1.83 ± 0.61
ICZ, 48 h	<i>A. fumigatus</i> (S)	1 (0.5-1)	0.15 ± 0.03	0.17 ± 0.05	-1.26 ± 0.27	-1.33 ± 0.40
	<i>A. fumigatus</i> (R)	>32	> 32	> 32	-0.04 ± 0.04	0.00 ± 0.00
	<i>A. flavus</i>	0.5	0.07 ± 0.01	0.21 ± 0.01	-1.17 ± 0.18	-6.06 ± 1.92
	<i>A. nidulans</i>	0.5 (0.25-0.5)	0.08 ± 0.01	0.17 ± 0.02	-3.44 ± 1.44	-1.87 ± 0.43
	<i>A. terreus</i>	0.5 (0.5-1)	0.11 ± 0.02	0.09 ± 0.02	-1.63 ± 0.53	-1.36 ± 0.33
	<i>A. ustus</i>	>32	0.48 ± 0.22	3.34 ± 1.41	-0.56 ± 0.16	-0.53 ± 0.12

^a Data were obtained by nonlinear regression analysis using the E_{max} model with variable slopes for the concentration effect curves obtained by spectrophotometric (SP) and colorimetric (XTT) methods after 24 and 48 h of incubation with serial twofold dilutions of amphotericin B (AB) and itraconazole (ICZ). 95% CI, 95% confidence intervals.

^b Data were the most frequently observed MIC and the range of MICs. MICs were determined visually by four different observers and three independent experiments.

two concentration effect curves for each drug and incubation period ($P > 0.05$) with the exception of the concentration effect curves of amphotericin B after 48 h, where statistically significantly steeper curves (higher absolute m values) were obtained by the colorimetric method than by the spectrophotometric method ($P < 0.01$). However, the slopes and the EC₅₀s of the fitted model were similar for the concentration effect curves obtained by the two methods (Table 2). Overall, the median coefficient variation of the log EC₅₀s and the slope m of the fitted model for the six strains among the replicates was 22 and 25%, respectively, for the colorimetric method and 37 and 38%, respectively, for the spectrophotometric method. Furthermore, the discrimination between the in vitro itraconazole-resistant strains and the other itraconazole-susceptible strains was clearer in concentration effect curves of the colorimetric method than those of spectrophotometric method (Fig. 3).

DISCUSSION

The tetrazolium salt XTT was converted by *Aspergillus* species only in the presence of an electron-coupling agent, as was found with yeasts (14). As opposed to mammalian cells (12) but similar to yeasts (15), among the two electron-coupling agents tested menadione was more potent than PMS. Since PMS exhibited a background higher than that found in previous studies (12, 13) and inhibitory effects at elevated concentrations were reported previously (1), menadione was chosen as the electron-coupling agent for the XTT assay of *Aspergillus* species.

The concentration of XTT is another important factor since it was found that high concentrations of XTT result in inhibition of formazan production while very low concentrations can result in poor conversion (15). No inhibition was observed among the three concentrations tested in this study. Preliminary studies showed that XTT was not toxic for conidia (unpublished

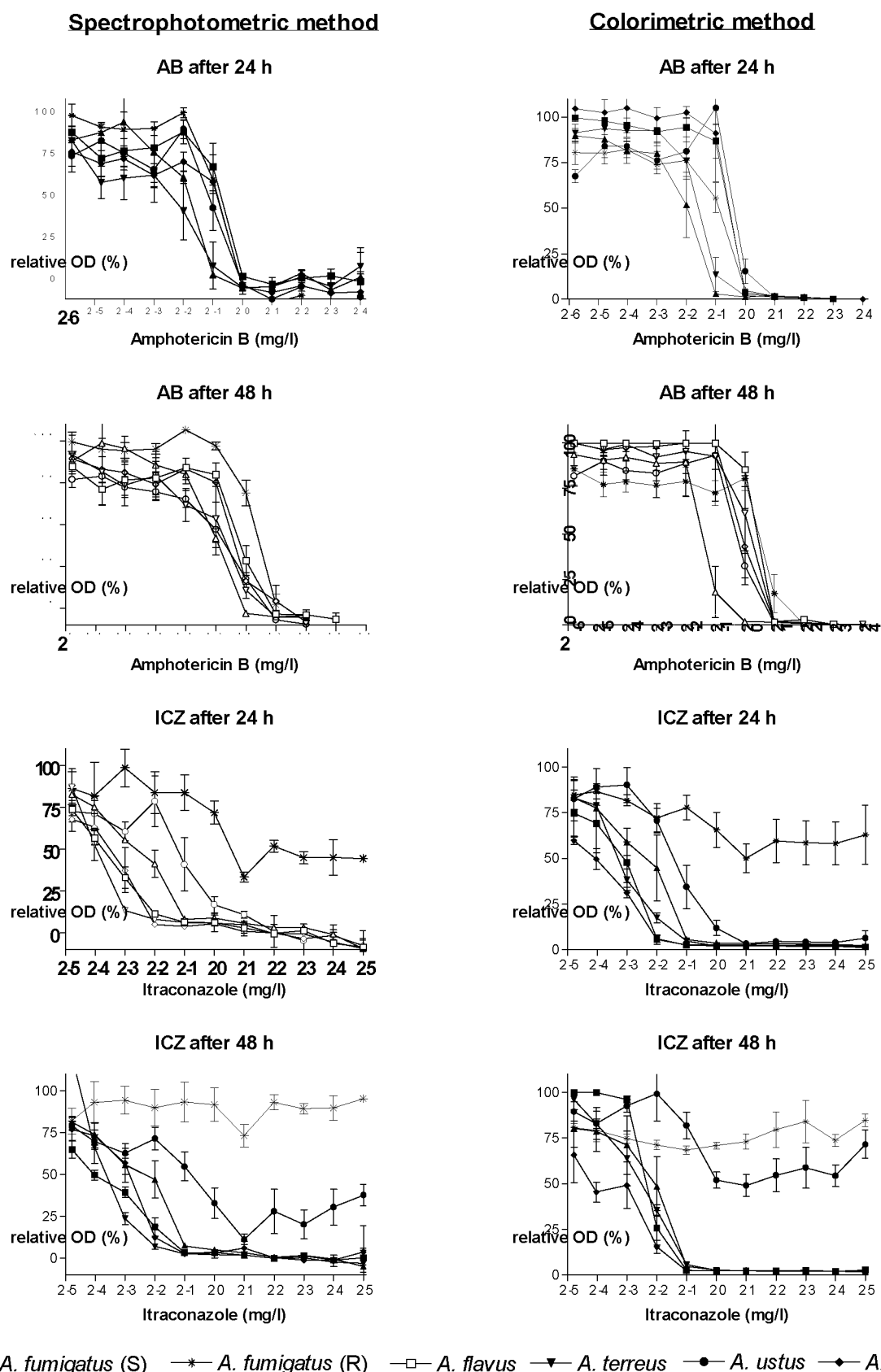


Figure 3. Concentration effect curves for amphotericin B (AB) and itraconazole (ICZ). Conidia of each *Aspergillus* spp. tested were incubated for 24 and 48 h and the OD of hyphal growth at 405 nm was measured for each well. Then, hyphae were exposed to 200 μ g of XTT/ml plus 25 μ M of menadione for 2 h and the OD at 450 nm was measured. Concentration effect curves based on the spectrophotometric method (left-hand) and colorimetric method (right-hand) were constructed, and the relative ODs for each drug concentration represent the amount of formazan produced and the fungal biomass, respectively, for each method compared with the growth control. *A. ustus* and *A. fumigatus* (R) showed NCCLS MICs higher than 2 mg of itraconazole/liter. Means with the standard errors of triplicates are represented for each strain.

observation). At higher concentrations of XTT (200 µg/ml), the rate of formazan production increased rapidly. Therefore, a concentration of 200 µg of XTT/ml was used for further studies. XTT and menadione at the above concentrations were stable when they were stored separately for up to 3 months at room temperature and 4, -20, and -70°C (unpublished data).

The linear relationship between the formazan production using 200 µg of XTT/ml and menadione with increasing inocula of *Aspergillus* species indicates that the XTT assay is a reliable indicator of fungal biomass. The linearity and the slopes of this relationship depended on the concentration of menadione for each of the *Aspergillus* species. At a concentration of 25 µM, high coefficients and slopes for all *Aspergillus* species tested were found, unlike with yeasts, for which lower concentrations of menadione (1 µM) were required to generate a linear relation between XTT conversion and CFU (15). For *Aspergillus* species, menadione concentrations higher than 25 µM generated a less linear CFU-OD relationship, which explains the conclusions of Jahn et al., who found that when XTT was used with 1,000 µM menadione, a less-well-defined correlation was observed (5).

The XTT assay was applied in the presence of antifungal drugs generating less-variable concentration effect curves. For amphotericin B, clear-cut endpoints were obtained since XTT conversion was absent once the MIC was exceeded, as was found previously (15). For itraconazole, shallow concentration effect curves were obtained due to a partial inhibition of growth and possible interference of the drug in the metabolic status of fungi. Furthermore, as was found in a previous study (14), discrimination between susceptible and resistant strains may be facilitated by using the XTT assay since resistant strains converted XTT even at a high concentration of antifungal drugs.

The need for the use of menadione in the XTT assay described here offers the possibility of increasing the sensitivity of this assay by adjusting the concentration of menadione. In this way, it would be possible to detect the metabolic capacity of slow-growing fungi. Also, incubation periods proposed by the NCCLS to determine the MICs may be shortened if conversion of XTT of the growth control is sufficient. However, the development of a tetrazolium salt which might not require the addition of an electron-coupling agent would be a favorable step since the need of an electron-coupling agent complicates the assay more and may increase variability (13). Variability may also be increased by the lack of a step for the termination of XTT conversion since small variation in incubation time would influence the formazan production.

In conclusion, the XTT-menadione system described in this study provides an assay which enables the quantification of metabolic activity of *Aspergillus* species and which could be applied for other filamentous fungi like it was shown with MTT (7).

ACKNOWLEDGMENTS

This work was supported by the European Commission Training and Mobility of Researchers grant ERBFMRXCT97-0145 to Joseph Meletiadis and by the Mycology Research Center of Nijmegen.

REFERENCES

1. Altman, F. L. 1976. Tetrazolium salts and formazans. *Prog. Histochem. Cytochem.* **9**:1-52.
2. Clancy, C. J., and M. H. Nguyen. 1997. Comparison of a photometric method with standardized methods of antifungal susceptibility testing of yeasts. *J. Clin. Microbiol.* **35**:2878-2882.
3. Greco, W. R., G. Bravo, and J. C. Parsons. 1995. The search for synergy: a critical review from a response surface perspective. *Pharmacol. Rev.* **47**:331-385.
4. Hawser, S. P., H. Norris, C. J. Jessup, and M. A. Ghannoum. 1998. Comparison of a 2,3-bis(2-methoxy-4-nitro-5-sulphophenyl)-5-(phenylamino) carbonyl]-2H-tetrazolium hydroxide (XTT) colorimetric method with the standardized National Committee for Clinical Laboratory Standards method of testing clinical yeast isolates for susceptibility to antifungal agents. *J. Clin. Microbiol.* **36**:1450-1452.
5. Jahn, B., E. Martin, A. Stueben, and S. Bhakdi. 1995. Susceptibility testing of *Candida albicans* and *Aspergillus* species by a simple microtiter menadione-augmented 3-(4,5-dimethyl-2-thiazolyl)-2,5-diphenyl-2H-tetrazolium bromide assay. *J. Clin. Microbiol.* **33**:661-667.
6. Levitz, S. M., and R. D. Diamond. 1985. A rapid colorimetric assay of fungal viability with the tetrazolium salt MTT. *J. Infect. Dis.* **152**:938-945.
7. Meletiadis, J., J. F. G. M. Meis, J. W. Mouton, J. P. Donnelly, and P. E. Verweij. 2000. Comparison of NCCLS and 3-(4,5-dimethyl-2-Thiazyl)-2,5-diphenyl-2H-tetrazolium bromide (MTT) methods of in vitro susceptibility testing of filamentous fungi and development of a new simplified method. *J. Clin. Microbiol.* **38**:2949-2954.
8. Meshulam, T., S. M. Levitz, L. Christin, and R. D. Diamond. 1995. A simplified new assay for assessment of fungal cell damage with the tetrazolium dye, (2,3)-bis-(2-methoxy-4-nitro-5-sulphenyl)-(2H)-tetrazolium-5-carboxanilide (XTT). *J. Infect. Dis.* **172**:1153-1156.
9. National Committee for Clinical Laboratory Standards. 1998. Reference method for broth dilution antifungal susceptibility testing of conidium forming filamentous fungi. Proposed standard M38-P. National Committee for Clinical Laboratory Standards, Wayne, Pa.

10. **Paull, D. K., H. Shoemaker, and M. R. Boyd.** 1998. The synthesis of XTT: a new tetrazolium reagent that is bio-reducible to a water-soluble formazan. *J. Heterocycl. Chem.* **25**:911-914.
11. **Pfaller, M. A., and M. G. Rinaldi.** 1993. Antifungal susceptibility testing. Current state of technology, limitations, and standardization. *Infect. Dis. Clin. N. Am.* **7**:435-444.
12. **Roehm, N. W., G. H. Rodgers, S. M. Hatfield, and A. L. Glasebrook.** 1991. An improved colorimetric assay for cell proliferation and viability utilizing the tetrazolium salt XTT. *J. Immunol. Methods* **142**:257-265.
13. **Scudiero, D. A., R. H. Shoemaker, K. D. Paull, A. Monks, S. Tierney, T. H. Nofziger, M. J. Currens, D. Seniff, and M. R. Boyd.** 1988. Evaluation of a soluble tetrazolium/formazan assay for cell growth and drug sensitivity in culture using human and other tumor cell lines. *Cancer Res.* **48**:4827-4833.
14. **Seidler, E.** 1991. The tetrazolium-formazan system: design and histochemistry. *Prog. Histochem. Cytochem.* **24**:1-86.
15. **Tellier, R., M. Krajden, G. A. Grigoriew, and I. Campbell.** 1992. Innovative endpoint determination system for antifungal susceptibility testing of yeasts. *Antimicrob. Agents Chemother.* **36**:1619-1625.



Chapter 2.4

Comparison of Spectrophotometric and Visual Readings of NCCLS Method and Evaluation of a Colorimetric Method Based on Reduction of a Soluble Tetrazolium Salt, 2,3-Bis {2-Methoxy-4-Nitro-5-[(Sulfenylamino) Carbonyl]-2H-Tetrazolium-Hydroxide}, for Antifungal Susceptibility Testing of *Aspergillus* Species

Journal of Clinical Microbiology 2001; 39: 4256-4263

COMPARISON OF SPECTROPHOTOMETRIC AND VISUAL READINGS OF NCCLS METHOD AND EVALUATION OF A COLORIMETRIC METHOD BASED ON REDUCTION OF A SOLUBLE TETRAZOLIUM SALT, 2,3-BIS{2-METHOXY-4-NITRO-5-[(SULFENYLAMINO) CARBONYL]-2H-TETRAZOLIUM-HYDROXIDE}, FOR ANTIFUNGAL SUSCEPTIBILITY TESTING OF *ASPERGILLUS* SPECIES

JOSEPH MELETIADIS¹, JOHAN W. MOUTON², JACQUES F. G. M. MEIS², BIANCA A. BOUMAN¹, J. PETER DONNELLY³, PAUL E. VERWEIJ¹, AND EUROFUNG NETWORK*

Departments of Medical Microbiology¹ and Hematology³, University Medical Center Nijmegen, and Department of Medical Microbiology and Infectious Diseases, Canisius-Wilhelmina Hospital², Nijmegen, The Netherlands

The susceptibilities of 25 clinical isolates of various *Aspergillus* species (*Aspergillus fumigatus*, *A. flavus*, *A. terreus*, *A. ustus*, and *A. nidulans*) to itraconazole (ICZ) and amphotericin B (AB) were determined using the standard proposed by NCCLS for antifungal susceptibility testing of filamentous fungi, a modification of this method using spectrophotometric readings, and a colorimetric method using the tetrazolium salt 2,3-bis{2-methoxy-4-nitro-5-[(sulfenylamino) carbonyl]-2H-tetrazolium-hydroxide} (XTT). Five MIC end points for ICZ (MIC-0, no visible growth or $\leq 5\%$ the growth control value [GC]; MIC-1, slight growth or 6 to 25% the GC; MIC-2, prominent reduction in growth or 26 to 50% the GC; MIC-3, slight reduction in growth or 51 to 75% the GC; and MIC-4, no reduction in growth or 76 to 100% the GC) and one for AB (MIC-0) were determined visually by four observers and spectrophotometrically. The intraexperimental (between the observers) and interexperimental (between the experiments) levels of agreement of the NCCLS and XTT methods exceeded 95% for MIC-0 of AB and MIC-0 and MIC-1 of ICZ. The MIC-2 of ICZ showed lower reproducibility, although spectrophotometric reading and/or incubation for 48 h increased the interexperimental reproducibility from 85 to >93%. Between visual and spectrophotometric readings, high levels of agreement were found for AB (97%) and MIC-1 (92%) and MIC-2 (88%) of ICZ. Poor agreement was found for MIC-0 of ICZ (51% after 24 h), since the spectrophotometric readings resulted in higher MIC-0 values than the visual readings. The agreement was increased to 98% by shifting the threshold level of MIC-0 from 5 to 10% relative optical density and by establishing an optical density of greater than 0.1 for the GC as the validation criterion. No statistically significant differences were found between the NCCLS method and the XTT method, with the levels of agreement exceeding 97% for MIC-0 of AB and 83% for MIC-0, MIC-1, and MIC-2 of ICZ. The XTT method and spectrophotometric readings can increase the sensitivity and the precision, respectively, of in vitro susceptibility testing of *Aspergillus* species.

Opportunistic systemic mycoses caused by filamentous fungi occur more frequently now than before partly as a consequence of the larger numbers of individuals receiving more potent immunosuppressive

therapy (1). The pathogens most frequently encountered belong to the genus *Aspergillus*, with *Aspergillus fumigatus* being responsible for over 90% of invasive infections in humans (10). Amphotericin B (AB) and itraconazole (ICZ) are the only licensed antifungal drugs available for treatment (4), although their efficacy is limited, perhaps partly because of drug resistance. Therefore, testing of the susceptibility of these pathogens may contribute to the management of patients. Such testing requires standardized and reproducible techniques (6, 7). Broth microdilution methods have been adopted, since they are less expensive and cumbersome than macrodilution methods and yield reproducible results (2, 5, 18). Fungal growth is assessed either visually by grading turbidity (16) or

*EC-TMR-EUROFUNG network (ERBFMRXCT97-0145). The Eurofung Network consists of the following participants: Emmanuel Roilides and Nicos Maglaveras, Aristotle University, Thessaloniki, Greece; Tore Abrahamsen and Peter Gaustad, Rikshospitalet National Hospital, Oslo, Norway; David W. Denning, University of Manchester, Manchester, United Kingdom; Paul E. Verweij and Jacques F. G. M. Meis, University of Nijmegen, Nijmegen, The Netherlands; Juan L. Rodriguez-Tudela, Instituto de Salud Carlos III, Madrid, Spain; and George Petrikos, Athens University, Athens, Greece.

spectrophotometrically by measuring optical density (OD) (3, 12). Alternatively, biomass can be determined colorimetrically using indicator substances that are reduced to colored products by viable microorganisms. Thus, fungal biomass is estimated by the metabolic activity of the fungus (7, 9, 13).

The hyphae and nonhomogeneous growth of filamentous fungi, together with a trailing effect of fungistatic drugs, complicate the determination of MICs and do not allow for precise quantification of fungal growth (13). Visual assessment of fungal growth lacks objectivity and precision (13, 19), and the accuracy of spectrophotometric readings may be hampered by clumps of mycelia (11, 15). Colorimetric methods may be an alternative, since precise quantification of hyphal growth is achieved and clear-cut end points can be generated (8). Tetrazolium salts have been used as colorimetric indicators, since fungi convert them to colored formazan derivatives, which can be quantified (18). The tetrazolium salt 3-(4,5-dimethyl-2-thiazyl)-2,5-diphenyl-2H-tetrazolium bromide (MTT) has been used for antifungal susceptibility testing of yeasts and has recently been shown to be useful for determining MICs for filamentous fungi (13, 14). However, the usefulness of this assay is limited, since dissolution of the formazan derivative is achieved in organic solvents and relatively large numbers of fungi are required (11, 15).

2,3-Bis{2-methoxy-4-nitro-5-[(sulfenylamino)carbonyl]-2H-tetrazolium-hydroxide} (XTT) is a new yellow tetrazolium salt which is converted by mitochondrial dehydrogenases of viable fungi to an orange formazan product (8, 18, 24). Unlike MTT-derived formazan, the product of XTT conversion is a water-soluble formazan, which obviates the need for solubilization steps (15, 21, 22). The XTT assay has been used for testing of the susceptibility of yeasts to antifungal agents and has yielded a high level of agreement with the NCCLS method for various *Candida* species and *Cryptococcus neoformans* (8). The same assay has been used to determine MICs for a small collection of filamentous fungi and has resulted in reproducible and comparable results relative to those obtained with the NCCLS method (23). A recently developed XTT assay for *Aspergillus* species resulted in well-defined dose-response curves for antifungal drugs (13a).

In this study, 25 clinical isolates of five *Aspergillus* species were tested three times against AB and ICZ using the method proposed by NCCLS (M38-P), and five MIC end points were determined visually by four observers. Given the problems encountered with the visual observation and spectrophotometric assessment of the hyphal growth of filamentous fungi, the results of M38-P were compared with a modification of this method using spectrophotometric

readings at 405 nm. Furthermore, in order to facilitate the determination of MICs for filamentous fungi, the activities of antifungal drugs were determined by a colorimetric method that uses the dye XTT as described previously (13a). The intraexperimental (between the observers) and interexperimental (between the experiments) agreements of the methods as well as the agreements between the NCCLS and colorimetric methods and between visual and spectrophotometric readings were calculated.

MATERIALS AND METHODS

Test isolates. Twenty-five clinical isolates of *Aspergillus* species (from our private collection) were selected for testing and included 5 isolates each of the following species: *A. fumigatus* (AZN5161, AZN5241, AZG7, AZN8248, and AZN8244), *A. flavus* (AZN137, AZN510, AZN2865, AZN4094, and AZN4132), *A. nidulans* (AZN2867, AZN8033, AZN8236, AZN8933, and AZN4606), *A. terreus* (AZN286, AZN515, AZN2868, AZN7320, and AZN9152), and *A. ustus* (AZN677, AZN2725, AZN6989, AZN9420, and AZN7843). *Candida parapsilosis* (ATCC 22019) and *C. krusei* (ATCC 6258) were used for quality control.

Isolates were cultured twice on Sabouraud glucose agar at 30°C for 5 to 7 days. All isolates were tested on three different days. Conidia of the isolates were obtained from fresh cultures each time.

Medium. RPMI 1640 medium (with L-glutamine but without bicarbonate) (GIBCO BRL, Life Technologies, Woerden, The Netherlands) buffered to pH 7.0 with 0.165 M 3-*N*-morpholinopropanesulfonic acid (MOPS) (Sigma-Aldrich Chemie GmbH, Steinheim, Germany) was used as the assay medium.

Inoculum. Conidia were collected with a cotton swab and suspended in sterile saline containing 0.05% Tween 20. After heavy particles were allowed to settle, the turbidity of the supernatants was measured spectrophotometrically (Spectronic 20D; Milton Roy, Rochester, N.Y.) at 530 nm, and the transmission was adjusted to 80 to 82% to yield an initial inoculum of 1×10^6 to 5×10^6 CFU/ml. Each suspension was diluted 1:50 in medium to obtain twice the desired inoculum. The inoculum size was confirmed by plating of serial dilutions on Sabouraud glucose agar plates, with final inocula ranging from 1×10^4 to 5×10^4 CFU/ml.

Antifungal susceptibility testing. The broth microdilution method of the NCCLS (M38-P) (16) was performed using 96-well flat-bottom microtitration trays. ICZ (Janssen-Cilag, Beerse, Belgium) and AB (Bristol-Myers Squibb, Woerden, The Netherlands) were dissolved in dimethyl sulfoxide (DMSO) and diluted serially in medium to yield final concentrations of 0.015 to 16 mg of AB/liter and 0.03 to 32 mg of ICZ/liter in a final volume of 200 μ l after the inoculation. A drug-free growth control that contained 0.5% DMSO in medium was included. Trays were kept at -70°C until the day of testing.

Incubation and MIC determination. After the microtitration trays were defrosted, they were inoculated with

100 µl of inoculum. The trays were agitated for 10 s and incubated at 37°C for 48 h. The MICs of the antifungal drugs were determined after 24 and 48 h of incubation by two methods (the NCCLS and XTT methods) and by two modes of reading (visual and spectrophotometric) as described below.

(i) NCCLS method. (a) Visual reading (NCCLS_{vis}).

Fungal growth was assessed visually by four different observers with the aid of a concave mirror and graded according to NCCLS guidelines as follows: 4, no reduction in growth; 3, slight reduction in growth; 2, prominent reduction in growth; 1, slight growth; and 0, absence of visual growth compared with the growth in the drug-free well. Only score 0 was recorded for AB. Four MIC end points (MIC-0, MIC-1, MIC-2, and MIC-3) were determined as the lowest drug concentrations showing growth scaled to the corresponding score (0, 1, 2, and 3, respectively). MIC-4 was determined as the highest drug concentration showing growth scaled to score 4.

(b) Spectrophotometric reading (NCCLS_{sp}). After the MICs were determined visually, the OD of each well was measured at 405 nm with a spectrophotometer (Rosys Anthos ht3; Anthos Labtec Instruments GmbH, Salzburg, Austria). After subtraction of the ODs of the blank, which consisted of noninoculated wells that had been incubated together with the inoculated wells, from the ODs of the inoculated wells, the percentage of growth for each well was correlated with the relative OD estimated by the following equation: $(OD_{405} \text{ of wells that contained the drug} / OD_{405} \text{ of the drug-free well}) \times 100$. Relative ODs after rounding were grouped in five levels: 4, 76 to 100% relative OD; 3, 51 to 75% relative OD; 2, 26 to 50% relative OD; 1, 6 to 25% relative OD; and 0, equal to or less than 5% relative OD. Five MIC end points were determined for ICZ based on the levels of relative ODs. MIC-0, MIC-1, MIC-2, and MIC-3 were determined as the lowest drug concentrations with relative ODs of levels 0, 1, 2, and 3, respectively. MIC-4 was determined as the highest drug concentration with a relative OD of level 4. Only MIC-0 was determined for AB.

Once these determinations were completed, the trays were returned to the incubator for another 24 h and read again visually and spectrophotometrically.

(ii) XTT method. The MICs were also determined colorimetrically using XTT (Sigma-Aldrich Chemie). Microtitration trays were prepared and incubated for 24 and 48 h at 37°C according to NCCLS guidelines as described above. Then, 50 µl of saline containing 1 mg of XTT/ml and 20.2 µg of menadione (Sigma-Aldrich Chemie)/ml was added to each well in order to obtain final concentrations of 200 µg of XTT/ml and 4.3 µg of MEN/ml (25 µM). MEN was first dissolved in acetone at a concentration of 430.5 µg/ml and then diluted 1/10 in saline. Incubation was continued at 37°C for 2 h in the dark to allow conversion of XTT to its formazan derivative. The OD was measured at 450 nm, after shaking, with a microtitration tray spectrophotometer reader. The color was assessed first visually by the same four observers and graded according to NCCLS guidelines (XTT_{vis}) and then spectrophotometrically based on relative ODs at 450 nm and grouped in five levels as described above (XTT_{sp}). Five MIC end points were determined for ICZ as described above. For AB, only MIC-0 was determined.

Study design. A multifactorial panel of data was generated based on five parameters studied, i.e., modes of reading, MIC end points, drugs, species, and incubation periods, in order to test the reproducibility of and the agreement between the NCCLS and XTT methods. Data from five readings (four observers and spectrophotometer), five MIC end points, two drugs, five species, five strains, two incubation periods, and three independent experiments were obtained for both methods. Four comparisons were done in order to find the levels of absolute and relative agreements within the observers and the experiments (intra- and interexperimental agreements, respectively), between the visual and the spectrophotometric readings for each method, and between the NCCLS and the XTT methods.

Analysis of results. The levels of agreement within the four observers and the three experiments as well as between the two methods and between the two modes of reading were calculated for each species-drug-MIC end point-incubation period combination. In order to approximate a normal distribution for statistical analysis, the drug concentrations were transformed by logarithmic transformation to \log_2 and the percentages of agreement were transformed by angular transformation (with the transformed value being the arcsine of the square root of the percentage). After the transformation, MIC end points were analyzed by two-way analysis of variance (ANOVA), which was applied to each drug-MIC end point-incubation period combination. *P* values of less than 0.05 were considered significant. Any systematic differences between the methods and the species were controlled by the interaction factor of two-way ANOVA. A *P* value of less than 0.05 indicated that the differences between the two methods are not the same for each species and therefore that the differences between the methods are species dependent. Discrepancies were analyzed by Fisher's exact test. The transformed percentages of agreement were used in order to estimate variations between the experiments, the species, and the strains and to analyze differences in intra- and interexperimental agreements between all MIC end points after 24 and 48 h by repeated-measures ANOVA. The 95% confidence intervals (95% CI) of the percentages of agreement were calculated using the Wald equation for proportions (Prism software; GraphPad Software, Inc., San Diego, Calif.). The high and low off-scale MICs were included in the analysis by conversion to the next higher and lower drug concentrations, respectively.

(i) Intraexperimental agreement. For the visual readings (NCCLS_{vis} and XTT_{vis}), the percentage of absolute or relative agreement between the four observers for each strain was defined as the proportion of the MIC end points which were identical or which belonged to the largest subset of four observations with a range of which not more than 3 dilutions, respectively. The levels of agreement between the four visual readings were calculated for each species and experiment, and the total percentage of agreement for all species and experiments was reported for each drug and MIC end point for the NCCLS_{vis} and XTT_{vis} methods after 24 and 48 h of incubation.

(ii) Interexperimental agreement. For each method and mode of reading, the percentage of absolute and relative agreements between the three experiments was defined as the proportion of the MIC end points determined by the four

Table 1. Susceptibilities of five strains of five *Aspergillus* spp. to AB and ICZ based on MIC-0 and MIC-2, respectively, after 24 and 48 h of incubation

Drug	Time	Species	Geometric mean (range) MIC, in mg/liter, determined by the following method:			
			NCCLS _{vis}	NCCLS _{sp}	XTT _{vis}	XTT _{sp}
AB	24 h	<i>A. fumigatus</i>	0.68 (0.125-4)	0.63 (0.5-2)	0.63 (0.25-2)	0.63 (0.5-2)
		<i>A. flavus</i>	1.19 (0.5-4)	1.20 (0.5-2)	1.11 (0.5-2)	1.15 (0.5-2)
		<i>A. nidulans</i>	0.74 (0.25-4)	0.72 (0.25-2)	0.68 (0.25-2)	0.66 (0.25-1)
		<i>A. terreus</i>	1.11 (0.5-4)	0.95 (0.5-4)	1.07 (0.5-2)	1.10 (0.5-2)
		<i>A. ustus</i>	1.11 (0.5-2)	0.88 (0.5-2)	0.92 (0.5-4)	1.12 (0.5-2)
	48 h	<i>A. fumigatus</i>	1.50 (1-4)	1.26 (1-4)	1.14 (0.5-4)	1.15 (0.5-4)
		<i>A. flavus</i>	1.64 (1-4)	1.38 (1-2)	1.57 (1-4)	1.45 (1-2)
		<i>A. nidulans</i>	1.10 (0.25-4)	0.87 (0.25-4)	0.97 (0.25-4)	0.95 (0.25-4)
		<i>A. terreus</i>	2.89 (2-4)	2.09 (2-4)	2.64 (2-4)	2.52 (2-4)
		<i>A. ustus</i>	1.91 (1-4)	1.36 (1-2)	1.53 (1-4)	1.47 (1-2)
ICZ	24 h	<i>A. fumigatus</i>	2.39 (0.015->32)	1.15 (0.125->32)	1.36 (0.125->32)	1.38 (0.125->32)
		<i>A. flavus</i>	0.14 (0.063-0.25)	0.10 (0.063-0.125)	0.14 (0.0125-0.5)	0.14 (0.063-0.25)
		<i>A. nidulans</i>	0.13 (0.031-0.5)	0.13 (0.063-0.25)	0.13 (0.062-0.5)	0.10 (0.062-0.5)
		<i>A. terreus</i>	0.09 (0.031-0.25)	0.09 (0.063-0.125)	0.12 (0.062-0.5)	0.11 (0.063-0.125)
		<i>A. ustus</i>	0.40 (0.062-1)	0.35 (0.063-1)	0.54 (0.062-1)	0.46 (0.063-1)
	48 h	<i>A. fumigatus</i>	2.89 (0.125->32)	2.41 (0.125->32)	2.96 (0.125->32)	2.10 (0.063->32)
		<i>A. flavus</i>	0.19 (0.125-0.5)	0.12 (0.063-0.25)	0.26 (0.125-1)	0.24 (0.125-0.5)
		<i>A. nidulans</i>	0.16 (0.062-0.25)	0.20 (0.063-2)	0.17 (0.031-0.5)	0.15 (0.031-0.5)
		<i>A. terreus</i>	0.15 (0.062-0.5)	0.14 (0.063-0.25)	0.29 (0.062-0.5)	0.23 (0.125-0.5)
		<i>A. ustus</i>	1.48 (0.125->32)	0.89 (0.5-1)	3.21 (0.125->32)	2.72 (0.25->32)

observers or the spectrophotometer which were identical or within 1 dilution of the median, respectively. The levels of agreement between the three experiments were calculated for each species, and the total percentage of agreement for all species was reported for each drug and MIC end point for the NCCLS_{vis}, NCCLS_{sp}, XTT_{vis}, and XTT_{sp} methods after 24 and 48 h of incubation.

(iii) Agreement between visual and spectrophotometric readings. For each method, the percentage of agreement between the visual and spectrophotometric readings was calculated as the proportion of the MIC end points determined visually by the four observers which fell within 1 dilution of the corresponding MIC end points determined spectrophotometrically. The total percentage of agreement for the three experiments and all species between NCCLS_{vis} and NCCLS_{sp} as well as between XTT_{vis} and XTT_{sp} was reported for each drug and MIC end point after 24 and 48 h of incubation, and the approximate 95% CI of percentages of agreement were calculated as described above.

(iv) Agreement between NCCLS and XTT methods. For each strain, the percentage of agreement between the NCCLS and XTT methods based on visual and spectrophotometric readings of each MIC end point was calculated as the proportion of the MIC end points determined by the NCCLS method, visually or spectrophotometrically, which fell within 1 dilution of the corresponding MIC end points of the XTT method, determined visually or spectrophotometrically, respectively. The total percentage of agreement between NCCLS_{vis} and XTT_{vis} and between NCCLS_{sp} and XTT_{sp} for the three experi-

ments was reported for each drug and MIC end point after 24 and 48 h of incubation, and the approximate 95% CI of percentages of agreement were calculated as described above.

RESULTS

MICs. The *Aspergillus* strains tested in this study had various susceptibilities to AB and ICZ, with MICs ranging between 0.125 and 4 mg/liter for AB and 0.015 to >32 mg/liter for ICZ. Most of the MICs of ICZ were less than 1 mg/liter, except for those for two strains of *A. fumigatus* (Table 1). For *A. ustus* strains, despite the fact that the MIC-2 values were less than 1 mg/liter, the MIC-0 values were higher than 2 mg/liter and up to >32 mg/liter (data not shown). The geometric means of the MICs of AB and for ICZ obtained by all methods after 24 and 48 h of incubation were similar, as shown in Table 1. Differences were observed with *A. fumigatus* and ICZ, for which the geometric mean of the MICs obtained by NCCLS_{vis} after 24 h was slightly higher than the corresponding value obtained by the other methods (2.4 and 1.4 mg/liter, respectively), and with *A. ustus* and ICZ, for which the geometric means of the MICs obtained by NCCLS_{vis} and NCCLS_{sp} after 48 h were lower than the values obtained by the corresponding XTT methods (1.5 and 0.9 mg/liter for NCCLS_{vis} and NCCLS_{sp} and 3.2 and 2.7 mg/liter for XTT_{vis} and XTT_{sp}, respectively).

Table 2. Overall absolute and relative (within 0 and 1 dilution, respectively) agreement within the four observers and the three experiments for all tested *Aspergillus* isolates

Agreement	Group ^a	Drug	Growth level ^b	Overall absolute (relative) % agreement for the indicated method after the following h of incubation:			
				24		48	
				NCCLS	XTT	NCCLS	XTT
Intraexperimental	1	ICZ	0	82.9 (99.1)	90.3 (97.7)	89.7 (99.4)	92.5 (99.5)
			1	83.2 (98.6)	77.6 (99.1)	76.1 (99.5)	82.0 (98.8)
			2	69.0 (88.8)	66.9 (87.6)	69.8 (95.3)	72.0 (94.9)
			3	62.4 (80.2)	59.1 (73.6)	65.5 (78.2)	65.0 (86.7)
			4	60.8 (71.7)	63.2 (71.8)	64.1 (77.0)	63.5 (70.3)
		AB	0	91.0 (99.8)	96.1 (99.9)	90.6 (100)	95.8 (100)
Interexperimental	2	ICZ	0	78.3 (97.6)	75.3 (95.6)	83.7 (99.4)	85.6 (99.3)
			1	69.6 (95.5)	74.5 (96.6)	78.3 (98.9)	77.0 (98.6)
			2	65.8 (85.7)	64.6 (85.3)	71.5 (94.3)	68.8 (93.3)
			3	62.8 (82.2)	57.7 (75.9)	67.7 (82.5)	69.1 (87.8)
			4	61.9 (73.8)	58.5 (68.4)	66.0 (79.3)	66.8 (77.2)
		AB	0	81.7 (99.0)	87.9 (99.7)	78.1 (99.7)	83.1 (99.7)
		3	0	54.7 (76.2)	64.4 (90.9)	75.4 (91.6)	87.3 (99.4)
			1	71.2 (99.7)	74.8 (95.7)	84.7 (97.6)	81.0 (97.2)
			2	65.6 (96.2)	63.4 (93.1)	72.3 (99.7)	67.0 (89.6)
			3	58.8 (71.4)	56.0 (80.2)	62.9 (89.6)	49.3 (88.9)
			4	61.7 (64.3)	61.7 (67.0)	59.5 (64.8)	56.1 (78.2)
		AB	0	78.9 (99.7)	88.2 (100)	92.4 (100)	89.6 (100)

^a Groups 1 and 2, NCCLS_{vis} and XTT_{vis}, 95% confidence intervals of absolute agreement ranged from ± 3.6 to $\pm 5.6\%$; group 3, NCCLS_{sp} and XTT_{sp}, 95% confidence intervals of absolute agreement ranged from ± 2.6 to $\pm 11.3\%$.

^b 0, no visible growth or $<5\%$; 1, slight growth or 5-25% of growth control; 2, prominent reduction of growth or 26-50% of growth control; 3, slight reduction in growth or 51-75% of growth control; 4, no reduction in growth or 76-100% of growth control.

(i) Intraexperimental agreement. For AB, the absolute agreement between the four observers was higher with the XTT_{vis} method (96%) than with the NCCLS_{vis} method (91%) after 24 and 48 h (Table 2). The lowest level of agreement was found for *A. ustus* with the NCCLS_{vis} method (75%); the agreement was higher with the XTT_{vis} method ($>88\%$). For ICZ, the absolute agreement was higher for MIC-0 and MIC-1 with both methods ($>76\%$) than for the other MIC end points. Based on MIC-0 and MIC-1, *A. ustus* (67%) and *A. fumigatus* (98%) showed the lowest and the highest levels of absolute agreement, respectively, among the tested species. The coefficient of variation of intraexperimental absolute agreement was always less than 10% among the experiments as well as among the species for both the NCCLS_{vis} and the XTT_{vis} methods. No statistically significant differences were found between the percentages of agreement of the NCCLS_{vis} and XTT_{vis} methods after 24 and 48 h of incubation.

(ii) Interexperimental agreement. For AB, the absolute agreement between the experiments was slightly higher for the XTT_{vis} method than for the NCCLS_{vis} method and was lower after 48 h of incubation than after 24 h for both methods (Table 2). When spectrophotometric readings were used, the

interexperimental agreement for the XTT_{sp} and NCCLS_{sp} methods was higher after 48 h of incubation than after 24 h. For ICZ, the reproducibility of the NCCLS_{vis} and XTT_{vis} methods was high ($>70\%$) with MIC-0 and MIC-1 and was always higher after 48 h. For these MIC end points, the lowest and highest levels of absolute agreement among the different species were found with *A. ustus* (64%) and *A. fumigatus* (93%), respectively. For the NCCLS_{sp} and XTT_{sp} methods, the highest reproducibility was found for MIC-1 (71-85%) with both methods after 24 and 48 h, with the exception of the XTT_{sp} method after 48 h, for which the MIC-0 showed the highest reproducibility (87%).

The reproducibility of MIC-0 with the NCCLS_{sp} method was very low after 24 h (55%) but improved after 48 h (75%) and with the XTT_{sp} method (87%). The coefficient of variation of interexperimental absolute agreement among the species was always less than 13% for visual readings, with an average coefficient of variation of 10%; for the spectrophotometric readings, the coefficient of variation was always less than 19%, with an average coefficient of variation of 13% for both methods. Unlike that of the spectrophotometric readings, the relative agreement of the visual readings increased statistically significantly

Table 3. Overall relative (within 1 dilution) agreement and 95% confidence intervals (95% CI) between the visual and spectrophotometric readings and between the NCCLS and XTT methods

Time (h)	Drug	Growth level ^a	% Agreement \pm 95% CI for the following comparisons:			
			Visual vs Spectrophotometric readings		NCCLS vs XTT methods	
			NCCLS _{vis} vs NCCLS _{sp} ^b	XTT _{vis} vs XTT _{sp} ^b	NCCLS _{vis} vs XTT _{vis} ^b	NCCLS _{sp} vs XTT _{sp} ^c
24	ICZ	0	51.4 \pm 5.7 ^d	90.8 \pm 3.3	88.0 \pm 3.7	60.0 \pm 11.1 ^e
		1	92.8 \pm 3.0	91.1 \pm 3.3	92.7 \pm 3.0	94.7 \pm 5.1
		2	87.7 \pm 3.8	86.0 \pm 4.0	86.8 \pm 3.9	82.7 \pm 8.6
		3	67.8 \pm 5.4 ^e	75.4 \pm 4.9 ^e	79.8 \pm 4.6 ^e	73.3 \pm 10.0 ^e
		4	68.1 \pm 22.6 ^d	67.9 \pm 5.3	68.3 \pm 5.4	73.3 \pm 10.0
	AB	0	96.7 \pm 2.0	99.3 \pm 0.9	96.7 \pm 2.0	98.7 \pm 2.5
48	ICZ	0	81.5 \pm 4.4	95.3 \pm 2.4	94.0 \pm 2.7	84.0 \pm 8.3
		1	91.6 \pm 3.1	90.9 \pm 3.3	85.1 \pm 4.1	77.3 \pm 9.5
		2	87.2 \pm 3.8	83.2 \pm 4.2	82.8 \pm 4.3	73.3 \pm 10.0
		3	72.5 \pm 5.1	69.5 \pm 5.2	78.0 \pm 4.7	54.7 \pm 11.3
		4	58.1 \pm 5.6	67.5 \pm 5.5 ^d	69.6 \pm 5.2	48.0 \pm 11.3
	AB	0	98.7 \pm 1.3	100.0 \pm 0.0	97.0 \pm 1.9	98.7 \pm 2.6

^a See Table 2, footnote b.^b A total of 300 comparisons.^c A total of 75 comparisons.^d The *P* value (obtained by the two way ANOVA of log₂MIC-endpoints derived by the two methods) was <0.01.^e The *P* value was <0.05.

after 48 h for both methods ($P < 0.05$).

(iii) Agreement between visual and spectrophotometric readings. For AB, the relative agreements between the NCCLS_{vis} and NCCLS_{sp} methods as well as between the XTT_{vis} and XTT_{sp} methods were high after 24 and 48 h (>96 and >99%, respectively) (Table 3). For ICZ, the levels of agreement between the XTT_{vis} and XTT_{sp} methods for MIC-0, MIC-1, and MIC-2 ranged from 83 to 95% after 24 and 48 h of incubation. Between the NCCLS_{vis} and NCCLS_{sp} methods, the agreements were higher for MIC-1 and MIC-2 after 24 h (93 and 88%, respectively) and 48 h (92 and 87%, respectively). Very low agreement was found for MIC-0 after 24 h (51%; $P < 0.01$), but it increased after 48 h (82%). Statistically significant differences were found for MIC-3 ($P < 0.01$) and MIC-4 ($P < 0.05$) of ICZ after 24 h with the NCCLS methods and for MIC-3 after 24 h ($P < 0.05$) and MIC-4 after 48 h ($P < 0.01$) of ICZ with the XTT methods. No statistically significant systematic differences between the two methods and the species for both drugs after 24 and 48 h of incubation for all MIC end points were found ($P > 0.15$). For MIC-0 of ICZ after 24 h of incubation, in 42 (56%) out of 75 comparisons (three experiments, five species, and five strains), the MIC-0 values of the NCCLS_{sp} method were higher than those of the NCCLS_{vis} method, and only six comparisons (8%) were the opposite. Furthermore, out of 35 comparisons in which differences of higher than 1 dilution were observed, the MIC-0 values of the spectrophotometric method were higher than those of the NCCLS method in 33 and vice versa in 2.

In order to study further the low levels of agree-

ment between the NCCLS_{vis} and NCCLS_{sp} methods for MIC-0 of ICZ after 24 h, the relative ODs of the NCCLS_{sp} method which corresponded to the MIC-0 values of the NCCLS_{vis} method were associated with the ODs of their growth controls for all 75 comparisons in a cross-sectional study. Various contingency tables were constructed based on different cutoff values for relative ODs of MIC-0 (5 and 10%) and ODs of the growth control as validation criteria (0, 0.05, and 0.1). The strongest association was found when a relative OD of 10% as a cutoff for MIC-0 was combined with an OD of 0.1 for the growth control as a validation criterion ($P < 0.0005$). The Spearman correlation coefficient between these two parameters was -0.35 ($P = 0.029$). Using the 10% relative OD as a cutoff for MIC-0 instead of 5% and an OD of 0.1 for the growth control as an evaluation criterion, the discrepancy between the NCCLS_{vis} and NCCLS_{sp} methods was reduced 10 times (from 28 to 2.7%) and the levels of agreement reached 98%. However, 27% of MIC-0 values of the NCCLS_{sp} method will be in agreement with those of the NCCLS_{vis} method, although the ODs of their growth controls could be less than 0.1. The levels of agreement between the XTT_{vis} and XTT_{sp} methods, especially for MIC-0, were higher after 24 and 48 h (91% and 95%, respectively).

(iv) Agreement between NCCLS and XTT methods. For AB, the levels of agreement between the NCCLS_{vis} and XTT_{vis} methods as well as between the NCCLS_{sp} and XTT_{sp} methods were higher than 97% (Table 3). For ICZ, the agreement between the NCCLS_{vis} and XTT_{vis} methods was higher than 83% for

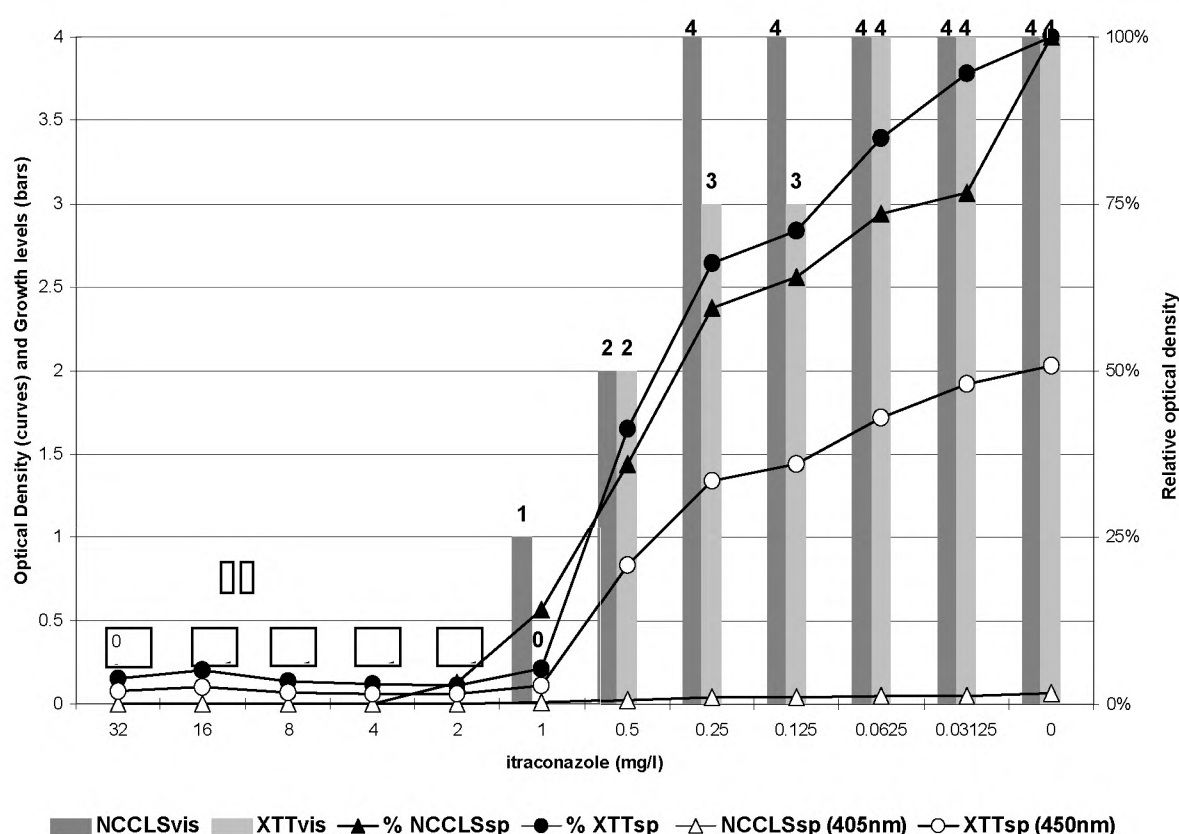


Figure 1. Results of susceptibility testing of an *A. ustus* strain against itraconazole in the NCCLS and XTT methods, with data determined visually and spectrophotometrically, after 24 h of incubation. The bars represent the growth levels obtained in the NCCLS_{vis} (dark bars) and XTT_{vis} (light bars) methods for each concentration on a scale of 0 (absence of growth or color) to 4 (no reduction of growth or color compared with the data for the drug-free control). The curves with the circles represent the OD at 450 nm (open symbols) and the relative OD (percentage) (closed symbols) obtained by the XTT_{sp} method. The curves with the triangles represent the OD at 405 nm (open symbols) and the relative OD (percentage) (closed symbols) obtained by the NCCLS_{sp} method.

MIC-0, MIC-1, and MIC-2, with MIC-1 showing the highest agreement after 24 h (93%) and MIC-0 doing so after 48 h (94%). Among the species, *A. ustus* showed the lowest level of agreement (82%). The levels of agreement between the NCCLS_{sp} and XTT_{sp} methods were lower with MIC-1 after 24 h and higher with MIC-0 after 48 h (95 and 84%, respectively). Statistically significant differences were found for MIC-3 of ICZ after 24 h between the NCCLS_{vis} and XTT_{vis} methods as well as between the NCCLS_{sp} and XTT_{sp} methods ($P < 0.05$). The statistically significant differences for MIC-0 of ICZ after 24 h between the NCCLS_{sp} and XTT_{sp} methods ($P < 0.05$) were due to the erroneous higher MICs obtained by the NCCLS_{sp} method. The discrepancies were reduced when the above-mentioned validation criteria were applied for the determination of MIC-0 by the NCCLS_{sp} method. No statistically significant systematic differences between the two methods and the species were obtained for both drugs after 24 and 48 h of incubation for all MIC end points ($P > 0.25$).

A representative graph is shown in Fig. 1, with

the results of NCCLS_{vis}, NCCLS_{sp}, XTT_{vis}, and XTT_{sp} for an *A. ustus* strain and ICZ. Growth at an OD at 405 nm of 0.047 with the NCCLS_{sp} method corresponded to formazan production of 2.0 OD units at 450 nm with the XTT_{sp} method.

DISCUSSION

The selection of an endpoint for MIC determination of antifungal drugs is an important factor of antifungal susceptibility testing of filamentous fungi which may increase the variability of these tests (5). This parameter is crucial especially for fungistatic drugs like ICZ since partial inhibition of the growth due to the delayed action of the drug (trailing phenomenon) may result in limited growth over a range of drug concentrations, which may elevate the MIC-0. Therefore, MIC-2 (prominent reduction of growth) was chosen for this drug (20). However, in previous studies MIC-1 (slight growth or 75% reduction of growth) showed higher interlaboratory agreement and similar

interexperimental agreement relative to MIC-2 (6, 12). In the present study, high levels of intra- and interexperimental agreement were found for MIC-0 and MIC-1 (>95%) as was found in our previous study (13). For MIC-2, the levels of intra- and interexperimental agreement were lower after 24 h (89 and 86%, respectively) although they increased after 48 h of incubation (95 and 94%, respectively). The interexperimental agreement for MIC-2 was improved when the spectrophotometric reading was used (96% after 24 h and 99% after 48 h). Similar results were obtained when XTT was used.

For fungicidal drugs such as AB, growth ceases abruptly after exposure to the drug which results in clear-cut end points (20). Therefore, the MIC-0 was chosen as the end point. In this study, in agreement with previous studies, high levels of inter- and intraexperimental agreement (>98%) were found after 24 and 48 h of incubation. Using the dye XTT, the absolute intra- and interexperimental agreements of visual determination were further increased.

It is assumed that spectrophotometric estimation of the growth of filamentous fungi is inaccurate because of nonhomogeneity (4, 5). However, in previous studies, high levels of agreement were found between visual and spectrophotometric readings at 405 and 570 nm for MIC-1 and MIC-2 for ICZ and MIC-0 for AB (3, 12). The same results were obtained in this study, since the levels of agreement for MIC-1 and MIC-2 were 92 and 87%, respectively, for ICZ and 97% for AB with MIC-0. However, the levels of agreement between visual and spectrophotometric readings at 405 nm for MIC-0 of ICZ were very low, especially after 24 h (51%; $P < 0.01$). In most cases, the MIC-0 values based on spectrophotometric readings were higher than those of visual readings. Further analysis of the discrepancies showed that this disagreement depended on the cutoff of relative OD as well as the OD of the growth control ($P < 0.0005$). In a previous study, an OD of 0.15 for the growth control was chosen as validation criterion for spectrophotometric readings of susceptibility testing of *Aspergillus* species although no evidence for the choice of threshold level was provided (17). Using a threshold level of 10% relative OD for MIC-0 and as a validation criterion an OD of the growth control of greater than 0.1, the discrepancies were reduced 10-fold and the agreement between visual and spectrophotometric readings was increased to 98%.

Spectrophotometric readings are in general more precise and reproducible than visual reading. Since the hyphal growth of *Aspergillus* species does not seem to present an obstacle, spectrophotometry can be used to determine the susceptibility of these fungi to antifungal drugs resulting in more precise quantification of hyphal growth than is attained by a visual reading. However, further optimization is required. The presence of phenol

red in RPMI 1640 medium may pose problems as it might lower the sensitivity of spectrophotometric readings. The absorbance of this medium is very high at 405 nm (OD, 0.15 to 0.2), a wavelength at which hyphae have the highest absorbance. At lower wavelengths, the background absorbance is decreased (OD at 630 nm, 0.06), but the absorbance of hyphae is also decreased (unpublished observations). Thus, due to high background absorbance, limited fungal growth is not detectable by spectrophotometer. Studies using RPMI 1640 medium without phenol red for in vitro susceptibility testing show identical results compared with the standard medium (23). Since phenol red was originally used to allow contamination of the medium to be detected, in antifungal susceptibility testing it serves no useful purpose; therefore, phenol red should be omitted.

Although spectrophotometric reading resulted in higher accuracy and reproducibility, lack in sensitivity was observed since growth higher than 0.1 OD is required for precise hyphal quantification. The sensitivity of spectrophotometric readings was increased with the colorimetric method, since ODs of up to 2.0 were achieved compared with 0.047 using the noncolorimetric method. In a previous study, a colorimetric method based on the dye XTT was applied for antifungal susceptibility testing of various yeasts against different azoles and flucytosine, resulting in high levels of agreement with the standard NCCLS method (8). XTT was applied for the first time for filamentous fungi by Sugar and Liu (23), who found lower MICs compared with the NCCLS method. These discrepancies between the two methods may be due to the different MIC end points that were chosen, namely, the MIC-0 defined as the first well showing no growth for the NCCLS method and a decrease in OD of greater than 50% for the XTT method (23). Variation in the colorimetric method may be caused by the absence of a step that stops the conversion, since extraction steps are not necessary. Since high levels of agreements were found between the spectrophotometric and the visual readings of the XTT method, the colorimetric method can be automated by using spectrophotometric readings. However, wells containing hyphae may interfere with OD measurements, since at 450 nm, where the formazan derivative is absorbed, hyphae also show high absorbance. These problems could be overcome by removing the formazan derivative from the wells where the fungi are growing, although it will increase the time required to generate results.

Strains for which MICs of antifungal agents are high were detectable with the colorimetric method, in some cases 24 h earlier than it was possible with visual reading. Furthermore, it was possible to distinguish between metabolically active hyphae and dead hyphae, which would both produce turbidity, which would be

seen as growth when examined visually, possibly resulting in a trailing effect. Besides helping to alleviate this problem, the colorimetric method should allow detection of small amounts of growth, more precise quantification, and earlier MIC determination than is possible with the noncolorimetric method.

In conclusion, for AB high levels of agreement were always obtained. For ICZ with both the NCCLS and the XTT methods, MIC-0 and MIC-1 showed the highest levels of intra- and interexperimental agreement. For MIC-2, similar levels of agreement were achieved either by prolonging the incubation period to 48 h or by using spectrophotometric reading after 24 h. The spectrophotometric readings can be used for antifungal susceptibility testing of *Aspergillus* species, since high levels of agreement with the visual readings were achieved for MIC-0, MIC-1, and MIC-2. The low agreement was found between the visual readings and the spectrophotometric readings of the NCCLS method for MIC-0 of ICZ was improved by shifting the threshold level to 10% relative OD and establishing an OD of 0.1 for the growth control as a validation criterion for the spectrophotometric readings. The XTT method based on both visual and spectrophotometric readings used in this study showed high levels of agreement with the NCCLS method, and higher levels of sensitivity and precision were achieved. Therefore, the colorimetric method could be used as an alternative method for antifungal susceptibility testing of *Aspergillus* species, although further work is required to study the robustness of this colorimetric method.

ACKNOWLEDGMENTS

This work was supported by the European Commission Training and Mobility of Researchers grant ERBFMRXCT97-0145 to Joseph Meletiadis and by the Mycology Research Center of Nijmegen.

REFERENCES

1. **Anaissie, E.** 1992. Opportunistic mycoses in the immunocompromised host: experience at a cancer center and review. *Clin. Infect. Dis.* **14**(Suppl. 1):43-53.
2. **Cormican, M. G., and M. A. Pfaller.** 1996. Standardization of antifungal susceptibility testing. *J. Antimicrob. Chemother.* **38**:561-578.
3. **Dannaoui, E., F. Persat, M. F. Monier, E. Borel, M. A. Piens, and S. Picot.** 1999. Use of spectro-photometric reading for in vitro antifungal susceptibility testing of *Aspergillus* spp. *Can. J. Microbiol.* **45**:871-874.
4. **Denning, D. W., S. A. Radford, K. L. Oakley, L. Hall, E. M. Johnson, and D. W. Warnock.** 1997. Correlation between in vitro susceptibility testing to itraconazole and in vivo outcome of *Aspergillus fumigatus* infection. *J. Antimicrob. Chemother.* **40**:401-441.
5. **Espinel-Ingroff, A., F. Barchiesi, K. C. Hazen, J. V. Martinez-Suarez, and G. Scalise.** 1998. Standardization of antifungal susceptibility testing and clinical relevance. *Med. Mycol.* **36**(Suppl. 1):68-78.
6. **Espinel-Ingroff, A., M. Bartlett, R. Bowden, N. X. Chin, C. Cooper, Jr., A. Fothergill, M. R. McGinnis, P. Menezes, S. A. Messer, P. W. Nelson, F. C. Odds, L. Pasarell, J. Peter, M. A. Pfaller, J. H. Rex, M. G. Rinaldi, G. S. Shankland, T. J. Walsh, and I. Weitzman.** 1997. Multicenter evaluation of proposed standardized procedure for antifungal susceptibility testing of filamentous fungi. *J. Clin. Microbiol.* **35**:139-143.
7. **Espinel-Ingroff, A., K. Dawson, M. Pfaller, E. Anaissie, B. Breslin, D. Dixon, A. Fothergill, V. Paetznick, J. Peter, M. G. Rinaldi, and T. J. Walsh.** 1995. Comparative and collaborative evaluation of standardization of antifungal susceptibility testing for filamentous fungi. *Antimicrob. Agents Chemother.* **39**:314-319.
8. **Hawser, S. P., H. Norris, C. J. Jessup, and M. A. Ghannoum.** 1998. Comparison of a 2,3-bis(2-methoxy-4-nitro-5-sulphophenyl)-5-[(phenylamino) carbonyl]-2H-tetrazolium hydroxide (XTT) colorimetric method with the standardized National Committee for Clinical Laboratory Standards method of testing clinical yeast isolates for susceptibility to antifungal agents. *J. Clin. Microbiol.* **36**:1450-1452.
9. **Jahn, B., E. Martin, A. Stueben, and S. Bhakdi.** 1995. Susceptibility testing of *Candida albicans* and *Aspergillus* species by a simple microtiter menadione-augmented 3-(4,5-dimethyl-2-thiazolyl)-2,5-diphenyl-2H-tetrazolium bromide assay. *J. Clin. Microbiol.* **33**:661-667.
10. **Latge, J. P.** 1999. *Aspergillus fumigatus* and aspergillosis. *Clin. Microbiol. Rev.* **12**:310-350.
11. **Levitz, S. M., and R. D. Diamond.** 1985. A rapid colorimetric assay of fungal viability with the tetrazolium salt MTT. *J. Infect. Dis.* **152**:938-945.
12. **Llop, C., I. Pujol, C. Aguilar, J. Sala, D. Riba, and J. Guarro.** 2000. Comparison of three methods of determining MICs for filamentous fungi using different end-point criteria and incubation periods. *Antimicrob. Agents Chemother.* **44**:239-242.
13. **Meletiadis, J., J. F. G. M. Meis, J. W. Mouton, J. P. Donnelly, and P. E. Verweij.** 2000. Comparison of NCCLS and 3-(4,5-dimethyl-2-thiazolyl)-2,5-diphenyl-2H-tetrazolium bromide (MTT) methods of in vitro susceptibility testing of filamentous fungi and development of a new simplified method. *J. Clin. Microbiol.* **38**:2949-2954.
- 13a. **Meletiadis, J., J. W. Mouton, J. F. G. M. Meis, B. A. Bouman, J. P. Donnelly, P. E. Verweij, and Eurofung Network.** 2001. Colorimetric assay for antifungal susceptibility testing of *Aspergillus* species. *J. Clin. Microbiol.* **39**:3402-3408.
14. **Meletiadis, J., J. W. Mouton, J. L. Rodriguez-Tudela, J. F. G. M. Meis, and P. E. Verweij.** 2000. In vitro interaction of terbinafine with itraconazole against clinical

- isolates of *Scedosporium prolificans*. Antimicrob. Agents Chemother. **44**:470-472.
15. **Meshulam, T., S. M. Levitz, L. Christin, and R. D. Diamond.** 1995. A simplified new assay for assessment of fungal cell damage with the tetrazolium dye, (2,3)-bis-(2-methoxy-4-nitro-5-sulphenyl)-(2H)-tetrazolium-5-carboxanilide (XTT). J. Infect. Dis. **172**:1153-1156.
 16. **National Committee for Clinical Laboratory Standards.** 1998. Reference method for broth dilution antifungal susceptibility testing of conidium forming filamentous fungi. Proposed standard M38-P. National Committee for Clinical Laboratory Standards, Wayne, Pa.
 17. **Odds, F. C., and H. Van den Bossche.** 2000. Antifungal activity of itraconazole compared with hydroxy-itraconazole in vitro. J. Antimicrob. Chemother. **45**:371-373.
 18. **Paull, D. K., H. Shoemaker, and M. R. Boyd.** 1998. The synthesis of XTT: a new tetrazolium reagent that is bio-reducible to a water-soluble formazan. J. Heterocycl. Chem. **25**:911-914.
 19. **Pfaller, M. A., and M. G. Rinaldi.** 1993. Antifungal susceptibility testing. Current state of technology, limitations, and standardization. Infect. Dis. Clin. North Am. **7**:435-444.
 20. **Rex, J. H., M. A. Pfaller, M. G. Rinaldi, A. Polak, and J. N. Galgiani.** 1993. Antifungal susceptibility testing. Clin. Microbiol. Rev. **6**:367-381.
 21. **Roehm, N. W., G. H. Rodgers, S. M. Hatfield, and A. L. Glasebrook.** 1991. An improved colorimetric assay for cell proliferation and viability utilizing the tetrazolium salt XTT. J. Immunol. Methods **142**:257-265.
 22. **Scudiero, D. A., R. H. Shoemaker, K. D. Paull, A. Monks, S. Tierney, T. H. Nofziger, M. J. Currens, D. Seniff, and M. R. Boyd.** 1988. Evaluation of a soluble tetrazolium/formazan assay for cell growth and drug sensitivity in culture using human and other tumor cell lines. Cancer Res. **48**:4827-4833.
 23. **Sugar, A. M., and X. Liu.** 1995. Comparison of three methods of antifungal susceptibility testing with the proposed NCCLS standard broth macrodilution assay: lack of effect of phenol red. Diagn. Microbiol. Infect. Dis. **21**:129-133.
 24. **Tellier, R., M. Krajden, G. A. Grigoriew, and I. Campbell.** 1992. Innovative end-point determination system for antifungal susceptibility testing of yeasts. Antimicrob. Agents Chemother. **36**:1619-1625.



CHAPTER

3

DRUG INTERACTION MODELING OF ANTIFUNGALS

- In vitro interaction of terbinafine with itraconazole against clinical isolates of *Scedosporium prolificans*
- Drug interaction modeling of in vitro combination of azoles with terbinafine against clinical *Scedosporium prolificans* isolates
- Assessing the in vitro interaction of antifungal drugs: Comparison of different drug interaction models

Chapter 3.1

In Vitro Interaction of Terbinafine with Itraconazole against Clinical Isolates of *Scedosporium prolificans*

Antimicrobial Agents and Chemotherapy 2000; 44: 470-472

IN VITRO INTERACTION OF TERBINAFINE WITH ITRACONAZOLE AGAINST CLINICAL ISOLATES OF *SCEDOSPORIUM PROLIFICANS*

JOSEPH MELETIADIS¹, JOHAN W. MOUTON², JUAN L. RODRIGUEZ-TUDELA³,
JACQUES F. G. M. MEIS^{1,2}, AND PAUL E. VERWEIJ¹

Department of Medical Microbiology, University Hospital Nijmegen¹, and Department of Medical Microbiology and Infectious Diseases, Canisius-Wilhelmina Hospital², Nijmegen, The Netherlands, and Unidad de Micología, Centro Nacional de Microbiología, Instituto de Salud Carlos III, Majadahonda (Madrid), Spain³

In order to develop new approaches for the chemotherapy of invasive infections caused by *Scedosporium prolificans*, the in vitro interaction between itraconazole and terbinafine against 20 clinical isolates was studied using a checkerboard microdilution method. Itraconazole and terbinafine alone were inactive against most isolates, but the combination was synergistic against 95 and 85% of isolates after 48 and 72 h of incubation, respectively. Antagonism was not observed. The MICs obtained with the terbinafine-itraconazole combination were within levels that can be achieved in plasma.

Invasive infections caused by *Scedosporium* species are uncommon but are generally fatal in immunocompromised patients, especially when they are caused by *Scedosporium prolificans* (2, 13). Treatment includes surgical debridement, if possible, and antifungal chemotherapy, although the optimal choice and duration of therapy are unknown. Azoles, such as miconazole and itraconazole, have been used with some success for the treatment of invasive infections with *Scedosporium apiospermum* (6), but treatment failures have also been reported (15). *S. prolificans* is considered multiresistant since low in vitro activities have been reported for amphotericin B, flucytosine, and the azoles (3). Even novel antifungal agents such as the triazoles voriconazole, posaconazole (SCH56592), and Syn-2869 (5, 9) and the echinocandins LY303366 and caspofungin (MK-0991) show limited or no in vitro activity against this fungus (4, 5). We have previously reported a patient with pulmonary pseudallescheriosis who failed itraconazole therapy but responded after treatment was changed to terbinafine (15). The *S. apiospermum* isolate was resistant to either drug alone but was susceptible in vitro to the terbinafine-itraconazole combination (N. S. Ryder and I. Leitner, Abstr. 38th Intersci. Conf. Antimicrob. Agents Chemother., abstr. J-155, 1998). In the present study we investigated whether terbinafine and itraconazole act synergistically against 20 clinical *S. prolificans* isolates to determine if this combination is a potentially useful combination in the treatment of these infections.

MATERIALS AND METHODS

All isolates were obtained from clinical specimens (3) and subcultured on Sabouraud glucose agar (SAB) plates with 0.5% chloramphenicol and incubated at room

temperature for 7 days. They were then subcultured again on SAB plates and incubated for another 5 to 7 days at 37°C, and spores were collected. *Paecilomyces variotii* (ATCC 22319) was used as a quality control strain, and all isolates were tested in duplicate.

MICs were determined by a broth microdilution method according to National Committee for Clinical Laboratory Standards guidelines (proposed standard M38-P) (11). Briefly, a suspension of spores was adjusted with a spectrophotometer (Spectronic 20D; Milton Roy, Rochester, N.Y.) to 68 to 70% transmission at a wavelength of 530 nm and diluted 10-fold to yield a final inoculum of 1×10^4 to 5×10^4 CFU/ml. The spectrophotometer transmissions were verified by enumeration of colonies per milliliter of serial dilution on SAB plates that were incubated at 35°C for 48 h. These cultures showed that the final inoculum varied between 1.5×10^4 and 3.5×10^4 CFU/ml. Terbinafine (Novartis, Basel, Switzerland) and itraconazole (Janssen Research Foundation, Beerse, Belgium) were tested in RPMI 1640 medium with L-glutamine and without bicarbonate (GIBCO BRL, Life Technologies, Breda, The Netherlands), buffered to pH 7.0 with 0.165 M MOPS (3-N-morpholinopropanesulfonic acid). The final concentrations ranged from 0.5 to 32 µg/ml for itraconazole and 0.06 to 64 µg/ml for terbinafine. Growth was graded on a scale of 0 to 4 as follows: 4 indicated no reduction in growth, 3 indicated a 25% reduction of growth, 2 indicated a 50% reduction of growth, 1 indicated a 75% reduction of growth, and 0 indicated an optically clear well. The MIC was defined as the lowest concentration of antifungal compound that inhibited growth by 50% or more.

A two-dimensional, two-agent broth microdilution checkerboard technique was used to study the interactions between itraconazole and terbinafine. Serial twofold dilutions of itraconazole and terbinafine, alone and in combination, were tested against final inocula of 1×10^4 to 5×10^4 CFU/ml. In order to obtain an exact percentage of growth for each well, the dye 3-(4,5-dimethyl-2-thiazyl)-2,5-diphenyl-2H-tetrazolium bromide (MTT; Sigma Chemical, St. Louis, MO.) was added together with the inoculum to each well at a

Table 1. MICs and Σ FICs of itraconazole (ICZ) and terbinafine (TB) alone and in combination against *S. proliferans* after 48 and 72 h of incubation

Isolate	MIC (μ g/ml)		Lowest Σ FIC at 48 h	MIC of the combination (ICZ/ TB)	MIC (μ g/ml)		Lowest Σ FIC at 72 h	MIC of the combination (ICZ/ TB)
	ICZ	TB			ICZ	TB		
7898	16	0.5	0.25	2/0.06	>32	4	0.14	1/0.5
7906	16	0.5	0.25	2/0.06	>32	4	0.25	8/0.5
7902	16	0.5	0.25	2/0.06	>32	4	0.31	4/1
7921	>32	0.5	0.18	4/0.06	>32	4	0.51	0.5/2
7946	16	1	0.19	2/0.06	>32	4	0.26	0.5/1
7891	>32	1	0.12	4/0.06	>32	4	0.16	1/0.5
7940	>32	0.5	0.52	1/0.25	>32	32	0.09	2/2
7886	>32	1	0.27	1/0.25	>32	>64	0.02	0.5/0.5
7901	>32	1	0.09	2/0.06	>32	>64	0.05	2/1
7924	>32	1	0.15	1/0.13	>32	>64	0.05	1/2
7920	>32	0.5	0.27	1/0.125	>32	>64	0.04	0.5/2
7894	>32	1	0.12	4/0.06	>32	4	0.38	8/1
7905	16	1	0.19	2/0.06	>32	8	0.52	1/4
7888	16	2	0.13	1/0.125	>32	>64	0.07	0.5/4
7908	>32	1	0.14	1/0.125	>32	>64	0.05	2/1
7913	>32	0.5	0.28	2/0.125	>32	>64	0.05	1/2
7930	16	1	0.12	1/0.06	>32	>64	0.05	1/2
7903	>32	8	0.09	2/05	>32	>64	2	>32/>64
7900	>32	2	0.10	2/0.13	>32	>64	0.25	16/1
7912	>32	>64	0.04	0.5/2	>32	>64	0.04	0.5/2

final concentration of 0.1 mg/ml (8). After 48 or 72 h of incubation, the content of each well was removed and 200 μ l of isopropanol containing 5% HCl (1 M) was added. After 30 min of incubation at room temperature and gentle agitation, the optical density (OD) was measured with a spectrophotometer (MS2 reader, Titertekplus; ICN Biomedical Ltd., Basingstoke, United Kingdom) at 550 nm (8). The OD of the blank, to which a conidium-free inoculum had been added, was subtracted from the OD values. The percentage of growth for each well was calculated by comparing the OD of a well with that of the drug-free control. For each itraconazole-terbinafine combination which showed the same percentage of growth with the MICs, the summation of the fractional inhibitory concentrations (Σ FIC) of each drug was calculated for these combinations as follows: (concentration of itraconazole in the combination/MIC of itraconazole) + (concentration of terbinafine in the combination/MIC of terbinafine). The interpretation of the Σ FIC was as follows: the synergistic effect was ≤ 0.5 , the indifferent effect was >0.5 but ≤ 4 , and the antagonistic effect was >4 (7). The results of experiments with the two agents alone and in combination were analyzed separately as well as together by calculating the mean ODs. Since all analyses yielded identical results, we present the results based on the mean OD from both experiments.

RESULTS

The MICs of terbinafine and itraconazole based on 50% reduction of growth for *P. variotii* were 0.125 and 0.25 μ g/ml, respectively. Itraconazole was

inactive in vitro against most isolates, with the MIC at which 90% of the isolates were inhibited being >32 μ g/ml after both 48 and 72 h of incubation (Table 1). An attempt was made to establish the exact MIC of itraconazole by an agar dilution method. Serial dilutions ranging from 32 to 512 μ g of itraconazole per ml were made in RPMI 1640 agar. The growth of none of the *S. proliferans* isolates was inhibited by any of these concentrations after 48 h of incubation. Therefore, a MIC of 64 μ g/ml was chosen for calculations for those isolates that grew in the wells that contained the highest concentration of itraconazole. The MIC of terbinafine at which 90% of the isolates were inhibited was 2 μ g/ml after 48 h but increased to 64 μ g/ml after 72 h. Synergism was found for 19 of 20 (95%) of the *S. proliferans* isolates after 48 h and for 17 of 20 (85%) of the isolates after 72 h of incubation (Table 1). For three isolates the effect of the combination appeared to be indifferent after 72 h of incubation, and antagonism was not observed.

DISCUSSION

Although drug interactions in vitro are difficult to assess, we believe that the observed synergism is significant for several reasons. (i) Despite the fact that we selected a stringent criterion for the definition of synergism, almost all isolates showed synergism after both 48 and 72 h of incubation. (ii) Because the MIC of

itraconazole was set at 64 µg/ml for most isolates, the calculated ΣFIC underestimates the actual level of synergism. Calculations with higher MICs of single drugs would have resulted in even lower ΣFIC. (iii) Itraconazole and terbinafine block different steps of the same pathway of fungal ergosterol biosynthesis, which supports the possibility of synergistic action. The classic example of proven synergism in this respect is the combination of trimethoprim with sulfonamides, which also interacts with consecutive steps of a common pathway. Furthermore, the combination of terbinafine with azoles has been shown to be synergistic in vitro for other fungi, including *Candida albicans* (1), *Candida glabrata*, and *Cryptococcus neoformans* (A. W. Fothergill, I. Leitner, J. G. Meingassner, N. S. Ryder, and M. G. Rinaldi, Abstr. 36th Intersci. Conf. Antimicrob. Agents Chemother., abstr. E53, 1996), and for *Pythium insidiosum* (14). Synergism has been reported for combinations of amphotericin B with azoles against *S. apiospermum* but the synergistic activity was less pronounced than for the terbinafine-itraconazole combination and occurred only for a limited number of isolates (16). In another study, the effect of amphotericin B combined with terbinafine was indifferent against *S. apiospermum*, but terbinafine with fluconazole was synergistic against the same isolate (Ryder and Leitner, 38th ICAAC, abstr. J-155). Terbinafine appears to interact synergistically with the class of azole antifungal drugs.

The MICs of the terbinafine-itraconazole combination are within the range that can be achieved in blood. The achievable maximum concentrations of terbinafine are approximately 1.7 µg/ml within 2 h of oral administration of a dose of 500 mg (10). Levels in serum above 3.0 µg/ml can be achieved with itraconazole (12), and even higher levels may be achieved with the oral solution or the intravenous formulation that is now undergoing clinical evaluation.

Invasive infections caused by *S. prolificans* are generally fatal, and at present there is no antifungal regimen that has been shown to be effective. The in vitro synergism of itraconazole and terbinafine that we demonstrated may prove effective for the treatment of these infections. Animal-model and clinical studies are warranted to further elucidate the potential of terbinafine-itraconazole combination therapy in difficult-to-treat infections by filamentous fungi.

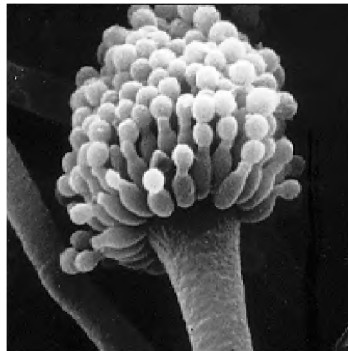
ACKNOWLEDGMENTS

This work was supported by the European Commission Training and Mobility of Researchers grant ERBFMRXCT97-0145 to Joseph Meletiadis.

REFERENCES

1. Barchiesi, F., L. Falconi Di Francesco, and G. Scalise. 1997. In vitro activities of terbinafine in combination with fluconazole and itraconazole against isolates of *Candida albicans* with reduced susceptibility to azoles. *Antimicrob. Agents Chemother.* **41**:1812-1814.
2. Berenguer, J., J. L. Rodriguez-Tudela, C. Richard, M. Alvarez, M. A. Sanz, L. Gaztelurrutia, J. Ayats, and J. V. Martinez-Suarez. 1997. Deep infections caused by *Scedosporium prolificans*. A report on 16 cases in Spain and a review of the literature. *Scedosporium prolificans* Spanish Study Group. *Medicine (Baltimore)* **76**:256-265.
3. Cuenca-Estrella, M., B. Ruiz-Díez, J. V. Martínez-Suárez, A. Monzón, and J. L. Rodríguez-Tudela. 1999. Comparative in vitro activity of voriconazole (UK-109,496) and six other antifungal agents against clinical isolates of *Scedosporium prolificans* and *Scedosporium apiospermum*. *J. Antimicrob. Chemother.* **43**:149-151.
4. Del Poeta, M., W. A. Schell, and J. R. Perfect. 1997. In vitro activity of pneumocandin L-743,872 against a variety of clinically important moulds. *Antimicrob. Agents Chemother.* **41**:1835-1836.
5. Espinel-Ingroff, A. 1998. Comparison of in vitro activities of the new triazole SCH56592 and the echinocandins MK-0991 (L-743,872) and LY303366 against opportunistic filamentous and dimorphic fungi and yeasts. *J. Clin. Microbiol.* **36**:2950-2956.
6. Garcia-Arata, M. I., M. J. Otero, M. Zomeno, M. A. de la Figuera, M. C. de las Cuevas, and M. Lopez-Brea. 1996. *Scedosporium apiospermum* pneumonia after autologous bone marrow transplantation. *Eur. J. Clin. Microbiol. Infect. Dis.* **15**:600-603.
7. Hallander, H. O., K. Dornbusch, L. Gezelius, K. Jacobson, and I. Karlsson. 1982. Synergism between aminoglycosides and cephalosporins with anti-pseudomonal activity: interaction index and killing curve method. *Antimicrob. Agents Chemother.* **22**:743-752.
8. Jahn, B., A. Stuben, and S. Bhakdi. 1996. Colorimetric susceptibility testing for *Aspergillus fumigatus*: comparison of menadione-augmented 3-(4,5-dimethyl-2-thiazolyl)-2,5-diphenyl-2H-tetra-zolium bromide and Alamar blue tests. *J. Clin. Microbiol.* **34**:2039-2041.
9. Johnson, E. M., A. Szekely, and D. W. Warnock. 1999. In vitro activity of Syn-2869, a novel triazole agent, against emerging and less common mould pathogens. *Antimicrob. Agents Chemother.* **43**:1260-1263.
10. Kovarik, J. M., E. A. Mueller, H. Zehender, J. Denouël, H. Caplan, and L. Millerioux. 1995. Multiple-dose pharmacokinetics and distribution in tissue of terbinafine and metabolites. *Antimicrob. Agents Chemother.* **39**:2738-2741.
11. National Committee for Clinical Laboratory Standards. 1998. Reference method for broth dilution antifungal susceptibility testing of conidium-forming fungi. Proposed standard M38-P. National Committee for Clinical Laboratory Standards, Villanova, Pa.
12. Patterson, T. F., J. Peters, S. M. Levine, A. Anzueto, C. L. Bryan, E. Y. Sako, O. L. Miller, J. H. Calhoun, and M. G. Rinaldi. 1996. Systemic availability of

- itraconazole in lung transplantation. *Antimicrob. Agents Chemother.* **40**:2217-2220.
13. **Salkin, I. F., M. R. McGinnis, M. J. Dykstra, and M. G. Rinaldi.** 1988. *Scedosporium inflatum*, an emerging pathogen. *J. Clin. Microbiol.* **26**:498-503.
14. **Shenp, J. L., B. K. English, L. Kaufman, T. A. Pearson, J. W. Thompson, R. A. Kaufman, G. Frisch, and M. G. Rinaldi.** 1998. Successful medical therapy for deeply invasive facial infection due to *Pythium insidiosum* in a child. *Clin. Infect. Dis.* **27**:1388-1393.
15. **Verweij, P. E., N. J. Cox, and J. F. G. M. Meis.** 1997. Oral terbinafine for treatment of pulmonary *Pseudallescheria boydii* infection refractory to itraconazole therapy. *Eur. J. Clin. Microbiol. Infect. Dis.* **16**:26-28.
16. **Walsh, T. J., J. Peter, D. A. McGough, A. W. Fothergill, M. G. Rinaldi, and P. A. Pizzo.** 1995. Activities of amphotericin B and antifungal azoles alone and in combination against *Pseudallescheria boydii*. *Antimicrob. Agents Chemother.* **39**:1361-1364.



Chapter 3.2

Drug Interaction Modeling of in vitro Combination of Azoles
with Terbinafine against Clinical
Scedosporium prolificans Isolates

Submitted for publication

DRUG INTERACTION MODELING OF IN VITRO COMBINATION OF AZOLES WITH TERBINAFINE AGAINST CLINICAL *SCEDOSPORIUM PROLIFICANS* ISOLATES

JOSEPH MELETIADIS¹, JOHAN W. MOUTON², JACQUES F. G. M. MEIS², AND PAUL E. VERWEIJ¹

Departments of Medical Microbiology, University Medical Center Nijmegen¹, Department of Medical Microbiology and Infectious Diseases, Canisius-Wilhelmina Hospital², Nijmegen, The Netherlands

The in vitro interaction between terbinafine and the azoles, voriconazole, miconazole and itraconazole against 5 clinical *Scedosporium prolificans* isolates after 48 and 72 h of incubation was tested with a microdilution checkerboard (12x8) technique. The antifungal effects of the drugs alone and in combination on the fungal biomass as well as on the metabolic activity of fungi was measured using a spectrophotometric and two colorimetric methods, based on MIC-1 and MIC-2 (the lowest drug concentration showing 75% and 50% growth inhibition, respectively). The nature and the intensity of the interactions were assessed using a non-parametric approach (FIC index model) and a fully parametric response surface approach (Greco model) of the Loewe additivity no interaction model (LA) as well as a non-parametric approach (Prichard model) and a parametric surface response approach of the Bliss independence no interaction model (BI). Statistically significant synergy was found between each of the three azoles and terbinafine in all cases although with different intensity. A 27 to 64-fold and 16 to 90-fold reduction of geometric mean of the azole and terbinafine MICs, respectively was observed when they were combined resulting in FIC indices lower than 1 down to 0.02. MIC-1 resulted in higher levels of synergy, which were more consistent between the two incubation periods than MIC-2. The strongest synergy among the azoles was found with miconazole using the BI-based models and voriconazole using the LA-based models. The synergistic effects both on fungal growth and metabolic activity were more potent after 72 h of incubation. Fully parametric approaches in combination with the modified colorimetric method might prove useful for testing the in vitro interaction of antifungal drugs against filamentous fungi.

S. prolificans is a filamentous fungus, which causes various types of human infections ranging from asymptomatic colonizations, and localized infections in immunocompetent individuals to disseminated infections usually in immunocompromised patients (7, 18). The mortality rate of invasive infections is high (92%) despite antifungal chemotherapy with amphotericin B, miconazole, fluconazole or itraconazole (18). However, the effectiveness of antifungal chemotherapy is uncertain since any success reported in the literature was associated with additional intervention such as surgery, immunomodulation or recovery of host defense. Furthermore, in vitro susceptibility tests indicate a multi-resistant fungus due to the very low growth inhibitory activities of conventional and new antifungal drugs (10, 12, 27). Therefore, new approaches for treating these infections are warranted. Promising results are coming up from the field of in vitro combination of antifungal drugs against fungi (3, 35, 41), especially after the recent findings of synergistic interaction between itraconazole and terbinafine against different fungi including *S. prolificans* (31, 32). Despite the fact that these two drugs were inactive alone, the in vitro combination of

them succeeded in inhibiting the fungal growth at concentrations achievable in plasma.

However, assessing the nature and intensity of drug interactions is still a debated area of chemotherapy. The in vitro interaction of two or more agents is dependent both on the methodology which is used to generate the data as well as on the way the results are analyzed, resulting to variable as well as controversial conclusions (6, 20, 35).

Despite the considerable progress which has been made in producing reproducible results with the M-38P standard proposed by the NCCLS (33), the in vitro antifungal susceptibility testing of filamentous fungi is faced with several problems regarding the choice of the proper testing method, reading system, MIC endpoint and incubation period (11, 15, 34, 39). Different results might be obtained by choosing different combinations of these parameters. This is even more complicated when two drugs are combined in vitro. Spectrophotometric and colorimetric modifications of the NCCLS method have been described, quantifying more precisely the fungal growth and being able to detect small changes in metabolic activity of fungi, respectively (26, 30). Based on these methods, the

effects of antifungal drugs either on the fungal biomass or on metabolic status of fungi can be measured.

However, even when the same methodology is used for testing the in vitro susceptibility to drug combinations variable conclusions might be inferred depending on the way data are analyzed. Many models and approaches have been described for the assessment of in vitro drug interactions and extensive reviews have summarized them (5, 6, 20, 38, 43). The assumption of no interaction has a central position in these debates since synergy and antagonism are defined as departures from this. Thus, when the observed effect is more or less than the effect predicted from the no interaction theory synergy or antagonism is claimed, respectively. Among the various no interaction models, Loewe additivity (LA) and Bliss independence (BI) are the two major competitor candidates for reference models (20). LA is based on the idea that a drug cannot interact with itself while BI on the idea that two drugs act independently with the probabilistic sense of independence. Based on these concepts, various models have been described based on both parametric and non-parametric approaches of these two reference models. These include estimates of the intensity of interaction and summary results incorporating statistically significance levels.

Given that a synergistic interaction might have great impact on approaches for controlling infections caused by *S. prolificans* in clinical practice (19, 25), the unbiased assessment of in vitro interaction of antifungal drugs is crucial. In this study, the interaction between three azoles, voriconazole, miconazole, and itraconazole, and an allylamine, terbinafine, was tested in vitro against 5 clinical isolates of *S. prolificans*. In order to reduce biases derived from factors related to the method of antifungal susceptibility testing as well as to theoretical and mathematical models for defining synergism, the in vitro interaction of antifungal drugs were determined with a recently described spectrophotometric and colorimetric method (26), after 48 and 72 h of incubation based on two MIC endpoints and assessed using two parametric and two non-parametric models based on Loewe additivity and Bliss independence, described in the literature.

MATERIALS AND METHODS

Isolates. Five *Scedosporium prolificans* strains from our private collection were used in this study namely AZN7898 and AZN7918 isolated from blood, AZN7901 and AZN7902 isolated from sputum and a reference strain AZN7906 (NCPF7108). The isolates were stored in 50% glycerol in water at -70°C . *Candida parapsilosis* (ATCC 22019) and *C. krusei* (ATCC 6258) were used as quality control (QC).

Antifungal drugs. Three antifungal drugs belonging to

azoles namely, miconazole (MW 479.15) (Janssen Research Foundation, Beerse, Belgium), itraconazole (MW 705.64) (Janssen Research Foundation), voriconazole (MW 349.32) (Pfizer Central Research, Sandwich, United Kingdom), and the allylamine terbinafine (MW 291.44) (Novartis, Basel, Switzerland) were used in this study. Miconazole and voriconazole were dissolved in dimethylsulfoxid (DMSO) (Merck, Darmstadt, Germany) at final concentrations of 25,600 mg/l and 6,400 mg/l, respectively. Terbinafine was dissolved in DMSO with 5% Tween 80 (Merck) and itraconazole in 0.1 M HCL/100% Aceton (1:1) (Merck) at final concentrations of 25600 mg/l and 12,800 mg/l, respectively.

Medium. The medium used was liquid RPMI 1640 (with L-glutamine, without sodium bicarbonate) (GIBCO BRL, Life Technologies, Woerden, The Netherlands) supplemented with 0.165 M 3-N-morpholinopropanesulfonic acid buffer (Sigma-Aldrich Chemie GmbH, Steinheim, Germany). The pH of the medium was adjusted to 7.0 ± 0.1 at 22°C .

Inoculum. Each isolate had been grown for 7 days on Sabouraud dextrose agar with 0.5% chloramphenicol at room temperature and was then subcultured on the same medium for a further 5-7 days at 37°C . Conidia were collected with a swab and suspended in sterile water. After the heavy particles were allowed to settle the turbidity of the supernatants were measured spectrophotometrically at 530 nm (Spectronic 20D; Milton Roy, Rochester, N.Y., USA) and its transmittance was adjusted to 68-70% by diluting. Each suspension was diluted 1:50 in RPMI 1640 to obtain 2x the final inoculum size ranging from 0.5×10^4 to 5×10^4 CFU/ml. Inoculum size was verified by plating 100 μl of serial dilutions of each inoculum onto a Sabouraud dextrose agar plate and incubated until growth became visible.

For the QCs, the transmittance of blastoconidia suspensions obtained from 1 to 2 day-old colonies was adjusted to 75-77% at 530 nm. The suspensions were diluted 1/1000 and a final inoculum ranging from 0.5×10^3 to 2.5×10^3 CFU/ml was used.

Susceptibility testing method. The in vitro interaction between the three azoles and the allylamine terbinafine was studied using a two-dimensional (12x8) checkerboard microdilution technique in sterile, 96-well flat-bottom microtitration plates described below. In order to choose the appropriate range of drug concentrations for the combination studies, the MICs of the individual drugs were determined in an exploratory study for each strain.

(i) Microtitration plates set up. For the combination studies, each drug was first serially diluted twofold in the corresponding solvents and then 100-fold in the medium according to the dilution scheme of NCCLS for water-insoluble drugs in order to obtain 4 times the final concentration. 50 μl of each drug concentration of the azole was added to columns 1 to 11 and then 50 μl of each concentration of terbinafine was added to rows A to G. In the wells of column 12, 50 μl of the medium containing 1% of the azole solvent was added and in wells of row H, 50 μl of the medium contained 1% of terbinafine solvent was added. Thus, column 12 and row H contained alone the azole and terbinafine, respectively and the well H12 was the drug-free well that served as growth control. The final concentrations

after the addition of 100 µl of inoculum ranged from 64 to 0.06 µg/ml for miconazole, 32 to 0.03 µg/ml for itraconazole, 16 to 0.015 for voriconazole, and 64 to 1 µg/ml for terbinafine. The microtitration plates were kept in -70°C until the day of the experiments.

(ii) Incubation and reading method. On the day of the test, microtitration plates were thawed and each well was inoculated with 100 µl of the inoculum suspension. After agitation for 15 sec, the microtitration plates were incubated for 72 h at 37°C. The growth in each well was quantified by using three methods: a spectrophotometric method after 48 and 72 h of incubation (SP48 and SP72, respectively) where the optical density (OD) at 405 nm of each well was measured, a colorimetric method utilizing the dye MTT after 72 h of incubation (COL72) where the conversion of the dye MTT to colored formazan derivative after 2 h of exposure by metabolic active fungi was measured at 550 nm and a modification of the latter colorimetric method after 48 and 72 h of incubation (mCOL48 and mCOL72, respectively) where the dye MTT was added to the inoculum and therefore fungi was exposed to the dye for 48 and 72 h as described previously (26). The percentage of growth in each well was calculated as the OD of each well/OD of the drug free well after subtracting the background OD obtained from microorganisms free microtiter plates were proceeded as the inoculated plates. Thus, growth- and metabolic inhibitory effects of the drugs alone and in combination were estimated based on the results of spectrophotometric and colorimetric methods, respectively.

Drug interaction modeling. In order to assess the nature of the in vitro interaction between the three azoles and terbinafine against each *S. proliferans* strain, the data obtained using the three reading methods, as described above, were analyzed using four different models. The models were parametric and non-parametric approaches of the following two no interaction theories: the Loewe additivity and the Bliss independence. In the Loewe additivity theory concentrations of the drugs, alone or in combination, that produce the same effect, are compared while in the Bliss independence based models the estimates of the combined effect based on the effect of the individual drugs were compared with these obtained by the experiment.

(i) Loewe additivity is described by the following equation: $1 = d_A/D_A + d_B/D_B$ where d_A and d_B are the concentrations of the drugs A and B in the combination which elicit a certain effect and D_A and D_B the iso-effective concentrations of the drugs A and B when acting alone. The non-parametric approach is based on the fractional inhibitory concentration index model expressed with the following equation:

$$\Sigma\text{FIC} = \text{FIC}_A + \text{FIC}_B = \frac{C_A^{\text{comb}}}{\text{MIC}_A^{\text{alone}}} + \frac{C_B^{\text{comb}}}{\text{MIC}_B^{\text{alone}}}$$

where C_A^{comb} and C_B^{comb} are the concentrations of the drugs A and B in a combination and $\text{MIC}_A^{\text{alone}}$ and $\text{MIC}_B^{\text{alone}}$ the concentrations of the drugs A and B when acting alone (23). The ΣFIC was calculated for all combinations of the two drugs, which showed the same growth as the MICs. For each data set, among all ΣFICs , the FIC index (FIC_i) was determined as the ΣFIC_{\min} (the lowest ΣFIC) only when the

ΣFIC_{\max} (the highest ΣFIC) was smaller than 4; otherwise the FIC_i was determined as the ΣFIC_{\max} (23) (Fig. 1Ai). Two MIC endpoints were used for the evaluation of each data set. These were the MIC-1 and MIC-2 and were defined as the lowest drug concentration showing 25% and 50% of growth compared to the growth control, respectively. Based on these endpoints two types of FIC indices were determined, FIC_i-1 and FIC_i-2, respectively. Off-scale MICs were converted to the next highest or lowest doubling concentration. Finally, the median and the range of FIC indices of the replicates were determined for both the MIC-1 and MIC-2. When the FIC indices in all four replicates were smaller than 1, significant synergy was claimed, when they were higher than 1 significant antagonism was claimed and in all other cases additivity or indifference was concluded. In addition isobolograms were plotted in order to visualize the departure from additivity (Fig. 1Aii).

The fully parametric surface approach described by Greco et al. (21) was used based on the following equation:

$$1 = \frac{D_A}{\text{IC}_{50,A} \left(\frac{E}{E_{\max} - E} \right)^{1/m_A}} + \frac{D_B}{\text{IC}_{50,B} \left(\frac{E}{E_{\max} - E} \right)^{1/m_B}} + \alpha \frac{D_A D_B}{\text{IC}_{50,A} \text{IC}_{50,B} \left(\frac{E}{E_{\max} - E} \right)^{0.5(1/m_A + 1/m_B)}}$$

where E is the OD (dependent variable) at the drug concentrations D_A and D_B (independent variables), E_{\max} is the maximal OD observed in the drug-free control, $\text{IC}_{50,A}$ and $\text{IC}_{50,B}$ are the drug concentrations producing 50% of the E_{\max} , m_A and m_B are the slopes of the concentration-effect curves (Hill coefficient) for the drugs A and B, respectively and α is the interaction parameter which describes the nature of the interaction. This model was fitted directly to experimental data (the average OD among the replicates for all concentrations of the two drugs alone or in combination) with a non-weighted, non-linear regression analysis using the MODLAB program (MEDIMATICS, Maastricht, The Netherlands, www.medimatics.nl). Goodness of fit criteria included the 95% confidence interval (CI) of the fitted parameters, the R^2 , the sum of the squares, correlation and covariance matrices and the residual plots.

When the parameter α was positive and 95% CI did not include 0, statistically significant synergy was claimed while when α was negative and its 95% CI did not include 0, statistically significant antagonism was claimed. In any other case Loewe additivity was concluded. The additivity surface was simulated by fixing all parameters of the Greco model to values obtained after the model fitted to experimental data except α which was fixed at 0. The fitted experimental surface calculated by the Greco model was then subtracted from the additivity surface calculated as described above. The percentage above (synergistic combinations) or below (antagonistic interactions) the additivity surface was plotted in three-dimensional graph and a contour plot was constructed in order to determine the range of drug concentrations producing synergistic effects (Fig. 1B).

(ii) Bliss independence is described by the equation $I_i = I_A + I_B - I_A \times I_B$ where I_i is the predicted percentage of inhibition of the theoretical combination of the drugs A and B and I_A , I_B are the experimental percentages of inhibition of each drug acting alone, respectively. Since $I = 1 - E$ where E is the percentage of growth and substituting to the former

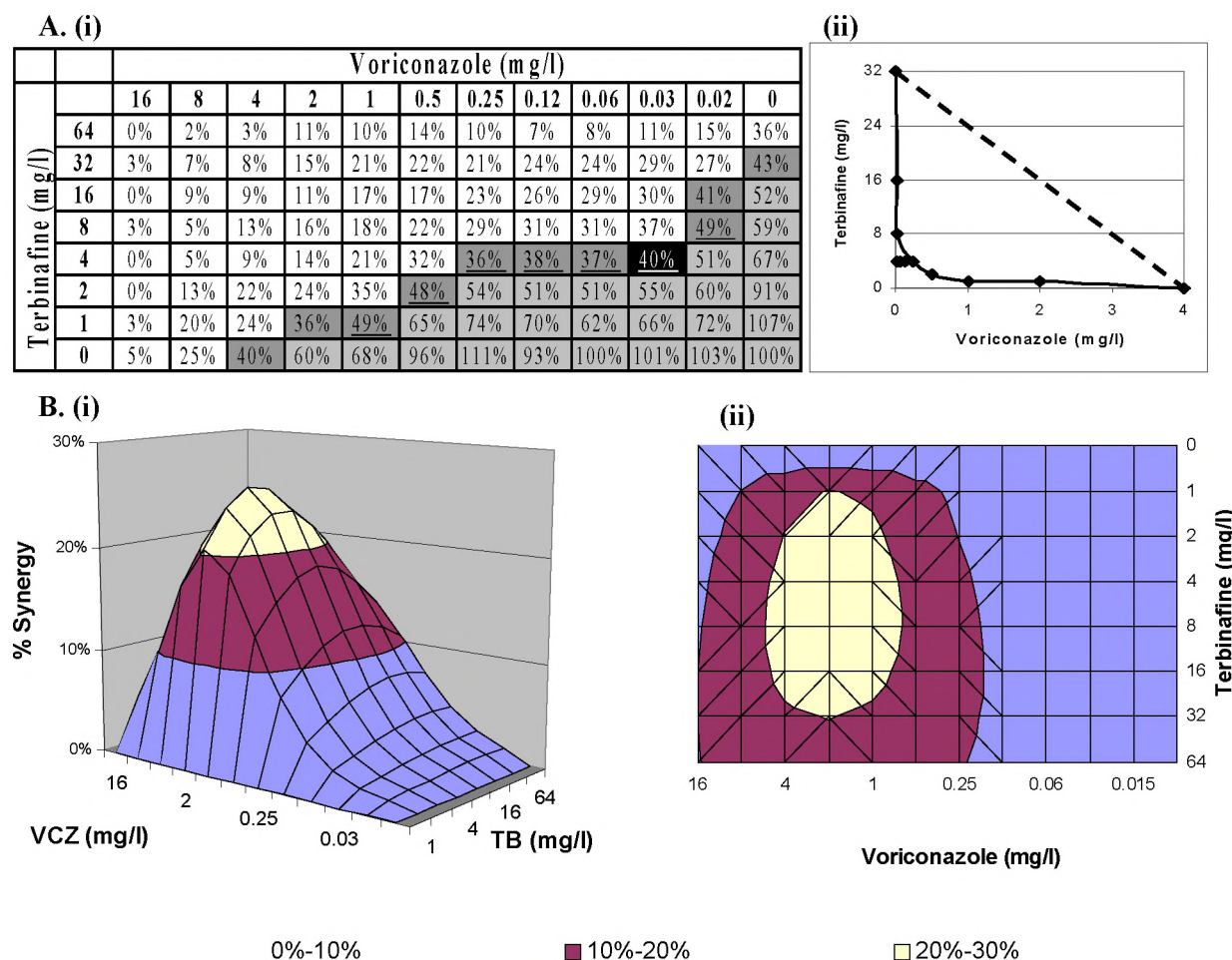


Figure 1. Assessment of the in vitro interaction between voriconazole (VCZ) and terbinafine (TB) against a clinical *S. proliferans* strain (AZN7898) based on Loewe additivity no interaction theory using the SP48 method. **A.** FIC index model (i). The checkerboard with the % of growth for each combination where are shown the combinations with more than 50% of growth (light gray area), the MICs-2 of VCZ and of TB and the iso-effective combination based on which the Σ FIC were calculated (dark gray area), the combinations with Σ FICs lower than 0.5 (underline wells) and the combination with lowest Σ FIC (0.20) (black well) which corresponded to the FICi-2. (ii). The corresponding isobologram with the additivity line (dashed line). **B.** Greco model. The three-dimensional (i) and the contour plot (ii) of the % of synergy with the following fitted parameters (\pm 95% CI): $IC_{50,TB} = 5.33 \pm 0.57$, $IC_{50,VCZ} = 2.63 \pm 0.31$, $m_{TB} = -0.51 \pm 0.04$, $m_{VCZ} = -1.1 \pm 0.11$, $\alpha = 13.9 \pm 1.6$.

equation, the following equation is derived: $E_i = E_A \times E_B$ where E_i is the predicted percentage of growth of the theoretical combination of the drugs A and B, respectively and E_A , E_B are the experimental percentages of inhibition and growth of each drug acting alone, respectively. Interaction is described by the difference ΔE between the predicted and measured percentage of growth at various concentrations. Because of the nature of interaction testing using microtiter plates with twofold dilution of either drug, this results in a ΔE for each drug combination. Using a three-dimensional plot the ΔE depicted on the Z-axis, this results in a surface plot. In the non-parametric surface approach described by Prichard et al. (36, 37), the E_A and E_B are obtained directly from the experimental data while in the parametric surface approach (14, 20) these values are derived from fitting the E_{max} model to the concentration-effect curves of each drug alone. Thus, for the latter approach E_A and E_B are obtained by the following equation: $E_{A,B} = E_{max} \times (D/IC_{50})^m / [1 + (D/IC_{50})^m]$ where E , D , E_{max} , IC_{50} and m are the same parameters for

drug A and B as described above. The parameters of the model were obtained by a non-weighted non-linear regression analysis using the GraphPad Prism Software (San Diego, CA). Data were normalized by using the percentages, and the maximum and the minimum of the E_{max} model corresponding with 100% and 0%, respectively, were kept constant. The fit of the model was interpreted using the run test and the R^2 values. After the E_{max} model was fitted to the data, the parameters generated were used to calculate the no interaction surface for each replicate separately.

For each combination of the two drugs in each of the four independent experiments, the observed OD of growth obtained from the experimental data was subtracted from the predicted OD calculated as described above for each model. When the average difference was positive without its 95% CI among the four replicates overlapping 0, statistically significant synergy was claimed, when the difference was negative without its 95% CI among the four replicates overlapping 0, antagonism was claimed. In any other case

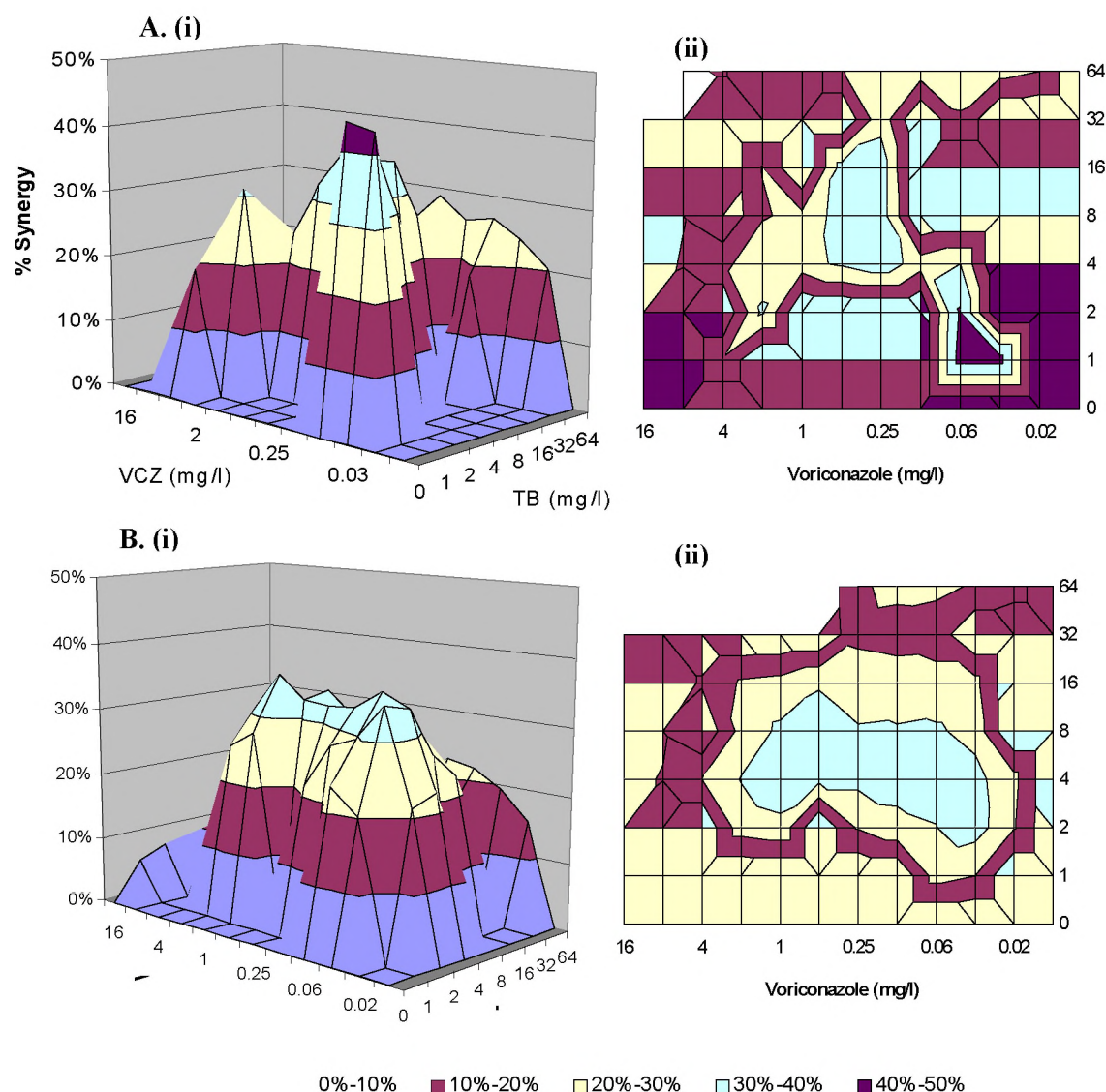


Figure 2. Assessment of the in vitro interaction between voriconazole (VCZ) and terbinafine (TB) against a clinical *S. proliferans* strain (AZN7898) based on Bliss independence no interaction theory using the SP48 method. **A.** The three-dimensional (i) and the contour plot (ii) of the % of synergy calculated with the non-parametric approach that resulted in 697% of synergy. **B.** The three-dimensional (i) and the contour plot (ii) of the % of synergy calculated with the parametric approach which resulted in 1118% of synergy with the following fitted parameters ($\pm 95\%CI$) of the E_{max} model: $IC_{50,TB} = 19.9 \pm 6.7$, $m_{TB} = -0.76 \pm 0.21$, $IC_{50,VCZ} = 2.8 \pm 0.7$, $m_{VCZ} = -1.3 \pm 0.37$.

Bliss independence was concluded. The values thus obtained for each combination were used to construct a three-dimensional plot. Peaks above and below the 0 plane indicate synergistic and antagonistic combinations, respectively while the 0 plane indicate no statistically significant interaction (Fig. 2). The contour plots were also constructed in order to visualize the drug concentrations producing an interaction.

Since the plot only shows the interactions for each separate combination of the concentrations, a value is needed to summarize the interaction surface. This was done by calculating the sum percentage of all statistically significant synergistic (ΣSYN) and antagonistic interactions (ΣANT). Interactions with $<100\%$ of statistically significant interactions were considered weak, 100-200% moderate, $>200\%$ strong.

RESULTS

Interaction between voriconazole and terbinafine. The in vitro antifungal effects of voriconazole and terbinafine were tested alone and in combination at concentrations of 0.015 to 16 mg/l and 1 to 64 mg/l, respectively. Using the spectrophotometric method and reading after 72 h (SP72), 75% growth inhibition was achieved for all strains at concentrations of 4 to 16 mg/l of voriconazole and higher than 64 mg/l of terbinafine. When the two drugs were combined the geometric mean (GM) of the MICs-1 decreased up to 27-fold and 20-fold, respectively based on FIC_i-1. MICs-1 were then shifted down to 0.03 mg/l of voriconazole and 2 mg/l of terbinafine (Table 1).

Table 1. Susceptibilities (geometric mean and range in mg/l) of 5 *S. prolificans* strains against voriconazole (VCZ), miconazole (MCZ) and itraconazole (ICZ) alone and in combination with terbinafine (TB) based on the 75% growth inhibition endpoint (MIC-1) using the SP72 method

Combination	Isolate	MIC-1 Alone		MIC-1 In combination	
		Azole	Terbinafine	Azole	Terbinafine
VCZ and TB	7898	9.51 (8-16)	>64 (>64)	0.71 (0.13-2)	9.51 (2-32)
	7901	6.73 (4-8)	>64 (>64)	0.25 (0.03-1)	6.73 (4-16)
	7902	6.73 (4-8)	>64 (>64)	0.5 (0.13-1)	8 (8)
	7906	8 (8)	>64 (>64)	1 (0.5-2)	9.51 (8-16)
	7918	9.51 (8-16)	>64 (>64)	1.19 (0.5-2)	11.31 (2-32)
MCZ and TB	7898	64 (32->64)	>64 (>64)	1.19 (0.25-4)	2.83 (2-4)
	7901	>64 (>64)	>64 (>64)	2.83 (2-4)	2 (1-4)
	7902	45.25 (8->64)	>64 (>64)	2 (0.13-8)	2 (2)
	7906	>64 (>64)	>64 (>64)	2.83 (2-4)	1.41 (1-4)
	7918	26.91 (8->64)	>64 (>64)	0.84 (0.13-2)	2.38 (2-4)
ICZ and TB	7898	>32 (>32)	>64 (>64)	1 (0.5-2)	16 (16)
	7901	>32 (>32)	>64 (64->64)	10.01 (4-16)	12.7 (8-16)
	7902	>32 (>32)	>64 (64->64)	4 (0.5-16)	8 (8)
	7906	>32 (>32)	>64 (>64)	3.17 (1-16)	8 (2-16)
	7918	>32 (>32)	>64 (>64)	4 (1-16)	10.08 (2-16)

A. Loewe additivity based models. (i) Non-parametric approach. The median FIC indices for each strain regarding the growth inhibitory effects (SP methods) were lower than 0.75 down to 0.02 indicating synergy. This was significant in most of the cases (Table 2). However, the degree of synergy as well as the significance level was dependent on the MIC-endpoint and incubation period used, with reading of MIC-1 after 48 h of incubation showing stronger synergy. Based on metabolic inhibitory effects strong synergy was found with the mCOL72 method. More variable results were obtained with COL method since FIC indices ranged from 0.02 up to 1.00 and discrepancies between FIC_i-1 and FIC_i-2 were found.

(ii) Parametric approach. The Greco model fit to the data well (median R^2 : 0.90, range: 0.83-0.96). The GM of IC₅₀s and the median slope m was 5.9 mg/l (range 0.96-2342) and -0.61 (range -0.16--1.46) for terbinafine and 4.2 mg/l (range 1.2-25) and -0.94 (range -0.45--1.79) for voriconazole, respectively. The interaction parameters α were positive and the 95% CI did not overlap 0 indicating statistically significant synergy in all cases (Table 2). The interaction parameter α ranged from 2.7-42 for all strains and methods except for one strain for which high α values were obtained.

B. Bliss independence based models. When the interaction was determined based on BI, statistically significant synergy ($P < 0.05$) was found using both non-parametric and parametric models. In most of the cases more than 200% and up to 1582% of synergy was found indicating strong synergy (Table 2). Overall lower levels of synergy were found with the COL72

method (median Σ SYN<165%). The SP methods resulted in higher levels of synergy after 48h of incubation (median Σ SYN>195%) while mCOL methods after 72 h of incubation (median Σ SYN >268%).

For the parametric approach, the E_{\max} model fit well to the data [R^2 : 0.90 (0.74-0.99)]. The GM of the IC₅₀s and the median slope m was 10.6 mg/l (range 1.6-67.4) and -0.92 (range -0.44--4.38) for terbinafine and 2.9 mg/l (range 0.24-16.7) and -1.2 (range -0.13--5.2) for voriconazole, respectively. Antagonistic effects were not observed although the SP72 and mCOL48 methods indicated some weak antagonistic combinations. The median absolute coefficient of variation of the differences between observed and predicted ODs among the replicates of all strains ranged from 41-232% (median 57%) for the SP methods, 68-166% (median 123%) for the COL method and 44-83% (median 53%) for the mCOL methods with the parametric approach and 49-165% (median 88%) for the SP method, 86-180% (median 105%) for the COL method and 45-64% (median 51%) for the mCOL methods with the non-parametric approach.

Interaction between miconazole and terbinafine. The in vitro antifungal effects of miconazole and terbinafine were tested alone and in combination at concentrations of 0.06 to 64 mg/l and 1 to 64 mg/l, respectively. Using the SP72 method, 75% growth inhibition was achieved for all strains at concentrations higher than 8 mg/l of miconazole and higher than 64 mg/l of terbinafine. When the two drugs were combined the geometric mean (GM) of the MICs-1 decreased 54

Table 2. In vitro interaction between voriconazole and terbinafine against *S. prolificans*

Method	Time	Isolate	Loewe additivity based models			Bliss independence based models			
			Non-parametric [median (range)]		Parametric	Non-parametric		Parametric	
			FICI-2	FICI-1	$\alpha \pm 95\% \text{ CI}$	ΣSYN	ΣANT	ΣSYN	ΣANT
Spectrophotometric	48 h	7898	0.13 (0.07-0.19)	0.10 (0.06-0.28)	13.9 \pm 1.6	700%	0%	1118%	0%
		7901	0.25 (0.08-0.75)	0.10 (0.05-0.13)	10.8 \pm 1.8	428%	0%	742%	0%
		7906	0.26 (0.13-0.38)	0.13 (0.06-0.25)	16.3 \pm 4.5	457%	0%	566%	0%
		7918	0.09 (0.04-0.13)	0.09 (0.04-0.09)	2479.8 \pm 289.1	409%	0%	702%	0%
		7902	0.14 (0.05-0.27)	0.09 (0.06-0.13)	42.2 \pm 7.3	709%	0%	987%	0%
		Median	0.14	0.10	16.30	457%	0%	742%	0%
Spectrophotometr	72 h	7898	0.07 (0.05-0.31)	0.14 (0.13-0.75)	13.0 \pm 3.4	1582%	0%	942%	0%
		7901	0.32 (0.04-0.75)	0.13 (0.07-0.25)	32.4 \pm 6.0	195%	-3%	702%	0%
		7906	0.38 (0.13-0.50)	0.28 (0.19-0.38)	8.4 \pm 3.3	57%	0%	67%	0%
		7918	0.08 (0.02-0.28)	0.27 (0.16-0.50)	1517.5 \pm 334.8	770%	-9%	520%	-12%
		7902	0.29 (0.13-0.31)	0.19 (0.08-0.25)	6.6 \pm 2.1	185%	0%	579%	-10%
		Median	0.29	0.19	14.04	195%	-2%	579%	0%
Colorimetric	72 h	7898	0.25 (0.02-0.63)	0.13 (0.04-0.16)	8.9 \pm 4.0	165%	0%	442%	0%
		7901	0.75 (0.50-1.00)	0.16 (0.13-0.16)	29.9 \pm 16.8	0%	0%	23%	0%
		7906	0.53 (0.07-0.75)	0.17 (0.07-0.19)	8.0 \pm 3.0	34%	0%	72%	0%
		7918	0.13 (0.08-0.25)	0.20 (0.04-0.31)	40.7 \pm 16.5	254%	0%	49%	0%
		7902	0.16 (0.08-0.50)	0.11 (0.04-0.19)	42.0 \pm 12.2	619%	0%	903%	0%
		Median	0.25	0.16	29.90	165%	0%	72%	0%
Modified Colorimetric	48 h	7898	0.25 (0.25-0.26)	0.25 (0.25-0.50)	1754.9 \pm 947.1	299%	-4%	373%	-5%
		7901	0.25 (0.25)	0.25 (0.19-0.25)	33.7 \pm 11.5	413%	-5%	564%	0%
		7906	0.25 (0.25)	0.27 (0.25-0.38)	2.7 \pm 1.5	532%	0%	753%	0%
		7918	0.25 (0.25-0.26)	0.13 (0.13-0.25)	9.9 \pm 4.1	214%	0%	75%	0%
		7902	0.26 (0.25-0.50)	0.27 (0.13-0.38)	8.2 \pm 2.5	72%	0%	236%	0%
		Median	0.25	0.25	9.9	299%	0%	373%	0%
Modified Colorimetric	72 h	7898	0.13 (0.08-0.13)	0.07 (0.06-0.07)	10.3 \pm 7.6	279%	0%	56%	0%
		7901	0.25 (0.09-0.38)	0.13 (0.07-0.13)	5.0 \pm 2.6	795%	0%	379%	0%
		7906	0.31 (0.13-0.31)	0.13 (0.06-0.13)	3.9 \pm 2.4	566%	0%	1072%	0%
		7918	0.13 (0.07-0.13)	0.14 (0.07-0.14)	4.7 \pm 2.9	579%	0%	513%	0%
		7902	0.13 (0.07-0.25)	0.09 (0.06-0.13)	14.8 \pm 5.0	464%	0%	468%	0%
		Median	0.13	0.13	5.0	566%	0%	468%	0%

to 90-fold for both drugs, respectively based on FICI-1 indices. MICs-1 were then shifted down to 0.125 mg/l of miconazole and 1 mg/l of terbinafine (Table 1).

A. Loewe additivity based models. Non-parametric approach. The median FIC indices for each strain regarding both the growth- and metabolic inhibitory effects were between 0.03 and 0.24 indicating synergy, which was significant in all cases (Table 3). The degree of synergy between 48 and 72 h was more consistent using the MIC-1 rather than the MIC-2 endpoint; for the latter endpoint weaker synergy was found after 48 h than after 72 h of incubation. This was even more pronounced with the mCOL methods. MICs-2 of the drugs in combination were lower than the lowest drug concentration using the COL72 method. Thus, the calculation of the FICI for many replicates was impossible.

(ii) Parametric approach. The Greco model fit

to the data well [R^2 ; 0.88 (0.76-0.93)]. The GM of IC_{50s} and the median slope m was 22.1 mg/l (range 0.23-7.2 $\times 10^3$) and -0.16 (range -0.1--0.53) for terbinafine and 4.2 mg/l (range 0.53-32.9) and -0.44 (range -0.27--4.4) for miconazole, respectively. Relatively high IC_{50s} of terbinafine were obtained after 72 h of incubation. The interaction parameters α were positive and the 95% CI did not overlap 0 indicating statistically significant synergy for each strain-method-incubation period however with different degrees of synergy (Table 3). The interaction parameter α ranged from 10-2.8 $\times 10^5$ indicating very strong synergy with higher values obtained with the SP72 and mCOL72.

B. Bliss independence based models. Statistically significant synergy ($P < 0.05$) was also found based on the parametric and non-parametric approach of BI since up to 1751% of synergy was found (Table 3). For the former, the E_{max} model fit well to the data

Table 3. In vitro interaction between miconazole and terbinafine against *S. prolificans*

Method	Time	Isolate	Loewe additivity based models			Bliss independence based models			
			Non-parametric [median (range)]		Parametric	Non-parametric		Parametric	
			FICI-2	FICI-1	$\alpha \pm 95\% \text{ CI}$	ΣSYN	ΣANT	ΣSYN	ΣANT
Spectrophotometr	48 h	7898	0.13 (0.02-0.28)	0.04 (0.01-0.05)	302.1 \pm 32.6	173%	0%	242%	0%
		7901	0.11 (0.02-0.14)	0.05 (0.02-0.06)	3072.0 \pm 441.7	243%	0%	396%	-35%
		7902	0.17 (0.14-0.28)	0.08 (0.01-0.28)	111.1 \pm 17.5	163%	0%	206%	-9%
		7906	0.17 (0.09-0.28)	0.04 (0.01-0.13)	565.0 \pm 110.7	160%	-8%	284%	-97%
		7918	0.06 (0.03-0.15)	0.03 (0.02-0.08)	9462.1 \pm 1194.5	460%	0%	615%	0%
		Median	0.13	0.04	565.0	173%	0%	284%	-9%
Spectrophotometr	72 h	7898	0.06 (0.02-0.09)	0.05 (0.03-0.08)	552.1 \pm 77.6	57%	0%	135%	-146%
		7901	0.05 (0.02-0.08)	0.05 (0.03-0.06)	5516.6 \pm 966.9	146%	-6%	365%	-144%
		7902	0.06 (0.03-0.28)	0.06 (0.03-0.14)	1374.9 \pm 242.9	10%	-19%	78%	-109%
		7906	0.09 (0.03-0.13)	0.05 (0.02-0.07)	434.5 \pm 124.9	67%	-12%	138%	-173%
		7918	0.06 (0.03-0.16)	0.05 (0.03-0.27)	5464.7 \pm 1082.9	392%	-8%	505%	-95%
		Median	0.06	0.05	1374.9	67%	-8%	138%	-144%
Colorimetric	72 h	7898	0.06 (0.03-0.09)	0.04 (0.02-0.06)	817.5 \pm 297.5	7%	0%	14%	-16%
		7901	0.19 (0.06-0.28)	0.03 (0.02-0.04)	180.1 \pm 50.3	17%	0%	92%	-95%
		7902	0.05 (0.02-0.08)	0.05 (0.02-0.08)	128.2 \pm 28.4	8%	0%	0%	-75%
		7906	0.03 (0.03)	0.05 (0.03-0.16)	55.5 \pm 23.8	0%	0%	0%	-97%
		7918	0.08 (0.03-0.19)	0.04 (0.02-0.09)	633.2 \pm 162.2	57%	0%	0%	0%
		Median	0.06	0.04	180.1	8%	0%	0%	-75%
Modified Colorimetric	48 h	7898	0.27 (0.27-0.28)	0.05 (0.04-0.13)	9.8 \pm 2.2	556%	-6%	567%	-10%
		7901	0.16 (0.09-0.31)	0.05 (0.04-0.05)	44.3 \pm 11.4	955%	0%	941%	-21%
		7902	0.27 (0.27-0.50)	0.04 (0.03-0.05)	34.1 \pm 8.2	354%	-5%	392%	-34%
		7906	0.38 (0.31-0.51)	0.04 (0.04-0.05)	18.5 \pm 5.0	539%	0%	526%	0%
		7918	0.27 (0.13-0.28)	0.31 (0.05-0.31)	3807.5 \pm 1479.4	259%	-9%	372%	0%
		Median	0.27	0.05	34.1	539%	-5%	526%	-10%
Modified Colorimetric	72 h	7898	0.03 (0.03-0.04)	0.06 (0.06-0.13)	9505.2 \pm 2824.2	487%	0%	518%	-93%
		7901	0.03 (0.02-0.04)	0.09 (0.06-0.09)	6768.1 \pm 2078.9	1051%	0%	1006%	-136%
		7902	0.03 (0.02-0.03)	0.06 (0.06-0.13)	7740.3 \pm 1887.3	1751%	0%	1295%	-89%
		7906	0.03 (0.02-0.04)	0.13 (0.06-0.13)	7872.5 \pm 3421.3	606%	-8%	517%	-103%
		7918	0.06 (0.03-0.09)	0.08 (0.06-0.08)	534.6 \pm 141.8	595%	-31%	538%	-26%
		Median	0.03	0.08	7740.3	606%	0%	538%	-93%

[R²; 0.88 (0.73-0.99)]. The GM of the IC₅₀s and the median slope m were 11.4 mg/l (range 0.57-1028) and -0.35 (range -0.10—0.86) for terbinafine and 4.43 mg/l (range 0.19-43.74) and -0.45 (-0.24—1.63) for miconazole, respectively. Higher levels of synergy were found with the parametric approach than with the non-parametric based on the growth inhibitory activities. Among methods, mCOL72 and mCOL48 generated the highest levels of synergy (median ΣSYN >526%) followed by the SP48 and SP72 (median ΣSYN <284%). Between the two incubation periods, stronger synergistic interactions were found after 48 h based on growth inhibitory effects and after 72 h based on metabolic inhibitory effects. By contrast the COL72 method resulted in weak statistically significant synergistic interactions with 3 strains in the parametric approach showing no statistically significant synergistic interactions.

Weak statistically significant antagonistic interactions (ΣANT <100%) were observed in all methods for many strains. Particularly with the parametric approach even moderate antagonistic interactions were observed (200-100% ΣANT). These interactions were predominantly observed at the high concentrations of miconazole and terbinafine i.e. 64 mg/l where precipitation was obvious in the wells. The median absolute coefficient of variation of the differences between observed and predicted ODs among the replicates of all strains ranged from 60-124% (median 95%) for the SP methods, 142-227% (median 173%) for the COL method and 24-49% (median 40%) for the mCOL methods with the parametric approach and from 69-191% (median 123%) for the SP methods, 118-343% (median 236%) for the COL method and 23-56 % (median 36%) for the mCOL methods with the non-parametric approach.

Table 4. In vitro interaction between itraconazole and terbinafine against *S. proliferans*

Method	Time	Isolate	Loewe additivity based models			Bliss independence based models			
			Non-parametric [median (range)]		Parametric	Non-parametric		Parametric	
			FICI-2	FICI-1	$\alpha \pm 95\% \text{ CI}$	ΣSYN	ΣANT	ΣSYN	ΣANT
Spectrophotometric	48 h	7898	0.13 (0.07-0.16)	0.19 (0.13-0.19)	4.3 ± 1.3	19%	-20%	244%	-45%
		7901	0.52 (0.51-0.52)	0.13 (0.13-0.19)	9.3 ± 1.8	36%	-25%	90%	-27%
		7902	0.07 (0.02-0.56)	0.13 (0.13-0.25)	203.8 ± 49.1	49%	0%	144%	0%
		7906	0.16 (0.04-0.51)	0.14 (0.13-0.19)	3.3 ± 0.8	230%	0%	291%	0%
		7918	0.51 (0.07-0.51)	0.13 (0.09-0.38)	25.1 ± 9.6	52%	0%	167%	0%
		Median	0.16	0.13	9.3	49%	0%	167%	0%
Spectrophotometric	72 h	7898	0.13 (0.07-0.56)	0.14 (0.13-0.16)	25.9 ± 8.2	76%	-31%	202%	-178%
		7901	0.75 (0.52-1.00)	0.31 (0.31-0.38)	57.2 ± 14.7	10%	-85%	7%	-98%
		7902	0.02 (0.02-0.28)	0.19 (0.07-0.38)	182.9 ± 48.1	41%	0%	90%	0%
		7906	0.13 (0.06-0.38)	0.16 (0.14-0.27)	8.1 ± 2.5	536%	0%	428%	0%
		7918	0.51 (0.06-0.52)	0.14 (0.09-0.38)	457.6 ± 148.5	81%	0%	180%	0%
		Median	0.13	0.16	57.2	76%	0%	180%	0%
Colorimetric	72 h	7898	0.07 (0.02-0.26)	0.16 (0.09-0.16)	202.9 ± 130.7	0%	-46%	0%	-109%
		7901	0.13 (0.01-0.16)	0.26 (0.25-0.27)	5.2 ± 3.3	7%	-83%	0%	0%
		7902	0.13 (0.01-1.02)	0.19 (0.14-0.25)	29.1 ± 20.5	10%	-53%	179%	-3%
		7906	0.04 (0.02-0.13)	0.13 (0.09-0.25)	23.7 ± 13.7	6%	-209%	16%	-404%
		7918	0.16 (0.08-0.26)	0.16 (0.13-0.16)	69.9 ± 59.7	380%	0%	384%	-4%
		Median	0.13	0.16	29.1	7%	-53%	16%	-4%
Modified Colorimetric	48 h	7898	0.34 (0.19-0.50)	0.27 (0.27-0.28)	105.4 ± 39.1	25%	-1%	69%	0%
		7901	0.14 (0.13-0.15)	0.20 (0.14-0.26)	802.1 ± 310.8	276%	0%	417%	0%
		7902	0.27 (0.25-0.28)	0.20 (0.16-0.25)	23.9 ± 9.4	105%	0%	209%	-14%
		7906	0.20 (0.16-0.25)	0.23 (0.19-0.27)	81.6 ± 28.0	31%	-14%	88%	0%
		7918	0.11 (0.06-0.16)	0.08 (0.02-0.14)	795.3 ± 435.9	79%	0%	49%	0%
		Median	0.20	0.20	105.4	79%	0%	88%	0%
Modified Colorimetric	72 h	7898	0.21 (0.14-0.28)	0.18 (0.04-0.31)	959.7 ± 542.4	146%	-16%	529%	-5%
		7901	0.04 (0.02-0.07)	0.15 (0.05-0.25)	5091.5 ± 3287.1	942%	0%	372%	-16%
		7902	0.30 (0.28-0.31)	0.05 (0.04-0.06)	404.7 ± 242.3	533%	0%	616%	-51%
		7906	0.28 (0.25-0.31)	0.06 (0.05-0.07)	2351.3 ± 1445.1	83%	-13%	300%	-33%
		7918	0.04 (0.03-0.05)	0.07 (0.05-0.09)	7673.7 ± 389.4	263%	0%	1354%	0%
		Median	0.21	0.07	959.7	263%	0%	529%	-16%

Interaction between itraconazole and terbinafine. The in vitro antifungal effects of itraconazole and terbinafine were tested alone and in combination at concentrations of 0.5 to 32 mg/l and 0.06 to 64 mg/l, respectively. Using the SP72 method, 75% growth inhibition was not observed for all strains at high concentrations up to 32 mg/l of itraconazole and 64 mg/l of terbinafine based on the results of SP72. When the two drugs were combined the geometric mean (GM) of the MICs-1 decreased up 64-fold for itraconazole and 16-fold for terbinafine based on FICI-1. MICs-1 were then shifted down to 0.5 mg/l of itraconazole and 2 mg/l of terbinafine (Table 1).

A. Loewe additivity based models. (i) Non-parametric approach. The median FIC indices for all strains regarding the growth and metabolic- inhibitory effects ranged from 0.07 to 0.21 indicating synergy. This was significant in all cases with mCOL methods, but not with SP and COL methods since FIC indices up

to 1.02 were found for some strains (Table 4). The highest degree of synergy was found after 72 h reading the MIC-1. The values of the FIC indices represented the minimal values since the off-scale MICs of both itraconazole and terbinafine alone did not allow the calculation of exact values.

(ii) Parametric approach. The Greco model fitted well to the data [R^2 ; 0.88 (0.69-0.95)]. The GM of IC₅₀s and the median slope m was 2.98 mg/l (range 0.15-93.6) and -0.68 (range -0.15-1.7) for terbinafine and 404.4 mg/l (range 17.5-7 x 10³) and -0.28 (range -0.16-26.7) for itraconazole, respectively. The α interaction parameters were positive and the 95% CI did not overlap 0 indicating statistically significant synergy for all strain-method-incubation period combinations (Table 4). The interaction parameter α ranged from 3.3 to 7.4 x 10⁴ indicating very strong synergy. High α values obtained with the mCOL72 method. In some cases none of the tested concentrations

of itraconazole resulted in 50% of growth. In these cases the Greco model resulted in IC_{50} s outside the range of concentrations tested and this affected the fit. Therefore the IC_{50} of itraconazole was fixed to the next highest doubling concentration.

B. Bliss independence based models. Statistically significant interactions ($P < 0.05$) were also found with the two approaches based on BI. High levels of synergy were found with mCOL methods (up to 1354% Σ SYN) followed by the SP methods (up to 536% Σ SYN). After 72 h of incubation the levels of synergy were higher than after 48 h. Strong statistically significant antagonistic interactions (up to -404% Σ ANT) were found with COL method particularly with the non-parametric approach. The parametric approach resulted in higher % of synergy than the non-parametric approach. For the former, the E_{max} model fitted well to the data [R^2 ; 0.95 (0.77-0.99)]. The GM of the IC_{50} s and the median slope m was 2.85 mg/l (range 0.23-155 mg/l) and -0.52 (-0.11--1.22) for terbinafine and 298.64 mg/l (range 5.2-5011 mg/l) and -0.43 (range -0.06--0.99) for itraconazole, respectively. Statistically significant antagonistic interactions were found particularly with the parametric approach after 72 h of incubation, which were strong in some cases (>200%). The median absolute coefficient of variation of the differences between observed and predicted ODs of all strains ranged from 58-157% (median 106%) for the SP methods, 59-222% (median 106%) for the COL method and 51-69% (median 61%) for mCOL methods with the parametric approach and 57-287% (median 154%) for the SP methods, 51-195% (median 115%) for the COL method and 58-89% (median 71%) for the mCOL methods with the non-parametric approach.

DISCUSSION

Strong synergistic interactions were found in vitro between terbinafine and three azoles, namely voriconazole, miconazole, and itraconazole, against 5 clinical *S. proliferans* isolates based on antifungal growth- and metabolic inhibitory effects after 48 and 72 h of incubation. These results were confirmed by parametric and non-parametric approaches of the Loewe additivity and the Bliss independence no-interaction theories, respectively.

This confirms previous studies where terbinafine was found to interact synergistically with itraconazole for 90% of *S. proliferans* isolates (32) and 43% of *Candida albicans* (3), with voriconazole against *Aspergillus* species (41) and with fluconazole for 40% of *C. albicans* isolates (3) based on the FIC index model. However, the results obtained with the FIC index model are dependent on the MIC endpoints used particularly for filamentous fungi where they are not

clear established. In this study the results based on both MIC endpoints showed significant synergy with MIC-1 resulting in higher levels of synergy and more consistent between the two incubation periods compared to MIC-2.

The interpretation of the FIC index in concluding synergism or antagonism is a problem in it self. Since the determination of the MIC is sensitive to dilution errors, and 2 fold dilutions are used in determining MICs, the accuracy of the MIC is usually taken as not more than within one dilution. Since the FIC indices are determined from two antifungals, the value of the FIC may also differ between experiments. In the interpretation of a single FIC index therefore, a value of >4 is usually applied to conclude antagonism, and ≤ 0.5 to conclude synergism (23). This is one of the approaches we also took in interpreting the results. However, because we performed replicate experiments (4 times) for each strain-combination studied we were also able to interpret the results of the FIC index model for all replicates as one outcome (synergy, antagonism or additivity), thereby constraining the inter-experimental error. Thus when the results of all four replicates were concordant, synergy or antagonism was claimed if FIC indices were below 1 or above 1, respectively. In all other cases additivity was concluded. Another alternative approach would have been a more statistical approach, by using the mean of the four replicates and the 95% confidence interval; if 1 does not include the 95% confidence interval synergism or antagonism could be concluded. However, because the distribution of the FIC indices is not normal we preferred the approach mentioned.

Assessing the nature of drug interactions using the FIC index model faces several other problems except the choice of the FIC indices- and MIC-endpoints such as the lack of a good summary and statistical interpretation of the results, and the imprecise approximation of the real FIC index when off-scale MICs are present. Therefore, the data were analyzed by a fully parametric approach described by Greco et al. (20). This model is based on the assumption that the concentration effect curves follow the E_{max} model (sigmoid curve with variable slopes), includes statistical significance levels of the interactions and summarizes them with a non-unit, concentration-independent interaction parameter. This model does not require replicates to obtain statistical measures (although the mean with the standard error of replicates can be included as weight factor) and is less sensitive to intra-experimental errors compared to the FIC index model. The model fitted to the data well since narrow 95% confidence intervals for all parameters and low sum of the squares were obtained. Statistically significant synergy was found in all cases. The model resulted in high interaction parameters particularly when the IC_{50} s

of the individual drugs were off-scale. This indicates very strong synergy since a drug with poor activity (very high IC_{50}) acquires activity when it is combined. However to obtain a reasonable fit, the IC_{50} s had to be fixed to certain values in some cases. The value of the interaction parameter for these cases might be uncertain because the extrapolation of E_{max} model outside the range of effects caused by a drug alone (i.e. itraconazole for which less than 50% inhibition was not observed at any concentration of the drug alone) is very dangerous. The values of interaction parameters found should then be regarded with extreme caution since the E_{max} model may not describe the concentration effect curve of itraconazole appropriately in the whole range of effects. However, results of previous studies have shown that the E_{max} model fitted well to concentration effect curves of itraconazole against other filamentous fungi (i.e. *Aspergillus* species) (29). In addition, the Greco model fitted to the entire data set (21) where effects of 0% up to 100% of inhibition were observed. Even though problems of fitting may arise when none of the tested combinations reduces the growth to 50%. Finally, results obtained with the Greco model, as for most of the regression analysis models, are dependent on various factors associated with the fitting procedure such as the initial parameters, the algorithms used for calculation the sum of the squares, variance models.

From the mechanistic point of view, the synergistic interaction between allylamines and azoles can be explained in a similar manner as the synergistic interaction between the antibacterials trimethoprim and the sulfonamides, which are acting at different steps of the same pathway. Allylamines inhibit the squalene epoxidase, a non-cytochrome P-450 enzyme in the pathway of ergosterol biosynthesis whereas azoles act at a more distal point in the same pathway by inhibiting the 14 α -demethylase of lanosterol (16, 40, 47). Among the three azoles, miconazole showed the strongest synergy with FIC indices as low as 0.03 using the MIC-1. The strong synergy of miconazole could be associated with its multiple mechanisms of action that probably involve alteration of fungal cell wall, alteration of the RNA and DNA metabolism, and intracellular accumulation of peroxides (4, 13) thereby increasing the sites of potential interactions. Although sequential blocking of a biochemical pathway might often result in synergy (17, 44), the appropriateness of using Loewe additivity as no interaction model for analyzing interactions of drugs with dissimilar actions was questioned first by Bliss (8). Furthermore, it was found that Bliss independence of the effects of the two drugs acting in such ways can be achieved (46) even when the concentration effect curves of the two drugs followed the E_{max} model (24) despite Berenbaum's critical arguments (6).

Even when Bliss independence was used as no interaction theory to analyze the interaction between the three azoles and terbinafine, strong statistically significant synergy was found in most of the cases. However, weak or not statistically significant synergistic interactions as well as strong statistically significant antagonistic interactions were found. The latter was mainly due to precipitation at high concentrations. A good summary of the results is lacking and replicates are required in order to obtain statistically significant results. Combinations with different interactions can be obtained and a full checkerboard design is required. Between the parametric and the non-parametric approach, higher levels of synergy were found with the former, which was also less variable between the two incubation periods. The parametric approach could be applied in frugal experiments with significant results particularly when the concentration effect curves are well defined. It might reduce the intraexperimental errors particularly in single drug-containing wells. However, both models are sensitive to inter-experimental variations. Precipitation at high concentrations affected more the results of the parametric approach than those of non-parametric resulting in strong statistically significant antagonistic interactions. Precipitation did not affect the results of the fully parametric Greco model since fully parametric approaches can fix experimental errors in total area of checkerboard by contrast with the semi-parametric like the parametric BI based model, which can do this only in the single drug containing wells. It would be interesting to compare all four models in interactions of different nature and degree using the same summary parameters and comparing the concentrations producing the synergistic effects.

Among the three azoles, the strongest synergy was produced with miconazole followed by itraconazole and voriconazole relying on Loewe additivity-based models and mainly on the Greco model since the calculation of the exact FIC indices for the interaction of itraconazole and terbinafine was not possible due to off-scale MICs of the former drug. Relying on Bliss independence-based models, voriconazole produced the strongest synergy followed by miconazole and itraconazole. This discrepancy, which might reflect different theoretical mechanisms, is caused by the different isobols obtained from the two models. As it was presented in Fig. 12 of the review by Greco et al. (20), the isobols based on Bliss independence are dependent on the magnitude of the slopes of the individual concentration effect curves. The smaller the slopes, the lesser Bliss synergistic interactions. Therefore, voriconazole with the largest absolute median slope resulted in the strongest synergy and itraconazole with the smallest absolute median slope resulted in the weakest synergy.

Using spectrophotometric and colorimetric methods, the three azoles interacted synergistically with terbinafine not only by restricting the fungal biomass but also by reducing the metabolic activity of the fungi. However, lower levels of synergy were found with the standard colorimetric method compared to the spectrophotometric method and to the modified colorimetric method. This was more pronounced when the combinations were analyzed with Bliss independence-based models. Less and weaker statistically significant synergistic interactions were found with the standard colorimetric method (fungi are exposed for 3 h to the dye MTT after 72 h incubation with the drug) despite that the spectrophotometric method after 72 h resulted in strong statistically significant synergistic interactions for all the strains. This was caused mainly by the large variation between the replicates obtained with the standard colorimetric method resulting in less statistically significant interactions. Interestingly, the modified colorimetric method showed the lowest levels of interexperimental variability, thus increasing its potential for application in the *in vitro* combination studies of antifungal drugs.

The dynamic aspect of synergy between azoles and terbinafine was assessed by using measurements after 48 and 72 h of incubation. The BI-based models resulted in higher levels of synergy after 48 h than after 72 h based on the spectrophotometric methods while the opposite was observed with the modified colorimetric methods particularly for the miconazole-terbinafine and voriconazole-terbinafine interactions. This could be associated with the relatively higher interexperimental variation observed after 72 h for the spectrophotometric methods and after 48 h for the modified colorimetric methods between the two incubation periods. The LA based models resulted in higher levels of synergy after 72 h than after 48 h particularly for the miconazole-terbinafine and itraconazole-terbinafine interactions. This could be explained with the growth curves of *S. prolificans* recently published (28) where after 72 h the growth control inserts the second transition period while the drug containing wells might be in the log phase, which exhibits the highest growth rate. Therefore, at that time the synergistic effects are more pronounced and larger differences in growth between the single-drug and the drug-combinations containing wells could be observed.

The synergistic interaction between these three azoles and terbinafine might have great clinical impact for controlling infections caused by *S. prolificans*. Peak serum levels in humans have been reported for terbinafine up to 3.6 mg/l (2), for voriconazole up to 2.5 mg/l (<http://www.aspergillus.man.ac.uk>), for miconazole up to 21.9 mg/l (13) and for itraconazole up to 1 mg/l (1). These levels are within the concentration range of these drugs, which produced the synergistic

effects when they were combined *in vitro*. Furthermore, successful outcome was reported in humans treated with itraconazole and terbinafine in invasive infections, which might be due to *in vivo* synergy between these two drugs (42, 45). Therefore, the combination therapy of an azole with terbinafine could be beneficial for the management of *S. prolificans* infections for several reasons such as (i) enhancement of the antifungal effects of the single drugs which in case of *S. prolificans* can be absent like for itraconazole, (ii) reduction of the required drug concentrations to produce the same effect as the drugs alone at levels achievable in serum, (iii) diminution of the side effects and (iv) production of fungicidal activities. Regarding the latter, although few of the combinations tested in this study appear to inhibit completely the growth at high concentrations, the fungicidal activity of these combinations should be further explored.

Despite the *in vitro* synergistic interaction between azoles and terbinafine, the therapeutic synergy of such combinations may be affected by pharmacokinetic and/or pharmacodynamic interactions that may take place *in vivo* (9, 22) diminishing, if not reversing, the positive effects observed *in vitro*. Therefore, the effectiveness of combination therapy should be tested initially in experimental infections in animal models. A murine model of scedosporiosis recently developed (J. Meletiadis, J. Curfs, J. F. G. M. Meis, and P. E. Verweij. Abstr. 40th International Congress of Antimicrobial Agents and Chemotherapy, abstr. 1670, 2000) might help to test the *in vivo* interaction between azoles and terbinafine in an attempt to confirm the *in vitro* results.

ACKNOWLEDGMENTS

This work was supported by the Mycology Research Center of Nijmegen.

References

1. **Bailey, E. M., D. J. Krakovsky, and M. J. Rybak.** 1990. The triazole antifungal agents: a review of itraconazole and fluconazole. *Pharmacotherapy* **10**:146-153.
2. **Balfour, J. A., and D. Faulds.** 1992. Terbinafine. A review of its pharmacodynamic and pharmacokinetic properties, and therapeutic potential in superficial mycoses. *Drugs* **43**:259-284.
3. **Barchiesi, F., L. F. Di Francesco, P. Compagnucci, D. Arzeni, A. Giacometti, and G. Scalise.** 1998. In-vitro interaction of terbinafine with amphotericin B, fluconazole and itraconazole against clinical isolates of *Candida albicans*. *J. Antimicrob. Chemother.* **41**:59-65.
4. **Barriere, S. L.** 1990. Pharmacology and pharmacokine-

- tics of traditional systemic antifungal agents. *Pharmacotherapy* **10**(Suppl 6):134-140.
5. **Berenbaum, M. C.** 1985. The expected effect of a combination of agents: the general solution. *J. Theor. Biol.* **114**:413-431.
 6. **Berenbaum, M. C.** 1989. What is synergy? *Pharmacol. Rev.* **41**:93-141.
 7. **Berenguer, J., J. L. Rodriguez-Tudela, C. Richard, M. Alvarez, M. A. Sanz, L. Gaztelurrutia, J. Ayats, and J. V. Martinez-Suarez.** 1997. Deep infections caused by *Scedosporium prolificans*. A report on 16 cases in Spain and a review of the literature. *Scedosporium prolificans* Spanish Study Group. *Medicine (Baltimore)* **76**:256-265.
 8. **Bliss, C. I.** 1939. The toxicity of poisons applied jointly. *Ann. Appl. Biol.* **26**:585-615.
 9. **Breckenridge, A.** 1992. Clinical significance of interactions with antifungal agents. *Br. J. Dermatol.* **126**(Suppl. 39):19-22.
 10. **Carrillo, A. J., and J. Guarro.** 2001. In vitro activities of four novel triazoles against *Scedosporium* spp. *Antimicrob. Agents Chemother.* **45**:2151-2153.
 11. **Cormican, M. G., and M. A. Pfaller.** 1996. Standardization of antifungal susceptibility testing. *J. Antimicrob. Chemother.* **38**:561-578.
 12. **Cuenca-Estrella, M., B. Ruiz-Diez, J. V. Martinez-Suarez, A. Monzon, and J. L. Rodriguez-Tudela.** 1999. Comparative in-vitro activity of voriconazole (UK-109,496) and six other antifungal agents against clinical isolates of *Scedosporium prolificans* and *Scedosporium apiospermum*. *J. Antimicrob. Chemother.* **43**:149-151.
 13. **Daneshmend, T. K., and D. W. Warnock.** 1983. Clinical pharmacokinetics of systemic antifungal drugs. *Clin. Pharmacokinet.* **8**:17-42.
 14. **Drusano, G. L., D. Z. D'Argenio, W. Symonds, P. A. Bilello, J. McDowell, B. Sadler, A. Bye, and J. A. Bilello.** 1998. Nucleoside analog 1592U89 and human immunodeficiency virus protease inhibitor 141W94 are synergistic in vitro. *Antimicrob. Agents Chemother.* **42**:2153-2159.
 15. **Espinel-Ingroff, A., F. Barchiesi, K. C. Hazen, J. V. Martinez-Suarez, and G. Scalise.** 1998. Standardization of antifungal susceptibility testing and clinical relevance. *Med. Mycol.* **36**:68-78.
 16. **Georgopapadakou, N. H., and T. J. Walsh.** 1996. Antifungal agents: chemotherapeutic targets and immunologic strategies. *Antimicrob. Agents Chemother.* **40**:279-291.
 17. **Goldin, A., and N. Mantel.** 1957. The employment of combination drugs in the chemotherapy of neoplasia: A review. *Cancer Res.* **17**:635-654.
 18. **Gosbell, I. B., M. L. Morris, J. H. Gallo, K. A. Weeks, S. A. Neville, A. H. Rogers, R. H. Andrews, and D. H. Ellis.** 1999. Clinical, pathologic and epidemiologic features of infection with *Scedosporium prolificans*: four cases and review. *Clin. Microbiol. Infect.* **5**:672-686.
 19. **Graybill, J. R.** 1996. The future of antifungal therapy. *Clin. Infect. Dis.* **22**(Suppl. 2):166-178.
 20. **Greco, W. R., G. Bravo, and J. C. Parsons.** 1995. The search for synergy: a critical review from a response surface perspective. *Pharmacol. Rev.* **47**:331-385.
 21. **Greco, W. R., H. S. Park, and Y. M. Rustum.** 1990. Application of a new approach for the quantitation of drug synergism to the combination of cis-diamminedichloroplatinum and 1-beta-D-arabinofuranosylcytosine. *Cancer Res.* **50**:5318-5327.
 22. **Gupta, A. K., H. I. Katz, and N. H. Shear.** 1999. Drug interactions with itraconazole, fluconazole, and terbinafine and their management. *J. Am. Acad. Dermatol.* **41**:237-249.
 23. **Hindler, J.** 1995. Antimicrobial susceptibility testing, p. 5.18.11-15.18.20. In H. D. Isenberg (ed.), *Clinical Microbiology Procedures Handbook*, Washington, D. C.
 24. **Jackson, R. C.** 1991. Synergistic and antagonistic drug interactions resulting from multiple inhibition of metabolic pathway, p. 363-408. In T. C. Chou, and D. C. Rideout (eds), *Synergism and antagonism in Chemotherapy*. Academic Press, New York.
 25. **Kauffman, C. A., and P. L. Carver.** 1997. Antifungal agents in the 1990s. Current status and future developments. *Drugs* **53**:539-549.
 26. **Meletiadiis, J., J. F. G. M. Meis, J. W. Mouton, J. P. Donnelly, and P. E. Verweij.** 2000. Comparison of NCCLS and 3-(4,5-dimethyl-2-Thiazyl)-2,5-diphenyl-2H-tetrazolium bromide (MTT) methods of in vitro susceptibility testing of filamentous fungi and development of a new simplified method. *J. Clin. Microbiol.* **38**:2949-2954.
 27. **Meletiadiis, J., J. F. G. M. Meis, J. W. Mouton, J. L. Rodriguez-Tudela, J. P. Donnelly, and P. E. Verweij.** 2002. In vitro activities of new and conventional antifungal agents against clinical *Scedosporium* isolates. *Antimicrob. Agents Chemother.* **46**:62-68.
 28. **Meletiadiis, J., J. F. G. M. Meis, J. W. Mouton, and P. E. Verweij.** 2001. Analysis of growth characteristics of filamentous fungi in different nutrient media. *J. Clin. Microbiol.* **39**:478-484.
 29. **Meletiadiis, J., J. W. Mouton, J. F. G. M. Meis, B. A. Bouman, J. P. Donnelly, and P. E. Verweij.** 2001. Colorimetric assay for antifungal susceptibility testing of *Aspergillus* species. *J. Clin. Microbiol.* **39**:3402-3408.
 30. **Meletiadiis, J., J. W. Mouton, J. F. G. M. Meis, B. A. Bouman, J. P. Donnelly, and P. E. Verweij.** 2000. Comparison of spectrophotometric and visual reading of NCCLS method and evaluation of a colorimetric method based on the reduction of a soluble tetrazolium/formazan, XTT, for antifungal susceptibility testing of *Aspergillus* species. *J. Clin. Microbiol.* **39**:4256-4263.
 31. **Meletiadiis, J., J. W. Mouton, J. F. G. M. Meis, and P. E. Verweij.** 2000. Combination chemotherapy for the treatment of invasive infections by *Scedosporium prolificans*. *Clin. Microbiol. Infect.* **6**:336-337.
 32. **Meletiadiis, J., J. W. Mouton, J. L. Rodriguez-Tudela, J. F. G. M. Meis, and P. E. Verweij.** 2000. In vitro interaction of terbinafine with itraconazole against clinical isolates of *Scedosporium prolificans*. *Antimicrob. Agents Chemother.* **44**:470-472.
 33. **NCCLS** 1998. Reference method for broth dilution antifungal susceptibility testing of conidium-forming filamentous fungi; proposed standard. Document M-38P. National Committee for Clinical Laboratory Standards, Wayne, Pa.

34. **Pfaller, M. A., J. H. Rex, and M. G. Rinaldi.** 1997. Antifungal susceptibility testing: technical advances and potential clinical applications. *Clin. Infect. Dis.* **24**:776-784.
35. **Polak, A.** 1999. The past, present and future of antimycotic combination therapy. *Mycoses* **42**:355-370.
36. **Prichard, M. N., L. E. Prichard, W. A. Baguley, M. R. Nassiri, and C. Shipman, Jr.** 1991. Three-dimensional analysis of the synergistic cytotoxicity of ganciclovir and zidovudine. *Antimicrob. Agents Chemother.* **35**:1060-1065.
37. **Prichard, M. N., L. E. Prichard, and C. Shipman, Jr.** 1993. Strategic design and three-dimensional analysis of antiviral drug combinations. *Antimicrob. Agents Chemother.* **37**:540-545.
38. **Prichard, M. N., and C. Shipman, Jr.** 1990. A three-dimensional model to analyze drug-drug interactions. *Antiviral Res.* **14**:181-205.
39. **Rex, J. H., M. A. Pfaller, T. J. Walsh, V. Chaturvedi, A. Espinel-Ingroff, M. A. Ghannoum, L. L. Gosey, F. C. Odds, M. G. Rinaldi, D. J. Sheehan, and D. W. Warnock.** 2001. Antifungal susceptibility testing: practical aspects and current challenges. *Clin. Microbiol. Rev.* **14**:643-658.
40. **Ryder, N. S.** 1992. Terbinafine: mode of action and properties of the squalene epoxidase inhibition. *Br. J. Dermatol.* **126**(Suppl. 39):2-7.
41. **Ryder, N. S., and I. Leitner.** 2001. Synergistic interaction of terbinafine with triazoles or amphotericin B against *Aspergillus* species. *Med. Mycol.* **39**:91-95.
42. **Shenep, J. L., B. K. English, L. Kaufman, T. A. Pearson, J. W. Thompson, R. A. Kaufman, G. Frisch, and M. G. Rinaldi.** 1998. Successful medical therapy for deeply invasive facial infection due to *Pythium insidiosum* in a child. *Clin. Infect. Dis.* **27**:1388-1393.
43. **Suhnel, J.** 1990. Evaluation of synergism or antagonism for the combined action of antiviral agents. *Antiviral Res.* **13**:23-39.
44. **Veldstra, H.** 1956. Synergism and potentiation with special reference to the combination of structural analogues. *Pharmacol. Rev.* **8**:339-387.
45. **Verweij, P. E., N. J. Cox, and J. F. G. M. Meis.** 1997. Oral terbinafine for treatment of pulmonary *Pseudallescheria boydii* infection refractory to itraconazole therapy. *Eur. J. Clin. Microbiol. Infect. Dis.* **16**:26-28.
46. **Webb, J. L.** 1963. Effect of more than one inhibitor, p. 66-79 & 487-512, *Enzymes and metabolic inhibitors*, vol. 1. Academic Press, New York.
47. **White, T. C., K. A. Marr, and R. A. Bowen.** 1998. Clinical, cellular, and molecular factors that contribute to antifungal drug resistance. *Clin. Microbiol. Rev.* **11**:382-402.



Chapter 3.3

Assessing the in vitro Interaction of Antifungal Drugs:
Comparison of Different Drug Interaction models

Submitted for publication

ASSESSING THE IN VITRO INTERACTION OF ANTIFUNGAL DRUGS: COMPARISON OF DIFFERENT DRUG INTERACTION MODELS

JOSEPH MELETIADIS¹, PAUL E. VERWEIJ¹, DEBBIE T. A. TE DORSTHORST², JACQUES F. G. M. MEIS²,
AND JOHAN W. MOUTON²

Departments of Medical Microbiology, University Medical Center Nijmegen¹ and Department of Medical Microbiology and Infectious Diseases, Canisius-Wilhelmina Hospital², Nijmegen, The Netherlands

The in vitro combination of various antifungal drugs [miconazole (MZ), itraconazole (IZ), fluconazole (FZ), amphotericin B (AB), 5-flucytosine (FC), and terbinafine (TB)] was tested against 17 clinical fungal isolates including yeasts [3 *Candida albicans* (CA), 5 *C. glabrata* (CG), and 3 *C. krusei* (CK)] and filamentous fungi [3 *Aspergillus fumigatus* (AF) and 3 *Scedosporium prolificans* (SP)] with a microdilution checkerboard technique based on spectrophotometric and colorimetric modifications of the NCCLS standards. The drug combinations–strains pairs were chosen in such a way to have interactions spanned from strong synergy to strong antagonism based on the fractional inhibitory concentration index (FIC index) model. Thus, there were found 5 synergistic (MZ + TB with SP and FC + FZ with CA), 5 additive/indifferent (AB + IZ with AF and FC + FZ with CK) and 6 antagonistic (FC + FZ against CG) interactions. The interactions were analyzed using standard (the FIC index model) and modern concentration effect response surface approaches (fully parametric model developed by Greco et al.) of drug interaction modeling including non-parametric and parametric models of two competing zero-interaction theories, the Loewe additivity and the Bliss independence (model developed by Prichard et al.). Despite its simplicity, the FIC index model resulted in variable conclusions depending on MIC endpoints determined and the interpretation endpoints used. Using the MIC-2 endpoints (lowest drug concentration showing 50% of growth) problems in calculating the FIC indices due to trailing phenomena and fungistatic-fungicidal combinations were reduced. High reproducibility was achieved in interpreting the FIC indices when the cutoffs of 0.25 and 4 (for single experiments) and the cutoff of 1 (for replicates) were used for the upper and lower limits of synergy and antagonism, respectively. Although the fully parametric Greco model did not describe precisely the entire response surfaces of antifungal drugs, it was able to differentiate synergistic from antagonistic interactions with a non-unit, reproducible, concentration-independent interaction parameter including its uncertainty without requiring replication. The assessment of antagonistic interactions with this model was problematic. The Bliss independence based models resulted in mosaics of synergistic and antagonistic interactions raising questions about the mechanism of actions of antifungal drugs in combination. The levels of 150% and –150% of the sum of all statistically significant interactions can be used as cutoffs for synergy and antagonism. Semi-parametric approaches need particular care since experimental errors are not eliminated from the entire response surface.

Despite the considerable progress in antifungal therapy of systemic mycoses, treatment options still involve several drawbacks such as the toxicity of the widely used fungicidal antifungal drug, amphotericin B, the fungistatic properties of the less toxic azoles, the development of resistance to itraconazole, fluconazole and 5-flucytosine, and the emergence of new pathogens resistant to conventional monotherapy (i.e. scedosporiosis) (12, 34, 47). Thus, the introduction of new azoles with better pharmacokinetic profiles and potent antifungal activities (i.e. voriconazole, posaconazole) and the development of new agents with novel antifungal actions (i.e. echinocandins, nikkomycins) have boosted the discussion about the potential of combination therapy in management of invasive fungal

infections (13, 19, 24, 34, 40). More systemic drugs are now available with different mechanism of action increasing thus the possibility for synergistic interactions. This progress necessitates the provision of the in vitro antifungal susceptibility testing with new approaches for testing and analyzing combination of antifungal drugs.

Although antifungal drugs may interact differently under different conditions in in vitro systems (21, 27), variable results can be obtained even when the same in vitro methodology is used depending on the way that the nature and the intensity of drug interactions are assessed (5, 6, 14, 34). The standard approach in the field of medical microbiology is the calculation of the fractional inhibitory concentration

index (FIC_i) (10, 18). Synergy or antagonism is concluded when the concentration of the drugs in a combination showing the same effect as the MIC are lower or higher, respectively than the MICs of the single acting drugs for more than 1 dilution step of the assay. Despite the simplicity of this model, there are several drawbacks of this model to describe correctly, reliably and precisely the multi-dimensional phenomenon of drug interaction. These include (i) the choice of the MIC endpoints particularly with the combination of fungistatic and fungicidal drugs (ii) the choice of endpoints for the interpretation of the FIC indices (iii) the sensitivity to intraexperimental errors particularly when a twofold dilution scheme is followed (iv) the imprecise approximation of the real FIC index when off-scale MICs are present (v) the lack of a good summary of the interactions (vi) the difficulty to interpret statistically the results (45). The multi-dimensional (drugs + effect) nature of the drug interactions has led to the development of new models based on response surface approaches (7, 42, 44). One of them is a fully parametric model described by Greco et al. which is an E_{\max} based model and fits to the entire data set with a non-linear regression analysis (15). Many of the above mentioned problems of the drug interaction modeling are overcome since the nature and the intensity of an interaction is summarized with a non-unit, concentration-independent interaction parameter including the uncertainty in the estimate.

However, both models mentioned above rely on the Loewe additivity (LA) zero-interaction theory. This theory is based on the simple idea that a drug by definition cannot interact with itself and therefore a combination of a drug with itself is additive and its effect is that what is expected from the concentration effect curves. Opponents claim that the LA theory is limited to drugs that act similarly or have similar concentration-effect curves. Although many zero-interaction theories can be found in the literature, the major competitor of LA for a reference model is the Bliss independence (BI). The latter theory relies on the idea that two drugs that act independently at any aspect follow the law of probability: the probability of either or both two independent events (i.e. the action of a drug which in case of susceptibility tests corresponds to the percentage of inhibition) to occur is the sum of the probabilities of each event to happen alone minus the multiplication of them. Opponent arguments of this theory consisted of paradoxical cases when sham combinations of the same drug are analyzed assuming the BI as zero-interaction theory and the fact that the equation of the drug actions with independent events, as it is assumed in the BI theory, is questionable given the complexity of systems like cells (6, 14).

Several models based on BI have been described elsewhere (14). One of these is the non-

parametric model described by Prichard et al. (35, 36) as well as the parametric approach of the latter model assuming that the concentration-effect relationship of each drug alone follows the E_{\max} model (9, 14). Both models emphasize the multidimensional nature of drug interactions and determine the interactions including statistically significant levels. Furthermore, they enable the presence of mosaics of synergistic and antagonistic combinations as opposed to the Greco model. However, both models lack a good summary, although various summary measures have been previously described (8, 14, 36).

Controversial results on the nature as well as the intensity of an in vitro interaction can be obtained using each of the above-described models (14). Given the increasing interest of combination antifungal therapy, an unbiased, objective and comprehensive analysis tool for the assessment of the in vitro combination of antifungal drugs is warranted. In order to compare all these models, 17 drug combination-fungus pairs including different antifungal drugs (miconazole, itraconazole, fluconazole, amphotericin B, 5-flucytosine, and terbinafine) and various species of yeasts (*Candida albicans*, *C. glabrata*, and *C. krusei*) and moulds (*Aspergillus fumigatus* and *Scedosporium prolificans*) were selected based on the FIC indices calculated from preliminary experiments. Thus, the collection consisted of 6 synergistic interactions (FIC_i ≤ 0.5), 6 additive/indifferent interactions (0.5 < FIC_i ≤ 4) and 5 antagonistic interactions (FIC_i > 4). Data obtained from two dimensional checkerboard microdilution techniques based on a spectrophotometric (for yeasts) and a colorimetric (for moulds) modification of the NCCLS standard for antifungal susceptibility testing, were analyzed with the four above mentioned models. Results concerning the parameters of concentration-effect curves of the drugs, the nature and the intensity of the interactions, as well as the drug concentrations, which showed the interactive effects estimated with each model, were compared to each other. Because the purpose of this study was the drug interaction modeling of antifungal agents, biological and clinical extrapolations of the results were limited towards this direction.

MATERIALS AND METHODS

Isolates. Six clinical isolates of filamentous fungi, 3 *Scedosporium prolificans*, AZN7901 (SP1), AZN7902 (SP2), and AZN7906 (SP3) and 3 *Aspergillus fumigatus*, AZN5241 (AF1), AZN58 (AF2), and AZN59 (AF3), and 11 yeast clinical isolates, 3 *Candida albicans*, AZN574 (CA1), AZN2308 (CA2), and AZN4518 (CA3), 3 *C. krusei*, AZN1-27 (CK1), AZN1-31 (CK2), and AZN1-32 (CK3), 5 *C. glabrata*, AZN608 (CG1), AZN1143 (CG2), AZN1-28 (CG3), AZN2-50 (CG4), and AZN2-57 (CG5) were used in

Table 1. Characteristics of drug combination-strains pairs used in the interaction studies

Interaction	FIC indices	Drug combination (concentration range in mg/l)	Time	Species	No. of Strains	Replicates	Checker-board	Method
Synergy	≤0.5	miconazole (64-0.06) + terbinafine (64-1)	72 h	<i>S. prolificans</i>	3	4	12x8	MTT colorimetric
Synergy	≤0.5	5-flucytosine (64-0.004) + fluconazole (128-0.125)	48 h	<i>C. albicans</i>	3	3	16x12	Spectrophotometric
Additive/ indifferent	0.5-4	amphotericin B (16-0.015) + itraconazole (16-0.015)	48 h	<i>A. fumigatus</i>	3	3	12x12	MTT colorimetric
Additive/ indifferent	0.5-4	5-flucytosine (64-0.004) + fluconazole (128-0.125)	48 h	<i>C. krusei</i>	3	3	16x12	Spectrophotometric
Antagonism	>4	5-flucytosine (64-0.004) + fluconazole (128-0.125)	48 h	<i>C. glabrata</i>	5	3	16x12	Spectrophotometric

this study. The isolates were stored in 50% glycerol in water at -70°C . *C. parapsilosis* (ATCC 22019) and *C. krusei* (ATCC 6258) were used as quality control (QC).

Antifungal drugs. Six antifungal drugs belonging to different classes of antifungal agents namely, the azoles miconazole (MZ) (Janssen Research Foundation, Beerse, Belgium), itraconazole (IZ) (Janssen Research Foundation), and fluconazole (FZ) (Pfizer, Capelle aan den IJssel, The Netherlands), the allylamine terbinafine (TB) (Novartis, Basel, Switzerland), the polyene amphotericin B (AB) (Bristol-Myers Squibb, Woerden, The Netherlands) and the pyrimidine 5-flucytosine (FC) (ICN, Pharmaceuticals, Zoetermeer, The Netherlands) were tested. In order to obtain stock solutions miconazole, itraconazole, terbinafine and amphotericin B were dissolved in 100% dimethylsulfoxid at concentrations of 25,600 mg/l, 12,800 mg/l, 25,600 mg/l and 6,400 mg/l, respectively and fluconazole and 5-flucytosine were dissolved in water at concentrations of 512 mg/l.

Antifungal susceptibility testing method. The in vitro activities of drugs alone and in combination were tested in 96-well flat-bottom microtitration plates with a two-dimensional checkerboard microdilution technique described previously (J. Meletiadis, J. W. Mouton, J. F. G. M. Meis, P. E. Verweij, submitted for publication) based on the standards proposed by the NCCLS for filamentous fungi (M-38P) and yeasts (M-27A) (28, 29). Briefly, serial twofold dilutions according to the dilution scheme for water insoluble and -soluble drugs of the NCCLS methods were prepared in the standard medium (liquid RPMI 1640 without sodium bicarbonate, with L-glutamine) (GIBCO BRL, Life Technologies, Woerden, The Netherlands) buffered with 0.165 M 3-N-morpholinepropanesulfonic acid (Sigma-Aldrich Chemie GmbH, Steinheim, Germany) at pH 7.0 in order to obtain 4 times the final concentration. 50 μl of each drug concentration was mixed into the wells with 50 μl of each concentration of the other drug including the drug-free controls (medium with the drug solvent at the final concentration) for the two drugs alone and together in order to obtain a two-dimension checkerboard. Yeast and mould conidia were collected with a swab from 1-2 and 5-7 day-old cultures in Sabouraud dextrose agar, respectively and conidia suspensions were adjusted spectrophotometrically. The conidia suspensions were diluted in order to obtain two times the final inoculum, which ranged from 1×10^4 to 5×10^4

CFU/ml for mould isolates and from 1×10^3 to 2.5×10^3 CFU/ml for yeast isolates in the standard medium. Then 100 μl of conidia suspension were inoculated into each well. The final concentrations of the drugs after the inoculation, alone and in combination are shown in Table 1.

Interaction studies. The strain-drug combination pairs were chosen based on the results of previous experiments (Table 1) in such a way to have interactions that spanned from strong synergy to strong antagonism based on the fractional inhibitory concentration index (FICI) model. The growth was quantified spectrophotometrically at 405 nm for the yeast strains and at 550 nm colorimetrically using a modification of the MTT method described previously for the mould strains (25). The percentage of growth for each well was calculated compared to that of the drug-free well. All tests were conducted in replicates on different days.

Drug interaction modeling. Data obtained as described above were analyzed using four different models. The models were parametric and non-parametric approaches of the following two zero-interaction theories: the Loewe additivity and the Bliss independence. In the Loewe additivity theory, concentrations of the drugs that produce the same effect alone and in combination, are compared, while in the Bliss independence theory, the estimates of the combined effect based on the effect of the individual drugs were compared with the effects obtained with the experiment.

(i) Loewe additivity (LA) is described by the following equation: $1 = d_A/D_A + d_B/D_B$ where d_A and d_B are the concentrations of the drugs A and B in the combination which elicit a certain effect and D_A and D_B the iso-effective concentrations of the drugs A and B when acting alone.

FIC index model. The non-parametric approach is based on the fractional inhibitory concentration index model expressed with the following equation:

$$\Sigma\text{FIC} = \text{FIC}_A + \text{FIC}_B = \frac{C_A^{\text{comb}}}{\text{MIC}_A^{\text{alone}}} + \frac{C_B^{\text{comb}}}{\text{MIC}_B^{\text{alone}}}$$

where $\text{MIC}_A^{\text{alone}}$ and $\text{MIC}_B^{\text{alone}}$ are the concentrations of the drugs A and B when acting alone and C_A^{comb} and C_B^{comb} are the concentrations of the drugs A and B at the iso-effective combinations (18). Since each replicate experiment yields several ΣFICs , among all ΣFICs calculated for each replicate, the ΣFIC_{\min} and ΣFIC_{\max} were determined corresponding to

the lowest and the highest ΣFIC , respectively. The reported ΣFIC (FIC index) was the ΣFIC_{\min} in all cases except when the ΣFIC_{\max} was higher than 4. In that case the ΣFIC_{\max} was reported as the FIC index (FICi) (18). Three MIC endpoints were used namely MIC-0, MIC-1 and MIC-2 defined as the lowest drug concentration showing 10%, 25% (or 20% for the yeast strains) and 50% of growth compared to the growth control, respectively. Thus, the following FIC indices were determined for each replicate, FICi-0, FICi-1 and FICi-2, respectively. Off-scale MICs were converted to the next highest or lowest twofold concentration. Since the FIC indices (FICis) are not normally distributed the median and the range of FICis among the replicates was calculated. Furthermore, the drug concentrations of the combination, which was corresponded to the FICi, was determined. This combination was actually the combination with the strongest effect (I_{\max}).

Greco model. The fully parametric surface approach described by Greco et al. (15) was used based on the following equation:

$$I = \frac{D_A}{IC_{50,A} \left(\frac{E}{E_{\max}} \cdot E \right)^{1/m_A}} + \frac{D_B}{IC_{50,B} \left(\frac{E}{E_{\max}} \cdot E \right)^{1/m_B}} + \alpha \frac{D_A D_B}{IC_{50,A} IC_{50,B} \left(\frac{E}{E_{\max}} \cdot E \right)^{0.5(1/m_A + 1/m_B)}}$$

where E is the percentage of growth (dependent variable) at the drug concentrations D_A and D_B (independent variables), E_{\max} is the maximal percentage of growth observed in the drug-free control, $IC_{50,A}$ and $IC_{50,B}$ are the drug concentrations producing 50% of the E_{\max} , m_A and m_B are the slopes of the concentration-effect curves (Hill coefficient) for the drugs A and B, respectively and α is the interaction parameter which describes the nature of the interaction. This model was fitted directly to all experimental data of a data set (percentages of growth for all concentrations of the two drugs alone or in combination) with a non-weighted, non-linear regression analysis using the MODLAB program (MEDIMATICS, Maastricht, The Netherlands, www.medimatics.nl). When the estimate of α was positive and its 95% confidence interval (95% CI) did not include 0, statistically significant synergy was claimed while when α was negative without its 95% CI overlapping 0, statistically significant antagonism was concluded. In any other case Loewe additivity/indifference was concluded.

Goodness of fit criteria included the 95% CI of the estimated parameters, the R^2 , the sum of the squares (SumSq), correlation and covariance matrices. In order to check for any systematic deviation of the model from the data, residual plots were constructed and deviation from the normal distribution was tested with the Kolmogorof-Smirnof (KS) test.

In order to determine the drug combination which produced the highest effect (synergistic or antagonistic), the additivity surface was simulated by fixing all parameters of the Greco model to values obtained after the model was fitted to experimental data except α which was fixed at 0. This surface was then subtracted from the fitted surface calculated by the Greco model. The drug model concentrations of the combination with the highest percentage of synergy or antagonism were reported.

(ii) Bliss independence (BI) is described by the equation $I_{\text{ind}} = I_A + I_B - I_A \times I_B$, where I_{ind} is the predicted percentage of inhibition based on the experimental percentages of inhibition I_A , I_B of each drug acting alone, respectively. The latter equation is equivalent to $E_{\text{ind}} = E_A \times E_B$, where E_{ind} is the predicted percentage of growth which describes the effect of a combination where the drugs are acting independently and E_A , E_B are the experimental percentages of growth of each drug acting alone, respectively. The difference ΔE between the predicted percentage of growth E_{ind} and the experimentally measured percentage of growth (E_{exp}) describes the interaction at each combination of the drug concentrations. A three dimensional plot can then be constructed resulting in a surface plot.

In the non-parametric surface approach described by Prichard et al. (37), the E_A and E_B are obtained directly from the experimental data while in the parametric surface approach (9) these values are derived from fitting the E_{\max} model to the concentration-effect curves of each drug alone. Thus, for the latter approach the E_{ind} was calculated with the following equation:

$$E_{\text{ind}} = \frac{(D_A/IC_{50,A})^{m_A} \cdot (D_B/IC_{50,B})^{m_B}}{[1 + (D_A/IC_{50,A})^{m_A}] \cdot [1 + (D_B/IC_{50,B})^{m_B}]}$$

where D_A , D_B , $IC_{50,A}$, $IC_{50,B}$, m_A and m_B are the same parameters as described above for drug A and B in the Greco model. The parameters of the model were obtained by a non-weighted non-linear regression analysis of concentration effect curves of each drug alone using the GraphPad Prism Software (San Diego, CA). Data were normalized by using the percentages. The maximum and the minimum of the E_{\max} model were kept constant during the fitting procedure at 100% and 0%, respectively. The goodness of fit was interpreted using the 95% CI of the estimates, the run tests and the R^2 values. The estimated parameters for each drug generated were subsequently used to calculate the zero-interaction surface for each experiment.

For each combination of the drugs in each of the independent replicate experiments, the E_{exp} was subtracted from the E_{ind} calculated with the non-parametric or the parametric model. When the mean difference was positive and its 95% CI did not include 0, statistically significant synergy was claimed for that specific combination of drug concentrations. When the mean difference was negative without its 95% CI overlapping 0, statistically significant antagonism was claimed for that specific combination of drug concentrations. In any other case Bliss independence was concluded. In the three-dimensional plots, peaks above and below the 0 plane indicate synergistic and antagonistic combinations, respectively, while the 0 plane itself indicate no statistically significant interactions.

Since the plots only show the interaction for each separate combination of concentrations, a value is needed to summarize the whole interaction surface for each strain. This was done in two different ways. In the first, the percentages of all statistically significant interactions were summed (ΣSSI). In the second, all statistically significant interactions were averaged and the mean percentage (MSSI) as well as its 95% CI was calculated. When the MSSI was positive and its

Table 2. Summarized results of the four drug interaction models based on species and drug combinations. The median (min, max) for the 3 strains and the three replicates is presented

Species (No. of Strains)	Drug combi- nations	LOEWE ADDITIVITY BASED MODELS			
		Non-parametric approach (FIC index)			Parametric (Greco)
		FICi-0	FICi-1	FICi-2	α^b
SP (3)	TB + MZ	ND ^a	0.09 (0.06, 0.13)	0.03 (0.02, 0.04)	84.1 (0.2, 54 x 10 ³)
CA (3)	FC + FZ	0.17 (0.09, 0.25)	0.08 (0.05, 0.13)	1.03 (0.28, 1.03)	18.9 (1.2, 61.6)
AF (3)	AB + IZ	1 (0.25, 2)	0.63 (0.27, 2)	0.25 (0.08, 0.51)	-0.14 (-0.30, 0.04)
CK (3)	FC + FZ	1 (0.5, 1)	1 (0.5, 1)	1 (0.5, 1.5)	-0.2 (-0.5, -0.13)
CG (5)	FC + FZ	8.5 (4.25, 9)	8.5 (4.25, 16.5)	8.25 (1.01, 32.5)	-0.22 (-0.51, -0.14)

BLISS INDEPENDENCE BASED MODELS					
		Non-parametric approach		Parametric approach	
		Σ SSI (%) ^c	MSSI (% \pm 95% CI) ^d	Σ SSI (%)	MSSI (% \pm 95% CI)
SP (3)	TB + MZ	1401 (1051, 1751)	28.4 (14.9 \pm 1.8, 28.7 \pm 2.2)	870 (413, 1206)	21.7 (9.2 \pm 3.4, 23.6 \pm 4.6)
CA (3)	FC + FZ	347 (123, 440)	11.3 (7.2 \pm 7.1, 18.3 \pm 3.8)	639 (194, 871)	15.2 (9.2 \pm 6.4, 20.2 \pm 2.8)
AF (3)	AB + IZ	30 (21, 39)	1.2 (-0.1 \pm 14.4, 4.8 \pm 9.8)	137 (82, 207)	4.7 (4.3 \pm 9.4, 12.2 \pm 6.8)
CK (3)	FC + FZ	70 (-56, 285)	13.9 (-13.9 \pm 17.1, 15.8 \pm 3.4)	102 (61, 152)	6.8 (3.6 \pm 22.9, 7.9 \pm 7.8)
CG (5)	FC + FZ	-498 (-805, -282)	-31.1 (-41.3 \pm 18.4, -27.4 \pm 12.6)	-419 (-914, -214)	-34.9 (-37.7 \pm 9.2, -30.6 \pm 24.6)

^a ND, not determined.^b The 95% confidence intervals did not overlap 0.^c Sum of all statistically significant interactions of a data set.^d Mean and 95% confidence interval of all statistically significant interactions of a data set.

95% CI did not include 0, statistically significant synergy was claimed for the entire data set. When the MSSI was negative without its 95% CI overlapping 0, statistically significant antagonism was concluded for the entire data set. In addition, the Σ SSI and the MSSI were calculated only for the statistically significant synergistic (Σ SYN and MSYN, respectively) and antagonistic (Σ ANT and MANT, respectively) separately. Finally, the drug concentrations of the combination that yielded the highest synergistic or antagonistic effect (I_{\max}) were determined.

Comparison of models. In order to compare the four models various parameters were chosen such as (i) the single drug parameters MIC-0, MIC-1 and MIC-2 of the FIC index model and the IC_{50} and the slope m of the Greco and the parametric BI-based model, (ii) the summary interaction parameters FICi-0, FICi-1 and FICi-2 of the FIC index model, α interaction parameter of the Greco model and Σ SSI and MSSI of the non-parametric and parametric BI-based models and (iii) the interactive drug concentrations which yielded the most potent interaction as determined with each model.

Furthermore, different endpoints were used to determine synergy, zero-interaction (additivity, indifference, independence) and antagonism for each model. The percentage of agreement was calculated and the results were analyzed with the kappa test. A kappa value of 1 indicates absolute agreement (100%). Kappa values between 0.90-1 indicate excellent agreement, 0.80-0.90 very good agreement, 0.61-0.80 good agreement, and <0.6 poor agreement.

The concentrations of the drugs were transformed logarithmically in order to approximate normal distribution. The differences between the models for all drug-strain combinations were analyzed with analysis of variance (ANOVA) followed by Bonferroni's multiple comparison tests. In all comparisons, differences with $P < 0.05$ were considered statistically significant.

RESULTS

FIC index model. The summarized results obtained with the FIC index model are presented in Table 2 for each species-drug combination. In the table, for all data sets for which the reported FICis were corresponded to the Σ FIC_{min}S (*S. prolificans*, *C. albicans*, *A. fumigatus*, and *C. krusei*), the Σ FIC_{max}S were lower than 2.5 (except for the third replicate of the AF2 strain for which the Σ FIC_{max} was 4) while for all data sets for which the reported FICis were corresponded to the Σ FIC_{max}S (*C. glabrata*), the Σ FIC_{min}S were greater than 0.5. This indicates that there were not both synergistic and antagonistic combinations within the same data set.

FIC indices varied from as low as 0.02 for *S. prolificans* strains with terbinafine and miconazole to as high as 32.5 for *C. glabrata* stains with 5-flucytosine and fluconazole indicating strong synergy and antagonism, respectively. The results of the median FICi-0, FICi-1 and FICi-2 were consistent for 3 of the 5 combinations (*S. prolificans*, *C. krusei*, and *C. glabrata*). In contrast, for *C. albicans* and *A. fumigatus*, the value of the FICi was dependent on the MIC endpoint chosen. For instance, using the FICi-0 for *C. albicans* one could conclude synergy (median FICi 0.17), while using the FICi-2 indifference would be concluded (median FICi-2 1.03). Since some of the variation of the results might be due to experimental errors, we looked at the variation between replicate experiments.

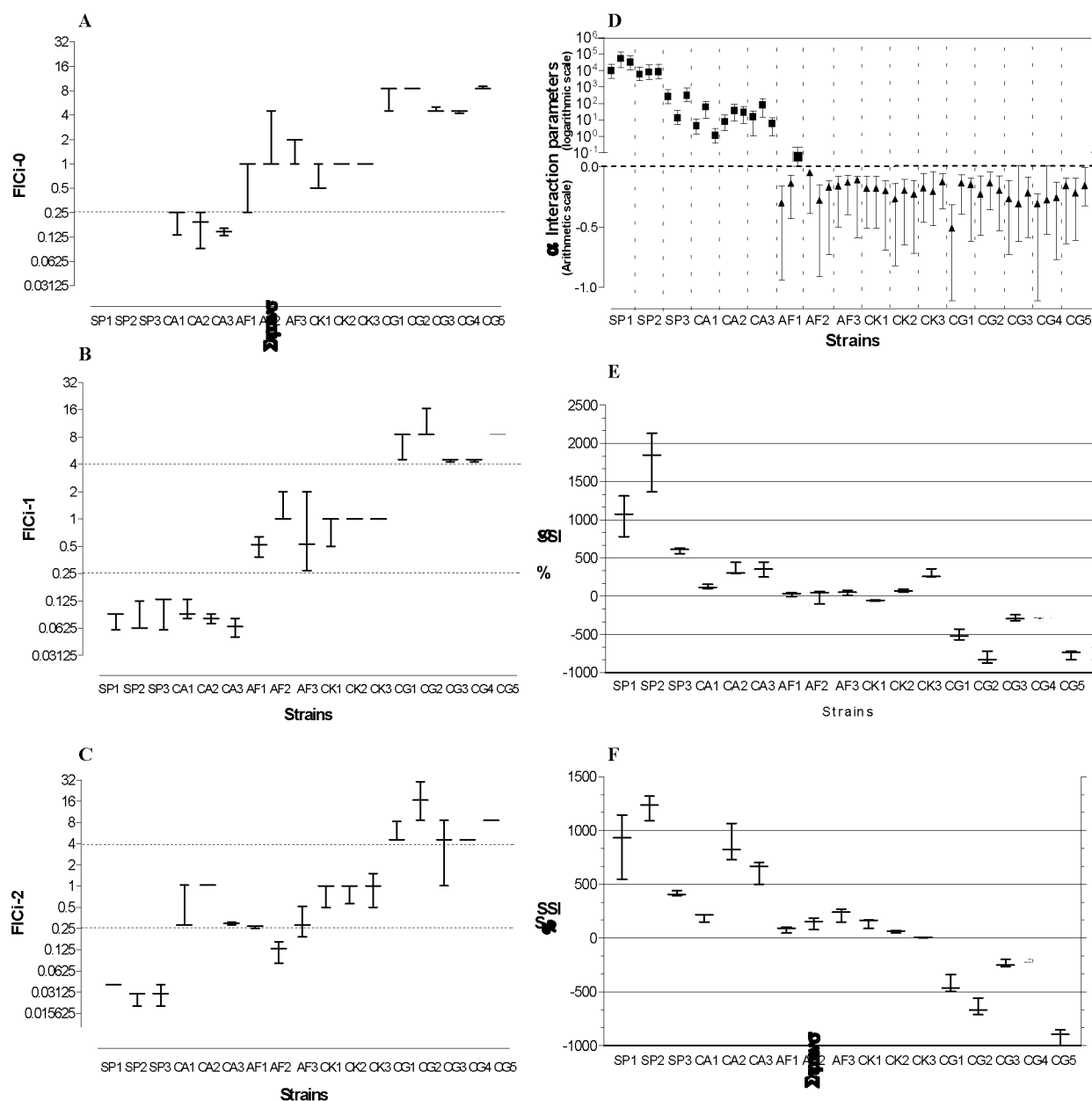


Figure 1. Graphical representation with the analytical results of the four models. The FICI-0 (A), FICI-1 (B) and FICI-2 (C) of the FIC index model, the α interaction parameters (D) of the Greco model and the % of Σ SSI of the non-parametric (E) and parametric (F) approach of Bliss independence. For all models except the Greco model the minimum, median and maximum among the replicates are presented for each strain with the three horizontal lines, respectively. For the Greco model the interaction parameter α with its 95% CI is presented for each replicate of each strain. Squares and triangles correspond to positive and negative α values, respectively.

Fig. 1 shows that most of the differences among the FIC indices of the replicates were within 3 \log_2 . By using the FICI-1, better discrimination was obtained between synergistic, additive/indifferent and antagonistic interactions (Fig. 1) when the cut-offs of 0.25 and 4 were used for the upper limit of synergy and additivity/indifference, respectively. By using these endpoints for the interpretation of the results the highest reproducibility among the replicates was found (100%) (data not shown). Using the FICI-0, the interactions could be classified as synergistic or antagonistic when all replicates resulted in indices lower or higher than 1,

respectively while in additive/indifferent interactions one or more replicates resulted in indices of 1.

Greco model. The fully parametric model was fitted to the entire data set of each replicate. The results of the interaction parameters α are summarized in Table 2. Statistically significant synergistic interactions were found for *S. prolificans* and *C. albicans* strains indicated by the positive interaction parameters and lower limit of their 95% CIs. Statistically significant antagonistic interactions were found for *A. fumigatus*, *C. krusei* and *C. glabrata* strains since the interaction parameters α and the upper limit of their 95% CIs were

negative. No additive interactions were found with the Greco model. As it is shown in Fig. 1, the model showed high reproducibility (98%) among the replicates since the results of all replicates were concordant with the exception of one replicate of the AF1 strain, which resulted in a positive α value by contrast with the other two replicates.

Regarding the goodness of fit, narrow 95% CIs ($<1\log_{10}$) of the fitted parameters were obtained and the R^2 and the SumSq of all fits ranged from 0.75 to 0.95 (median 0.91) and from 0.3 to 7.4 (median 1.3), respectively. However, when the residuals of each fit were tested with the KS test statistically significant deviation from the normal distribution was found for all strains ($P < 0.05$) except for the *S. proliferans* strains and two replicates of the AF1 strain. The residual plots together with the three-dimensional graphs of the response surface constructed by plotting the experimental data (experimental response surface) and data predicted with the Greco model (fitted response surface) revealed the areas where the model deviated from the data (Fig. 2).

For all fits with negative interaction parameters observed mainly with *C. glabrata* strains, the model deviated from the data at high concentrations of fluconazole and low concentrations of 5-flucytosine (Fig. 2Ci and ii). For this area of concentrations, the model yielded higher percentages of growth compared to the data at relatively lower concentrations of 5-flucytosine while the opposite observed at relatively higher concentrations as it is shown in Fig. 2Ciii with the two groups of residuals above and below the 0 plane. For the fits with positive interaction parameters two patterns of deviation were found. In yeasts (i.e. *C. albicans* strains), the model deviated at intermediate concentrations of fluconazole and low concentration of 5-flucytosine (Fig. 2Bi and ii) where the fitted response surface was above and below, respectively of the experimental data (Fig. 2Biii). In moulds (i.e. *S. proliferans* strains), despite the fact that the residuals did not deviate statistically significantly from the normal distribution, the Greco model deviated from the data at high concentrations of the two drugs where the fitted response surface did not follow the same pattern of curvature as the experimental response surface resulting in higher percentages of growth (Fig. 2A).

Bliss independence based models. The results for all strains are summarized in Table 2 where the sum and the mean of all statistically significant interactions (Σ SSI and MSSI, respectively) were used as summaries for each strain. *S. proliferans* strains showed the highest Σ SSI and the *C. glabrata* strains the lowest based on both the non-parametric and parametric approaches. The MSSI was statistically significant positive for the *S. proliferans* strains, but statistically significant negative for the *C. glabrata* strains. Between the two

approaches, the non-parametric approach resulted in stronger interactions for *S. proliferans* and *C. glabrata* strains, while the parametric approach did this for the remaining strains.

Although the absolute values of the Σ SSI were different between the non-parametric and parametric approach, the nature of the interaction determined with these two models was the same for most strains with the exception of one *C. krusei* strain. As it is shown in Fig. 1, better discrimination between the different interaction groups (synergistic, independent, and antagonistic) was obtained with the parametric approach. When the MSSI was correlated with the Σ SSI, the former became statistically significant positive and negative when the Σ SSI was higher than 100% and lower than -100%, respectively with the non-parametric approach. With the parametric approach, the same was found for the levels of 150% and -150% Σ SSI, respectively.

Regarding the goodness of fit of the E_{\max} model for the parametric approach, the R^2 ranged from 0.88 to 1 (median 0.98) and the SumSq ranged from 0.01-0.06 (median 0.27) for the concentration effect curves of 5-flucytosine. For the concentration effect curves of fluconazole for all *Candida* strains except *C. albicans*, the R^2 ranged from 0.85-1 (median 0.97) and the SumSq ranged from 0.01-0.35 (median 0.05). Low R^2 (0.47-0.98, median 0.64) and high SumSq (0.04-0.31, median 0.22) were found for *C. albicans* strains. For miconazole, terbinafine, amphotericin B and itraconazole the R^2 and the SumSq ranged from 0.72-1 (median 0.86) and 0.01-0.2 (median 0.05). Low R^2 (0.43-0.57) and high SumSq (0.17-0.32) were found for itraconazole against the AF2 strain. Run tests resulted in non-statistically significant deviation of the E_{\max} model for the concentration effect curves of all drugs.

Although the Σ SSI and MSSI were used for each strain as summary parameters of the BI-based models, both models resulted in a mosaic of synergy and antagonism at different concentrations of the two drugs. This mosaic is presented three dimensionally in Fig. 3. Synergistic combinations which are indicated with the volumes above the 0 plane coexist with antagonist combinations which are indicated with the volumes below the 0 plane for most of the strains. The analytical results for each strain are shown in Fig. 4 where the sum and the mean of all statistically significant synergistic (Σ SYN and MSYN) and antagonistic (Σ ANT and MANT) interactions are presented separately. Based on the non-parametric approach, *S. proliferans* strains showed the largest Σ SYN (600-1800%) and the *C. glabrata* strains showed the largest Σ ANT (300-800%) without showing both types of interactions. The remaining strains showed both Σ SYN and Σ ANT with the former being higher than the latter in most of the cases as it is shown in Fig. 4A with the light gray bars

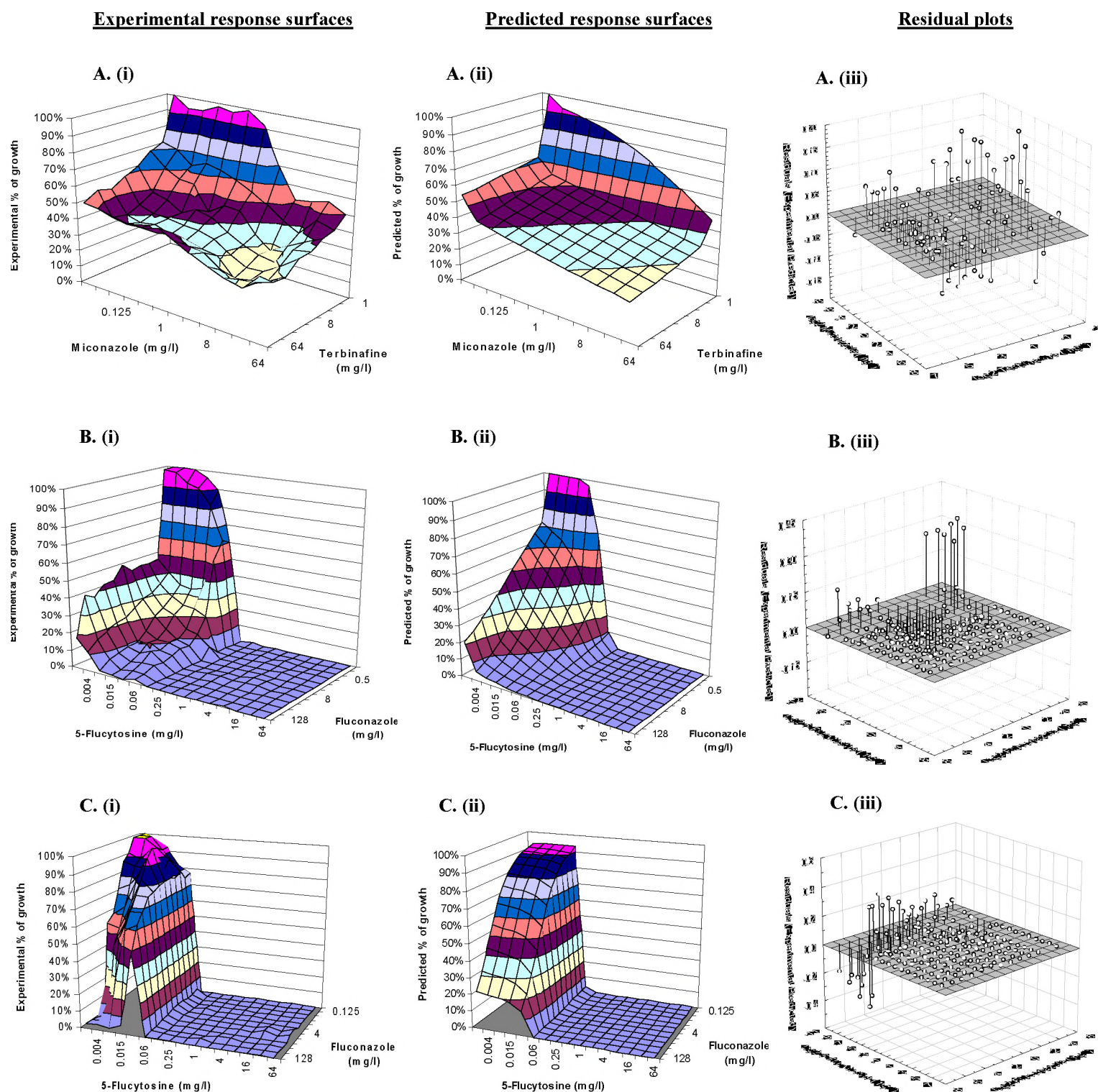


Figure 2. Response surfaces of the experimental data (i) and the data predicted with the Greco model (ii) as well as the residual plots (iii). **A.** Combination of miconazole and terbinafine against a *Scedosporium prolificans* strain (SP3) for which the FIC_i-1 and FIC_i-2 were 0.13 and 0.02 respectively. The interaction parameter $\alpha \pm 95\%$ CI derived from the Greco model was 271 ± 120 indicating very strong synergy. The normality test of the residuals resulted in non systematic deviation of the model (KS = 0.854, $P = 0.46$). **B.** Combination of fluconazole and 5-flucytosine against a *Candida albicans* strain (CA2) for which the FIC_i-0, FIC_i-1 and FIC_i-2 were 0.09, 0.09 and 1.03 respectively. The Greco model resulted in an interaction parameter of 37.08 ± 10 indicating synergy. The normality test of the residuals resulted in systematic deviation of the model (KS = 3.659, $P < 0.0001$). **C.** Combination of fluconazole and 5-flucytosine against a *Candida glabrata* strain (CG2) for which the FIC_i-0, FIC_i-1 and FIC_i-2 were 8.5 respectively. The interaction parameter $\alpha \pm 95\%$ CI derived with the Greco model was -0.23 ± 0.10 indicating antagonism. The normality test of the residuals resulted in systematic deviation of the model (KS = 5.376, $P < 0.0001$).

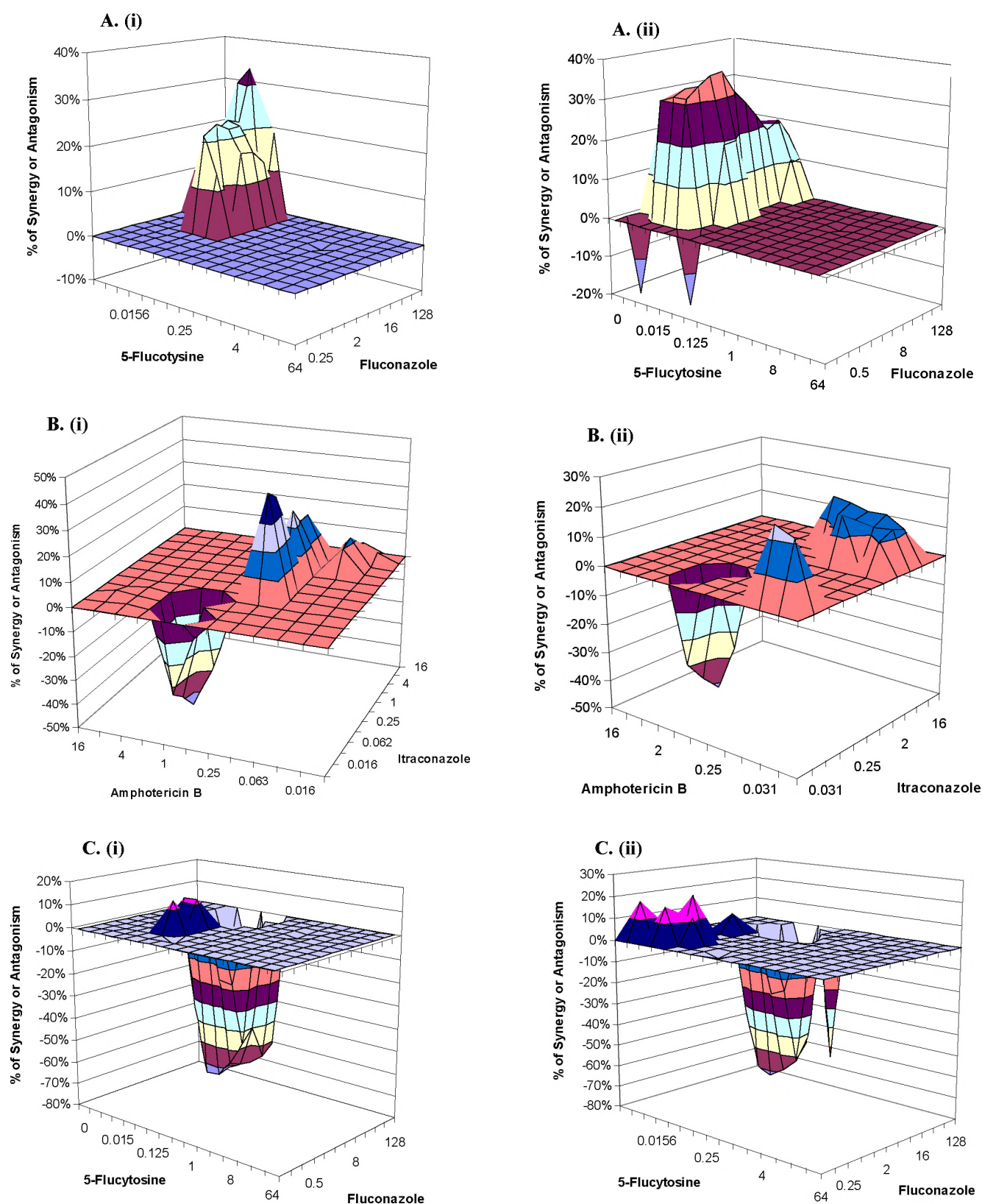


Figure 3. Interaction surfaces obtained with the non-parametric (i) and the parametric (ii) approach of Bliss independence where the % of synergy (above the 0 plane) and antagonism (below the 0 plane) are shown. **A.** The combination of fluconazole and 5-flucytosine against *Candida albicans* strain, (CA2), resulted in 347% Σ SSI and $18.3 \pm 3.8\%$ MSSI $\pm 95\%$ CI with the non-parametric approach of BI and 871% Σ SSI and $20.2 \pm 3.8\%$ MSSI $\pm 95\%$ CI with the parametric approach. **B.** The combination of itraconazole and amphotericin B against *Aspergillus fumigatus* strain, (AF1), resulted in 21% Σ SSI and $1.2 \pm 11.6\%$ MSSI with the non-parametric approach of BI and 82% Σ SSI and $4.3 \pm 9.4\%$ MSSI with the parametric approach. **C.** The combination of fluconazole and 5-flucytosine against *Candida glabrata* strain, (CG4), resulted in -740% Σ SSI and $-27.4 \pm 12.6\%$ MSSI with the non-parametric approach of BI and 914% Σ SSI and $36.6 \pm 12.6\%$ MSSI with the parametric approach.

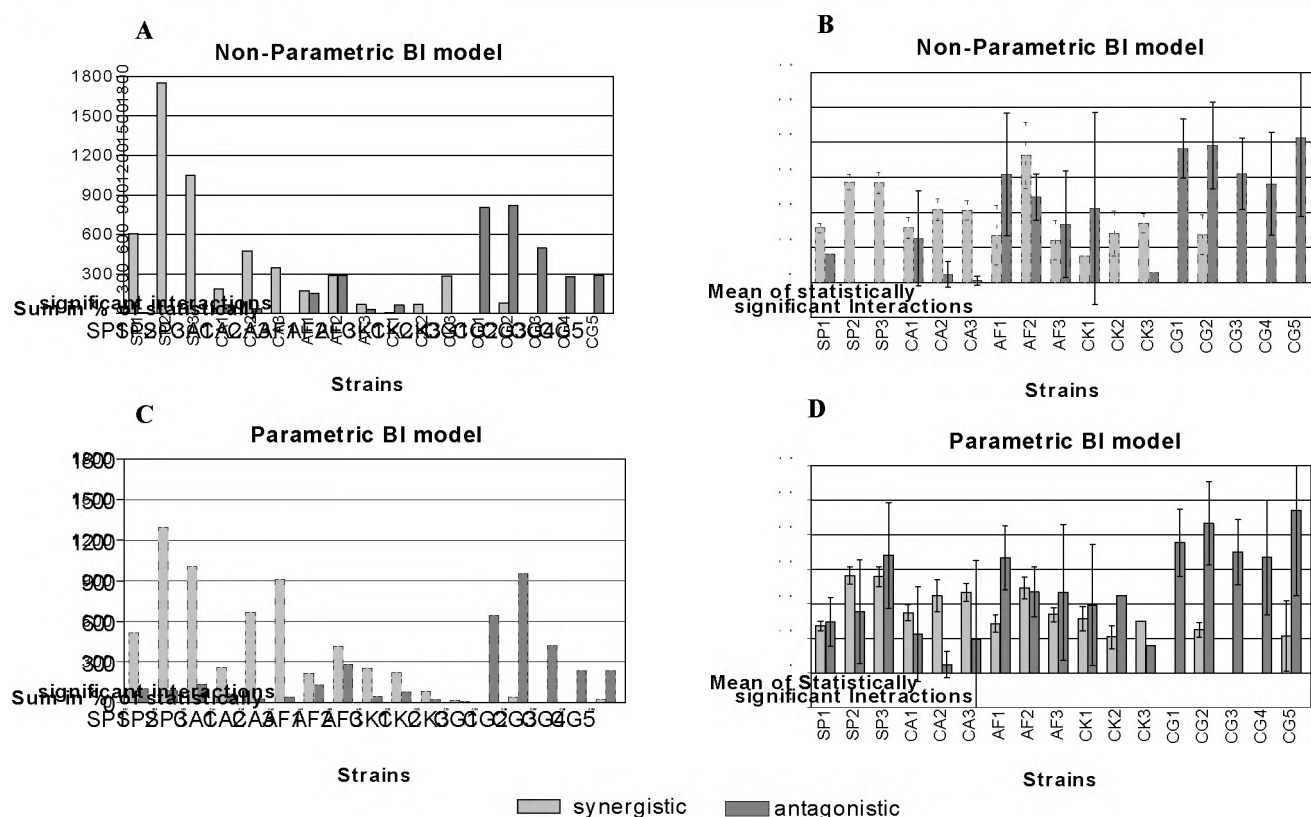


Figure 4. Graphical representation of the analytical results of the non-parametric and parametric approach of Bliss independence (BI). The sum and the mean with the 95% CI of all statistically significant synergistic and antagonistic interactions are presented separately for each strain.

dark gray bars, respectively. Based on the non-parametric approach, *S. proliferans* strains showed the largest Σ SYN (600-1800%) and the *C. glabrata* strains showed the largest Σ ANT (300-800%) without showing both types of interactions. The remaining strains showed both Σ SYN and Σ ANT with the former being higher than the latter in most of the cases as it is shown in Fig. 4A with the light gray bars dark gray bars, respectively. Using the MSYN and MANT, the same results were obtained, with the MSYN being statistically significant higher than the MANT for the *S. proliferans* strains and vice versa for the *C. glabrata* strains as it is shown in Fig. 4B.

Although the same conclusions were inferred with the parametric approach, the latter model resulted in some but weak Σ ANT for *S. proliferans* strains (Fig. 4C) and MSYN which was not statistically significant different from the MANT (Fig. 4D). However, the 95% CI of MSYN and MANT could not be calculated in some cases since only one combination showed the effect.

Comparison of the models. (i) Single drug parameters. The parameters of the concentration effect curves of the drugs acting alone that were used to determine the interactions with 1) the FIC index model, 2) the Greco model and 3) the parametric BI-based model are summarized in Table 3 for each species and

drug. No specific parameters were estimated for the non-parametric BI model. Among the three MIC endpoints calculated with the FIC index model, statistically significant differences ($P < 0.01$) were found between the MIC-2 and the other two MIC endpoints (ANOVA). These differences were observed mainly with the azoles and in particularly with fluconazole tested with the *C. albicans* strains where a 8-fold difference between the median MIC-2 and MIC-1 was found. Overall, the IC_{50} s estimated with the Greco model and parametric BI-based model were not statistically significant different from each other. The differences between the median IC_{50} s of each drug-species combination were within 2 twofold dilutions with the exception of the *S. proliferans* strains. For these strains the IC_{50} s of terbinafine obtained with the Greco model were higher than those obtained with the parametric BI model. The IC_{50} s estimated both with the Greco model and the parametric BI-based model were statistically significant different from MIC-0 and MIC-1 but not from MIC-2. The slopes estimated with the two latter parametric models were not statistically significant different.

(ii) Summary interaction parameters. Statistically significant correlation was found among all summary interaction parameters (Table 4). All correlations between the FIC index model and the other

Table 3. Single drug parameters. Median (range) among all strains and replicates of different parameters (MICs, IC50s in mg/l and slopes m) calculated with the FIC index model, the Greco model and the parametric Bliss independence (BI) model

Spp.	Drug	FIC index model			Greco model		Parametric BI model	
		MIC-0	MIC-1	MIC-2	IC50	- m	IC50	- m
CA	FC	0.13 (0.06-0.25)	0.13 (0.06-0.13)	0.13 (0.06-0.13)	0.07 (0.06-0.08)	4.7 (2.7-7.2)	0.07 (0.05-0.07)	4.3 (1.6-7.1)
	FZ	256 (16-256)	128 (16-256)	0.25 (0.06-1)	0.64 (0.06-0.36)	0.3 (0.2-0.4)	0.94 (0.19-2.96)	0.3 (0.2-0.5)
SP	TB	>64	>64	>64	33 (0.2-40)[$\times 10^3$]	0.09 (0.07-0.11)	51 (14-29 $\times 10^3$)	0.3 (0.1-0.6)
	MZ	>64	>64	16 (8->64)	35 (15-222)	0.4 (0.3-0.5)	19 (11-33)	1 (0.5-1.5)
CK	FC	16 (8-32)	16 (8-32)	4 (2-16)	5.14 (3.23-15.21)	1.5 (1-3.7)	3.28 (1.44-11.2)	1.6 (0.9-5.0)
	FZ	32 (16-64)	32 (16-64)	32 (16-64)	20.6 (13.8-52.1)	5.4 (4.3-34.7)	16.6 (10.7-38.7)	7.3 (2-19.6)
AF	AB	1 (0.5-2)	0.5 (0.5-2)	0.5 (0.5-1)	0.40 (0.29-1.23)	4.3 (2-21.4)	0.39 (0.23-1)	5.6 (2.3-19.8)
	IZ	32 (16->32)	32 (2->32)	8 (1->32)	1.87 (0.27-7.58)	0.7 (0.2-1.1)	5.41 (0.62-32.1)	0.5 (0.3-0.9)
CG	FC	0.06 (0.03-0.25)	0.06 (0.03-0.25)	0.06 (0.03-0.25)	0.05 (0.03-0.15)	6.7 (1.9-296.6)	0.03 (0.01-0.13)	3.8 (1.7-8.2)
	FZ	16 (16-64)	16 (8-64)	16 (4-64)	28.3 (17.5-128)	1.1 (0.7-2.1)	8.2 (2.1-54)	1.9 (0.7-8.1)
Overall		32 (0.031-256)	16 (0.031-256)	8 (0.03-128)	3.7 (0.03-40 $\times 10^3$)	1.5 (0.07-296)	3 (0.013-102)	1.9 (0.13-19.8)

models were negative.

Among the summary parameters of LA-based models, the strongest correlation was found between the interaction parameter α and the FICi-1 ($r_s = -0.74$) followed by FICi-2 ($r_s = -0.583$). To determine whether the value of the α interaction parameters could predict the magnitude of the FIC indices, combinations with negative and positive α interaction parameters were analyzed separately. No statistically significant correlation was found for the α negative interaction parameters and the corresponding FIC indices (the strongest correlation was with FICi-2, $r_s = -0.22$). For the positive α interaction parameters statistically significant correlation was found with the FICi-2 ($r_s = -0.63$, $P = 0.009$).

To explore further the relationship between α

interaction parameters and FIC indices, the α interaction parameters were plotted against the corresponding FIC indices from low to high α values separately for interactions with negative (Fig. 5A) and positive interaction parameters (Fig. 5B). Two patterns were detected. For negative interaction parameters, high α values (close to 0) tended to correspond to high FIC indices (Fig. 5A). While for positive interaction parameters, small α values (close to 0) tended to correspond to high FIC indices (close to 1) (Fig. 5B). Thus, although with the FIC index model the magnitude of synergy and antagonism is related with the degree of departure of the FIC indices from 1 (i.e. the larger the degree of departure, the stronger interactions), with the Greco model this seems to hold only for positive interactions (i.e. the larger the degree of departure of α

Table 4. Correlation^a between different summary parameters of parametric and non parametric approaches of Loewe additivity and Bliss independence

Summary parameters of each model		Loewe additivity (LA)				Bliss independence (BI) ^b			
		FIC index			Greco α	Non-parametric		Parametric	
		FICi-0	FICi-1	FICi-2		Σ SSI	MSSI	Σ SSI	MSSI
FIC index (LA)	FICi-0	1	0.943	0.789	-0.544	-0.879	-0.777	-0.916	-0.903
	FICi-1		1	0.783	-0.748	-0.904	-0.815	-0.952	-0.953
	FICi-2			1	-0.583	-0.807	-0.726	-0.814	-0.799
Greco (LA)	α				1	0.760	0.718	0.782	0.757
Non-parametric BI	Σ SSI					1	0.944	0.887	0.885
	MSSI						1	0.801	0.816
Parametric BI	Σ SSI							1	0.980
	MSSI								1

^a All correlations were significant at 0.01 level.

^b For the correlation of the summary parameters obtained with LA- and those obtained with BI- based models the median parameter of the three replicates obtained with the LA-based models was used.

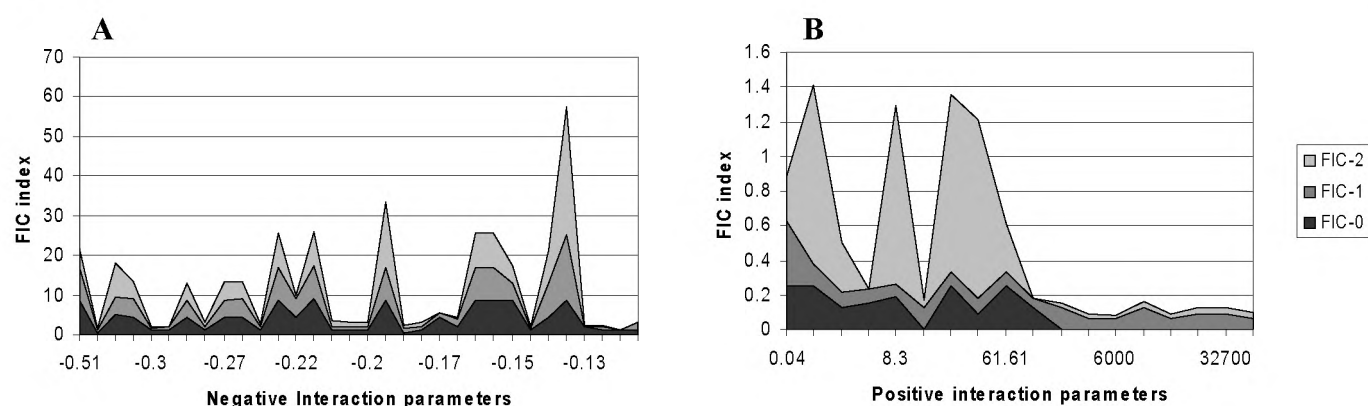


Figure 5. Correlation between the FIC indices and the α interaction parameters obtained with the Greco model. For interactions with negative interaction parameters (A) lower α values corresponded to higher FIC indices while for interactions with positive interaction parameters (B) the opposite was observed.

interaction parameter from 0, the stronger the synergy) since for negative interaction parameters the opposite was observed (i.e. the larger the degree of departure of α interaction parameter from 0, the weaker the antagonism).

Given, that replicates are required to obtain a summary parameter for BI-based models as opposed to LA-based models where each replicate resulted in a summary parameter, for the correlations between the BI- and LA- based models the median summary parameter of LA-based models among the replicates were used. Thus, between the summary parameters of BI-based models high correlation coefficients were obtained when the Σ SSI rather than the MSSI was used. Between the LA- and BI-based models, the interaction parameter α of the Greco model and the FICI-1 of the FIC index model were highly correlated with Σ SSI of

both the parametric ($r_s = 0.782$ and 0.953 , respectively) and the non-parametric ($r_s = 0.760$ and $r_s = 0.904$, respectively). Statistically significant correlation was found between the BI-based models and the FIC index model even when combinations with positive and negative Σ SSI were analyzed separately.

(iii) Highly interactive drug concentrations.

The concentrations of drugs that showed the strongest synergistic or antagonistic interaction (I_{\max}) determined with each model, are summarized in Table 5 for each species-drug pair. Although generally no statistically significant differences were found among the models, the I_{\max} determined with the Greco model tended to be at high concentrations (median concentration 6 mg/l) closer to those determined with the FICI-1 (median I_{\max} concentration 3 mg/l). The BI-based models showed the strongest interactions at lower concentration (median

Table 5. Median (range) drug concentrations in mg/l among all strains and replicates of the combination that showed the highest interactive effect as determined by each model

Spp.	Drug	Loewe additivity				Bliss independence	
		FICI-0	FICI-1	FICI-2	Greco	Non-Parametric	Parametric
CA	FC	0.016 (0.008-0.031)	0.008 (0.004-0.016)	0.004 (0.004-0.004)	0.06 (0.03-0.06)	0.03 (0.02-0.03)	0.03 (0.03-0.03)
	FZ	12 (1-32)	3 (1-4)	0.25 (0.25-0.25)	1.5 (0.25-4)	64 (8-64)	1 (1-2)
SP	TB	ND ^a	4 (4-8)	2 (2-4)	64 (64-64)	0.13 (0.03-0.25)	4 (4-8)
	MZ	ND	4 (4-8)	0.125 (0.016-2)	16 (4-32)	0.25 (0.13-0.25)	1 (0.25-4)
CK	FC	0.004 (0.004-16)	0.004 (0.004-16)	0.004 (0.004-8)	8 (4-64)	0.25 (0.13-4)	0.008 (0.008-2)
	FZ	32 (0.25-32)	32 (0.25-64)	16 (1-32)	32 (8-128)	2 (0.5-64)	1 (0.125-1)
AF	AB	1 (0.25-2)	0.5 (0.016-1)	0.031 (0.016-0.125)	0.5 (0.5-1)	0.03 (0.03-0.125)	0.03 (0.03-0.03)
	IZ	0.016 (0.016-2)	0.5 (0.016-8)	2 (0.125-8)	16 (0.06-16)	0.25 (0.125-1)	1 (0.125-4)
CG	FC	0.031 (0.016-0.25)	0.031 (0.016-0.125)	0.031 (0.016-0.125)	0.03 (0.03-0.25)	0.02 (0.02-0.03)	0.02 (0.02-0.02)
	FZ	256 (128-256)	128 (64-256)	128 (32-256)	64 (16-128)	16 (16-64)	16 (16-64)
Overall		0.63 (0.004-256)	3 (0.004-256)	0.25 (0.004-256)	6 (0.03-128)	0.75 (0.016-64)	1 (0.008-64)

^a ND, not determined

Table 6. Agreement in % (kappa value) between the four models using different endpoints for the definition of synergy (SYN), additivity/indifference (ADD), independence (IND) and antagonism (ANT)

Models and Interpretation endpoints		Agreement in % (kappa value)		
Greco model	FIC index	FICi-0	FICi-1	FICi-2
SYN; $\alpha \pm 95\%CI > 0$, ANT; $\alpha \pm 95\%CI < 0$	SYN < 0.25 , ANT ≥ 0.25	90% (0.66)	96% (0.91)	73% (0.38)
SYN; $\alpha \pm 95\%CI > 0$, ANT; $\alpha \pm 95\%CI < 0$	SYN < 0.5 , ANT ≥ 0.5	100% (1.00)	98% (0.96)	76% (0.50)
SYN; $\alpha \pm 95\%CI > 0$, ANT; $\alpha \pm 95\%CI < 0$	SYN < 1 , ANT ≥ 1	95% (0.87)	90% (0.78)	70% (0.40)
SYN; $\alpha \pm 95\%CI > 0$, ANT; $\alpha \pm 95\%CI < 0$	SYN < 2 , ANT ≥ 2	66% (0.36)	70% (0.45)	64% (0.36)
Non parametric BI	FIC index	FICi-0	FICi-1	FICi-2
SYN; $\Sigma SSI > 100\%$ IND; $100\% < \Sigma SSI < -100\%$ ANT; $\Sigma SSI < -100\%$	SYN; range FICi < 1 , ADD; range FICi incl. 1 ANT; range FICi > 1	93% (0.89)	82% (0.72)	69% (0.52)
SYN; $MSSI \pm 95\%CI > 0$ IND; $MSSI \pm 95\%CI = 0$ ANT; $MSSI \pm 95\%CI < 0$	SYN; range FICi < 1 , ADD; range FICi incl. 1 ANT; range FICi > 1	85% (0.78)	76% (0.63)	56% (0.33)
Parametric BI	FIC index	FICi-0	FICi-1	FICi-2
SYN; $\Sigma SSI > 150\%$ IND; $150\% < \Sigma SSI < -150\%$ ANT; $\Sigma SSI < -150\%$	SYN; range FICis < 1 , ADD; range FICis incl. 1 ANT; range FICi > 1	93% (0.89)	94% (0.91)	76% (0.0.64)
SYN; $MSSI \pm 95\%CI > 0$ IND; $MSSI \pm 95\%CI = 0$ ANT; $MSSI \pm 95\%CI < 0$	SYN; range FICis < 1 , ADD; range FICis incl. 1 ANT; range FICi > 1	86% (0.91)	88% (0.81)	68% (0.52)
Greco model	Non parametric BI			
SYN; $\alpha \pm 95\%CI > 0$ ANT; $\alpha \pm 95\%CI < 0$	SYN; $\Sigma SSI > 100\%$ ANT; $\Sigma SSI \leq 100\%$		94% (0.88)	
SYN; $\alpha \pm 95\%CI > 0$ ANT; $\alpha \pm 95\%CI < 0$	SYN; $MSSI \pm 95\%CI > 0$ ANT; $MSSI \pm 95\%CI \leq 0$		83% (0.62)	
Greco model	Parametric BI			
SYN; $\alpha \pm 95\%CI > 0$ ANT; $\alpha \pm 95\%CI < 0$	SYN; $\Sigma SSI > 150\%$ ANT; $\Sigma SSI \leq 150\%$		94% (0.88)	
SYN; $\alpha \pm 95\%CI > 0$ ANT; $\alpha \pm 95\%CI < 0$	SYN; $MSSI \pm 95\%CI > 0$ ANT; $MSSI \pm 95\%CI \leq 0$		94% (0.88)	
Parametric BI	Non parametric BI			
SYN; $\Sigma SSI > 150\%$ IND; $150\% \leq \Sigma SSI < -150\%$ ANT; $\Sigma SSI \leq -150\%$	SYN; $\Sigma SSI > 100\%$ IND; $100\% \leq \Sigma SSI < -100\%$ ANT; $\Sigma SSI \leq -100\%$		94% (0.91)	
SYN; $MSSI \pm 95\%CI > 0$ IND; $MSSI \pm 95\%CI = 0$ ANT; $MSSI \pm 95\%CI < 0$	SYN; $MSSI \pm 95\%CI > 0$ IND; $MSSI \pm 95\%CI = 0$ ANT; $MSSI \pm 95\%CI < 0$		77% (0.64)	

I_{max} concentrations 0.75 and 1 mg/l for the non-parametric and the parametric approach, respectively) closer to those determined with the FICi-0 (median I_{max} concentration 0.63 mg/l).

(iv) **Agreement between the models.** The levels of agreement between the models based on the interpretation of the results are summarized in Table 6 together with the results of the kappa test. Given that no additive interactions were found with the Greco model, for the comparisons with this model a unique cutoff was used for the determination of synergy and antagonism. Furthermore, for the comparisons between the BI- and

LA-based models, the interpretation of median interaction parameter among the replicates was used for the Greco model while for the FIC index model synergy or antagonism was defined when all replicates resulted in FIC indices lower or higher than the chosen cutoff, respectively. In any other case additivity/indifference was concluded.

Between the Greco model and the FIC index model, the highest level of agreement was found when the cutoff of 0.5 was used for the interpretation of the results of FICi-0 (100%) followed by FICi-1 (98%). Between the FIC index and the non-parametric BI-

based model high levels of agreement were found when the FIC_i-0 and the levels of 100% and -100% Σ SSI were used for the interpretation of the results, respectively.

Between the FIC index and the parametric BI-based model high levels of agreement were found when the cutoff of 1 for FIC_i-1 or FIC_i-0 and the level of 150% and -150% Σ SSI were used for the interpretation of the results, respectively. The same results were found when the Greco model was compared with the BI models. Between the BI-based models higher levels of agreement were found with the Σ SSI (94%) using the above mentioned endpoints than with the MSSSI (77%).

DISCUSSION

Different drug interaction models were used in this study in order to analyze the in vitro interaction of different antifungal drugs against various fungal species using the microdilution checkerboard technique. Interactions that varied in nature and degree, as assessed with the standard model in the field of medical microbiology, the FIC index model, were included and head-to-head comparisons with three other models were made.

The first and major problem in determination of the FIC index is the choice of the MIC endpoints for the two drugs alone and in combination (45). Although complete inhibition of growth is the endpoint often used with antibiotics this is not possible in the case of *S. prolificans* strains tested against terbinafine and miconazole since complete inhibition of growth (MIC-0) is not observed at any concentration of the drug alone or in combination. The interaction however was synergistic based on 75% (MIC-1) and 50% (MIC-2) inhibition of growth. Even when the MIC-0 was defined as in cases of *C. albicans* strains with 5-flucytosine and fluconazole, and *A. fumigatus* strains with amphotericin B and itraconazole, different FIC indices were obtained when the MIC-2 was used reversing the interpretation of the results from synergistic and additive/indifferent to additive and synergistic, respectively. These discrepancies were due to trailing phenomena observed with *C. albicans* strains when the drugs were tested alone. Trailing was reduced when the two drugs were combined (see Tables 2 and 5) confirming previous study (16). MIC-0 was more sensitive to trailing than the other MIC endpoints. In the case of *A. fumigatus* strains, the fungicidal action of amphotericin B at high concentrations of amphotericin B may cover the fungistatic action of itraconazole and vice versa at sub-MIC concentrations of amphotericin B and high concentrations of itraconazole. MIC-2 endpoint was more sensitive to this effect than the other MICs. However, the discrepancies between FIC_i-0, -1

and -2 were mainly due to off-scale MICs of itraconazole alone and in combination when the MIC-0 and MIC-1 were used, resulting in approximated FIC indices. The same phenomena were observed with *S. prolificans* strains where all MICs of terbinafine and miconazole alone were higher than the highest concentration tested and with a *C. glabrata* strain where the MICs-2 of fluconazole and 5-flucytosine in combination were lower than the lowest concentrations tested.

Another drawback of the FIC index model is the summary parameter for each data set and the interpretation of this parameter. According to the guidelines, among all Σ FIC indices calculated for each iso-effective combination, the Σ FIC_{min} is reported as the FIC_i unless Σ FIC_{max} exceeds 4. Synergy is claimed when the FIC_i is lower than 0.5 and antagonism when FIC_i is higher than 4. These cutoffs were chosen in this study in order to diminish the effect of the intraexperimental error (± 1 dilution) of antifungal susceptibility testing since a two-fold dilution scheme was followed (38, 39). The drawback of this approach is that the Σ FIC of a single well attempts to describe the whole checkerboard without taking into account the interactions occurring at other concentrations and levels of effect and without including its uncertainty. Furthermore, outliers can affect the results, particularly when checkerboards were abnormal and therefore subjective exclusion or inclusion of iso-effective wells was necessary.

In order to constrain the inter-experimental error, replicates were performed resulting in FIC indices in most of the cases within 3 log₂ (i.e. 0.25-1 or 1-4). For the interpretation of the results, different endpoints were used in literature. Based on reproducibility of the results, high reproducibility was found with FIC_i-1 (100%) as well as the FIC_i-0 (94%) when the cutoffs of 0.25 and 4 were used for the upper and the lower limit of synergy and antagonism, respectively in order to interpret each replicate individually. These cutoffs are 2 log₂ below and above the additivity level 1 and can be obtained after taking into account 1 doubling dilution error (often observed with the NCCLS methodology) for both drugs, alone or in combination, at any direction of the checkerboard. Although, different cutoffs can be found in the literature (22, 30, 46, 48) the cutoffs recommended from the guidelines (18) and commonly used for the upper and lower limit of synergy and additivity/indifference are the 0.5 and 4, respectively. These cutoffs although arbitrary are more stringent for defining antagonism than synergy since the cutoff of synergy (i.e. 0.5) is 1 log₂ while the cutoff of antagonism (i.e. 4) is 2 log₂ different than 1 (additivity). Therefore, from this point of view is better to use the cutoffs 0.25 and 4 for the upper and the lower limit of

synergy and antagonism, respectively as it is also illustrated in previous studies (3, 31).

However, by using stringent and arbitrary criteria to describe in vitro interactions, the problems of the inherent errors in laboratory tests might be pushed out of sight but they are not disappeared. Furthermore, given that most of the FIC indices are lying between 0.5-1 (1, 2, 32, 46), large amount of information about the drug interactions can be lost which might be in vivo important (4). There are several approaches to overcome these problems without losing important information such as smaller dilution steps, overlapping dilution series, continuous dilutions, more accurate techniques or replication (3, 4, 16). When replicates were analyzed, high reproducibility was found in the present study when synergy and antagonism was concluded if all replicates resulted in FIC indices lower or higher than 1, respectively and additivity or indifference when at least one replicate resulted in a FIC_i of 1. In addition, the departure of the FIC index from 1 can be evaluated statistically by checking if the 95% confidence interval overlapped 1 in which case no statistically significant interaction should be concluded.

In order to overcome the above mentioned drawbacks of the FIC index model, another model based on Loewe additivity zero-interaction theory was used in this study; the fully parametric model described by Greco et al. (15). This model was initially developed to describe anticancer drug interactions and thenceforth found many applications to different data sets (9, 33, 41, 45). This model tries to describe the effect at each combination of the two drugs including an interaction parameter, constant for the entire response surface, which indicates the departure from the additive surface. Thus, when this parameter is positive the experimental surface is below the additive one indicating synergy while when the parameter is negative the former is above the latter, indicating antagonism. This model enables us to check if the model fits adequately to the data as well as if the interaction is statistically significant. The model is based on the assumption that the concentration effect curves of each drug alone follow the E_{\max} model (sigmoid curve) and that true concentration dependent interactions are rare. Since the E_{\max} model describes adequately the concentration effect curves of all antifungal drugs tested in this study, which has also been shown by previous studies (26), the appropriateness of the Greco model to assess the interaction of antifungal drugs was further explored.

The model fitted well to the data derived from all drug-combination-strain pairs based on the R^2 and sum of the squares. However, when the residuals were analyzed statistically and graphically, the model deviated systematically from the data. This deviation was statistically significant in all fits with negative interaction parameters (antagonistic interactions) and

was located at drug concentrations at which the experimental response surface was above the additive (antagonistic combinations). For this area, the Greco model did not follow the curvature of the experimental response surface and it resulted in growth although experimentally no growth was observed. For the fits with positive interaction parameters (synergistic interactions), statistically significant deviation was found for the *C. albicans* strains. This deviation was due to the trailing phenomena observed with fluconazole, which also resulted in bad fit of the E_{\max} model when the latter was fitted to the concentration effect curves of fluconazole for the *C. albicans* strains. In order to diminish the effect of trailing, the concentration-effect curves for trailers could be normalized by setting as 0% the growth observed in concentrations at which the trailing is apparent. For the *S. proliferans* strains tested with miconazole and terbinafine, although a statistically significant deviation of the model was not found, residual plots and three-dimensional graphs revealed the area where the model did not describe the experimental surface precisely. This area was located at relatively high concentrations where the largest bowing of the response surface was observed (Fig. 2Ai). For this area the Greco model resulted in a more flat response surface (Fig. 2Aii).

The Greco model assumes that the concentration effect curves of each drug at any level of the other drug follow the E_{\max} model with variable parameters (IC_{50} and slopes) as is clearer shown in Fig. 2Cii. However, in the case of antagonistic interactions where the response surface concaves up and bell shaped concentration effect curves are apparent (see the concentration effect curve of 5-flucytosine in the presence of 128 mg/l of fluconazole in Fig. 2Ci) the E_{\max} model does not seem to hold true. These bell shaped curves are also observed, although less clear, in synergistic interactions as is shown in Fig. 2Ai where the response surface concaves down (concentration effect curve of terbinafine in presence of 8 mg/l of miconazole). This deviation of the model is more pronounced with strong interactions and declines as the interaction parameter approaches 0. This deviation is not reported in previous studies where the Greco model was used because low (close to 0) interaction parameters were found in these studies and data about the goodness of fit except the 95% CI are not presented in most of them (9, 33, 41, 45).

Based on the results derived with the Greco model, no additivity was found which might indicate the sensitivity of the model to detect even weak interactions. The results were very reproducible since all replicates except one were concordant. Although positive interaction parameters covered a broad range of values, from 1-10000, the negative interaction parameters were bounded in a narrow range from -0.04

to -0.51 indicating possibly the inability of the model to differentiate different degrees of antagonistic interactions as was also discussed above in relation to the difficulty of the Greco model to describe the response surfaces.

One of the assumptions of the Greco model is that antagonistic combinations cannot coexist with synergistic ones in the same data set and if such a case is found it is due to artifacts or experimental errors (43). However, Berenbaum summarized many types of interactions where both antagonism and synergy are present at different concentrations (6). These types of interactions cannot be described with the Greco model. Concentration dependent interactions was found for *Candida albicans* tested with the combination of fluconazole with fluphenazine where antagonism was observed at low concentrations of fluconazole and synergy at higher concentrations (17). These results were also supported by molecular studies on the mechanism of action. Similar phenomena were observed when itraconazole was combined with fluphenazine against itraconazole resistant *Aspergillus fumigatus* strains (J. Afeltra, personal communication). Since biphasic types of interactions might really exist, two other models were used to analyze the interaction of antifungal drugs, which can accommodate mosaics of interactions.

These models are based on Bliss independence zero-interaction theory without any assumption about the shape of the concentration effect curves of the drugs (non-parametric approach) or with the assumption that the latter's followed the E_{\max} model (parametric approach). With these models, the type of interaction was assessed for each combination of the tested drug concentrations. Both models resulted in a mix of statistically significant synergistic and antagonistic combinations for most of the data sets with the relative proportion ranged from purely synergistic for the *S. prolificans* strains to purely antagonistic for *C. glabrata* strains. The levels of synergy or antagonism determined with the non-parametric and the parametric model were comparable in most of the cases except for *S. prolificans* strains and for *C. albicans* and *A. fumigatus* strains where more antagonistic and synergistic interactions, respectively were found with the parametric approach. For the *S. prolificans* strains the antagonistic interactions were found at high concentrations of the drugs where precipitation was obvious resulting in overgrowth in those wells. This affected the parametric approach since with this approach experimental errors are selectively eliminated with the fitting process only in the single drug containing wells and not in all directions of the checkerboard. For *C. albicans* and *A. fumigatus* strains, the bad fit of the E_{\max} model to the concentration effect curves of fluconazole and itraconazole, due to trailing

effects and in vitro resistance, respectively resulted in higher % of growth for each concentration of the drugs present alone. Consequently the independent response surface determined with the parametric approach was shifted at higher levels compared to that of the non-parametric approach resulting therefore in higher levels of synergy.

Although the few antagonistic combinations found in particular with the parametric approach for the *S. prolificans* strains, could be explained with precipitation at high concentrations of the drugs, the presence of both types of interactions at different concentrations could raise points for discussion about the mechanistic explanation of these observations. For instance, when itraconazole was combined with amphotericin B against *Aspergillus fumigatus*, antagonistic interactions were found at concentrations around the MIC of amphotericin B (2-0.5 mg/l) and synergistic ones at sub-MIC concentrations of amphotericin B (<0.5 mg/l) (Fig. 3Bi). Whether the antagonistic effects are related to the lack of ergosterol due to sterol biosynthesis inhibition by itraconazole and the synergistic ones to the increased uptake of itraconazole inside the fungus due to damages of cell membrane caused by low concentrations of amphotericin B, suggested by previous studies (20, 23), need to be confirmed with molecular studies. Then, it would also be possible to evaluate mechanistically the validity of each of the zero-interaction theories used in the present study to assess the interaction of antifungal drugs. However, the same biphasic effect was observed also with the FIC index model, which resulted in lower FIC indices (synergy) based on the MIC-2 (which actually is observed at lower concentrations of itraconazole) and higher FIC indices (additive/indifference) based on the MIC-0 (which actually is observed at higher concentrations of itraconazole).

In order to summarize the results obtained with the BI-based model for further comparisons and with any reserve about their legalization from the mechanistic point of view two approaches were followed. For each data set the sum and the mean together with its 95% CI of all statistically significant interactions were calculated. The approach developed by Prichard et al. (36) where the volumes (% of interaction x the concentrations of the two drugs) above and below the 0 plane were calculated, was not followed since the final results are unequally influenced by small in degree interactions occurred at high concentrations. Thus, based on the sum and the mean of statistically significant interactions, the latter was positive without its 95% CI overlapping 0, when the sum was higher than 100% and negative when the sum was lower than -100% for the non-parametric approach while the same hold true for the parametric approach

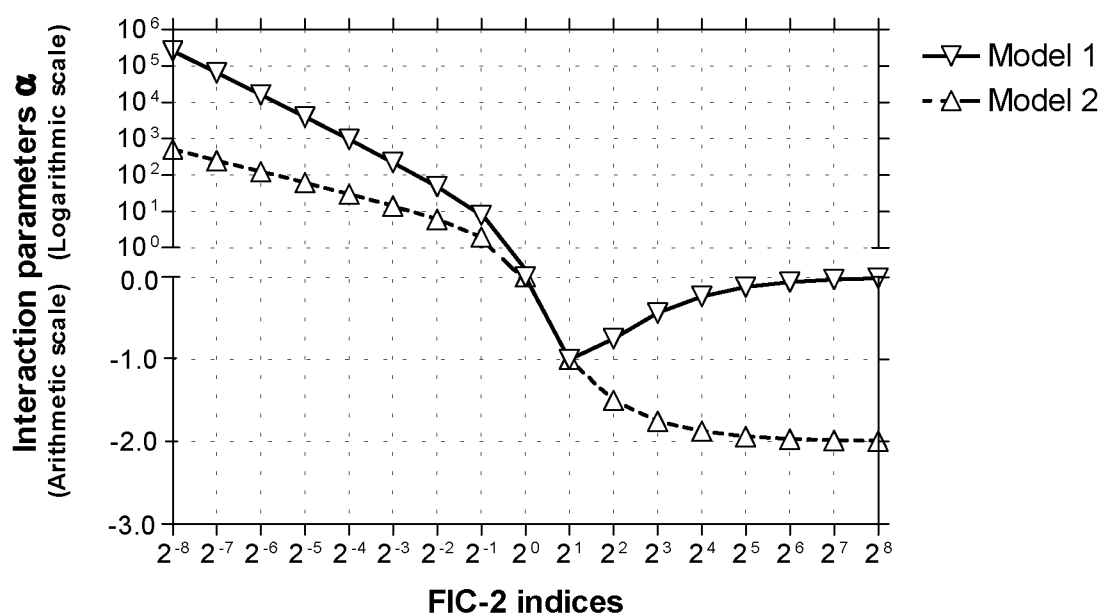


Figure 6. Graphical representation of the relationship between the interaction parameter α and the FIC-2 index (assuming that $FIC_A = FIC_B$) defined by two models. The model 1 is the Greco model used in the present study which defined the following equation for the FICi-2- α relationship: $FICi-2 = 1 - \alpha \times FIC_A \times FIC_B$. The model 2 is an alternative model for the Greco model described first by Finney et al. (11) and defines the following equation for the FICi-2- α relationship: $FICi-2 = 1 - \alpha (FIC_A \times FIC_B)^{1/2}$. Note the non-monotonic behavior of the Greco model by contrast with model 2. For negative interaction parameters, the model 1 has an asymptote at 0 while the model 2 at -2.

based on 150% sum of statistically significant interactions. This suggests that these cutoffs may serve as cutoffs for statistically significant synergy and antagonism, respectively. Between the two approaches of BI, higher reproducibility among the replicates was found with the non-parametric approach since the range of the sum of statistically significant interactions was within 150% for most of the strains.

Despite the pro and the con of each model, the most important point is the nature of an interaction determined with each model and discrepancy between them. Therefore a head to head comparison was performed including primary parameters (MICs, IC_{50} s, slopes m) used for the calculation of the summary interaction parameters (FICI, α , Σ SSI, and MSSI) of each model based on which the combinations were classified to different interaction groups (synergy, zero-interaction, or antagonism). Non statistically significant differences among the MICs-2 determined with the FIC index model and the IC_{50} s determined with the Greco and the parametric BI model (within 2 doubling dilutions) as well as between the slopes of the concentration effect curves determined by the two latter models were found. This indicates that the E_{max} model could be used to determine the in vitro susceptibility of fungi and that fully parametric approaches do not affect the concentration effect curves of the single drugs.

When the summary parameters of each model were correlated, statistically significant correlation was

found for all models. A strong correlation was found between the FICI-1, the interaction parameter α , the Σ SSI of both BI-based models and the MSSI of the parametric BI-based model. For the FIC index and the Greco model, no statistically significant correlation was found between the FIC indices and the α values, when the interactions with negative interaction parameters were analyzed separately. This might indicate the qualitative nature of the Greco model for combinations with negative interaction parameters as discussed above. However, since the FIC index model is itself an approximation of the intensity of the interactions such an assumption needs further exploration. Negative correlation was found between the FIC index model and the other models since high FIC indices corresponded with low values of the other summary parameters. However, this monotonic relationship was not found for the α interaction parameters obtained with the Greco model since a biphasic correlation was found as depicted in Fig. 5.

This innate property of the model is shown in Fig. 6 where hypothetical FIC indices calculated at the level of 50% of E_{max} (i.e. FICi-2) were plotted against the interaction parameter α according to the following equation $FICi-2 = 1 - \alpha \times FIC_A \times FIC_B$. The latter equation is derived after rearrangement of the Greco model given that the sum of the first two terms on the right part of the Greco equation is the FICi-2 and the term $[E/(E_{max}-E)]^{0.5(mA + mB)}$ at 50% of effect equals 1

independent of the value of the slopes m . In the same graph the $\text{FICi-2-}\alpha$ relationship as defined by an alternative model introduced first by Finney et al. (11) is also plotted. This model was suggested by Greco et al. (14) in order to overcome the rise up at high concentrations observed with the first model. This rise up is more pronounced at α values lower than -0.5 and therefore they were not observed in the present study since most of the α values were higher. This second model differs from the Greco model only in the third part of the Greco equation in that this part squared. Although this model shows a monotonic relationship with the FIC index, as is shown in Fig. 6, preliminary studies showed that it shares the same drawbacks, although to lesser extent, as the first model inferring the same conclusions. In the Fig. 6 is also depicted why narrow range of negative α interaction parameters found in this study since there is a minimum at -1 and a maximum at 0 for the α values and why the degree of antagonism is reversibly related with the magnitude of the α values as discussed above for the experimental data since increase of the FIC index is associated with increase of the interaction parameter α (closer to 0) for negative values as opposed for the positive interaction parameters.

The comparison of the models based on the interpretations of the results showed high levels of agreement between the Greco and the FIC index model when the cutoff of 0.5 was used to interpret the FICi-0 and the FICi-1 . Although one might expect the cutoff of 1 to show the highest agreement, the cutoff of 0.5 is within the experimental error of antifungal susceptibility methodology used in this study. This error affects more the results of the FIC index model. From the same point of view, the highest levels of agreement between the BI-based models and the FIC index model were found when the cutoffs of 0.5 and 4 were used to determine the upper limit of synergy and additivity/indifference respectively when only the median FIC index among the three replicates rather than the FIC indices of all replicates was used for the comparisons (data not presented). However, when all three replicates used to determine synergy (all FIC indices lower than 1) antagonism (FIC indices greater than 1) and additivity/indifference (in any other case), satisfactory levels of agreement were found (45). For the BI models the corresponding levels of synergy and antagonism were 100% and -100% ΣSSI for the non-parametric approach and 150% and -150% ΣSSI for the parametric approach, respectively as discussed above. The latter resulted in higher levels of agreement with the other models using both the ΣSSI and MSSI for the interpretation of the results.

The drug concentrations, which showed the highest interactive effect (I_{\max}), were not statistically significant different among the four models. The I_{\max}

drug concentrations determined with Greco model were the highest and they were similar to those determined using the FICi-1 of the FIC index model. The I_{\max} drug concentrations determined with the BI models were relatively lower and similar to those determined using the FICi-0 of the FIC index model. These conclusions confirm previous observations (14, 15) where the largest synergy was found at concentrations near but not exactly at the IC_{50} s of the two drugs and that the isobols are more bowed (stronger synergy) at 90% of pharmacological effect i.e. 10% of growth.

In conclusions, for the assessment of the interaction of antifungal drugs the FIC index model is easy and does not require sophisticated approaches. The FIC index based on MIC-2 (50% of growth) should be used in order to overcome problems coming from trailing effects and fungistatic-fungicidal combinations. However, interactions assessed based on other MIC endpoints might also be important to describe the concentration-dependent nature of a drug combination. The cutoffs of 0.25 and 4 for single experiments and 1 when replicates are performed for the upper and lower limits of synergy and antagonism respectively should be used for the interpretation of the results. However, the drawbacks of this model such as the monodimensional nature, lack of good summary including statistical significance levels and the sensitivity to experimental errors remain.

For the BI models, the level of 100% (for non-parametric approach) and 150% (for parametric approach) sum of statistically significant interactions with any mechanistic reserve could be used to differentiate synergistic from antagonistic interactions. Particular care should be given in parametric approaches for the choice of the model (especially with resistant and trailing strains) and because fitting process eliminates errors selectively in single drug concentrations and not in entire response surfaces. With the BI models, the multifactorial nature of drug interactions is emphasized and statistical significance levels are included. However, replicates are required, the results are depended on the range of concentrations tested, variation within the replicates can affect the levels and the nature of statistically significant interactions and comparisons between different data sets are difficult.

The Greco model describes the interactions with a single concentration-independent non-unit interaction parameter, does not require replicates, includes statistically significant levels and it is reproducible and less sensitive to experimental errors. However, it does not describe precisely the response surface of antifungal combinations and therefore the interaction parameters may be approximations. Quantitative results might be difficult to obtain particularly for antagonistic interactions, and a non-monotonic relationship with the

FIC index model exists. As it is pointed by Greco et al. the latter model is a model to assess drug interactions and therefore efforts to develop a model, which would describe precisely the response surface, should be continued.

Finally, the models could be evaluated from the biological point of the interactions if the mechanism of actions were fully understood, although this might be complicated in growth assays where population factors and in vitro parameters could affect the interaction (6). Therefore, drug interaction modeling should be focused on concentration effect response surface approaches. A comprehensive drug interaction model, which would describe the entire response surface and assess the interaction with a single parameter, is an attractive approach. However, even if the concentration effect relationship of single drugs are well characterized and parameterized, the development of such a model applicable to different interactions and tested against different microorganisms in various in vitro conditions is questionable. Therefore, different models might be required to assess the various combinations and possible interactions and to predict the clinical outcome of combination therapy.

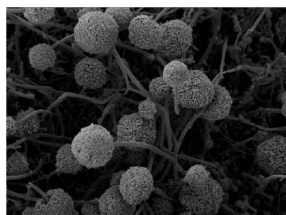
ACKNOWLEDGMENTS

This work was supported by the Mycology Research Center of Nijmegen.

REFERENCES

1. Atherton, F. R., M. J. Hall, C. H. Hassall, S. W. Holmes, R. W. Lambert, W. J. Lloyd, L. J. Nisbet, P. S. Ringrose, and D. Westmacott. 1981. Antibacterial properties of alafosfalin combined with cephalexin. *Antimicrob. Agents Chemother.* **20**:470-476.
2. Barchiesi, F., L. Falconi Di Francesco, and G. Scalise. 1997. In vitro activities of terbinafine in combination with fluconazole and itraconazole against isolates of *Candida albicans* with reduced susceptibility to azoles. *Antimicrob. Agents Chemother.* **41**:1812-1814.
3. Berenbaum, M. C. 1980. Correlations between methods for measurement of synergy. *J. Infect. Dis.* **142**:476-480.
4. Berenbaum, M. C. 1987. Minor synergy and antagonism may be clinically important. *J. Antimicrob. Chemother.* **19**:271-273.
5. Berenbaum, M. C. 1977. Synergy, additivism and antagonism in immunosuppression. A critical review. *Clin. Exp. Immunol.* **28**:1-18.
6. Berenbaum, M. C. 1989. What is synergy? *Pharmacol. Rev.* **41**:93-141.
7. Carter, W. H., Jr., and G. L. Wampler. 1986. Review of the application of response surface methodology in the combination therapy of cancer. *Cancer Treat. Rep.* **70**:133-140.
8. Drewinko, B., C. Green, and T. L. Loo. 1976. Combination chemotherapy in vitro with cis-dichlorodiammineplatinum(II). *Cancer Treat. Rep.* **60**:1619-1625.
9. Drusano, G. L., D. Z. D'Argenio, W. Symonds, P. A. Bilello, J. McDowell, B. Sadler, A. Bye, and J. A. Bilello. 1998. Nucleoside analog 1592U89 and human immunodeficiency virus protease inhibitor 141W94 are synergistic in vitro. *Antimicrob. Agents Chemother.* **42**:2153-2159.
10. Elliopoulos 1993. Antimicrobial combinations, p. 432-492. In V. Lorian (ed.), *Antibiotics in Laboratory Medicine*. 3rd edition. The Williams and Wilkins Co., Baltimore.
11. Finney, D. J. 1952. Probit analysis, 2nd ed. Cambridge University Press, Cambridge, UK.
12. Graybill, J. R. 1992. Future directions of antifungal chemotherapy. *Clin. Infect. Dis.* **14**(Suppl. 1):170-181.
13. Graybill, J. R. 1996. The future of antifungal therapy. *Clin. Infect. Dis.* **22**(Suppl. 2):166-178.
14. Greco, W. R., G. Bravo, and J. C. Parsons. 1995. The search for synergy: a critical review from a response surface perspective. *Pharmacol. Rev.* **47**:331-385.
15. Greco, W. R., H. S. Park, and Y. M. Rustum. 1990. Application of a new approach for the quantitation of drug synergism to the combination of cis-diamminedichloroplatinum and 1-beta-D-arabinofuranosylcytosine. *Cancer Res.* **50**:5318-5327.
16. Hamilton-Miller, J. M. 1985. Rationalization of terminology and methodology in the study of antibiotic interaction. *J. Antimicrob. Chemother.* **15**:655-658.
17. Henry, K. W., M. C. Cruz, S. K. Katiyar, and T. D. Edlind. 1999. Antagonism of azole activity against *Candida albicans* following induction of multidrug resistance genes by selected antimicrobial agents. *Antimicrob. Agents Chemother.* **43**:1968-1974.
18. Hindler, J. 1995. Antimicrobial susceptibility testing, p. 5.18.11-15.18.20. In H. D. Isenberg (ed.), *Clinical Microbiology Procedures Handbook*, Washington, D. C.
19. Kauffman, C. A., and P. L. Carver. 1997. Antifungal agents in the 1990s. Current status and future developments. *Drugs* **53**:539-549.
20. Kontoyiannis, D. P., R. E. Lewis, N. Sagar, G. May, R. A. Prince, and K. V. Rolston. 2000. Itra-conazole-amphotericin B antagonism in *Aspergillus fumigatus*: an Etest-based strategy. *Antimicrob. Agents Chemother.* **44**:2915-2918.
21. Lewis, R. E., D. J. Diekema, S. A. Messer, M. A. Pfaller, and M. E. Klepser. 2002. Comparison of Etest, checkerboard dilution and time-kill studies for the detection of synergy or antagonism between antifungal agents tested against *Candida* species. *J. Antimicrob. Chemother.* **49**:345-351.
22. Lorian, V. 1991. *Antibiotics in laboratory medicine*, 3rd ed. Williams & Wilkins, Baltimore, Md.
23. Maesaki, S., S. Kohno, M. Kaku, H. Koga, and K. Hara. 1994. Effects of antifungal agent combinations administered simultaneously and sequentially against *Aspergillus fumigatus*. *Antimicrob. Agents Chemother.* **38**:2843-2845.
24. Maschmeyer, G. 2002. New antifungal agents-treatment standards are beginning to grow old. *J. Antimicrob.*

- Chemother. **49**:239-241.
25. Meletiadis, J., J. F. G. M. Meis, J. W. Mouton, J. P. Donnelly, and P. E. Verweij. 2000. Comparison of NCCLS and 3-(4,5-dimethyl-2-Thiazyl)-2,5-diphenyl-2H-tetrazolium bromide (MTT) methods of in vitro susceptibility testing of filamentous fungi and development of a new simplified method. *J. Clin. Microbiol.* **38**:2949-2954.
 26. Meletiadis, J., J. W. Mouton, J. F. G. M. Meis, B. A. Bouman, J. P. Donnelly, and P. E. Verweij. 2001. Colorimetric assay for antifungal susceptibility testing of *Aspergillus* species. *J. Clin. Microbiol.* **39**:3402-3408.
 27. Nakajima, R., A. Kitamura, K. Someya, M. Tanaka, and K. Sato. 1995. In vitro and in vivo antifungal activities of DU-6859a, a fluoroquinolone, in combination with amphotericin B and fluconazole against pathogenic fungi. *Antimicrob. Agents Chemother.* **39**:1517-1521.
 28. NCCLS 1998. Reference method for broth dilution antifungal susceptibility testing of conidium-forming filamentous fungi; proposed standard. Document M-38P. National Committee for Clinical Laboratory Standards, Wayne, Pa.
 29. NCCLS 1995. Reference method for broth dilution antifungal susceptibility testing of yeasts. M-27A. National Committee for Clinical Laboratory Standards. Wayne, Pa.
 30. Nguyen, M. H., F. Barchiesi, D. A. McGough, V. L. Yu, and M. G. Rinaldi. 1995. In vitro evaluation of combination of fluconazole and flucytosine against *Cryptococcus neoformans* var. *neoformans*. *Antimicrob. Agents Chemother.* **39**:1691-1695.
 31. Norden, C. W., H. Wentzel, and E. Keleti. 1979. Comparison of techniques for measurement of in vitro antibiotic synergism. *J. Infect. Dis.* **140**:629-633.
 32. Odds, F. C. 1982. Interactions among amphotericin B, 5-fluorocytosine, ketoconazole, and miconazole against pathogenic fungi in vitro. *Antimicrob. Agents Chemother.* **22**:763-770.
 33. Patick, A. K., T. J. Boritzki, and L. A. Bloom. 1997. Activities of the human immunodeficiency virus type 1 (HIV-1) protease inhibitor nelfinavir mesylate in combination with reverse transcriptase and protease inhibitors against acute HIV-1 infection in vitro. *Antimicrob. Agents Chemother.* **41**:2159-2164.
 34. Polak, A. 1999. The past, present and future of antimycotic combination therapy. *Mycoses* **42**:355-370.
 35. Prichard, M. N., L. E. Prichard, W. A. Baguley, M. R. Nassiri, and C. Shipman, Jr. 1991. Three-dimensional analysis of the synergistic cytotoxicity of ganciclovir and zidovudine. *Antimicrob. Agents Chemother.* **35**:1060-1065.
 36. Prichard, M. N., L. E. Prichard, and C. Shipman, Jr. 1993. Strategic design and three-dimensional analysis of antiviral drug combinations. *Antimicrob. Agents Chemother.* **37**:540-545.
 37. Prichard, M. N., and C. Shipman, Jr. 1990. A three-dimensional model to analyze drug-drug interactions. *Antiviral Res.* **14**:181-205.
 38. Rex, J. H., M. A. Pfaller, M. G. Rinaldi, A. Polak, and J. N. Galgiani. 1993. Antifungal susceptibility testing. *Clin. Microbiol. Rev.* **6**:367-381.
 39. Rex, J. H., M. A. Pfaller, T. J. Walsh, V. Chaturvedi, A. Espinel-Ingroff, M. A. Ghannoum, L. L. Gosey, F. C. Odds, M. G. Rinaldi, D. J. Sheehan, and D. W. Warnock. 2001. Antifungal susceptibility testing: practical aspects and current challenges. *Clin. Microbiol. Rev.* **14**:643-658.
 40. Sheehan, D. J., C. A. Hitchcock, and C. M. Sibley. 1999. Current and emerging azole antifungal agents. *Clin. Microbiol. Rev.* **12**:40-79.
 41. Snyder, S., D. Z. D'Argenio, O. Weislow, J. A. Bilello, and G. L. Drusano. 2000. The triple combination indinavir-zidovudine-lamivudine is highly synergistic. *Antimicrob. Agents Chemother.* **44**:1051-1058.
 42. Solana, R. P., V. M. Chinchilli, W. H. Carter, Jr., J. D. Wilson, and R. A. Carchman. 1987. The evaluation of biological interactions using response surface methodology. *Cell. Biol. Toxicol.* **3**:263-277.
 43. Suhnel, J. 1992. Re: W. R. Greco et al., Application of a new approach for the quantitation of drug synergism to the combination of cis-diamminedichloroplatinum and 1-beta-D-arabinofuranosylcytosine. *Cancer Res.*, **50**:5318-5327, 1990. *Cancer Res.* **52**:4560-4561.
 44. Suhnel, J. 1992. Zero interaction response surfaces, interaction functions and difference response surfaces for combinations of biologically active agents. *Arzneimittelforschung* **42**:1251-1258.
 45. te Dorsthorst, D. T., P. E. Verweij, J. F. G. M. Meis, N. C. Punt, and J. W. Mouton. 2002. Comparison of fractional Inhibitory concentration index with response surface modeling for characterization of in vitro interaction of antifungals against itraconazole-susceptible and -resistant *Aspergillus fumigatus* isolates. *Antimicrob. Agents Chemother.* **46**:702-707.
 46. Walsh, T. J., J. Peter, D. A. McGough, A. W. Fothergill, M. G. Rinaldi, and P. A. Pizzo. 1995. Activities of amphotericin B and antifungal azoles alone and in combination against *Pseudallescheria boydii*. *Antimicrob. Agents Chemother.* **39**:1361-1364.
 47. Warnock, D. W. 1998. Fungal infections in neutropenia: current problems and chemotherapeutic control. *J. Antimicrob. Chemother.* **41**(Suppl. D):95-105.
 48. White, R. L., D. S. Burgess, M. Manduru, and J. A. Bosso. 1996. Comparison of three different in vitro methods of detecting synergy: time-kill, checkerboard, and Etest. *Antimicrob. Agents Chemother.* **40**:1914-1918.



CHAPTER

4

GENERAL CONCLUSIONS

- Summary
- Samenvatting (summary in Dutch)
- Περίληψη (summary in Greek)
- Future perspectives

Adapted from Reviews in Medical Microbiology 2002; 13: (in press)

4.1 SUMMARY

Combination therapy might be an alternative chemotherapeutic approach for management of infections caused by filamentous fungi given the limited *in vivo* efficacy of antifungal monotherapy. Among the benefits of combination therapy are the enhancement of efficacy of antifungal therapy, reduction of appearance of resistant strains and broadening of the spectrum of antifungal activities. Drug levels that are required to produce an antifungal effect can be reduced to achievable serum levels and therefore side effects of highly toxic drugs might be diminished. In addition pharmacokinetic profiles of antifungal drugs can be improved when pharmacokinetic interactions take place. Fungicidal activities might be produced and faster and better curative effects can be obtained. Since evaluation of the efficacy of combination therapy in clinical circumstances is not easy, *in vitro* testing of combination of antifungal drugs could give information about the nature and the intensity of drug interactions (1, 9). However, assessing drug interactions depends both on *in vitro* drug susceptibility testing as well as on the interaction model used for the analysis. Therefore, in this thesis two parameters of *in vitro* antifungal susceptibility testing of filamentous fungi, the medium and the quantification of fungal growth, were investigated (**Chapter 2**) and different drug interaction models were used for analyzing the *in vitro* combination of various antifungal drugs (**Chapter 3**).

In **Chapter 2.1**, a microbroth kinetic system was developed in order to analyze the growth curves of three species of filamentous fungi (*Rhizopus microsporus*, *Aspergillus fumigatus*, and *Scedosporium prolificans*) in five different nutrient media. In general, five distinct phases could be distinguished in the growth of filamentous fungi, namely, the lag-phase, the first transition period, the log-phase, the second transition period, and the stationary-phase. The different growth phases of filamentous fungi were barely distinguishable in RPMI 1640 in which the poorest growth was observed for all fungi even when the medium was supplemented with 2% glucose. *R. microsporus* and *A. fumigatus* grew better in Sabouraud and yeast nitrogen base medium than in RPMI 1640 with growth rates 3 to 4 times higher. None of the media provided optimal growth of *S. prolificans*. The germination of conidia and spores as well as the elongation rates of hyphae were enhanced in antibiotic medium 3 and delayed in yeast nitrogen base medium.

In **Chapter 2.2**, a colorimetric method based on the reduction of the tetrazolium salt dye 3-(4,5-Dimethyl-2-Thiazyl)-2,5-Diphenyl-2H-Tetrazolium Bromide (MTT) was evaluated for the MIC determination of six different antifungal drugs (miconazole, voriconazole, itraconazole, UR9825, terbinafine, and

amphotericin B) against six different species of filamentous fungi (*A. fumigatus*, *A. flavus*, *S. apiospermum*, *S. prolificans*, *Fusarium solani*, and *F. oxysporum*). Furthermore, a new simplified assay that incorporates the dye MTT with the initial inoculum and in which the fungi are incubated with the dye for 48 h or more was developed. High levels of agreement were found between the MTT and the NCCLS method for all drugs and species tested. Among the three genera tested and the two MIC endpoints used, the highest levels of agreement were found with *Aspergillus* spp. (97%) and with the MIC-0 endpoint (97%). However, the percentage of hyphal growth as determined visually by the NCCLS method showed several discrepancies when they were compared with the percentages of MTT reduction. The new assay was easier to perform and more sensitive than the earlier MTT method showing comparable levels of agreement and reproducibility with the other two methods.

In **Chapter 2.3**, another colorimetric assay based on the new tetrazolium salt 2,3-bis{2-methoxy-4-nitro-5-[(sulphenylamino) carbonyl]-2H-tetrazolium-hydroxide} (XTT) was developed and optimized for testing the susceptibility of various *Aspergillus* spp. to amphotericin B and itraconazole. This salt is converted by viable fungi to a water-soluble formazan in the presence of an electron-coupling agent. The combination of 200 µg/ml of XTT with 25 µM of menadione resulted in high production of formazan within 2 h of exposure allowing the detection of hyphae generated by low inocula of 10² CFU/ml after 24 h of incubation. Under these settings the formazan production correlated linearly with the fungal biomass and less variable concentration effect curves for amphotericin B and itraconazole were obtained.

In **Chapter 2.4**, spectrophotometric reading was compared with the visual reading of the NCCLS method for antifungal susceptibility testing of 25 *Aspergillus* strains belonging to different species. Furthermore, results obtained with the XTT method were compared with those obtained with the NCCLS method. The intra- (between the observers) and inter- (between the experiments) experimental agreement of the NCCLS and the XTT method exceeded 95% for MIC-0 for amphotericin B and MIC-0, and 1 for itraconazole. Between visual and spectrophotometric readings, high levels of agreement were found for amphotericin B (≈97%) and MIC-1 (≈92%) and MIC-2 (≈88%) for itraconazole. Poor agreement was found for MIC-0 of itraconazole (51% after 24 h) since the spectrophotometric readings resulted in higher MICs-0 than the visual. The agreement increased to 98% by shifting the threshold level of MIC-0 from 5% to 10% relative OD and by establishing an optical density larger than 0.1 for the growth control as validation criterion. No statistical significant differences were

found between the NCCLS method and the XTT method with the levels of agreement exceeding 97% for MIC-0 of amphotericin B and 83% for MIC-0, 1 and 2 of itraconazole.

In **Chapter 3.1**, the in vitro combination of itraconazole and terbinafine was tested against 20 clinical *S. proliferans* isolates using the modified MTT method described in Chapter 2. The results were analyzed based on the FIC index model and showed synergy for 18 out of 20 strains. Although both drugs had poor activity alone, when they were used in combination up to 8-fold reduction of the MICs of the single drugs was observed and the antifungal activity occurred at concentrations achievable during treatment.

In **Chapter 3.2**, in order to generalize the results of the previous study and to exclude methodological and analysis bias, the in vitro combination of terbinafine with three azoles, namely itraconazole, voriconazole and miconazole was tested against five clinical *S. proliferans* isolates using the spectrophotometric method described in Chapter 2.4, the colorimetric MTT and the modified method described in Chapter 2.2. In addition, the results were analyzed with parametric and non-parametric approaches of the Loewe additivity and Bliss independence zero interaction theories. Synergy was found in all cases with different intensity. Among the three azoles, based on Loewe additivity theory miconazole showed the strongest synergy while based on Bliss independence theory voriconazole did so. Less variable results were obtained with the modified MTT method. The fully parametric model described by Greco et al. (7) applied well to the data resulting in reproducible and easily interpretable results.

In **Chapter 3.3**, the appropriateness as well as the advantages and disadvantages of each of the four models used in the previous study were extensively explored by modeling the interaction of various antifungal drugs against different fungal species. For this purpose combinations of different interactions, spanning from strong synergy to strong antagonism, were chosen. Despite its simplicity, results of the FIC index model depended on the choice of MIC endpoints and interpretation endpoints. Furthermore it lacked of good summary. Although the model described by Prichard et al. (10) resulted in a concentration dependent mosaic of interactions, replicates were required for statistical evaluation of the results, good summary was absent and the results were dependent on the concentration range used. The fully parametric model described by Greco et al., although it did not describe precisely the response surface of antifungal combinations, was able to distinguish synergistic and antagonistic interactions and summarized the interaction with a non-unit concentration independent

interaction parameter including statistically significance levels without requiring replicates.

4.2 SAMENVATTING (SUMMARY IN DUTCH)

Combinatie therapie is een mogelijk alternatief voor de behandeling van infecties veroorzaakt door filamenteuze schimmels met het oog op de beperkte effectiviteit van monotherapie. De voordelen van combinatie therapie zijn onder andere versterking van de effectiviteit, vermindering van selectie van resistente stammen, en verbreding van het spectrum van antifungale activiteit. Hoge plasma spiegels die nodig zijn om een antischimmel effect te bewerkstelligen kunnen bij combinatie therapie verlaagd worden waardoor de bijwerkingen van deze vaak toxische middelen verminderd wordt. Daarnaast kunnen de farmacokinetische profielen verbeterd worden door de interacties die plaatsvinden. Fungicide activiteit kan door combinatie bewerkstelligd worden en daarmee tot snellere en betere curatieve effecten aanleiding geven. Aangezien de evaluatie van de effectiviteit van combinatie therapie bij patiënten niet eenvoudig is, kan in vitro testen van combinaties van antifungale middelen informatie geven over de aard en intensiteit van de geneesmiddel interactie (1, 9). Echter, het bepalen van de geneesmiddel interactie is afhankelijk van zowel de methode van in vitro gevoeligheidsbepaling als het interactie model dat gebruikt wordt voor analyse. Derhalve werden in dit proefschrift twee parameters onderzocht die betrekking hebben op de methode van in vitro gevoeligheidsbepaling, namelijk het medium en de kwantificering van schimmel groei (**hoofdstuk 2**) en werden verschillende modellen vergeleken die de interactie van verschillende antifungale geneesmiddel combinaties beschrijven (**hoofdstuk 3**).

In **hoofdstuk 2.1** werd een microdilutie kinetisch systeem beschreven waarmee de groeikarakteristieken van filamenteuze schimmels (*Rhizopus microsporus*, *Aspergillus fumigatus* en *Scedosporium proliferans*) en vijf verschillende media werden onderzocht. In het algemeen konden in de groei van deze filamenteuze schimmels vijf fases onderscheiden worden, namelijk de lag-fase, de eerste transitie periode, de log-fase, de tweede transitie periode en een stationaire fase. De verschillende groeifases van filamenteuze schimmels waren nauwelijks te onderscheiden in RPMI 1640 waarin de groei van alle schimmels het minst was, zelfs als 2% glucose aan het medium was toegevoegd. *R. microsporus* en *A. fumigatus* groeiden 3 tot 4 maal beter in Sabouraud en yeast nitrogen base medium dan in RPMI 1640. Geen van de media ondersteunde de groei van *S. proliferans* optimaal. De ontkieming van conidia

en sporen alsmede de elongatie snelheden van hyfen waren versterkt in antibiotic medium 3 en vertraagd in yeast nitrogen base medium.

In **hoofdstuk 2.2** werd een colorimetrische methode, gebaseerd op de reductie van een tetrazolium zout kleurstof 3-(4,5-Dimethyl-2-Thiazyl)-2,5 Diphenyl-2H-Tetrazolium bromide (MTT), geëvalueerd voor de bepaling van de minimaal remmende concentratie (MIC) van zes verschillende antifungale middelen (miconazol, voriconazol, itraconazol, UR9825, terbinafine en amfotericine B) tegen zes verschillende soorten filamenteuze schimmels (*A. fumigatus*, *A. flavus*, *S. apiospermum*, *S. prolificans*, *Fusarium solani* en *F. oxysporum*). Tevens werd een nieuwe gesimplificeerde methode geëvalueerd waarbij de kleurstof MTT aan het initiële inoculum werd toegevoegd en met de schimmels gedurende 48 uur geïncubeerd. Een hoge mate van overeenstemming in MIC tussen MTT en NCCLS methoden werd gevonden voor alle middelen en geteste soorten. Onder de drie geteste genera en twee MIC eindpunten, werd de hoogste mate van overeenstemming gevonden voor *Aspergillus* spp. (97%) met een MIC-0 eindpunt (97%). Echter, het percentage groei dat, conform de NCCLS richtlijn, visueel bepaald werd vertoonde discrepanties vergeleken bij de percentages van MTT reductie. Deze nieuwe methode was eenvoudiger om uit te voeren en gevoeliger dan de eerdere MTT methode, waarbij de mate van overeenstemming en reproduceerbaarheid vergelijkbaar was met de andere MTT methoden.

In **hoofdstuk 2.3** werd een andere colorimetrische methode, gebaseerd op een nieuw tetrazolium zout 2,3-bis{2-methoxy-4-nitro-5-[(sulphenylamino) carbonyl]-H-tetrazoliumhydroxide} (XTT), beschreven en geoptimaliseerd voor de gevoeligheidsbepaling van *Aspergillus* spp. voor amfotericine B en itraconazol. Dit zout wordt, in aanwezigheid van een electronbindende stof, door levende schimmels omgezet in het wateroplosbare formazan. De combinatie van 200 µg/ml XTT met 25 µM menadion resulteerde in de hoogste productie van formazan bij een incubatie periode van 2 uur. Hiermee was het mogelijk hyfen, ontstaan uit een inoculum van 10^2 CFU/ml, te detecteren na 24 uur incubatie. Bij deze condities was er een lineair verband tussen schimmel biomassa en formazan productie en was de variabiliteit bij de concentratie-effect curven voor amfotericine B en itraconazol minimaal.

In **hoofdstuk 2.4** werden spectrofotometrisch en visueel aflezen van de NCCLS methode met elkaar vergeleken voor gevoeligheidsbepalingen van 25 *Aspergillus* stammen van verschillende species. Tevens werd de XTT methode vergeleken met de NCCLS methode. De intra (tussen waarnemers) en inter (tussen experimenten) experimentele overeenstemming van de NCCLS en XTT methode waren groter dan 95% voor

MIC-0 voor amfotericine B en MIC-0 en MIC-1 voor itraconazol. Tussen visueel en spectrofotometrisch aflezen werd een hoge mate van overeenstemming gevonden voor amfotericine B ($\approx 97\%$) en MIC-1 ($\approx 97\%$) en MIC-2 ($\approx 88\%$) voor itraconazol. Matige overeenstemming werd gevonden voor MIC-0 voor itraconazol (51% na 24 uur) omdat de spectrofotometrische bepalingen hogere MIC-0s gaven dan de visuele. De overeenstemming nam toe tot 98% door de afleesgrens te verschuiven van 5% naar 10% relatieve OD en als validatie criterium een optische dichtheid van groter dan 0.1 te gebruiken. Er werden geen statistisch significante verschillen gevonden tussen de NCCLS methode en de XTT methode met een hoge mate van overeenstemming voor MIC-0 voor amfotericine B (97%) en voor MIC-0, -1, -2 voor itraconazol (83%).

In **hoofdstuk 3.1** werd in vitro de activiteit van de combinatie van itraconazol en terbinafine getest tegen 20 klinische *S. prolificans* isolaten met de gemodificeerde MTT methode zoals beschreven in hoofdstuk 2. De resultaten werden geanalyseerd met behulp van de FIC index en synergie werd gevonden voor 18 van de 20 isolaten. Hoewel de activiteit van beide middelen apart gering was, leidde de combinatie tot een 8-voudige reductie van de MICs van de middelen afzonderlijk en waren de middelen actief bij een concentratie die binnen de therapeutische breedte ligt.

In **hoofdstuk 3.2** werd, om de resultaten van de vorige studie te kunnen generaliseren en om bias gerelateerd aan methoden en analyse in vitro de combinatie van terbinafine met drie azolen te weten itraconazol, voriconazol en miconazol getest tegen vijf *S. prolificans* stammen gebruik makend van de (gemodificeerde) colorimetrische methoden zoals beschreven in hoofdstuk 2.4. Tevens werden de resultaten geanalyseerd met parametrische en non-parametrische benaderingen van Loewe additiviteit en Bliss onafhankelijke nul interactie theorieën. Van de drie azolen gaf de Loewe additiviteit aan dat miconazol de sterkste synergistische interactie liet zien terwijl de Bliss benadering suggereerde dat dit het geval was voor voriconazol. De minste variabiliteit werd bereikt met de gemodificeerde MTT methode. Het volledig parametrisch model, zoals beschreven door Greco (7), was goed toepasbaar op de experimentele gegevens en resulteerde in reproduceerbare en eenvoudig te interpreteren resultaten.

In **hoofdstuk 3.3**, werd de geschiktheid alsmede de voor- en nadelen van elk van de vier modellen die beschreven zijn in het vorige hoofdstuk in groter detail onderzocht door de interacties van verschillende antifungale middelen tegen verschillen schimmels te modelleren. Hiertoe werden combinaties van verschillende interacties geselecteerd variërend van

sterk synergistisch tot sterk antagonistisch. Ondanks zijn eenvoud, waren de resultaten van het FIC index model sterk afhankelijk van de keuze van de MIC eindpunten en de interpretatie criteria. Verder konden de resultaten niet goed samengevat worden. Alhoewel het model van Prichard (10) leidt tot een concentratie afhankelijk mozaïek van interacties en meerdere herhalingen van experimenten nodig waren om deze statistisch te evalueren, konden de resultaten niet voldoende samengevat worden en waren de resultaten afhankelijk van de gekozen reeks van concentraties. Het volledig parametrisch model van Greco kon niet met precisie de oppervlakte respons van de antifungale combinatie beschrijven, maar met dit model konden synergistische en antagonistische interacties onderscheiden worden en kon de interactie samengevat worden in een non-unit concentratie onafhankelijk interactie parameter die zonder replica's toegankelijk was voor statistische berekeningen.

4.3 ΠΕΡΙΛΗΨΗ (SUMMARY IN GREEK)

Η συνδυασμένη θεραπεία είναι ενδεχόμενο να αποτελεί καλή εναλλακτική χημειοθεραπευτική αγωγή για την καταπολέμηση λοιμώξεων που προκαλούνται από νηματοειδείς μύκητες δεδομένης της περιορισμένης in vivo αποτελεσματικότητας της αντιμυκητιακής μονοθεραπείας. Ανάμεσα στα οφέλη της συνδυασμένης θεραπείας συγκαταλέγονται η ενίσχυση της δράσης των αντιμυκητιακών φαρμάκων, η μείωση της εμφάνισης ανθεκτικών στελεχών και η διεύρυνση του φάσματος της αντιμυκητιακής δράσης. Οι συγκεντρώσεις των αντιμυκητιακών φαρμάκων που απαιτούνται για να είναι δραστικά μπορεί να μειωθούν σε επίπεδα που είναι εφικτά στο αίμα και έτσι να περιοριστούν οι παρενέργειες ισχυρά τοξικών φαρμάκων. Επιπλέον, φαρμακοκινητικά χαρακτηριστικά αντιμυκητιακών φαρμάκων μπορεί να βελτιωθούν σε περίπτωση που λάβουν χώρα φαρμακοκινητικές αλληλεπιδράσεις. Είναι ενδεχόμενο να προκύψουν μυκητοκτόνες δράσεις και να επιτευχθούν συντομότερα και καλύτερα θεραπευτικά αποτελέσματα. Επειδή όμως η αποτίμηση της αποτελεσματικότητας της συνδυασμένης χημειοθεραπείας σε κλινικές συνθήκες δεν είναι εύκολη, in vitro πειράματα συνδυασμών αντιμυκητιακών φαρμάκων θα μπορούσαν να δώσουν πληροφορίες για το είδος και την ένταση των αλληλεπιδράσεων μεταξύ των φαρμάκων (1, 9). Ωστόσο, η αποτίμηση των φαρμακευτικών αλληλεπιδράσεων εξαρτάται τόσο από τις in vitro δοκιμές ευαισθησίας όσο και από το μοντέλο αλληλεπίδρασης που χρησιμοποιείται για την ανάλυση των αποτελεσμάτων. Γι' αυτούς τους λόγους, στην παρούσα διατριβή ερευνήθηκαν δύο παράμετροι in vitro δοκιμών ευαισθησίας νηματοειδών μυκήτων, το θρεπτικό υλικό και η ποσοτικοποίηση της μυκητιακής

ανάπτυξης (κεφάλαιο 2). Επιπλέον, χρησιμοποιήθηκαν διαφορετικά μοντέλα φαρμακευτικών αλληλεπιδράσεων για να αναλυθούν in vitro συνδυασμοί διαφόρων αντιμυκητιακών φαρμάκων (κεφάλαιο 3).

Στο κεφάλαιο 2.1, αναπτύχθηκε ένα μικρής κλίμακας κινητικό σύστημα σε υγρό υλικό για να αναλυθούν οι καμπύλες αύξησης τριών ειδών νηματοειδών μυκήτων (*Rhizopus microsporus*, *Aspergillus fumigatus*, και *Scedosporium prolificans*) σε πέντε διαφορετικά θρεπτικά υλικά. Γενικά, μπόρεσαν να διακριθούν πέντε ξεχωριστές φάσεις κατά την αύξηση των μυκήτων, η λανθάνουσα φάση, η πρώτη μεταβατική περίοδος, η λογαριθμική φάση, η δεύτερη μεταβατική περίοδος και η φάση στασιμότητας. Οι διαφορετικές φάσεις αύξησης των νηματοειδών μυκήτων ήταν ελάχιστα διακριτές στο θρεπτικό υλικό RPMI 1640, στο οποίο παρατηρήθηκε η φτωχότερη αύξηση για όλους τους μύκητες ακόμη και όταν προστέθηκε συμπλήρωμα γλυκόζης 2%. Ο *R. microsporus* και ο *A. fumigatus* αναπτύχθηκαν στα θρεπτικά υλικά Sabouraud και Yeast Nitrogen Base καλύτερα απ' ό,τι στο RPMI 1640 με ρυθμούς αύξησης 3 έως 4 φορές υψηλότερους. Κανένα από τα θρεπτικά υλικά δεν υποστήριξε ικανοποιητική αύξηση του *S. prolificans*. Η εκβλάστηση των κονιδίων και των σπορίων καθώς και η επιμήκυνση των υφών επιταχύνθηκε στο θρεπτικό υλικό antibiotic medium 3 και επιβραδύνθηκε στο Yeast Nitrogen Base.

Στο κεφάλαιο 2.2, αξιολογήθηκε μια χρωματομετρική μέθοδος βασισμένη στην αναγωγή ενός άλατος του τετραζολίου, η χρωστική 3-(4,5-διμέθυλ-2-θειαζύλ) 2,5 διφενύλ-2H- τετραζόλιο βρομίδιο (MTT) για τον προσδιορισμό της ελάχιστης ανασταλτικής πυκνότητας (MIC) έξι διαφορετικών αντιμυκητιακών φαρμάκων (μικοναζόλη, βορικοναζόλη, ιτρακοναζόλη, UR9825, τερμινافίνη και αμφοτερικίνη B) ενάντια σε έξι διαφορετικά είδη νηματοειδών μυκήτων (*Aspergillus fumigatus*, *A. flavus*, *Scedosporium prolificans*, *S. apiospermum*, *Fusarium solani* και *F. oxysporum*). Επιπλέον, αναπτύχθηκε μια καινούργια απλοποιημένη μέθοδος κατά την οποία η χρωστική MTT ενσωματώνεται στο αρχικό ενοφθάλμισμα και οι μύκητες επωάζονται με την χρωστική για 48 ή και περισσότερες ώρες. Υψηλά επίπεδα συμφωνίας βρέθηκαν μεταξύ της MTT και της NCCLS μεθόδου για όλα τα φάρμακα και είδη μυκήτων που ελέγχθηκαν. Ανάμεσα στα τρία γένη που μελετήθηκαν και τους δύο τύπους δεικτών MIC που χρησιμοποιήθηκαν, τα υψηλότερα επίπεδα συμφωνίας βρέθηκαν με τα είδη του *Aspergillus* (97%) και τον MIC-0 δείκτη (97%). Ωστόσο, τα ποσοστά ανάπτυξης των υφών όπως προσδιορίστηκαν οπτικά με την NCCLS μέθοδο ήταν αρκετές φορές σε ασυμφωνία όταν συγκρίθηκαν με τα ποσοστά μετατροπής της χρωστικής MTT. Η καινούργια μέθοδος ήταν ευκολότερη και πιο ευαίσθητη από την παλαιότερη

μέθοδο MTT δείχνοντας παρόμοια επίπεδα συμφωνίας και επαναληψιμότητας με τις άλλες δύο μεθόδους.

Στο **κεφάλαιο 2.3**, αναπτύχθηκε μια άλλη χρωματομετρική μέθοδος βασισμένη σε ένα νέο άλας του τετραζόλιου, το 2,3-δισ (2-μεθοξύ-4-νιτρο-5-[(σουλφενυλαμινο) καρμπονυλ]-2H-τετραζόλιο υδροξείδιο (XTT), και βελτιστοποιήθηκε για δοκιμές ευαισθησίας διάφορων ειδών *Aspergillus* στην αμφοτερικίνη B και ιτρακοναζόλη. Αυτό το άλας μετρατρέπεται από ζώντες μύκητες σε μια υδατοδιαλυτή φορμαζάνη παρουσία ενός ηλεκτρονιο-συζευκτικού παράγοντα. Ο συνδυασμός 200 µg/ml XTT με 25 µM μεναδιόνης είχε ως αποτέλεσμα την παραγωγή φορμαζάνης μέσα σε 2 ώρες έκθεσης επιτρέποντας την ανίχνευση υφών που προέκυψαν από αρχικό ενοφθάλμισμα 10^2 κονιδίων/ml μετά από 24 ώρες επώσης. Κάτω από αυτές τις συνθήκες, η παραγωγή φορμαζάνης συσχετιζόταν ευθύγραμµα με την μυκητιακή βιοµάζα και αποκλήθηκαν λιγότερο μεταβλητές καμπύλες συγκέντρωσης-αύξης.

Στο **κεφάλαιο 2.4**, συγκρίθηκαν η φασματοφωτομετρική και η οπτική ανάγνωση της NCCLS μεθόδου σε δοκιμές ευαισθησίας 25 στελεχών *Aspergillus* που ανήκαν σε διαφορετικά είδη σε αντιμυκητιακά φάρμακα. Επιπλέον, τα αποτελέσματα που αποκτήθηκαν με την XTT μέθοδο συγκρίθηκαν με αυτά της NCCLS μεθόδου. Η ενδοπειραματική (μεταξύ των παρατηρητών) και διαπειραματική (μεταξύ των πειραμάτων) συμφωνία της NCCLS και της XTT μεθόδου υπερέβη το 95% για τον MIC-0 δείκτη της αμφοτερικίνης B και τον MIC-0 και -1 της ιτρακοναζόλης. Μεταξύ οπτικής και φασματοφωτομετρικής ανάγνωσης, υψηλά επίπεδα συμφωνίας βρέθηκαν για την αμφοτερικίνη B ($\approx 97\%$) και με τους δείκτες MIC-1 ($\approx 92\%$) και MIC-2 ($\approx 88\%$) για την ιτρακοναζόλη. Χαμηλά επίπεδα συμφωνίας βρέθηκαν με τον MIC-0 δείκτη για την ιτρακοναζόλη ($\approx 51\%$ μετά από 24 ώρες) επειδή οι MIC-0 δείκτες της φασματοφωτομετρικής ανάγνωσης ήταν υψηλότεροι από τους αντίστοιχους της οπτικής ανάγνωσης. Η συμφωνία αυξήθηκε σε 98% μετατοπίζοντας το όριο του MIC-0 δείκτη από 5% σε 10% σχετικής οπτικής πυκνότητας και καθιερώνοντας μια οπτική πυκνότητα μεγαλύτερη του 0.1 για την αύξηση του μάρτυρα (αύξηση μύκητα απουσία αντιμυκητιακού) ως κριτήριο αξιοπιστίας. Μη στατιστικά σημαντικές διαφορές βρέθηκαν μεταξύ των μεθόδων NCCLS και XTT με επίπεδα συμφωνίας που ξεπερνούσαν το 97% για τον MIC-0 δείκτη της αμφοτερικίνης B και 83% για τους δείκτες MIC-0, -1 και -2 της ιτρακοναζόλης.

Στο **κεφάλαιο 3.1**, ο *in vitro* συνδυασμός της ιτρακοναζόλης με την τερμπιναφίνη δοκιμάστηκε σε 20 κλινικά στελέχη *S. proliferans* χρησιμοποιώντας την τροποποιημένη μέθοδο MTT που περιγράφηκε στο κεφάλαιο 2.2. Τα αποτελέσματα αναλύθηκαν με βάση το μοντέλο του κλασματικού δείκτη ανασταλτικών

συγκεντρώσεων (δείκτης FIC) και βρέθηκε συνέργεια σε 18 από τα 20 στελέχη. Αν και τα δύο αντιμυκητιακά φάρμακα είχαν μικρή δράση μόνα τους, όταν χρησιμοποιήθηκαν σε συνδυασμό, παρατηρήθηκε μέχρι και οκταπλάσια μείωση των δεικτών MIC που επιτύγχαναν τα φάρμακα μόνα τους και αντιμυκητιακή δράση εμφανίστηκε σε συγκεντρώσεις που ήταν θεραπευτικά εφικτές.

Στο **κεφάλαιο 3.2**, για να γενικευθούν τα αποτελέσματα της προηγούμενης μελέτης και να αποκλειστεί τυχόν αναλυτικό και μεθοδολογικό συστηματικό σφάλμα, δοκιμάστηκε ο *in vitro* συνδυασμός της τερμπιναφίνης με τρεις αζόλες, την ιτρακοναζόλη, την βορικοναζόλη και την μικοναζόλη, σε 5 κλινικά στελέχη *S. proliferans* χρησιμοποιώντας την φασματοφωτομετρική μέθοδο που περιγράφηκε στο κεφάλαιο 2.4, την χρωματομετρική μέθοδο MTT και την τροποποιημένη μέθοδο MTT που περιγράφηκαν στο κεφάλαιο 2.2. Επιπλέον, τα αποτελέσματα αναλύθηκαν με παραμετρικές και μη παραμετρικές προσεγγίσεις των θεωριών «της προσθετικής κατά Loewe» και «της ανεξαρτησίας κατά Bliss» για την απουσία φαρμακευτικής αλληλεπίδρασης. Συνέργεια βρέθηκε σε όλες τις περιπτώσεις διαφορετικής όμως εντάσεως. Μεταξύ των τριών αζολών, με βάση τη θεωρία της προσθετικής κατά Loewe, η μικοναζόλη παρουσίασε την ισχυρότερη συνέργεια ενώ με βάση τη θεωρία της ανεξαρτησίας κατά Bliss, η βορικοναζόλη παρουσίασε την ισχυρότερη συνέργεια. Με την τροποποιημένη μέθοδο MTT αποκτήθηκαν αποτελέσματα με μικρότερες διακυμάνσεις. Το πλήρως παραμετρικό μοντέλο που περιγραφηκό από τον Greco και τους συνεργάτες του (7) έδειξε ικανοποιητική εφαρμογή στα δεδομένα δίνοντας επαναλήψιμα και εύκολα ερμηνεύσιμα αποτελέσματα.

Στο **κεφάλαιο 3.3**, εξετάστηκαν διεξοδικά η καταλληλότητα καθώς και τα πλεονεκτήματα και μειονεκτήματα των τεσσάρων μοντέλων που χρησιμοποιήθηκαν στην προηγούμενη μελέτη, προτυποποιώντας την αλληλεπίδραση διαφόρων αντιμυκητιακών φαρμάκων ενάντια σε διαφορετικά είδη μυκήτων. Γι' αυτό το λόγο επιλέχθηκαν συνδυασμοί με διαφορετικές αλληλεπιδράσεις εκτεινόμενες από ισχυρή συνέργεια μέχρι ισχυρό ανταγωνισμό. Παρά την απλότητα του, τα αποτελέσματά του μοντέλου του δείκτη FIC εξαρτιόταν από την επιλογή των δεικτών MIC και των ορίων που χρησιμοποιήθηκαν για την ερμηνεία των αποτελεσμάτων. Επιπρόσθετα, το μοντέλο του δείκτη FIC στερείτο καλής σύνοψης των αποτελεσμάτων. Από την άλλη πλευρά, αν και το μοντέλο που περιγράφηκε από τον Prichard και τους συνεργάτες του (10) είχε ως αποτέλεσμα ένα μωσαϊκό αλληλεπιδράσεων ανάλογα με την συγκέντρωση του φαρμάκου, απαιτούνταν επαναληπτικά πειράματα για στατιστικά αξιολογήσιμα αποτελέσματα, έλειπε καλή σύνοψη των αποτελεσμάτων και τα αποτελέσματα

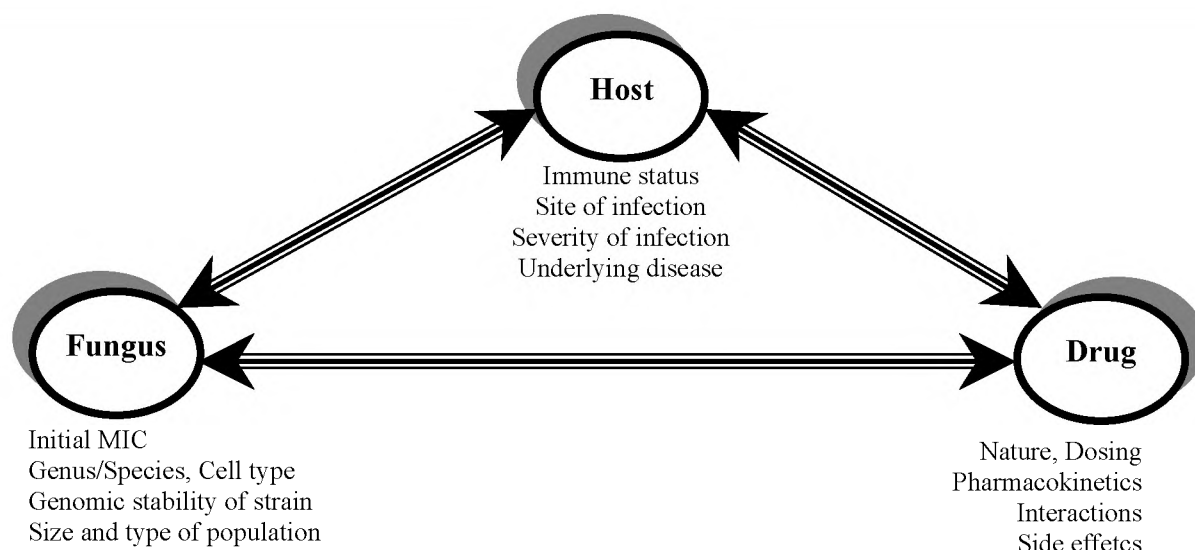


Figure 1. Factors that may contribute to clinical resistance.

εξαρτιόνταν από την περιοχή των συγκεντρώσεων που χρησιμοποιήθηκε. Το πλήρως παραμετρικό μοντέλο που αναπτύχθηκε από τον Greco και τους συνεργάτες του, αν και δεν περιέγραψε επακριβώς την επιφάνεια απόκρισης των αντιμυκητιακών συνδυασμών, ήταν ικανό να διαχωρίσει συνεργατικές και ανταγωνιστικές αλληλεπιδράσεις και να συνοψίσει τις αλληλεπιδράσεις με μια παράμετρο αλληλεπίδρασης, χωρίς μονάδα, ανεξάρτητη των συγκεντρώσεων συμπεριλαμβάνοντας στατιστικά σημαντικά επίπεδα χωρίς να απαιτούνται επαναληπτικά πειράματα.

4.4 FUTURE PERSPECTIVES

The need for standardized and clinically relevant antifungal susceptibility testing (AST) of filamentous fungi became obvious as a result of an increase in the incidence rates of opportunistic fungal infections and in the number of available antifungal drugs. Ideally, the ultimate role of susceptibility testing is to correlate the *in vitro* results with the *in vivo* activity thereby predicting the outcome of therapy with an antifungal agent in a reproducible way (5). However, clinical outcome may be affected by various factors related to the host, drug, and fungus and interactions between them (Fig. 1) (14). Therapeutic failure might be the result of clinical resistance, which is associated with a variety of factors shown in Fig. 1 and/or of microbiological resistance (intrinsic or acquired during therapy), which is associated with the fungal pathogen and described by the minimal inhibitory concentration (MIC) determined with the *in vitro* susceptibility testing methodologies (3).

Since MICs are not physical or chemical measurements, the results of *in vitro* drug susceptibility testing are a function of the condition of methodology used. Although some parameters have little effect on the results of AST, their effect may increase when all these parameters are combined simultaneously (4, 11). Furthermore, given the significant morphological and physiological variation of filamentous fungi, species-specific adjustments of AST might be required in order to obtain reliable results. This is illustrated by the poor and differential growth of different mould genera in RPMI 1640 medium. However, to optimize AST for moulds, truly microbiologically resistant strains are required. Although, resistance could be explored using clinical data or data obtained from animal models, an objective view of microbiological resistance could be obtained based on molecular studies where resistance would be associated with particular mechanisms at this level.

In addition, MICs are parameters that describe a static situation where the concentration of drug remains constant over time. *In vivo* the concentration of drugs fluctuates over time in a different way depending on the site of infection (2). The fungus is exposed to different concentrations at each time point. This changes the antifungal activity of the drugs. Therefore, pharmacokinetic data should be taken into account for assessing the *in vivo* antifungal activity (12). This can be done with *in vitro* pharmacodynamic models where the human pharmacokinetics are simulated or in animal models, where host factors are also accounted, by establishing pharmacodynamic indices associated with the MICs (e.g. time that the drug concentration exceeds the MIC, the ratio of the maximal drug concentration to

the MIC, the ratio of the area under the curve to the MIC) (8).

In such systems, precise quantification of even small amounts of fungal growth is required in order to describe the concentration dependent effect accurately. The colorimetric methods described in this thesis provide sensitive, reproducible, easy to perform, and rapid assays for precise quantification of filamentous growth and objective MIC determination. This potential is considered by the subcommittee of the European Committee on Antimicrobial Susceptibility Testing for reference methodology for in vitro AST of filamentous fungi. Based on these assays the entire concentration-effect curves of antifungal drugs can be characterized and modeled, providing more information about the action of antifungal drugs. Particularly for amphotericin B, for which the concentration-effect curve is very steep using twofold dilutions, a wider range of dilutions (1.5-fold or arithmetically increased dilutions) would give more information about the antifungal action and might enable the separation of resistant strains from susceptible ones, a critical problem of the current in vitro AST methodology.

The real time monitoring of filamentous growth described in this thesis would enable not only the automation of AST but also the modeling of antifungal effects on filamentous fungi; possibilities which were precluded with visual determination of growth. With this system the filamentous growth can be studied kinetically and the effect of antifungal drugs pharmacodynamically. In addition pharmacodynamic studies like the assessment of post antifungal effects in filamentous fungi are facilitated with this system (13). Furthermore, the effect of drugs alone or in combination, simultaneously or sequentially administered, can be studied from the perspective of the growth curves.

In vitro combination of antifungal drugs is an area of AST where more focus is needed, given the clinical implications of the results obtained from combination studies. Although the Loewe additivity has fewer drawbacks as a reference zero interaction theory, the Bliss independence cannot be implicitly excluded. The differences between these two theories might reflect differences in mechanism of action of the drugs. Such conclusions require precise description of response surfaces of each drug interaction excluding the noise, derived from experimental variations. This in combination with molecular studies on mechanisms of action of antifungal drugs would help to establish a zero interaction theory.

Fully parametric models are an attractive approach for analyzing drug interactions since they provide a quantitative measure of the intensity of interaction including statistical analysis, reduce the full data set of an experiment to a smaller set of parameters

and facilitate prediction of the response under new conditions. Furthermore, they are appropriate for complex situations such as three or four drug combinations, they have the potential to explain all the characteristics of a complex system and they tend to be tolerant of a wider spectrum of experimental designs. Finally, they are objective, rigorous, and consistent with modern statistical concepts and they can be used as the pharmacodynamic component of composite pharmacokinetic/pharmacodynamic models (6).

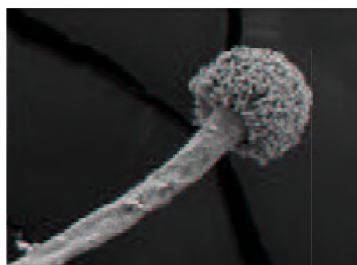
However, further investigation is required to find the best model for the interaction of antifungal drugs given the inability of the Greco model to describe precisely the response surface of antifungal agents against fungi. Although, more than one model might be required to describe such interactions, the choice of the best model would be difficult and to a certain degree it would be arbitrary. A good model should allow each agent's individual concentration-effect curve to be different and accommodate more than two agents. It should describe synergy and antagonism in different regions of the concentration-effect surface and follow the correct course even in regions for which there are no data. Furthermore, it should closely follow the overall average data without following random fluctuations and include a data variation model for fitting data with modern statistical approaches.

Finally, the system of real time monitoring of fungal growth, the colorimetric methods in combination with modern approaches of drug interaction modeling would equip the in vitro AST of filamentous fungi with powerful tools for thorough understanding of interactions of antifungal drugs enabling the pharmacokinetic-pharmacodynamic modeling for filamentous fungi. In vitro data could be used to explore the benefits of combination therapy and to optimize the dosing regimens with an ultimate goal, to cure patients with opportunistic infections caused by filamentous fungi.

REFERENCES

1. **Berenbaum, M. C.** 1989. What is synergy? *Pharmacol. Rev.* **41**:93-141.
2. **Dodds, E. S., R. H. Drew, and J. R. Perfect.** 2000. Antifungal pharmacodynamics: review of the literature and clinical applications. *Pharmacotherapy* **20**:1335-1355.
3. **Espinel-Ingroff, A.** 2000. Clinical utility of in vitro antifungal susceptibility testing. *Rev. Esp. Quimioter.* **13**:161-166.
4. **Espinel-Ingroff, A., F. Barchiesi, K. C. Hazen, J. V. Martinez-Suarez, and G. Scalise.** 1998. Standardization of antifungal susceptibility testing and clinical relevance. *Med. Mycol.* **36**:68-78.

5. **Ghannoum, M. A.** 1997. Susceptibility testing of fungi and correlation with clinical outcome. *J. Chemother.* **9**(Suppl 1):19-24.
6. **Greco, W. R., G. Bravo, and J. C. Parsons.** 1995. The search for synergy: a critical review from a response surface perspective. *Pharmacol. Rev.* **47**:331-85.
7. **Greco, W. R., H. S. Park, and Y. M. Rustum.** 1990. Application of a new approach for the quantitation of drug synergism to the combination of cis-diamminedichloroplatinum and 1-beta-D- arabinofuranosylcytosine. *Cancer Res.* **50**:5318-5327.
8. **MacGowan, A., C. Rogers, and K. Bowker.** 2001. In vitro models, in vivo models, and pharmacokinetics: what can we learn from in vitro models? *Clin. Infect. Dis.* **33**(Suppl 3):214-220.
9. **Polak, A.** 1990. Combination therapy in systemic mycosis. *J. Chemother.* **2**:211-217.
10. **Prichard, M. N., L. E. Prichard, and C. Shipman, Jr.** 1993. Strategic design and three-dimensional analysis of antiviral drug combinations. *Antimicrob. Agents Chemother.* **37**:540-545.
11. **Rambali, B., J. A. Fernandez, L. Van Nuffel, F. Woestenborghs, L. Baert, D. L. Massart, and F. C. Odds.** 2001. Susceptibility testing of pathogenic fungi with itraconazole: a process analysis of test variables. *J. Antimicrob. Chemother.* **48**:163-177.
12. **Rex, J. H., M. A. Pfaller, T. J. Walsh, V. Chaturvedi, A. Espinel-Ingroff, M. A. Ghannoum, L. L. Gosey, F. C. Odds, M. G. Rinaldi, D. J. Sheehan, and D. W. Warnock.** 2001. Antifungal susceptibility testing: practical aspects and current challenges. *Clin. Microbiol. Rev.* **14**:643-658.
13. **Vitale, R., J. W. Mouton, J. Afeltra, J. F. G. M. Meis, and P. E. Verweij.** 2002. Method for measuring postantifungal effect in *Aspergillus* species. *Antimicrob. Agents Chemother.* **46**:1960-1965.
14. **White, T. C., K. A. Marr, and R. A. Bowden.** 1998. Clinical, cellular, and molecular factors that contribute to antifungal drug resistance. *Clin. Microbiol. Rev.* **11**:382-402.



ACKNOWLEDGMENTS

Despite that this part is usually mentioned at the end, it is leading the completion of the Ph. D. thesis since the latter has been realized through the support of many people who have contributed in different aspects for the initiation, performance, and completion of these studies. Those people I would like to thank wholeheartedly here.

Dr. Paul E. Verweij, supervisor and co-promoter of this thesis, I would like to thank you not only for your scientific support in offering new ideas, directing my research and optimizing my experimental work but also for the trust that you showed in me to undertake many responsibilities which contributed substantially to my maturation as scientist. Thank you also for introducing another style in my work, more organized and cooler, especially when deadlines were approaching and you replied to me "Don't worry. We have time". For all these and for your support all this period, beste Paul, dank je wel.

Dr. Jacques F. G. M. Meis, co-promoter of this thesis, I would like to thank you for sharing with me your scientific experience and motivating me for greater efforts as well as for your critical comments in the manuscripts even after they were submitted. I want also to thank you for introducing me in the scientific world with the best words, for your support any time that I needed and for being so friendly. Beste Jacques, dank je wel.

Many thanks to **Professor dr. Ben E. de Pauw** for promoting this thesis and the nice environment that he made in all our meetings in which he always had something to surprise me starting with the unforgettable slogans and ending with his impressive knowledge of ancient Greek language. Beste Ben, dank je wel.

Dr. Johan W. Mouton, co-author of papers of this thesis, I would like to thank you for your exciting new ideas during hot discussions and for your critical comments in my manuscripts. Beste Johan, dank je wel.

Dr. J. Peter Donnelly, co-author of papers of this thesis, I would like to thank you for the extensive discussions we had analyzing in deep many scientific and not only, problems as well as for your excellent examples of English language such as "Only God and strippers reveal, while data show". Dear Peter, thank you.

Dr. Andreas Voss, I would like to thank you for the party advises as well as the high tech support. Lieber Andreas, danke sehr.

Dr. Jo Curfs, next door neighbor to my office, I would like to thank you for introducing me to mice and for your company every time that I was lost in my computer. Beste Jo, dank je wel.

Dr. Willem J. G. Melchers, head of the molecular biology laboratory, I would like to thank you for giving me the opportunity to work in your lab on molecular diagnostics and for the interesting discussions that we had about the DNA world. **Patrick van den Hurk**, I would like to thank you for your technical support for the molecular techniques and for the nice collaboration we had. Beste Willem en Patrick, dank jullie wel.

Dr. Emmanuel Roilides, coordinator of the Eurofung program, I would like to thank you not only because you first brought me in contact with medical mycology but also for your continuous encouragement and your crucial advises in important breakpoints in my life. Thank you for the assiduity of the Greek summary and for your excellent coordination of the Eurofung program giving me the possibility to be a member of a very productive group with high standards. Αγαπητέ κ. Ροιλίδη, σας ευχαριστώ.

At this point I would like also to thank the participants of the Eurofung program for achieving to have a high quality program with outstanding meetings and discussions, which promote further my research. Many thanks to all Eurofung fellows for the wonderful time that we had every time that we met each other by sharing our experiences and celebrating our successes in each Congress (after of course the scientific program). Thank you all.

Roxane Vitale, Javier Afeltra and Eric Dannaoui, Eurofung fellows in Nijmegen and coworkers, I would like to thank you for your excellent collaboration during this period and the knowledge that I gained from our unlimited discussions during the breaks as well as for our wonderful friendship that we build up through all the problems that we passed starting with the Dutch weather until personal decisions. Queridos Roxy and Javier, muchas gracias. Cher Eric, merci beaucoup.

Ton Rijs, technician of medical mycology laboratory, I would like to thank you not only for your excellent technical support and for teaching me the medical mycology of the lab but also for your support during the first period of my stay in Nijmegen. **Hein van der Lee**, I would like also to thank you for your technical support any time that asked for and for your friendly environment in the lab as well as for your helpful but sometimes dangerous advises about special Dutch beers. **Ilse Breuker**, I would also like to thank you for kind technical support, which was accompanied always with a smile. Beste Ton, Hein en Ilse, dank jullie wel.

I would like to thank all the students that they performed their graduation studies in our laboratory for the nice moments we had and especially, **Jos J. Kerremans** and **Esther Kramer** with whom several projects were completed. I would like also to thank **Debbie T. A te Dorsthorst**, Ph. D. student, for the nice collaboration we had.

Special thanks to **Bianca A. Bouman**, co-author of papers of this thesis, not only for her technical support in several projects and her invaluable help until late in the evening when I had to handle hundreds of microtiter plates and mice but also for the design and lay-out of this booklet and for her personal support during all this period. Beste Bianca, dank je wel.

Last but not least, I would like to thank my parents for the warm Greek environment with home

made Greek food during the weekends I visited them in Hannover, Germany and for the psychological support during all this period. Αγαπητοί μου γονείς, σας ευχαριστώ.

I would like also to thank my friends in Hannover which accompanied me in my weekend escapes having a lot of fun and my friends in Greece who succeeded to be here, despite the long distance, every day when my mailbox was flashing with news from my home country. Αγαπητοί μου φίλοι, ευχαριστώ.

Finally I would like to thank all the people of the Department of Medical Microbiology for the friendly and nice atmosphere making me feel at home as well as all those who have contributed for a nice stay in the Netherlands.

CURRICULUM VITAE

Joseph Meletiadis was born on 13th of July of 1975 in Hannover, Germany. Four years later he moved to Nea Roda, Chalkidiki, Greece where he finished the primary school.

In 1989 he finished the first three years of secondary school in Greek Gymnasium in Ierissos, Chalkidiki, Greece. He completed the remaining three years of secondary school in Greek Lyzeum in Hannover, Germany with the degree excellent (19/20). He then participated in Panhellenic University Entry examinations, which he passed with the degree excellent (18/20).

In 1993 he started his university studies in Biology School of Aristotle University of Thessaloniki, Greece. After 4 years and having completed successfully (10/10) the graduate project entitled "Cloning and Expression of the Immediate Early (IE-1) Gene of Human Herpesvirus-6 (HHV-6) in eukaryotic cells" in Laboratory of Molecular Biology and General Microbiology, Biology School, Aristotle University of Thessaloniki, Greece in 1997 he graduated from Biology school with the degree of very good (7.84/10).

After he performed his military duties in the Greek army, he worked on a research project entitled "Direct effects of cytokines and corticosteroids on *Candida albicans*" in the Infectious Diseases Laboratory, Hippokration Hospital of Thessaloniki, Greece until 1998.

In October of 1998, he started his PhD studies, described in this thesis, at the department of Medical Microbiology as part of a multicenter European Commission Training and Mobility of Research program (EC-TMR-EUROFUNG network ERBFMRXCT97-0145). During this period, he participated in several graduation projects and multicenter collaborative studies.

In 2000, he was awarded by the European Society of Clinical Microbiology and Infections Diseases with the "ESCMID fellowship 2000 award". His research in medical mycology will be continued at the National Institutes of Health, Bethesda, USA in the Immunocompromised Host Section, Pediatric Oncology Branch of the National Cancer Institute.

LIST OF PUBLICATIONS

1. **Meletiadis, J., J. F. G. M. Meis, R. Horre, and P. E. Verweij.** 1999. In vitro antifungal activity of six drugs against 13 clinical isolates of *Ochroconis gallopava*. *Stud. Mycol.* **43**:226-228.
2. **Meletiadis, J., J. F. G. M. Meis, G. S. de Hoog, and P. E. Verweij.** 2000. In vitro susceptibility of 11 clinical isolates of *Exophiala* species to six antifungal drugs. *Mycoses* **43**:309-312.
3. **Meletiadis, J., J. W. Mouton, J. L. Rodriguez-Tudela, J. F. G. M. Meis, and P. E. Verweij.** 2000. In vitro interaction of terbinafine with itraconazole against clinical isolates of *Scedosporium prolificans*. *Antimicrob. Agents Chemother.* **44**:470-472.
4. **Meletiadis, J., J. F. G. M. Meis, J. W. Mouton, J. P. Donnelly, and P. E. Verweij.** 2000. Comparison of NCCLS and 3-(4,5-Dimethyl-2-Thiazyl)-2,5-Diphenyl-2H-Tetrazolium Bromide (MTT) methods of in vitro susceptibility testing of filamentous fungi and development of a new simplified method. *J. Clin. Microbiol.* **38**:2949-2954.
5. **Meletiadis, J., J. W. Mouton, J. F. G. M. Meis, and P. E. Verweij.** 2000. Combination chemotherapy for the treatment of invasive infections by *Scedosporium prolificans*. *Clin. Microbiol. Infect.* **6**:336-337.
6. **Meletiadis, J., J. F. G. M. Meis, J. W. Mouton, and P. E. Verweij.** 2001. Analysis of growth characteristics of filamentous fungi in different nutrient media. *J. Clin. Microbiol.* **39**:478-484.
7. **Meletiadis, J., J. W. Mouton, J. F. G. M. Meis, B. A. Bouman, J. Peter Donnelly, P. E. Verweij and EUROFUNG network.** 2001. Colorimetric assay for antifungal susceptibility testing of *Aspergillus* species. *J. Clin. Microbiol.* **39**:3402-3408.
8. **Meletiadis, J., J. F. G. M. Meis, B. A. Bouman, J. W. Mouton, P. E. Verweij and EUROFUNG network.** 2001. Comparison of spectrophotometric and visual readings of NCCLS method and evaluation of a colorimetric method based on reduction of a soluble tetrazolium salt 2,3-bis{2-methoxy-4-nitro-5-[(sulphenylamino) carbonyl]-2H-tetrazolium hydroxide} for antifungal susceptibility testing of *Aspergillus* species. *J. Clin. Microbiol.* **39**:4256-4263.
9. **Meletiadis, J., J. W. Mouton, J. F. G. M. Meis, and P. E. Verweij and EUROFUNG network.** 2002. In vitro activities of new and conventional antifungal agents against *Scedosporium* isolates. *Antimicrob. Agents Chemother.* **46**:62-68.
10. **Meletiadis, J., J. W. Mouton, J. F. G. M. Meis, B. A. Bouman, P. E. Verweij and EUROFUNG network.** 2002. Comparison of E-test and the Sensititre colorimetric method with the NCCLS proposed standard for antifungal susceptibility testing of *Aspergillus* species. *J. Clin. Microbiol.* **40**:(in press).
11. **te Dorsthorst, D. T. A., P. E. Verweij, J. Meletiadis, M. Bergervoet, N. C. Punt, J. F. G. M. Meis, and J. W. Mouton.** 2002. In vitro interaction of flucytosine against 35 yeast isolates determined by both the fractional inhibitory concentration index and the response surface approach. *Antimicrob. Agents Chemother.* **46**:(in press).
12. **Meletiadis, J., J. W. Mouton, J. F. G. M. Meis, and P. E. Verweij.** 2002. Methodological issues related to drug interaction modeling for filamentous fungi. *Rev. Med. Microbiol.* **13**:(in press).
13. **Dannaoui, E., J. Meletiadis, J. W. Mouton, J. F. G. M. Meis, and P. E. Verweij.** 2002. In vitro susceptibilities of zygomycetes to new and conventional antifungals. *J. Antimicrob. Chemother.* (in press).
14. **Meletiadis, J., P. van den Hurk, W. J. G. Melchers, G. Jannes, J. F. G. M. Meis and P. E. Verweij.** 2002. Evaluation of a polymerase chain reaction-line probe assay system for the detection of medically important fungi in bronchoalveolar lavage fluids. *Med. Mycol.* (in press).
15. **Meletiadis, J., J. W. Mouton, J. F. G. M. Meis, and P. E. Verweij.** Drug interaction modeling of in vitro combination of azoles with terbinafine against clinical *Scedosporium prolificans* isolates (submitted).
16. **Meletiadis, J., D. T. A. te Dorsthorst, J. W. Mouton, J. F. G. M. Meis, P. E. Verweij.** Assessing the in vitro interaction of antifungal drugs: Comparison of different drug interaction models (submitted).
17. **Meletiadis, J., D. T. A. te Dorsthorst, J. W. Mouton, J. F. G. M. Meis, and P. E. Verweij.** Early determination of in vitro antifungal resistance of filamentous fungi based on growth curves (submitted).
18. **Meletiadis, J., J. Curfs, J. F. G. M. Meis, and P. E. Verweij.** A non-neutropenic murine model for invasive scedosporiosis (submitted).
